Alzheimer's Disease and Frontotemporal Dementia

Methods and Protocols

Edited by

Erik D. Roberson

Center for Neurodegeneration and Experimental Therapeutics,
Departments of Neurology and Neurobiology,
University of Alabama at Birmingham, AL, USA

Humana Press

Editor
Erik D. Roberson, M.D., Ph.D.
Center for Neurodegeneration and Experimental Therapeutics
Departments of Neurology and Neurobiology
University of Alabama at Birmingham, AL
USA
eroberson@uab.edu

ISSN 1064-3745 e-ISSN 1940-6029
ISBN 978-1-60761-743-3 e-ISBN 978-1-60761-744-0
DOI 10.1007/978-1-60761-744-0
Springer New York Dordrecht Heidelberg London

Library of Congress Control Number: 2010938365

Humana Press is part of Springer Science+Business Media (www.springer.com)

Preface

Alzheimer's disease (AD) is the most common neurodegenerative disorder and one of the most feared diseases due to the manner in which it robs its victims of their memories. Frontotemporal dementia (FTD) is perhaps somewhat less well known among the public, but it is also a prominent cause of dementia that produces devastating changes in personality and a decline in interpersonal interactions. The two conditions are often considered siblings, for while they are distinct disorders targeting different brain regions and producing unique clinical symptoms, there is some overlap in their molecular neuropathology (such as the presence of inclusions containing the microtubule-associated protein tau) and genetic risk factors (such as apolipoprotein E).

Both conditions were originally described around the turn of the last century but languished without significant research effort for decades. In the 1980s, breakthroughs in pathobiochemistry and genetics led to identification of molecular players in these diseases, enabling a very fruitful period of biomedical research that continues to intensify. Recent years have seen a growing interest in the neurobiology of neuronal dysfunction in these conditions with increasing application of complex techniques from molecular and cellular neuroscience. Thus, the diversity and sophistication of methods and protocols used for research on AD and FTD continue to grow. It is not uncommon, and actually is expected in many journals, to see publications that include techniques as divergent in their required expertise as behavior, electrophysiology, confocal microscopy, and hardcore biochemistry. Consequently, projects in AD and FTD research may require individual investigators to branch out into complex approaches for which they have not received abundant hands-on training. The goal of this book is to make many of those techniques more accessible.

The book is intended for scientists of all kinds studying AD and FTD. Realizing that many of the approaches will be foreign to some users, the protocols are presented in a step-by-step fashion with complete materials lists and user notes describing the "real story" about how to make the method work.

The book begins with an overview of the two diseases and modern approaches to research on them. Many of the molecules associated with AD and FTD are notoriously difficult to work with, so the first half of the book (Chaps. 2–10) details specialized protocols for working with amyloid-β peptide, tau, and apolipoprotein E. The second part (Chaps. 11–18) focuses on experimental systems for studying AD and FTD, including cell and animal models, and outcome measures that can be used to assess neuronal function in these systems.

Birmingham AL, USA *Erik D. Roberson*

Contents

Preface . . . . . *v*
Contributors . . . . . *ix*

1 Contemporary Approaches to Alzheimer's Disease and Frontotemporal Dementia 1
Erik D. Roberson

PART I WORKING WITH AD- AND FTD-RELATED MOLECULES

2 Preparing Synthetic Aβ in Different Aggregation States 13
W. Blaine Stine, Lisa Jungbauer, Chunjiang Yu, and Mary Jo LaDu

3 Isolation of Low-n Amyloid β-Protein Oligomers from Cultured Cells, CSF, and Brain 33
Ganesh M. Shankar, Alfred T. Welzel, Jessica M. McDonald, Dennis J. Selkoe, and Dominic M. Walsh

4 Detecting Aβ*56 Oligomers in Brain Tissues 45
Mathew A. Sherman and Sylvain E. Lesné

5 Assessing Aβ Aggregation State by Atomic Force Microscopy 57
Justin Legleiter

6 Measuring APP Carboxy-Terminal Fragments 71
Luke A. Esposito

7 Detection of APP Intracellular Domain in Brain Tissue 85
Sanjay W. Pimplikar and Anupama Suryanarayana

8 Cell-Based Assays for Regulators of Tau Biology 93
Umesh K. Jinwal and Chad A. Dickey

9 Split GFP Complementation Assay for Quantitative Measurement of Tau Aggregation In Situ 109
Wanjoo Chun, Geoffrey S. Waldo, and Gail V.W. Johnson

10 Apolipoprotein E Expression and Purification 125
Yvonne Newhouse and Karl H. Weisgraber

PART II MODEL SYSTEMS AND OUTCOME MEASURES

11 Aβ Toxicity in Primary Cultured Neurons 141
Adriana Ferreira, Roxana C. Sinjoanu, Alexandra Nicholson, and Sara Kleinschmidt

12 Manipulation of Gene Expression in the Central Nervous System with Lentiviral Vectors 155
Binggui Sun and Li Gan

13 Selecting a Mouse Model of Alzheimer's Disease 169
Jeannie Chin

14 Monitoring Spatial Learning and Memory in Alzheimer's Disease Mouse Models Using the Morris Water Maze 191
Kimberly Scearce-Levie

15 Step-by-Step In Situ Hybridization Method for Localizing Gene Expression Changes in the Brain 207
Jorge J. Palop, Erik D. Roberson, and Inma Cobos

16 Real-Time Visualization of Axonal Transport in Neurons 231
Yasuko Osakada and Bianxiao Cui

17 Quantifying Biomarkers of Cognitive Dysfunction and Neuronal Network Hyperexcitability in Mouse Models of Alzheimer's Disease: Depletion of Calcium-Dependent Proteins and Inhibitory Hippocampal Remodeling 245
Jorge J. Palop, Lennart Mucke, and Erik D. Roberson

18 Epigenetic Changes in the Brain: Measuring Global Histone Modifications 263
Gavin Rumbaugh and Courtney A. Miller

Index *275*

Contributors

Jeannie Chin • *Department of Neuroscience and Farber Institute for Neurosciences, Thomas Jefferson University, Philadelphia, PA, USA*

Wanjoo Chun • *Department of Pharmacology, College of Medicine, Kangwon National University, Chunchon, Korea*

Inma Cobos • *Nina Ireland Laboratory of Developmental Neurobiology, Department of Psychiatry, University of California, San Francisco, San Francisco, CA, USA*

Bianxiao Cui • *Department of Chemistry, Stanford University, Stanford, CA, USA*

Chad A. Dickey • *Department of Molecular Medicine, Byrd Alzheimer's Institute, University of South Florida, Tampa, FL, USA*

Luke A. Esposito • *ProteoTech, Inc, Kirkland, WA, USA*

Adriana Ferreira • *Department of Cell and Molecular Biology, Feinberg School of Medicine, Northwestern University, Chicago, IL, USA*

Li Gan • *Department of Neurology, Gladstone Institute of Neurological Disease, University of California, San Francisco, San Francisco, CA, USA*

Umesh K. Jinwal • *Department of Molecular Medicine, Byrd Alzheimer's Institute, University of South Florida, Tampa, FL, USA*

Gail V.W. Johnson • *Department of Anesthesiology, University of Rochester Medical Center, Rochester, NY, USA*

Lisa Jungbauer • *Department of Anatomy and Cell Biology, University of Illinois at Chicago, Chicago, IL, USA*

Sara Kleinschmidt • *Department of Cell and Molecular Biology, Feinberg School of Medicine, Northwestern University, Chicago, IL, USA*

Mary Jo LaDu • *Department of Anatomy and Cell Biology, University of Illinois at Chicago, Chicago, IL, USA*

Justin Legleiter • *The C. Eugene Bennett Department of Chemistry, West Virginia University, Morgantown, WV, USA*

Sylvain E. Lesné • *Department of Neuroscience, Institute for Translational Neuroscience, University of Minnesota, Minneapolis, MN, USA*

Jessica M. McDonald • *Laboratory for Neurodegenerative Research, The Conway Institute for Biomolecular and Biomedical Research, University College Dublin, Belfield Dublin, Ireland*

Courtney A. Miller • *Department of Metabolism & Aging and Department of Neuroscience, The Scripps Research Institute Florida, Jupiter, FL, USA*

Lennart Mucke • *Gladstone Institute of Neurological Disease, University of California, San Francisco, San Francisco, CA, USA*

Yvonne Newhouse • *Gladstone Institute of Neurological Disease, University of California, San Francisco, San Francisco, CA, USA*

Alexandra Nicholson • *Department of Cell and Molecular Biology, Feinberg School of Medicine, Northwestern University, Chicago, IL, USA*

Yasuko Osakada • *Department of Chemistry, Stanford University, Stanford, CA, USA*
Jorge J. Palop • *Department of Neurology, Gladstone Institute of Neurological Disease, University of California, San Francisco, San Francisco, CA, USA*
Sanjay W. Pimplikar • *Department of Neurosciences, Lerner Research Institute, Cleveland Clinic, Cleveland, OH, USA*
Erik D. Roberson • *Departments of Neurology and Neurobiology, Center for Neurodegeneration and Experimental Therapeutics, University of Alabama at Birmingham, Birmingham, AL, USA*
Gavin Rumbaugh • *Department of Neuroscience, The Scripps Research Institute Florida, Jupiter, FL, USA*
Kimberly Scearce-Levie • *Genentech, Inc, South San Francisco, CA, USA*
Dennis J. Selkoe • *Center for Neurologic Diseases, Brigham & Women's Hospital and Harvard Medical School, Boston, MA, USA*
Ganesh M. Shankar • *Center for Neurologic Diseases, Brigham & Women's Hospital and Harvard Medical School, Boston, MA, USA*
Mathew A. Sherman • *Department of Neuroscience, Institute for Translational Neuroscience, University of Minnesota, Minneapolis, MN, USA*
Roxana C. Sinjoanu • *Department of Cell and Molecular Biology, Feinberg School of Medicine, Northwestern University, Chicago, IL, USA*
W. Blaine Stine • *Department of Anatomy and Cell Biology, University of Illinois at Chicago, Chicago, IL, USA*
Binggui Sun • *Department of Neurology, Gladstone Institute of Neurological Disease, University of California, San Francisco, San Francisco, CA, USA*
Anupama Suryanarayana • *Department of Neurosciences, Lerner Research Institute, Cleveland Clinic, Cleveland, OH, USA*
Geoffrey S. Waldo • *Bioscience Division, Los Alamos National Laboratory, Los Alamos, NM, USA*
Dominic M. Walsh • *Laboratory for Neurodegenerative Research, The Conway Institute for Biomolecular and Biomedical Research, University College Dublin, Belfield Dublin, Ireland*
Karl H. Weisgraber • *Gladstone Institute of Neurological Disease, University of California, San Francisco, San Francisco, CA, USA*
Alfred T. Welzel • *Laboratory for Neurodegenerative Research, The Conway Institute for Biomolecular and Biomedical Research, University College Dublin, Belfield Dublin, Ireland*
Chunjiang Yu • *Department of Anatomy and Cell Biology, University of Illinois at Chicago, Chicago, IL, USA*

Chapter 8

Cell-Based Assays for Regulators of Tau Biology

Umesh K. Jinwal and Chad A. Dickey

Abstract

Understanding the molecular mechanisms of Alzheimer's disease (AD) is a challenging endeavor, namely, due to the fact that the disease only occurs in the central nervous system of elderly humans. Thus, model systems simply do not accurately portray this cellular landscape. While we cannot ask many mechanistic questions using the human brain as our test subject, cell culture techniques that have emerged at least provide us with the ability to pose fundamental biochemical questions, which may ultimately lead to translational outcomes for AD. In particular, the intracellular microtubule-associated protein tau that accumulates in AD is found in normal cells. Manipulating these cells may allow us to address basic questions about tau biology that would provide novel therapeutic strategies down the road. Here, we describe several techniques to explore tau cell biology using the Odyssey® Infrared Imaging system (Odyssey system) from LI-COR Biosciences. We provide a detailed protocol on how to perform a scalable drug screening assay called the In-Cell Western and follow-up these screens with standard Western analysis to confirm whether "hits" are valid by more traditional means. We provide some tips on where mistakes are most likely to occur, and we interpret our standard Western data, providing some estimation as to the composition of the banding pattern that is typical for this enigmatic protein.

Key words: Odyssey, Tau, In-Cell Western, Near-infrared, Fluorescence, Cell culture

1. Introduction

For most neurodegenerative protein aggregation disorders, intracellular accumulation of an aberrant form of the parent protein initiates the cascade that ultimately culminates in the presentation of a pathological marker detected by histochemistry in post-mortem tissue. While these postmortem analyses have been critical to establish the foundation of these diseases, it is the early events that seed the pathology that will likely be the best targets for therapeutic design. The microtubule-associated protein tau accumulates into tangles in Alzheimer's disease (AD), although the pathogenic process leading up to this is still largely unclear.

Erik D. Roberson (ed.), *Alzheimer's Disease and Frontotemporal Dementia*, Methods in Molecular Biology, vol. 670,
DOI 10.1007/978-1-60761-744-0_8,

While mouse modeling has furthered our understanding of the disease process, these studies carry a high cost, both in time and resources. Therefore, the emergence of cell culture models has been critical for understanding the mechanisms at play in tau pathogenicity. With these models, we have been able to take advantage of a number of emerging technologies that are helping us define our understanding of the mechanisms involved with tau biology (1–3). Moreover, we are continuing to discover therapeutic targets that might prove most effective in our fight against AD and other tauopathies. In this chapter, we describe the methods using the Odyssey® Infrared Imaging system from LI-COR Biosciences, which has allowed us to begin to address questions in a semi-high throughput quantitative format previously not achievable for the tau protein. Screening the effects of small molecules, siRNAs and even biological agents, such as growth factors and cytokines, can be done in a high volume within a two-day protocol. The dual-color capability provides an option for greater control and reliability of the assay in a single run. Herein, we provide basic protocols to analyze total tau levels relative to GAPDH; however, this technique can be applied to any number of intracellular targets, provided antibody specificity is high. We also describe validation studies using the Odyssey system for more traditional Western blotting.

1.1. In-Cell Western

The LI-COR Biosciences In-Cell Western (ICW) assay is suited for drug discovery assay development where protein quantification is important in the cellular environment. It incorporates the use of near infrared-labeled secondary antibodies, which can be independently detected with the dual laser Odyssey system at 680 nm and 800 nm, to detect any combination of two proteins, provided species-specific antibodies are available. The assay can quantify proteins within a monolayer of fixed cells in 96 or 384-well microplates, making this platform a cross between high-throughput immunofluorescent chemistry and Western blotting; however, with this increased throughput, resolution is lost, making follow-up validation studies critical. This procedure is unique from typical plate reader-based applications and other biological system applications, such as the Typhoon from GE, because of the use of near-infrared laser scanning. Near-infrared light has a longer wavelength than light in the visible range. Therefore, near-infrared light can travel farther and pass through certain surfaces without losing intensity. Thus, the Odyssey system is the most affordable of a handful of devices that allows for this type of application. The signal from the Odyssey system is linear and, thus, the values provided by the system software allow for relative quantitation within each plate scanned. Moreover, a normalization template can be used for variance across plates, allowing for multiplate assay analyses. Here, we describe a protocol specific for analyzing

tau levels relative to GAPDH; however, this application could be applied to a number of other proteins. That being said, a large amount of effort went into optimizing the conditions described herein to specifically develop our assay around the tau protein; specifically, cell line and antibody selections.

1.2. Western Blotting with the Odyssey System

Protein blotting has become the most routine tool to detect specific proteins in a given sample of tissue homogenate or extract. Recent advances in chemiluminescent technologies have greatly increased the ease-of-use and rapidity for this procedure. Now, with the advent of the Odyssey system, Western blotting for two individual proteins can be performed simultaneously without the need of film or a dark room. Moreover, as opposed to signals produced by enzymatic labeling reactions, this latest technology uses linear fluorescent chemistry, allowing for true quantitative analyses to be done. Here, we describe Western blotting using the Odyssey system since standard Western analysis is a very common laboratory practice. Nevertheless, in Fig. 3c, we have utilized standard Western blotting for comparison with near-infrared detection.

2. Materials

2.1. In-Cell Western

2.1.1. Cell Culture and Treatment

1. Cell line: H4 neuroglioma highly adherent cell line.
2. Cell culture facility.
3. 96-well tissue culture plates, black shell, optically clear bottom (see Note 3).
4. Tissue culture flasks (T-75).
5. 25 ml Reagent reservoirs.
6. Sterile filtered pipette tips.
7. 12-Channel multichannel pipetter.
8. Trypsin/EDTA solution.
9. DMEM + 10% Fetal Bovine Serum (FBS).
10. Opti-MEM, no additives.
11. Compounds from a chemical library (10 mM stocks; Prestwick Chemical or Microsource, Gaylordsville, CT).
12. Standard 96-well tissue culture plates.
13. 17-AAG (17-(Allylamino)-17-demethoxygeldanamycin), (A.G. Scientific, San Diego, CA).

2.1.2. In-Cell Western Assay

1. Fixing solution: 3.7% formaldehyde in PBS.
2. Triton washing solution: 0.1% Triton X-100 in PBS.

3. Odyssey blocking buffer, neat.
4. Orbital shaker.
5. 96-well plate automatic washer (recommended).
6. Mouse monoclonal anti-GAPDH antibody (Biodesign, Saco, ME).
7. Rabbit polyclonal antitotal tau antibody (Dako, Carpinteria, CA).
8. Primary dilution buffer: 1:1 mixture of Odyssey blocking buffer and 1× PBS + 0.2% Tween-20 (see Note 1).
9. Goat antirabbit antibody labeled with Alexa-Fluor 680 (Molecular Probes).
10. Goat antimouse antibody labeled with IRDye 800 (Rockland Laboratories).
11. Secondary dilution buffer: 1:1 mixture of Odyssey blocking buffer and 1× PBS + 0.4% Tween-20.
12. Tween washing solution: 0.1% Tween-20 in PBS.
13. Aluminum foil or black boxes.
14. Odyssey Infrared Imaging system (LI-COR Biosciences, Nebraska USA).

2.2. Western Validation of Hits

2.2.1. Cell Lysis

1. 6-well tissue culture plates.
2. Vacuum source connected to a tube and a pasteur glass pipette for aspiration of media.
3. 1× Dulbecco's phosphate-buffered saline (DPBS).
4. Cell lifters.
5. Pipettes and tips from 10 µl to 1,000 µl.
6. Microcentrifuge tubes, 1.5 ml.
7. Sonicator.
8. Lysis Buffer: 50 mM Tris–HCl pH 7.5, 100 mM NaCl, 15 mM EDTA, 0.1% Triton X-100, 1%SDS, 1× Protease Inhibitor (CalBiochem, Gibbstown, NJ), Phosphatase Inhibitor cocktail 1 and 2 (Sigma, St. Louis, MO), 1 mM PMSF.

2.2.2. Protein Estimation

1. BCA Protein Assay Reagents A and B.
2. 1 µg/µl Bovine Serum Albumin (BSA).
3. 37°C Incubator.
4. Clear 96-well plate.
5. Spectrophotometer to read protein at 562 nm.

2.2.3. Western Blotting with the Odyssey System

1. Square plastic Petri dishes.
2. 10% Tris-Glycine, 1.0 mm Precast Gels, 12-well.

3. Thick blot papers, 1 cm larger than the membrane.
4. Immobilon-FL-PVDF membrane (see Note 11), cut 1 mm larger than the gel size.
5. Saran wrap.
6. Protein gel apparatus.
7. Western Transfer apparatus.
8. Power supply.
9. Heating block for heating samples at 95°C.
10. Rotary shaker.
11. Rocking mixer.
12. Odyssey Infrared Imaging system (LI-COR Biosciences).
13. 2× Laemmli sample buffer.
14. 2-Mercaptoethanol.
15. PBST: 0.2% Tween-20 in PBS.
16. Mouse monoclonal anti-GAPDH antibody (Biodesign).
17. Rabbit polyclonal antitotal tau antibody (Dako).
18. Goat antirabbit antibody labeled with Alexa-Fluor 680 (Molecular Probes).
19. Goat antimouse antibody labeled with IRDye 800 (Rockland Laboratories).
20. Odyssey blocking buffer, neat (LI-COR Biosciences).

3. Methods

3.1. In-Cell Western

3.1.1. Cell Culture and Treatments

Ensure that all cell culture work prior to fixation is performed in a Biological safety cabinet under sterile conditions. Do not forget to turn on airflow before starting work.

1. Grow H4 neuroglioma cells in DMEM containing 10% FBS (complete media) in a T75 tissue culture flask until confluency is reached (see Note 2).
2. Aspirate media and add 5 ml of Trypsin-EDTA solution to your flask. Once cells detach, remove 4 ml of this suspension and dispense 1 ml of cells into each of four individual 50 ml tubes. Replace media in flask.
3. Add 20 ml of complete media to each of the four 50 ml tubes. Cover and invert to distribute suspension.
4. Decant the contents of one tube into a sterile 25 ml reagent reservoir, and using a multichannel pipetter, dispense 200 µl/well into a sterile 96-well tissue culture treated plate (Black shell, optically clear bottom; see Note 3). Repeat with three

additional 96-well plates. During distribution, ensure that the cell suspension is evenly disbursed by triturating with the multichannel pipetter (see Note 4).

5. Incubate cells at 37°C in 5% CO_2 until they reach 95–100% confluency.
6. Remove the complete media from each well using a multichannel vacuum manifold and replace with 200 µl of serum-free Opti-MEM media.
7. In a standard 96-well assay plate, prepare 1 mM compound stocks from one plate of a commercially available library (we have used the GenesisPlus library from Microsource and the Prestwick Chemical library) by diluting in Opti-MEM. As a positive control, prepare a 100 µM stock of the Hsp90 inhibitor, 17-(Allylamino)-17-demethoxygeldanamycin (17-AAG). A vehicle control of DMSO should also be prepared using a volume equivalent to the highest concentration of drug. Most libraries come with the first and last columns empty to add controls. Add the 17-AAG stock to wells A, C, E, and G to the first column; add vehicle to wells B, D, F, and H of the first column.
8. Using a multichannel pipetter, add 2 µl from row A of the drug dilution plate to rows B, C, and D of the cell culture plates, creating triplicates for each compound in row A of the compound library (Fig. 1). Add 2 µl from row B of the drug dilution plate to rows E, F, and G of the cell culture plates, creating triplicates for each compound in row B of the compound library. Repeat for rows C–H in other culture plates (see Note 5). Incubate at 37°C for 24 h.

3.1.2. In-Cell Western Assay (Per Four Plates)

1. Prepare fresh 3.7% fixing solution by adding 5 ml of 37% formaldehyde to 45 ml of PBS.
2. Remove media from the cells using a multichannel vacuum manifold. Wash three times with 1× PBS.
3. Immediately and carefully add 150 µl of fixing solution by pipetting down the side of the wells to avoid detaching the cells. Incubate for 20 min at room temperature (RT) with no shaking.
4. Prepare Triton washing solution by adding 5 ml of 10% Triton X-100 into 495 ml of PBS.
5. Remove the fixing solution from cells using a multichannel vacuum manifold.
6. Wash cells with 200 µl of Triton washing solution for 5 min, with gentle shaking on a rotary shaker to permeabilize the cells. Repeat wash step three more times (see Note 4). Do not allow cells to dry out.

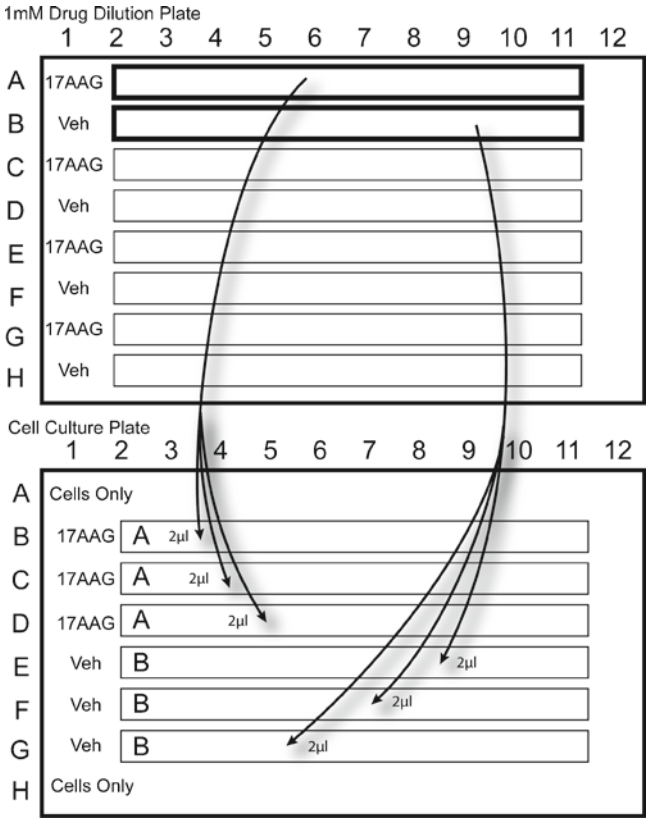

Fig. 1. Procedure for diluting drugs from a 1 mM stock drug dilution plate directly into cell culture plates. In a standard 96-well assay plate, prepare 1 mM compound stocks from one plate of a commercially available library by diluting in Opti-MEM. As a positive control, prepare a 100 μM stock of the Hsp90 inhibitor, 17-(Allylamino)-17-demethoxygeldanamycin (17-AAG). A vehicle control (Veh) of DMSO should also be prepared using a volume equivalent to the highest concentration of drug. Most libraries come with the first and last columns empty to add controls. Add the 17-AAG stock to wells A, C, E, and G to the first column; add vehicle to wells B, D, F, and H of the first column. Using a multichannel pipetter, add 2 μl from row A of the drug dilution plate to rows B, C, and D of the cell culture plates, creating triplicates for each compound in row A of the compound library. Add 2 μl from row B of the drug dilution plate to rows E, F, and G of the cell culture plates, creating triplicates for each compound in row B of the compound library. Repeat for rows C–H in other culture plates.

7. Remove the Triton Washing Solution using an automated plate washer.
8. Carefully, add 150 μl of Odyssey blocking buffer down the side of the wells into each well. Incubate at RT for 1.5 h with gentle shaking on a rotary shaker.
9. Dilute mouse anti-GAPDH at 1:1,000 and rabbit antitau at 1:1,000 in primary dilution buffer (8 ml of blocking buffer and 8 ml of PBS + 0.2% Tween-20). Remove the blocking buffer from the cell-containing wells using vacuum, and add

50 µl of this antibody mixture to rows B–G of all plates (see Note 6).

10. Add 50 µl of Odyssey blocking buffer to the top row of empty wells to control for evaporation due to overnight incubation.
11. Cover the plates and incubate overnight at 4°C with no shaking.
12. Prepare Tween washing solution by adding 1 ml 20% Tween-20 to 999 ml of PBS.
13. Wash the plates five times, incubating for 5 min between each wash at RT with gentle shaking on a rotator.
14. Dilute goat antirabbit Alexa Fluor 680 (1:500 dilution) and Goat/sheep antimouse IRDye 800CW (1:500 dilution) in secondary dilution buffer (10 ml of blocking buffer and 10 ml of 1× PBS + 0.4% Tween-20). Preparations should be made for low-light applications from this point forward.
15. Add 50 µl of this secondary antibody solution to all 96 wells of each of the four plates, wrap the plates with aluminum foil or store in black box to protect from light.
16. Incubate at RT for 60 min with gentle rotational shaking.
17. Wash the plates five times, incubating for 5 min between each wash at RT with gentle shaking on a rotator. Protect from light by wrapping the plate with aluminum foil.
18. Perform one final wash with 1× PBS without any detergent.
19. After this final wash, plates can be gently blotted dry using a Kimwipe or sterile towel.
20. Wipe the bottom plate surface and Odyssey imager scanning bed with lint-free paper. Scan plate immediately or wrap the plate with aluminum foil and store at 4°C for several weeks. Plates can also be stored long term at –20°C, although some signal intensity will be lost.
21. Adjust the settings of Odyssey Imager: use medium quality, 169 µm resolution, 3.0 mm focus offset, and intensity settings of five for both 700 nm and 800 nm channel. Start scanning simultaneously at 700 nm and 800 nm. These intensity settings may vary; however, plates can be scanned multiple times without consequence (see Note 7).
22. Once scanned, refer to the Odyssey application software manual for detailed methodology regarding data analysis (see Notes 8 and 9).
23. Figure 2 provides a detailed flow diagram for this procedure.

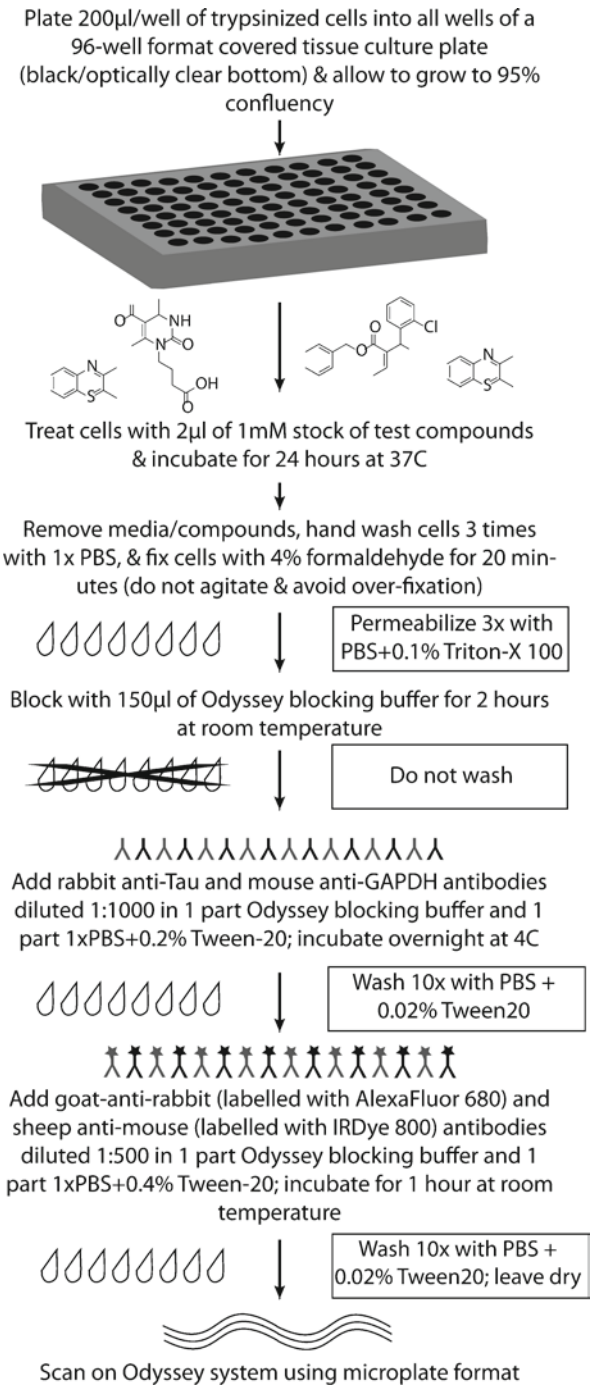

Fig. 2. Flow diagram of the In-Cell Western procedure. This diagram provides the minimal basics for the In-Cell Western procedure in a schematic single-page format.

3.2. Western Validation of Hits

3.2.1. Cell Culture and Treatment

1. Maintain H4 cells in complete media.
2. Remove media from the flask containing 95% confluent cells and add 5 ml of trypsin-EDTA to the flask and incubate for 2–5 min in the 37°C incubator.
3. Dispense 0.5 ml of suspended cells into a 15 ml conical tube and add 12 ml of complete media. Mix by tituration. Dispense 2 ml of cells into each well of a 6-well plate. Repeat two more times.
4. Incubate cells at 37°C in 5% CO_2 until 95% confluency is reached.
5. Prepare dilutions of the two hits and the toxic compound. Use the following concentrations: 10, 3, 1, 0.3, and 0 μM. Prepare each of these in 2 ml of Opti-MEM. Thus, there should be 15 tubes with 2 ml drug suspensions (see Note 10).
6. Remove complete media from cells and replace with these drug suspensions, one tube per well. Incubate cells at 37°C in 5% CO_2 for 24 h.

3.2.2. Cell Lysis

1. Remove media from the wells by vacuum aspiration and rinse cells gently with 1 ml of PBS.
2. Add 50 μl of Lysis buffer in the well and scrape cells using a cell lifter.
3. Transfer the lysed cells into 1.5 ml tubes and pulse sonicate for 30 s at 4°C.
4. Centrifuge at 13,500 × *g* for 10 min at 4°C and transfer supernatant into a new 1.5 ml tube. Discard pellet.
5. Perform BCA protein assay or store supernatant at –20°C.

3.2.3. Protein Estimation

1. Use a clear 96-well plate to do protein estimation.
2. Prepare BCA reagent by diluting Reagent B 1:50 in reagent A (e.g., add 200 μl of reagent B in to 9.8 ml of Reagent A.) BSA is provided as a standard protein to establish a standard curve.
3. All standards, samples and blanks should be run in triplicate.
4. The standard curve should be as follows for cell culture studies: dilute a 1 mg/ml stock of BSA with water to final concentrations of 1, 2, 5, 10, 15, 20, and 25 μg/ml. 25 μl water as a blank control should also be included for normalization.
5. 1 μl of each sample should then be added to other wells containing 24 μl of water.
6. Add 175 μl of BCA reagent to each well, mix by gentle rotation and incubate for 30 min at 37°C.
7. Measure optical density at 562 nm using a visible light spectrophotometer and use these values to generate a standard curve and determine protein concentrations.

3.2.4. Western Blotting with the Odyssey System

1. To investigate total tau levels by Western blot, a high amount of protein is typically required. Therefore, prepare 50 μg of total protein from H4 lysates and mix with equal volumes of 2× Laemmli sample buffer containing β-mercaptoethanol.
2. Heat denature these samples at 95°C for 10 min.
3. Centrifuge at 16,000 × *g* for 1 min at RT.
4. Load either the first or sixth lane of a 12-well 10% SDS-PAGE gel with a molecular weight ladder containing at least three standards in the 65–35 kDa range.
5. Load the samples in order from highest drug concentration to lowest drug concentration. Group samples by specific treatments, not concentrations. For example 10, 3, 1, 0.3, and 0 μM for Hit 1, followed by 10, 3, 1, 0.3, and 0 μM for the toxic hit.
6. Run the gel and transfer per standard procedures. The only caveat for running an Odyssey Western blot is to use PVDF-FL from Millipore in lieu of other membrane materials (see Note 11).
7. Following transfer, place the membrane in a square petri dish and block the membrane with Odyssey blocking buffer for 2 h at RT.
8. Dilute mouse anti-GAPDH at 1:5,000 and rabbit antitau at 1:5,000 in primary dilution buffer (5 ml of blocking buffer and 5 ml of PBS + 0.2% Tween-20). Decant the blocking buffer from the membrane and add the antibody mixture. Wrap with foil and incubate overnight at 4°C on a platform rocker.
9. Remove antibody mixture and wash the membrane with PBST (PBS with 0.2% Tween-20) for 10 min, repeating three times.
10. Dilute goat antirabbit Alexa Fluor 680 (1:1,000 dilution) and Goat/sheep antimouse IRDye 800CW (1:1,000 dilution) in secondary dilution buffer (5 ml of blocking buffer and 5 ml of 1× PBS + 0.4% Tween-20).
11. Decant wash buffer and add the secondary antibody mixture. Preparations should be made for low-light applications from this point forward (i.e., cover dish with foil).
12. Remove antibody mixture and wash the membrane with PBST for 10 min, repeating three times.
13. Remove PBST and replace with 1× PBS. Membrane can be scanned immediately or stored at 4°C for later (see Notes 12–17).

4. Notes

1. The most important note for this assay is the adherence to the reagents and supplies specified. In particular, it is important to use PBS and not TBS.
2. It is important to test the properties of your cell line with regard to adherence. We have utilized a number of cell lines and some work well while others do not. H4, CHO, and HeLa seem to be the most suitable for this assay.
3. Plate selection is important. The optically clear plates work great, but they are costly. Some plastics have less autofluorescence than others. These can be tested if the cost becomes prohibitive.
4. Automation is a central key for the reproducibility of this assay. Multichannel pipetters, plate washers, etc., where possible, dramatically improves the results.
5. It is essential that only the inner 60 wells of the tissue culture plate be used for your test samples, but that the outer wells contain cells and media.
6. The near-infrared channel corresponding to 800 nm/green fluorescence exhibits slightly lower intensity than the 680 nm/red channel. Thus, our loading control, GAPDH, was always used with the 800 nm dye.
7. Saturation is a problem with the fluorescent detection of the Odyssey system. When antibody concentrations are too high, saturation will occur, which manifests as a white signal. The scanning intensity can be adjusted before the scan, reducing this phenomenon; however, it may require that the entire experiment be rerun if it cannot be corrected. Therefore, it is very important that antibodies be titrated carefully to avoid this problem at the end of a large experiment.
8. Once the data has been collected from the In-Cell Western assay, we must begin the process of validating whether these compounds directly affect tau biology. We have summarized an example of results in Fig. 3a. One main concern with this type of assay is controlling for toxicity. By using GAPDH as one of our proteins, its levels can be used to estimate this. If GAPDH levels are significantly decreased, irrespective of tau levels, it suggests to us that this agent is simply killing cells (Fig. 3a). In this same assay, we considered two compounds to be "hits" because they appear to reduced tau (red) without reducing GAPDH (green). The overlay of the screen shows this contrast more clearly (yellow). These would be the best lead molecules for further testing. We also have internal

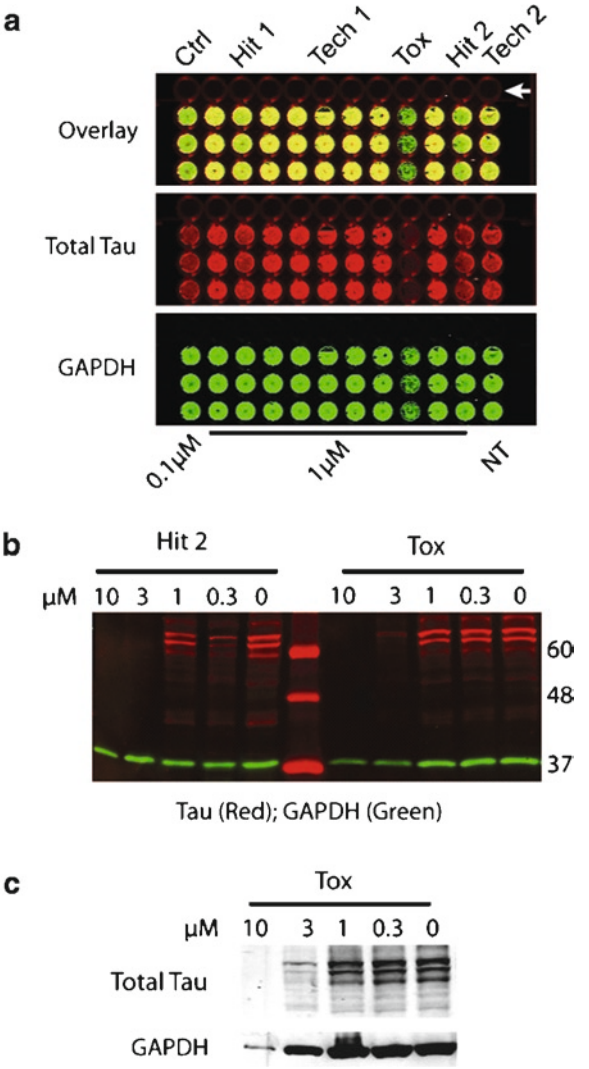

Fig. 3. Tau and GAPDH levels from drug-treated H4 cells following In-Cell and Odyssey Western analysis. (**a**) Images for one row of compounds run in triplicate with 17-AAG as a control (column 1, *indicated as Ctrl*) and untreated controls (column 12, indicated as Tech 2 at *top* and NT at *bottom*). Total tau is shown in *red*, GAPDH in *green*, and the overlay in *yellow*. The *white arrow* indicates *row A* of the plate showing no signal despite the presence of cells. This controls for autofluorescence. Presumptively effective drugs are designated as Hit 1 and Hit 2, showing reduced *red fluorescence* (Tau) with minimal loss of *green fluorescence* (GAPDH). Tox indicates that a toxic effect was observed, where GAPDH and Tau levels were both reduced. Tech1 demonstrates a common technical problem associated with cell adhesion. Tech2 demonstrates a common technical problem with nonuniform fluorescence across plates, particularly in the outer wells. (**b**) Dose response to Hit 2 and Tox as determined by standard Odyssey Western analysis. *Green bands* indicate GAPDH signal; *red bands* indicate Total tau signal. The molecular weight ladder in the *Sixth lane* fluoresces *red* and molecular weights are indicated on the *right*. (**c**) Dose response to Tox by Western blot using chemiluminscent detection.

validation within each plate because of the use of 17AAG as a positive control (Ctrl; Fig. 3a). Our vehicle control was in the bottom half of the plate (not shown). Now that we have hits to analyze, the next step in the process will be concentration optimization and validation by Western blot.

9. Figure 3a also illustrates two important technical challenges with the In-Cell Western; cell adhesion and signal distribution across plates. These are indicated as Tech 1 and Tech 2. Tech 1 shows that even extremely hearty cells like H4 can become detached during the In-Cell Western process despite fastidious care being taken. Thus, other less adherent cell lines can pose significant problems for assay development. Tech 2 shows perhaps the most difficult challenge with these assays; that being the growth kinetics of cells across 96-well plates. Gas exchange and heat properties vary for the outer wells relative to the inner core of 60 wells in a 96-well plate. While we have not been able to prevent this, we have adapted to the problem. For every assay, we include a control plate with no treatment across wells. Following the In-Cell Western protocol, we can then use this control plate as a normalization template for the growth dynamics of cells in that given run.

10. Toxicity with any compound is a concern for cell culture. Prior to preparing the samples and performing the Odyssey Western, toxicity assessment can be performed on the supernatant from cells 4 h after drug treatment using a CytoTox LDH analysis kit.
11. Always use the PVDF-FL membrane for Odyssey Westerns. This particular polymer has been specially designed to demonstrate extremely low autofluorescence.
12. Remove air bubbles between the membrane and scanning surface prior to scanning.
13. Use flat forceps to move membrane, particularly when applying the membrane to the scanning surface; never touch membrane with bare hands.
14. If signals are intense, there may be “bleed through” of the 800 nm signal with the 680 nm laser such that green signal shows up as a red signal, or vice versa. This can be titrated out using the appropriate concentration of antibody. This is particularly important if the proteins being investigated have a similar molecular weight.
15. If signals are too intense, wash the membrane with PBS containing up to 0.5% Tween-20 for 1 h and scan again.
16. If signals are not clear, reimmerse the membrane in methanol, wash with 1× PBS, and reapply a second round of secondary

antibodies at higher concentrations while reducing the stringency of the dilution buffer.

17. Tau biochemical analyses by Western blot can also be a challenge, and understanding these nuances is critical for interpretation of results. By Western blot, tau manifests not as a single band, but as multiple bands anywhere between 70 and 30 kDa. This can make analysis of tau Western blots difficult; however, a large amount of effort has been taken to understand why these bands emerge, and we will clarify some of those reasons here. First, tau is alternatively spliced into six isoforms (4). In cell culture, the species predominantly produced lack exon 10, leaving three primary isoforms ranging from 65 to 50 kDa (5). Some treatments may influence splicing factors that could change this pattern, allowing the other three isoforms to emerge. Tau is also heavily modified post-translationally. Each isoform can be differentially phosphorylated at any number of its >20 phosphorylation sites (6), dramatically altering its migration through a gel. It can be nitrated (7), glycosylated (8) and ubiquitinated (9). Tau can also be cleaved by proteases to produce smaller fragments that can range anywhere between 40 and 17 kDa (10). Therefore, it is critical to try and develop a mechanistic model for each test compound based on its known mechanism of action, which will help direct future experimental design.

Acknowledgments

This work was supported by the Alzheimer's Association and the NIA K99/R00AG031291.

References

1. Dickey, C. A., Eriksen, J., Kamal, A., Burrows, F., Kasibhatla, S., Eckman, C. B., Hutton, M., and Petrucelli, L. (2005) Development of a high throughput drug screening assay for the detection of changes in tau levels – proof of concept with HSP90 inhibitors. *Curr Alzheimer Res* **2**, 231–8.
2. Dickey, C. A., Ash, P., Klosak, N., Lee, W. C., Petrucelli, L., Hutton, M., and Eckman, C. B. (2006) Pharmacologic reductions of total tau levels; implications for the role of microtubule dynamics in regulating tau expression. *Mol Neurodegener* **1**, 6.
3. Dickey, C. A., Dunmore, J., Lu, B., Wang, J. W., Lee, W. C., Kamal, A., Burrows, F., Eckman, C., Hutton, M., and Petrucelli, L. (2006) HSP induction mediates selective clearance of tau phosphorylated at proline-directed Ser/Thr sites but not KXGS (MARK) sites. *Faseb J* **20**, 753–5.
4. Goedert, M., Spillantini, M. G., Jakes, R., Rutherford, D., and Crowther, R. A. (1989) Multiple isoforms of human microtubule-associated protein tau: sequences and localization in neurofibrillary tangles of Alzheimer's disease. *Neuron* **3**, 519–26.
5. Ko, L. W., DeTure, M., Sahara, N., Chihab, R., and Yen, S. H. (2002) Cellular models for tau filament assembly. *J Mol Neurosci* **19**, 311–6.
6. Mandelkow, E. M., Biernat, J., Drewes, G., Gustke, N., Trinczek, B., and Mandelkow, E. (1995) Tau domains, phosphorylation, and

interactions with microtubules. *Neurobiol Aging* **16**, 355–62; discussion 62–3.

7. Reynolds, M. R., Berry, R. W., and Binder, L. I. (2005) Site-specific nitration differentially influences tau assembly in vitro. *Biochemistry* **44**, 13997–4009.
8. Arnold, C. S., Johnson, G. V., Cole, R. N., Dong, D. L., Lee, M., and Hart, G. W. (1996) The microtubule-associated protein tau is extensively modified with O-linked N-acetylglucosamine. *J Biol Chem* **271**, 28741–4.
9. Dickey, C. A., Yue, M., Lin, W. L., Dickson, D. W., Dunmore, J. H., Lee, W. C., Zehr, C., West, G., Cao, S., Clark, A. M., Caldwell, G. A., Caldwell, K. A., Eckman, C., Patterson, C., Hutton, M., and Petrucelli, L. (2006) Deletion of the ubiquitin ligase CHIP leads to the accumulation, but not the aggregation, of both endogenous phospho- and caspase-3-cleaved tau species. *J Neurosci* **26**, 6985–96.
10. Gamblin, T. C., Chen, F., Zambrano, A., Abraha, A., Lagalwar, S., Guillozet, A. L., Lu, M., Fu, Y., Garcia-Sierra, F., LaPointe, N., Miller, R., Berry, R. W., Binder, L. I., and Cryns, V. L. (2003) Caspase cleavage of tau: linking amyloid and neurofibrillary tangles in Alzheimer's disease. *Proc Natl Acad Sci U S A* **100**, 10032–7.

Chapter 1

Contemporary Approaches to Alzheimer's Disease and Frontotemporal Dementia

Erik D. Roberson

Abstract

Alzheimer's disease and frontotemporal dementia are two of the most common neurodegenerative dementias. Here, we review the clinical presentation, genetic causes, typical neuropathology, and current treatments for these disorders. We then review molecules involved in their pathogenesis and protocols for working with these species and conclude with a discussion of experimental systems and outcome measures for studying these disorders.

Key words: Dementia, Mild cognitive impairment, Memory, Personality change, Disinhibition, Aging, Methods, Protocols, Aβ, β-Amyloid, Tau, Apolipoprotein E, Progranulin, TDP-43

1. Alzheimer's Disease

Alzheimer's disease (AD) is the most common neurodegenerative disease. Age is the strongest risk factor, and advances in health care that enable more people to live into their 80s and 90s have led to a steady increase in the incidence of AD (1).

Memory impairment is the earliest and most prominent symptom of AD. The typical patient might first notice mild problems with episodic memory, such as repeating themselves in conversation or forgetting recent events. Initially, the symptoms do not cause significant functional impairment, and at this stage the patient is considered to have amnestic mild cognitive impairment (aMCI). As the disease and symptoms worsen, functional impairment in daily activities becomes manifest, such as with problems balancing the checkbook, preparing meals, or managing medications. At this point, unless another likely cause is identified, the patient meets criteria for a clinical diagnosis of probable AD.

Erik D. Roberson (ed.), *Alzheimer's Disease and Frontotemporal Dementia*, Methods in Molecular Biology, vol. 670,
DOI 10.1007/978-1-60761-744-0_1,

The disease is inexorably progressive and fatal, with median survival about 12 years from onset of symptoms (2). Definite diagnosis is made neuropathologically, based on the presence of the pathological hallmarks of AD: amyloid plaques and neurofibrillary tangles.

Three genes have been identified as causes of rare, autosomal dominant, early onset AD. *APP*, encoding amyloid precursor protein, was the first to be identified (3), followed by *PSEN1* and *PSEN2*, encoding presenilin 1 and 2 (4–6). All three genes are involved in the production of amyloid-β peptide (Aβ). APP is the precursor protein from which Aβ is generated, and the presenilins are components of the γ-secretase enzyme complex that cleaves Aβ from APP (7, 8).

Current treatments for AD have only modest benefits (9). Around the time of diagnosis, one of three widely available cholinesterase inhibitors is often used to boost cholinergic function. In the middle stages of the disease, these agents are often paired with memantine, which prevents overstimulation of NMDA-type glutamate receptors. Many other agents specifically targeting the molecular processes involved in pathogenesis (and developed using some of the techniques described in his volume) are currently in clinical trials, and there is hope that some of these agents will provide more dramatic therapeutic benefit (10).

2. Frontotemporal Dementia

Frontotemporal dementia (FTD) is a term variably used to refer either to a specific clinical syndrome (more specifically called "behavioral variant FTD" or bvFTD) or to a family of neurodegenerative conditions that includes bvFTD and several related disorders (a group also called "frontotemporal lobar degeneration" or FTLD) (11, 12).

The clinical disorders falling under the umbrella of FTLD include bvFTD, semantic dementia, progressive nonfluent aphasia, and FTD with motor neuron disease (FTD-MND) (13). The bvFTD is characterized by personality changes and loss of insight, emotion, and social interactions (14). In semantic dementia, patients develop a fluent aphasia with loss of semantic knowledge about objects (15). Patients with progressive nonfluent aphasia exhibit progressive deterioration in expressive language with agrammatic, effortful speech (16). FTD-MND produces a combination of behavioral symptoms and frontal executive dysfunction in combination with weakness due to motor neuron degeneration (17).

Just as the clinical syndromes associated with FTD are more diverse than in AD, the neuropathology of FTD is also more complex (18). About half of the cases have some form of

tau-positive inclusions, while most of the others have inclusions composed of ubiquitinated TAR DNA-binding protein of 43 kDa (TDP-43). A small percentage have inclusions of the "fused in sarcoma" (FUS) gene product (19).

Families in which FTD is inherited in an autosomal dominant manner have also provided important clues to the molecular pathogenesis of the disease (20). Roughly 5% of all FTD cases are due to mutations in the *MAPT* gene encoding tau; all of these cases have tau pathology (21–24). Roughly 5% of FTD cases harbor mutation in the *GRN* gene encoding progranulin (25–27); these cases display TDP-43 pathology (28). Other, much less common genetic causes of FTD include mutations in *CHMP2B* (29, 30) or *VCP* (31, 32).

There are no FDA-approved treatments for FTD, although selective serotonin reuptake inhibitors are often used (33, 34). The lack of effective treatments for FTD underlines the need for intense research to develop new therapeutic strategies for targeting this disorder.

3. Molecules Involved in AD and FTD

As described in Subheadings 1 and 2, the identification of proteins accumulating in inclusion bodies and of genes causing inherited disease has greatly advanced our understanding of the molecular basis of AD and FTD.

Aβ is a 40- or 42-amino acid fragment of APP, which has normal functions in regulating synaptic transmission (35, 36), but which accumulates to toxic levels in AD. One of the most important properties of Aβ is its ability to aggregate into multimers, including dimers and trimers (37, 38), dodecamers (39), larger oligomers (40), protofibrils, and the long fibrils that compose amyloid plaques. The size of an Aβ aggregate is a critical determinant of its toxicity (41, 42). Unfortunately, the diverse array of possible aggregation states makes working with Aβ very challenging. In Chapter 2, Mary Jo LaDu and colleagues present protocols for preparing synthetic Aβ monomers, oligomers, and fibrils. In Chapter 3, Dominic Walsh, Dennis Selkoe, and colleagues describe purification of small Aβ oligomers (dimers and trimers) from cultured cells and from CSF and brain tissue. In Chapter 4, Sylvain Lesné and colleagues describe the isolation of Aβ*56, a larger oligomer shown to correlate with cognitive deficits in a mouse model of AD (39). In Chapter 5, Justin Legleiter describes protocols for using atomic force microscopy to evaluate the aggregation state of Aβ.

Aβ is not the only important product generated from its precursor, APP. The initial step in the production of Aβ from APP is

the cleavage of the extracellular portion of APP, which generates carboxy-terminal fragments (CTFs). The second step is the cleavage of the CTFs by γ-secretase, which produces Aβ and the APP intracellular domain (AICD). Thus, production of Aβ is coupled to generation of other biologically active species, and independent assays for each of these species can aid in the interpretation of data from experiments in which multiple APP fragments are present. In Chapter 6, Luke Esposito describes a method for quantifying CTFs and for examining different sized Aβ fragments using acid urea gels. And in Chapter 7, Sanjay Pimplikar and colleagues describe a protocol for detecting AICD in cell lysates.

The microtubule-associated protein tau, a component of the cytoskeleton, aggregates into neurofibrillary tangles, the other pathological hallmark of AD (43–46). Tau is also the most common genetic cause of FTD (20) and accumulates in about half of all FTD cases. One important aspect of tau biology is its level of expression; reducing tau expression was shown to be beneficial in mouse models of both AD and FTD (47, 48). In Chapter 8, Chad Dickey et al. describe an in-cell western assay that they have used to screen for regulators of tau expression (49). Another important aspect of tau is its ability to aggregate; in Chapter 9, Gail Johnson and colleagues describe a method they have developed using split GFP technology to quantitatively measure the effect of various agents on tau aggregation (50).

ApoE is the main genetic risk factor for AD; relative to the more common ε3 allele, the more pathologic ε4 allele increases AD risk several-fold (51). ApoE also has an influence on the evolution of FTD (52). As a lipoprotein, the biochemistry of apoE is quite sophisticated. In Chapter 10, Karl Weisgraber and colleagues describe a biochemical purification protocol they have developed to generate different apoE isoforms for use in experiments.

4. Experimental Systems for AD and FTD

A variety of experimental systems can be used to study these diseases. Many questions related to the effects of Aβ can be addressed using primary cultured neurons and a protocol for assessing the toxic effects of Aβ on cultured cells is presented by Adrianna Ferriera and colleagues in Chapter 11. Viral vectors have also proved an important tool for modeling neurodegenerative diseases, and in Chapter 12, Li Gan and colleagues detail a method for using lentivirus in the central nervous system. And of course, mouse models are a mainstay of research on these diseases (53). Given the myriad models available, the choice of which to use in a given situation can be dizzying, and in Chapter 13, Jeannie Chin provides a summary of important features of

major AD models and a discussion of factors to consider in choosing a mouse model.

After choosing a model system, it is important to define outcome measures with which to gauge the severity of impairments and/or the effects of potential treatments. Some, such as determining amyloid plaque burden, are well established. But it has become clear that plaques often are not a reliable indicator of neuronal function (39, 54–60); so other functional methods are increasingly applied. The ultimate functional measure is behavior, and the Morris water maze is a classic test of hippocampus-dependent memory function. Murine neurobehavioral assessment can be intimidating to newcomers in the field, so in Chapter 14, Kimberly Scearce-Levie presents a step-by-step guide to acquiring and analyzing water maze data. In Chapter 15, Jorge Palop and colleagues describe a detailed method for in situ hybridization to quantify and localize gene expression changes in the brain. Axonal transport impairment has been demonstrated in both AD and FTD, as well as in animal models (61); in Chapter 16, Bianxiao Cui and colleagues present a method for real-time evaluation of axonal transport. Recent findings have highlighted the importance of epileptiform activity in AD-related cognitive impairment (62, 63), and in Chapter 17, Jorge Palop et al. outline immunohistochemical biomarkers of this aberrant activity, which correlate well with behavioral impairment. Finally, one of the new frontiers in neurobiology, especially learning and memory, is the role of epigenetics: covalent modifications of DNA and histone proteins (64). There is now early evidence of a role for epigenetic changes in neurodegenerative disease (65, 66), and in Chapter 18, Courtney Miller and colleagues describe how to purify histone proteins and assess epigenetic post-translational modifications.

References

1. Ferri, C. P., Prince, M., Brayne, C., Brodaty, H., Fratiglioni, L., Ganguli, M., Hall, K., Hasegawa, K., Hendrie, H., Huang, Y., Jorm, A., Mathers, C., Menezes, P. R., Rimmer, E., and Scazufca, M. (2005) Global prevalence of dementia: a Delphi consensus study. *Lancet* **366**, 2112–17.
2. Roberson, E. D., Hesse, J. H., Rose, K. D., Slama, H., Johnson, J. K., Yaffe, K., Forman, M. S., Miller, C. A., Trojanowski, J. Q., Kramer, J. H., and Miller, B. L. (2005) Frontotemporal dementia progresses to death faster than Alzheimer disease. *Neurology* **65**, 719–25.
3. Goate, A., Chartier-Harlin, M.-C., Mullan, M., Brown, J., Crawford, F., Fidani, L., Giuffra, L., Haynes, A., Irving, N., James, L., Mant, R., Newton, P., Rooke, K., Roques, P., Talbot, C., Pericak-Vance, M., Roses, A., Williamson, R., Rossor, M., Owen, M., and Hardy, J. (1991) Segregation of a missense mutation in the amyloid precursor protein gene with familial Alzheimer's disease. *Nature* **349**, 704–6.
4. Levy-Lahad, E., Wasco, W., Poorkaj, P., Romano, D. M., Oshima, J., Pettingell, W. H., Yu, C. E., Jondro, P. D., Schmidt, S. D., Wang, K., Crowley, A. C., Fu, Y.-H., Guenette, S. Y., Galas, D., Nemens, E., Wijsman, E. M., Bird, T. D., Schellenberg, G. D., and Tanzi, R. E. (1995) Candidate gene for the chromosome 1 familial Alzheimer's disease locus. *Science* **269**, 973–77.
5. Rogaev, E. I., Sherrington, R., Rogaeva, E. A., Levesque, G., Ikeda, M., Liang, Y., Chi, H.,

Lin, C., Holman, K., Tsuda, T., Mar, L., Sorbi, S., Nacmias, B., Piacentini, S., Amaducci, L., Chumakov, I., Cohen, D., Lannfelt, L., Fraser, P. E., Rommens, J. M., and St George-Hyslop, P. H. (1995) Familial Alzheimer's disease in kindreds with missense mutations in a gene on chromosome 1 related to the Alzheimer's disease type 3 gene. *Nature* **376**, 775–78.

6. Sherrington, R., Rogaev, E. I., Liang, Y., Rogaeva, E. A., Levesque, G., Ikeda, M., Chi, H., Lin, C., Li, G., Holman, K., Tsuda, T., Mar, L., Foncin, J.-F., Bruni, A. C., Montesi, M. P., Sorbi, S., Rainero, I., Pinessi, L., Nee, L., Chumakov, I., Pollen, D., Brookes, A., Sanseau, P., Polinsky, R. J., Wasco, W., Da Silva, H. A. R., Haines, J. L., Pericak-Vance, M. A., Tanzi, R. E., Roses, A. D., Fraser, P. E., Rommens, J. M., and St George-Hyslop, P. H. (1995) Cloning of a gene bearing missense mutations in early-onset familial Alzheimer's disease. *Nature* **375**, 754–60.
7. De Strooper, B., Saftig, P., Craessaerts, K., Vanderstichele, H., Guhde, G., Annaert, W., Von Figura, K., and Van Leuven, F. (1998) Deficiency of presenilin-1 inhibits the normal cleavage of amyloid precursor protein. *Nature* **391**, 387–90.
8. Edbauer, D., Winkler, E., Regula, J. T., Pesold, B., Steiner, H., and Haass, C. (2003) Reconstitution of g-secretase activity. *Nat. Cell Biol.* **5**, 486–8.
9. Farlow, M. R., Miller, M. L., and Pejovic, V. (2008) Treatment options in Alzheimer's disease: maximizing benefit, managing expectations. *Dement. Geriatr. Cogn. Disord.* **25**, 408–22.
10. Roberson, E. D., and Mucke, L. (2006) 100 years and counting: prospects for defeating Alzheimer's disease. *Science* **314**, 781–84.
11. Roberson, E. D. (2006) Frontotemporal dementia. *Curr. Neurol. Neurosci. Rep.* **6**, 481–89.
12. Josephs, K. A. (2008) Frontotemporal dementia and related disorders: deciphering the enigma. *Ann. Neurol.* **64**, 4–14.
13. Kertesz, A. (2009) Clinical features and diagnosis of frontotemporal dementia. *Front. Neurol. Neurosci.* **24**, 140–48.
14. Rascovsky, K., Hodges, J. R., Kipps, C. M., Johnson, J. K., Seeley, W. W., Mendez, M. F., Knopman, D., Kertesz, A., Mesulam, M., Salmon, D. P., Galasko, D., Chow, T. W., Decarli, C., Hillis, A., Josephs, K., Kramer, J. H., Weintraub, S., Grossman, M., Gorno-Tempini, M. L., and Miller, B. M. (2007) Diagnostic criteria for the behavioral variant of frontotemporal dementia (bvFTD): current limitations and future directions. *Alzheimer Dis. Assoc. Disord.* **21**, S14–18.
15. Hodges, J. R., and Patterson, K. (2007) Semantic dementia: a unique clinicopathological syndrome. *Lancet Neurol.* **6**, 1004–14.
16. Ogar, J. M., Dronkers, N. F., Brambati, S. M., Miller, B. L., and Gorno-Tempini, M. L. (2007) Progressive nonfluent aphasia and its characteristic motor speech deficits. *Alzheimer Dis. Assoc. Disord.* **21**, S23–30.
17. Lillo, P., and Hodges, J. R. (2009) Frontotemporal dementia and motor neurone disease: overlapping clinic-pathological disorders. *J. Clin. Neurosci.* **16**, 1131–35.
18. Neumann, M., Tolnay, M., and Mackenzie, I. R. (2009) The molecular basis of frontotemporal dementia. *Expert Rev. Mol. Med.* **11**, e23.
19. Neumann, M., Rademakers, R., Roeber, S., Baker, M., Kretzschmar, H. A., and Mackenzie, I. R. (2009) A new subtype of frontotemporal lobar degeneration with FUS pathology. *Brain* **132**, 2922–31.
20. Seelaar, H., Kamphorst, W., Rosso, S. M., Azmani, A., Masdjedi, R., de Koning, I., Maat-Kievit, J. A., Anar, B., Kaat, L. D., Breedveld, G. J., Dooijes, D., Rozemuller, J. M., Bronner, I. F., Rizzu, P., and van Swieten, J. C. (2008) Distinct genetic forms of frontotemporal dementia. *Neurology* **71**, 1220–26.
21. Hutton, M., Lendon, C. L., Rizzu, P., Baker, M., Froelich, S., Houlden, H., Pickering-Brown, S., Chakraverty, S., Isaacs, A., Grover, A., Hackett, J., Adamson, J., Lincoln, S., Dickson, D., Davies, P., Petersen, R. C., Stevens, M., De Graaff, E., Wauters, E., Van Baren, J., Hillebrand, M., Joosse, M., Kwon, J. M., and Nowotny, P. (1998) Association of missense and 5′-splice-site mutations in tau with the inherited dementia FTDP-17. *Nature* **393**, 702–5.
22. Poorkaj, P., Bird, T. D., Wijsman, E., Nemens, E., Garruto, R. M., Anderson, L., Andreadis, A., Wiederholt, W. C., Raskind, M., and Schellenberg, G. D. (1998) Tau is a candidate gene for chromosome 17 frontotemporal dementia. *Ann. Neurol.* **43**, 815–25.
23. Spillantini, M. G., Murrell, J. R., Goedert, M., Farlow, M. R., Klug, A., and Ghetti, B. (1998) Mutation in the tau gene in familial multiple system tauopathy with presenile dementia. *Proc. Natl. Acad. Sci. U.S.A.* **95**, 7737–41.
24. Clark, L. N., Poorkaj, P., Wszolek, Z., Geschwind, D. H., Nasreddine, Z. S., Miller, B., Li, D., Payami, H., Awert, F., Markopoulou, K., Andreadis, A., D'Souza, I., Lee, V. M. Y., Reed, L., Trojanowski, J. Q., Zhukareva, V., Bird, T., Schellenberg, G., and Wilhelmsen, K. C. (1998) Pathogenic implications of

mutations in the tau gene in pallido-ponto-nigral degeneration and related neurodegenerative disorders linked to chromosome 17. *Proc. Natl. Acad. Sci. U.S.A.* **95**, 13103–7.

25. Baker, M., Mackenzie, I. R., Pickering-Brown, S. M., Gass, J., Rademakers, R., Lindholm, C., Snowden, J., Adamson, J., Sadovnick, A. D., Rollinson, S., Cannon, A., Dwosh, E., Neary, D., Melquist, S., Richardson, A., Dickson, D., Berger, Z., Eriksen, J., Robinson, T., Zehr, C., Dickey, C. A., Crook, R., McGowan, E., Mann, D., Boeve, B., Feldman, H., and Hutton, M. (2006) Mutations in progranulin cause tau-negative frontotemporal dementia linked to chromosome 17. *Nature* **442**, 916–19.
26. Cruts, M., Gijselinck, I., van der Zee, J., Engelborghs, S., Wils, H., Pirici, D., Rademakers, R., Vandenberghe, R., Dermaut, B., Martin, J. J., van Duijn, C., Peeters, K., Sciot, R., Santens, P., De Pooter, T., Mattheijssens, M., Van den Broeck, M., Cuijt, I., Vennekens, K., De Deyn, P. P., Kumar-Singh, S., and Van Broeckhoven, C. (2006) Null mutations in progranulin cause ubiquitin-positive frontotemporal dementia linked to chromosome 17q21. *Nature* **442**, 920–24.
27. Gass, J., Cannon, A., Mackenzie, I. R., Boeve, B., Baker, M., Adamson, J., Crook, R., Melquist, S., Kuntz, K., Petersen, R., Josephs, K., Pickering-Brown, S. M., Graff-Radford, N., Uitti, R., Dickson, D., Wszolek, Z., Gonzalez, J., Beach, T. G., Bigio, E., Johnson, N., Weintraub, S., Mesulam, M., White, C. L., 3rd, Woodruff, B., Caselli, R., Hsiung, G. Y., Feldman, H., Knopman, D., Hutton, M., and Rademakers, R. (2006) Mutations in progranulin are a major cause of ubiquitin-positive frontotemporal lobar degeneration. *Hum. Mol. Genet.* **15**, 2988–3001.
28. Mackenzie, I. R. (2007) The neuropathology and clinical phenotype of FTD with progranulin mutations. *Acta Neuropathol.* **114**, 49–54.
29. Skibinski, G., Parkinson, N. J., Brown, J. M., Chakrabarti, L., Lloyd, S. L., Hummerich, H., Nielsen, J. E., Hodges, J. R., Spillantini, M. G., Thusgaard, T., Brandner, S., Brun, A., Rossor, M. N., Gade, A., Johannsen, P., Sorensen, S. A., Gydesen, S., Fisher, E. M., and Collinge, J. (2005) Mutations in the endosomal ESCRTIII-complex subunit CHMP2B in frontotemporal dementia. *Nat. Genet.* **37**, 806–8.
30. Urwin, H., Ghazi-Noori, S., Collinge, J., and Isaacs, A. (2009) The role of CHMP2B in frontotemporal dementia. *Biochem. Soc. Trans.* **37**, 208–12.
31. Watts, G. D., Wymer, J., Kovach, M. J., Mehta, S. G., Mumm, S., Darvish, D., Pestronk, A., Whyte, M. P., and Kimonis, V. E. (2004) Inclusion body myopathy associated with Paget disease of bone and frontotemporal dementia is caused by mutant valosin-containing protein. *Nat. Genet.* **36**, 377–81.
32. Kimonis, V. E., Fulchiero, E., Vesa, J., and Watts, G. (2008) VCP disease associated with myopathy, Paget disease of bone and frontotemporal dementia: review of a unique disorder. *Biochim. Biophys. Acta* **1782**, 744–48.
33. Vossel, K. A., and Miller, B. L. (2008) New approaches to the treatment of frontotemporal lobar degeneration. *Curr. Opin. Neurol.* **21**, 708–16.
34. Mendez, M. F. (2009) Frontotemporal dementia: therapeutic interventions. *Front. Neurol. Neurosci.* **24**, 168–78.
35. Kamenetz, F., Tomita, T., Hsieh, H., Seabrook, G., Borchelt, D., Iwatsubo, T., Sisodia, S., and Malinow, R. (2003) APP processing and synaptic function. *Neuron* **37**, 925–37.
36. Abramov, E., Dolev, I., Fogel, H., Ciccotosto, G. D., Ruff, E., and Slutsky, I. (2009) Amyloid-β as a positive endogenous regulator of release probability at hippocampal synapses. *Nat. Neurosci.* **12**, 1567–76.
37. Podlisny, M. B., Walsh, D. M., Amarante, P., Ostaszewski, B. L., Stimson, E. R., Maggio, J. E., Teplow, D. B., and Selkoe, D. J. (1998) Oligomerization of endogenous and synthetic amyloid beta-protein at nanomolar levels in cell culture and stabilization of monomer by congo red. *Biochemistry* **37**, 3602–11.
38. Shankar, G. M., Li, S., Mehta, T. H., Garcia-Munoz, A., Shepardson, N. E., Smith, I., Brett, F. M., Farrell, M. A., Rowan, M. J., Lemere, C. A., Regan, C. M., Walsh, D. M., Sabatini, B. L., and Selkoe, D. J. (2008) Amyloid-b protein dimers isolated directly from Alzheimer's brains impair synaptic plasticity and memory. *Nat. Med.* **14**, 837–42.
39. Lesné, S., MT, K., Kotilinek, L., Kayed, R., Glabe, C. G., Yang, A., Gallagher, M., and Ashe, K. H. (2006) A specific amyloid-β protein assembly in the brain impairs memory. *Nature* **440**, 352–57.
40. Lambert, M. P., Barlow, A. K., Chromy, B. A., Edwards, C., Freed, R., Liosatos, M., Morgan, T. E., Rozovsky, I., Trommer, B., Viola, K. L., Wals, P., Zhang, C., Finch, C. E., Krafft, G. A., and Klein, W. L. (1998) Diffusible, nonfibrillar ligands derived from $A\beta_{1-42}$ are potent central nervous system neurotoxins. *Proc. Natl. Acad. Sci. U.S.A.* **95**, 6448–53.
41. Klein, W. L., Krafft, G. A., and Finch, C. E. (2001) Targeting small Ab oligomers: the solution to an Alzheimer's disease conundrum. *Trends Neurosci.* **24**, 219–24.

42. Dahlgren, K. N., Manelli, A. M., Stine, W. B., Jr., Baker, L. K., Krafft, G. A., and LaDu, M. J. (2002) Oligomeric and fibrillar species of amyloid-b peptides differentially affect neuronal viability. *J. Biol. Chem.* **277**, 32046–53.
43. Wood, J. G., Mirra, S. S., Pollock, N. J., and Binder, L. I. (1986) Neurofibrillary tangles of Alzheimer disease share antigenic determinants with the axonal microtubule-associated protein tau (t). *Proc. Natl. Acad. Sci. U.S.A.* **83**, 4040–3.
44. Kosik, K. S., Joachim, C. L., and Selkoe, D. J. (1986) Microtubule-associated protein tau (t) is a major antigenic component of paired helical filaments in Alzheimer disease. *Proc. Natl. Acad. Sci. U.S.A.* **83**, 4044–8.
45. Grundke-Iqbal, I., Iqbal, K., Quinlan, M., Tung, Y. C., Zaidi, M. S., and Wisniewski, H. M. (1986) Microtubule-associated protein tau. A component of Alzheimer paired helical filaments. *J. Biol. Chem.* **261**, 6084–9.
46. Lee, V. M., Balin, B. J., Otvos, L., Jr., and Trojanowski, J. Q. (1991) A68: a major subunit of paired helical filaments and derivatized forms of normal Tau. *Science* **251**, 675–8.
47. SantaCruz, K., Lewis, J., Spires, T., Paulson, J., Kotilinek, L., Ingelsson, M., Guimaraes, A., DeTure, M., Ramsden, M., McGowan, E., Forster, C., Yue, M., Orne, J., Janus, C., Mariash, A., Kuskowski, M., Hyman, B., Hutton, M., and Ashe, K. H. (2005) Tau suppression in a neurodegenerative mouse model improves memory function. *Science* **309**, 476–81.
48. Roberson, E. D., Scearce-Levie, K., Palop, J. J., Yan, F., Cheng, I. H., Wu, T., Gerstein, H., Yu, G.-Q., and Mucke, L. (2007) Reducing endogenous tau ameliorates amyloid b-induced deficits in an Alzheimer's disease mouse model. *Science* **316**, 750–54.
49. Dickey, C. A., Dunmore, J., Lu, B., Wang, J. W., Lee, W. C., Kamal, A., Burrows, F., Eckman, C., Hutton, M., and Petrucelli, L. (2006) HSP induction mediates selective clearance of tau phosphorylated at proline-directed Ser/Thr sites but not KXGS (MARK) sites. *FASEB J.* **20**, 753–55.
50. Chun, W., Waldo, G. S., and Johnson, G. V. (2007) Split GFP complementation assay: a novel approach to quantitatively measure aggregation of tau *in situ*: effects of GSK3β activation and caspase 3 cleavage. *J. Neurochem.* **103**, 2529–39.
51. Farrer, L. A., Cupples, L. A., Haines, J. L., Hyman, B., Kukull, W. A., Mayeux, R., Myers, R. H., Pericak-Vance, M. A., Risch, N., and van Duijn, C. M. (1997) Effects of age, sex, and ethnicity on the association between apolipoprotein E genotype and Alzheimer disease. A meta-analysis. *J. Am. Med. Assoc.* **278**, 1349–56.
52. Agosta, F., Vossel, K. A., Miller, B. L., Migliaccio, R., Bonasera, S. J., Filippi, M., Boxer, A. L., Karydas, A., Possin, K. L., and Gorno-Tempini, M. L. (2009) Apolipoprotein E ε4 is associated with disease-specific effects on brain atrophy in Alzheimer's disease and frontotemporal dementia. *Proc. Natl. Acad. Sci. U.S.A.* **106**, 2018–22.
53. Götz, J., and Ittner, L. M. (2008) Animal models of Alzheimer's disease and frontotemporal dementia. *Nat. Rev. Neurosci.* **9**, 532–44.
54. Holcomb, L., Gordon, M. N., McGowan, E., Yu, X., Benkovic, S., Jantzen, P., Wright, K., Saad, I., Mueller, R., Morgan, D., Sanders, S., Zehr, C., O'Campo, K., Hardy, J., Prada, C. M., Eckman, C., Younkin, S., Hsiao, K., and Duff, K. (1998) Accelerated Alzheimer-type phenotype in transgenic mice carrying both mutant amyloid precursor protein and presenilin 1 transgenes. *Nat. Med.* **4**, 97–100.
55. Westerman, M. A., Cooper-Blacketer, D., Mariash, A., Kotilinek, L., Kawarabayashi, T., Younkin, L. H., Carlson, G. A., Younkin, S. G., and Ashe, K. H. (2002) The relationship between Aβ and memory in the Tg2576 mouse model of Alzheimer's disease. *J. Neurosci.* **22**, 1858–67.
56. Kobayashi, D. T., and Chen, K. S. (2005) Behavioral phenotypes of amyloid-based genetically modified mouse models of Alzheimer's disease. *Genes Brain Behav.* **4**, 173–96.
57. Palop, J. J., Jones, B., Kekonius, L., Chin, J., Yu, G.-Q., Raber, J., Masliah, E., and Mucke, L. (2003) Neuronal depletion of calcium-dependent proteins in the dentate gyrus is tightly linked to Alzheimer's disease-related cognitive deficits. *Proc. Natl. Acad. Sci. U.S.A.* **100**, 9572–77.
58. Arriagada, P. V., Growdon, J. H., Hedley-Whyte, E. T., and Hyman, B. T. (1992) Neurofibrillary tangles but not senile plaques parallel duration and severity of Alzheimer's disease. *Neurology* **42**, 631–39.
59. Ingelsson, M., Fukumoto, H., Newell, K. L., Growdon, J. H., Hedley-Whyte, E. T., Frosch, M. P., Albert, M. S., Hyman, B. T., and Irizarry, M. C. (2004) Early Aβ accumulation and progressive synaptic loss, gliosis, and tangle formation in AD brain. *Neurology* **62**, 925–31.
60. Giannakopoulos, P., Gold, G., Kövari, E., von Gunten, A., Imhof, A., Bouras, C., and Hof, P. R. (2007) Assessing the cognitive impact of Alzheimer disease pathology and vascular burden in the aging brain: the Geneva experience. *Acta Neuropathol.* **113**, 1–12.

61. De Vos, K. J., Grierson, A. J., Ackerley, S., and Miller, C. C. (2008) Role of axonal transport in neurodegenerative diseases. *Annu. Rev. Neurosci.* **31**, 151–73.
62. Palop, J. J., Chin, J., Roberson, E. D., Wang, J., Thwin, M. T., Bien-Ly, N., Yoo, J., Ho, K. O., Yu, G.-Q., Kreitzer, A., Finkbeiner, S., Noebels, J. L., and Mucke, L. (2007) Aberrant excitatory neuronal activity and compensatory remodeling of inhibitory hippocampal circuits in mouse models of Alzheimer's disease. *Neuron* **55**, 697–711.
63. Palop, J. J., and Mucke, L. (2009) Epilepsy and cognitive impairments in Alzheimer disease. *Arch. Neurol.* **66**, 435–40.
64. Levenson, J. M., and Sweatt, J. D. (2005) Epigenetic mechanisms in memory formation. *Nat. Rev. Neurosci.* **6**, 108–18.
65. Ricobaraza, A., Cuadrado-Tejedor, M., Pérez-Mediavilla, A., Frechilla, D., Del Río, J., and García-Osta, A. (2009) Phenylbutyrate ameliorates cognitive deficit and reduces tau pathology in an Alzheimer's disease mouse model. *Neuropsychopharmacology* **34**, 1721–32.
66. Kilgore, M., Miller, C. A., Fass, D. M., Hennig, K. M., Haggarty, S. J., Sweatt, J. D., and Rumbaugh, G. (2010) Inhibitors of class 1 histone deacetylases reverse contextual memory deficits in a mouse model of Alzheimer's disease. *Neuropsychopharmacology* **35**, 870–80.

Chapter 2

Preparing Synthetic Aβ in Different Aggregation States

W. Blaine Stine, Lisa Jungbauer, Chunjiang Yu, and Mary Jo LaDu

Abstract

This chapter outlines protocols that produce homogenous preparations of oligomeric and fibrillar amyloid -β peptide (Aβ). While there are several isoforms of this peptide, the 42 amino acid form is the focus because of its genetic and pathological link to Alzheimer's disease (AD). Past decades of AD research highlight the dependence of Aβ42 function on its structural assembly state. Biochemical, cellular and in vivo studies of Aβ42 usually begin with purified peptide obtained by chemical synthesis or recombinant expression. The initial steps to solubilize and prepare these purified dry peptide stocks are critical to controlling the structural assembly of Aβ. To develop homogenous Aβ42 assemblies, we initially monomerize the peptide, erasing any "structural history" that could seed aggregation, by using a strong solvent. It is this starting material that has allowed us to define and optimize conditions that consistently produce homogenous solutions of soluble oligomeric and fibrillar Aβ42 assemblies. These preparations have been developed and characterized by using atomic force microscopy (AFM) to identify the structurally discrete species formed by Aβ42 under specific solution conditions. These preparations have been used extensively to demonstrate a variety of functional differences between oligomeric and fibrillar Aβ42. We also present a protocol for fluorescently labeling oligomeric Aβ42 that does not affect structure, as measured by AFM, or function, as measured by a cellular uptake assay. These reagents are critical experimental tools that allow for defining specific structure/function connections.

Key words: Amyloid-beta, Oligomer, Fibril, Aggregation, Atomic force microscopy

1. Introduction

Currently, research is focused on soluble oligomeric assemblies of Aβ42 as the proximate cause of the neuropathology that defines AD. Controlling Aβ assembly is critically important as Aβ structure determines its function (Figs. 1 and 2). Numerous experiments have addressed methods to characterize Aβ structure (for review, refs. (1, 2)). These studies demonstrate that peptide conformation and aggregation behavior are highly dependent on initial solvent conditions (Fig. 3) and subsequent solution conditions (Fig. 1a). Oligomer preparations are defined using a variety of different

Erik D. Roberson (ed.), *Alzheimer's Disease and Frontotemporal Dementia*, Methods in Molecular Biology, vol. 670,
DOI 10.1007/978-1-60761-744-0_2,

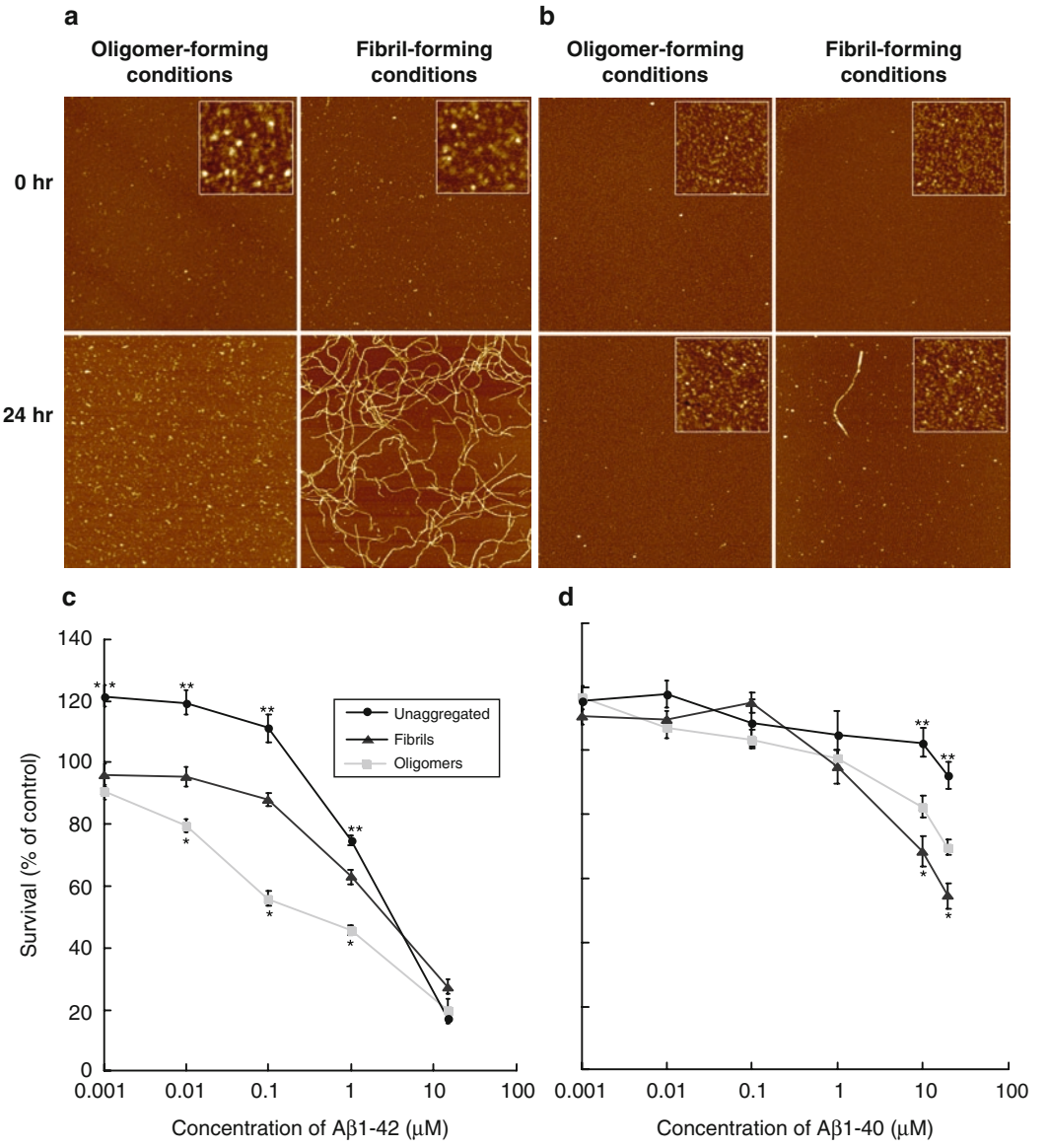

Fig. 1. Structure and neurotoxicity of oligomeric or fibrillar Aβ42 and Aβ40 assemblies. (**a**, **b**) Aβ42, but not Aβ40, forms oligomeric and fibrillar assemblies. 5 mM HFIP-treated Aβ42 (**a**) or Aβ40 (**b**) in DMSO was diluted to 100 μM in ice-cold F-12 culture media for oligomers, or 10 mM HCl for fibrils. Oligomer and fibril preparations were incubated for 24 h at 4°C and 37°C, respectively. Samples before (0 h) and after incubation (24 h) were mounted for AFM analysis at 10 μM. Representative 2 × 2 μm x–y, 10 nm total z-range AFM images. Inset images 200 × 200 nm x–y, 2 nm total z-range. Reprinted from Stine et al., JBC, 2003, with permission from ASBMB. (**c**, **d**) Oligomeric Aβ42, but not Aβ40, reduces neuronal viability significantly more than fibrillar and unaggregated species. Unaggregated, oligomeric, and fibrillar preparations of Aβ42 (**c**) or Aβ40 (**d**) were incubated with N2A cells for 20 h. Oligomeric and fibrillar preparations of Aβ were prepared as described above. For unaggregated peptide preparations, the 5 mM Aβ in DMSO was diluted directly into cell culture media. The MTT assay was used as an indicator of cell viability. Graph represents the mean ± SEM for $n \geq 10$ from triplicate wells from at least three separate experiments using different Aβ preparations. * Significant difference between Aβ assemblies prepared in oligomers and fibrils conditions ($p < 0.001$). ** Significantdifference between unaggregated and both Aβ assemblies prepared oligomers and fibrils conditions ($p < 0.001$). Reprinted from Dahlgren et al., JBC 2002, with permission from ASBMB.

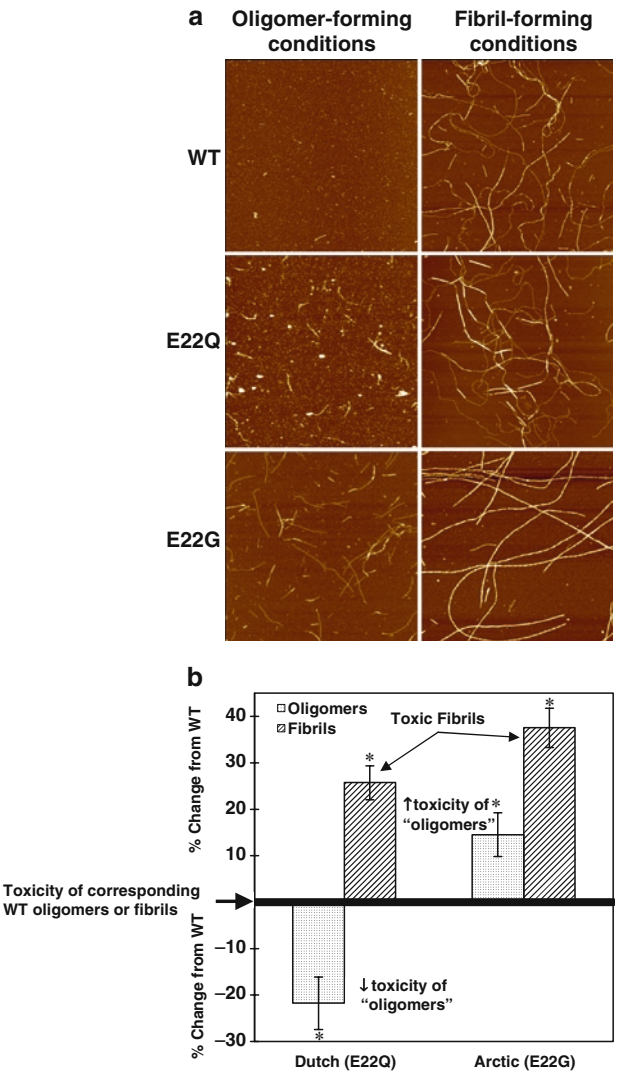

Fig. 2. Structure and neurotoxicity of oligomeric or fibrillar wild type (WT), Dutch (E22Q), and Arctic (E22G) Aβ42. (**a**) Oligomeric and fibrillar preparations of Aβ were prepared as described in Subheadings 3.3 and 3.4 and imaged at 10 μM. Both E22Q and E22G Aβ42 exhibit enhanced fibril formation, even under oligomer-forming conditions. Representative 2×2 μm, 10 nm total z-range AFM images of 100 μM Aβ. Reprinted from Dahlgren et al., JBC, 2002, with permission from ASBMB. (**b**) The "toxic fibrils" formed by E22Q and E22G are significantly more toxic than WT oligomers. Changes to structural assembly states of mutant Aβ42 observed by AFM (above) translate into changes in function as measured by cellular toxicity. N2A cells were treated for 20 h with 0.1 μM of WT Aβ42 oligomers and fibrils, or mutant E22Q Aβ42 or mutant E22G Aβ42 assemblies from oligomer and fibril-forming conditions. MTT assay was used as an indicator of cell viability. The data represent $n \geq 8$ triplicate wells from at least two separate experiments using different Aβ preparations. * Significant difference between oligomers and fibrils ($p < 0.01$). Reprinted with modifications from Dahlgren et al., JBC, 2002, with permission from ASBMB.

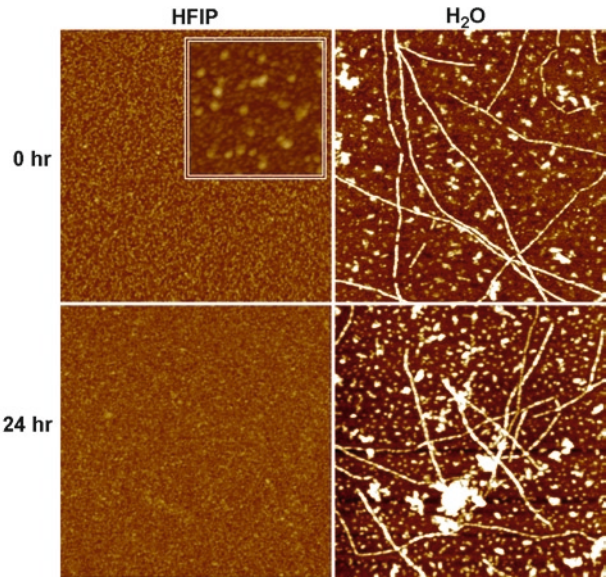

Fig. 3. AFM analysis of Aβ42 solubilized in HFIP and H_2O. Lyophilized synthetic Aβ42 was solubilized to 5 mM in 100% HFIP or deionized H_2O. 5 mM stock solutions were incubated for 24 h at RT. Samples before (0 h) and after incubation (24 h) were mounted for AFM analysis at 10 μM. Representative 1×1 μm x–y, 5 nm total z-range AFM images. Inset image 390×390 nm x–y, 5 nm total z-range. Reprinted with modifications from Stine et al., JBC, 2003, with permission from ASBMB.

methods, including neurotoxic activities, isolation techniques (primarily size exclusion chromatography (SEC)), size estimation such as by SDS or native PAGE, imaging techniques, and reactivity with various Aβ conformation-specific antibodies. These multiple operative definitions of oligomeric Aβ have resulted in a literature that is often difficult to interpret and almost impossible to compare. A rigorous approach is particularly important with Aβ42, which aggregates faster and to a significantly greater extent than Aβ40 and other shorter forms of the peptide (Fig. 1a, b).

AFM is particularly well suited to the analysis of amyloidogenic peptides and proteins that can assemble into a variety of structurally discrete species, specifically those like Aβ. Polydispersity of morphologies and sizes often complicates or precludes the use of other biophysical techniques (such as NMR or light scattering methods), or is masked by solvent incompatibilities of the bulk solution (as for secondary structure detected by far-UV circular dichroism). Techniques based on separation by size (SDS-PAGE, Native PAGE and SEC) may lead to apparent multimers/sizes arising from technical artifacts due to matrix effects. AFM is one of the few techniques that provide direct, high-resolution, 3-dimensional morphological images of the broad range of structures present in a single scan without the need for chemical manipulation of the sample. Numerous studies have demonstrated several

advantages of tapping mode AFM for Aβ42 morphological characterization (3–8). We have used AFM for developing conditions that consistently produce homogenous preparations of oligomeric or fibrillar assemblies of Aβ42 (9, 10). We have used these preparations extensively to demonstrate significant functional differences between Aβ42 oligomers and fibrils using a variety of experimental models (for example, Figs. 1c and 2b) (9, 11–14).

1.1. Overview of Experimental Methods to Prepare and Characterize Defined Aβ Assemblies (Unaggregated, Oligomers, Fibrils, and "Plaques-in-a-Dish")

To directly assess the conformation-dependent differences among Aβ assemblies, we have developed protocols for the preparation of homogeneous unaggregated, oligomeric, and fibrillar Aβ42 (9, 10) (Figs. 1 and 4). Because Aβ42 is the isoform of the peptide most associated with AD, we chose to utilize it almost exclusively, with Aβ40 used occasionally as a negative control (Fig. 1b, d). Using AFM to image Aβ42, we remove preexisting aggregates and β-sheet secondary structure from Aβ42 with a strong fluorinated alcohol, hexafluoroisopropanol (HFIP) (Fig. 3), followed by solubilization of the now monomerized peptide in dimethylsulfoxide (DMSO). Starting with this monomeric peptide preparation, we further developed two aggregation protocols that consistently produce extensively oligomeric or fibrillar populations of Aβ42 (Fig. 1). For the "unaggregated" peptide preparation, the DMSO-solubilized peptide is diluted in the experimental solution (for example, culture media) and used immediately (Fig. 1a, 0 h). To grow a "plaque in a dish," follow the fibril forming procedure, with the addition of salt at physiological concentrations (Fig. 5a2).

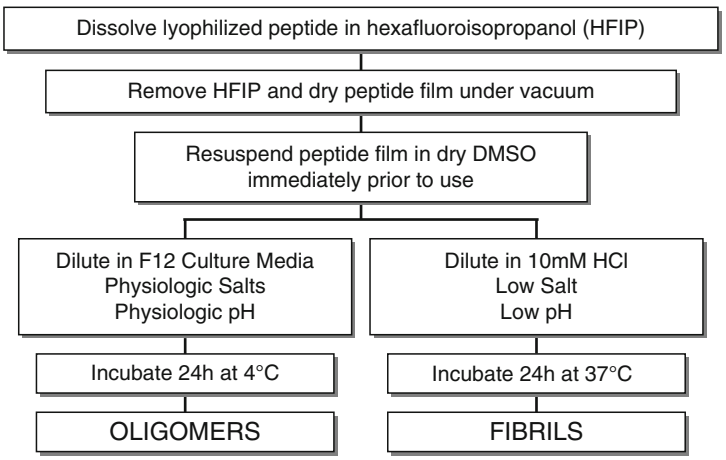

Fig. 4. Schematic diagram summarizing the solubilization and aggregation conditions developed for preparing oligomeric and fibrillar Aβ42. Synthetic Aβ42 is dissolved to 1 mM in 100% HFIP, HFIP is evaporated, and the dry peptide is stored at −20°C. For the aggregation protocols, the peptide is first resuspended in dry DMSO to 5 mM. For oligomeric conditions, F-12 (without phenol red) culture media is added to bring the peptide to a final concentration of 100 μM, and incubated at 4°C for 24 h. For fibrillar conditions, 10 mM HCl is added to bring the peptide to a final concentration of 100 μM, and incubated for 24 h at 37°C. Reprinted from Dahlgren et al., JBC, 2002, with permission from ASBMB.

Note that AFM is an optimal method for determining the aggregation state of Aβ42 as it is difficult to consistently identify Aβ42 assemblies by Western analysis of SDS-PAGE (Fig. 5) (15).

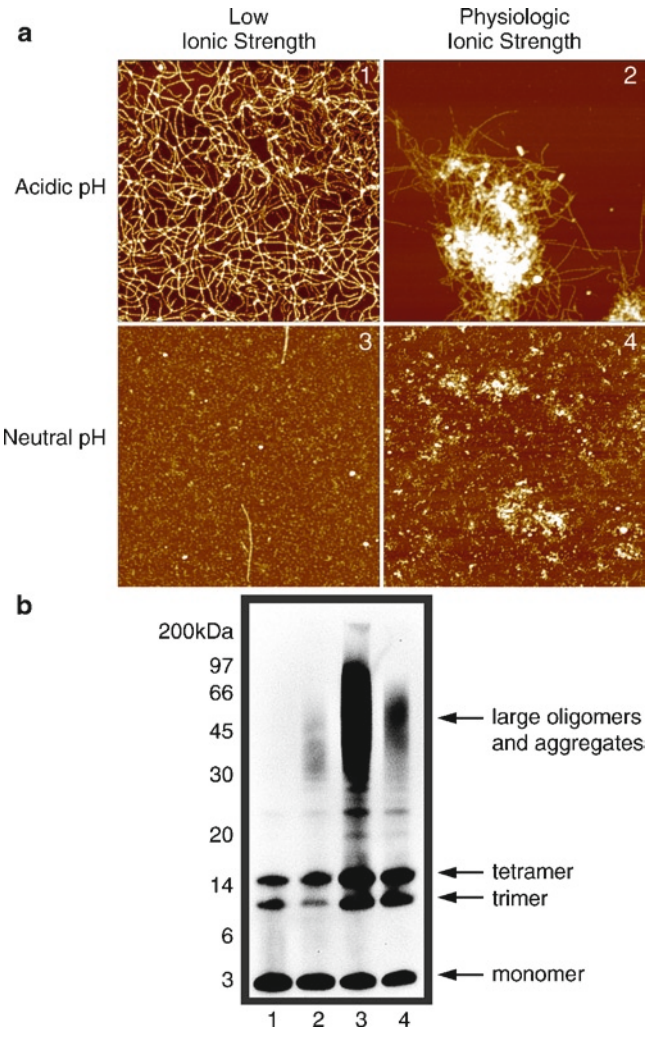

Fig. 5. Diverse Aβ42 assemblies imaged by AFM are not preserved by SDS-PAGE. (**a**) AFM images of Aβ42 fibrils, "plaque in a dish," oligomers, and coalesced oligomers. 5 mM Aβ42 in DMSO was diluted to 100 μM in either 10 mM HCl (1, *acidic pH, low ionic strength*), 10 mM HCl + 150 mM NaCl (2, *acidic pH*, *physiologic ionic strength*), 10 mM Tris, pH 7.4 (3, *neutral pH, low ionic strength*), or 10 mM Tris, and pH 7.4 + 150 mM NaCl (4, *neutral pH*, *physiologic ionic strength*). Samples were prepared after a 2 h incubation at 37°C. Representative 2 × 2 μm x–y, 10 nm total z-range AFM images are shown, except for panel 2, which is scaled to 2 × 2μm x–y, 25 nm total z-range. Reprinted from Stine et al., JBC, 2003, with permission from ASBMB. (**b**) Western analysis of SDS-PAGE does not produce an immunoreactive pattern that correlates with AFM images in Panel A. Representative Western blots of Aβ42 assemblies prepared as described above, separated by SDS-PAGE on a 12% NuPAGE BisTRIS gel and probed with the monoclonal antibody 6E10 (recognizing residues 1–16 of Aβ). Samples were visualized by enhanced chemiluminescence. Lanes numbers correspond to panel numbers in (**a**): HCl (lane 1), HCl + NaCl (lane 2), Tris (lane 3), and Tris + NaCl (lane 4). Reprinted from Stine et al., JBC, 2003, with permission from ASBMB.

These distinct assemblies are derived from chemically identical and structurally homogeneous starting materials and are thus particularly well suited for comparative structure–function studies. We have demonstrated that in vitro, oligomeric Aβ42 is ~10-fold more neurotoxic than the fibrillar (plaque-forming) assembly, and ~40-fold more toxic than the unaggregated peptide, with oligomeric Aβ42-induced toxicity significant at 10 nM (Fig. 1c). Under Aβ42 oligomer- and fibril-forming conditions, Aβ40 remains predominantly as unassembled monomer (Fig. 1b) and had significantly less effect on neuronal viability than preparations of Aβ42 (Fig. 1d). We applied the aggregation protocols developed for wild type (WT) Aβ42 to Aβ42 with the Dutch (E22Q) or Arctic (E22G) mutations (Fig. 2). Oligomeric preparations of the mutant peptides exhibited extensive protofibril and fibril formation, respectively, but were not consistently different from WT Aβ42 in terms of inhibition of neuronal viability. However, fibrillar preparations of the mutants appeared larger in diameter and induced significantly more inhibition of neuronal viability than WT Aβ42 fibril preparations. These data demonstrate that protocols developed to produce oligomeric and fibrillar Aβ42 are useful in distinguishing the structural and functional differences between Aβ42, Aβ40, and Aβ containing known genetic mutations.

1.2. Preparation and Use of Fluorophore-Labeled Aβ42 Assemblies

As researchers become increasingly conscientious of utilizing structurally uniform, well-characterized Aβ preparations, the same criteria need to be applied to fluorophore-labeled-Aβ, prior to their widespread use as experimental tools. Numerous recent studies utilizing fluorophore-labeled Aβ42 peptides demonstrate this need for defined methods of consistently preparing well-characterized fluorescent Aβ assemblies (16–31). The fluorescent Aβ42 reagents used to date are prepared from different sources of Aβ assemblies, in many cases using Aβ42 preparations that have not yet been structurally/morphologically characterized. Thus, structural comparisons between the unlabeled and labeled Aβ assemblies are not possible. Establishing the specific structural form of the assemblies, by AFM and other methods, is necessary to be able to interpret and compare results from the various fluorescent Aβ42 species. We present a method for preparing Alexa Fluor® 488-labeled Aβ oligomers, extending our structural and functional characterization to fluorophore-labeling of Aβ42 oligomers. Structural characterization by AFM establishes a method for labeling uniform oligomeric assemblies that is comparable to unlabeled oligomeric Aβ42 (Fig. 6a). To compare function, we demonstrate that the uptake of labeled and unlabeled oligomeric Aβ42 by neurons in vitro is also similar (Fig. 6b) (see Note 1). These well-characterized fluorophore-Aβ42 oligomers are an exciting new reagent for use in a variety of studies designed to elucidate critical cellular and molecular mechanisms underlying the functions of this Aβ42 assembly form in AD.

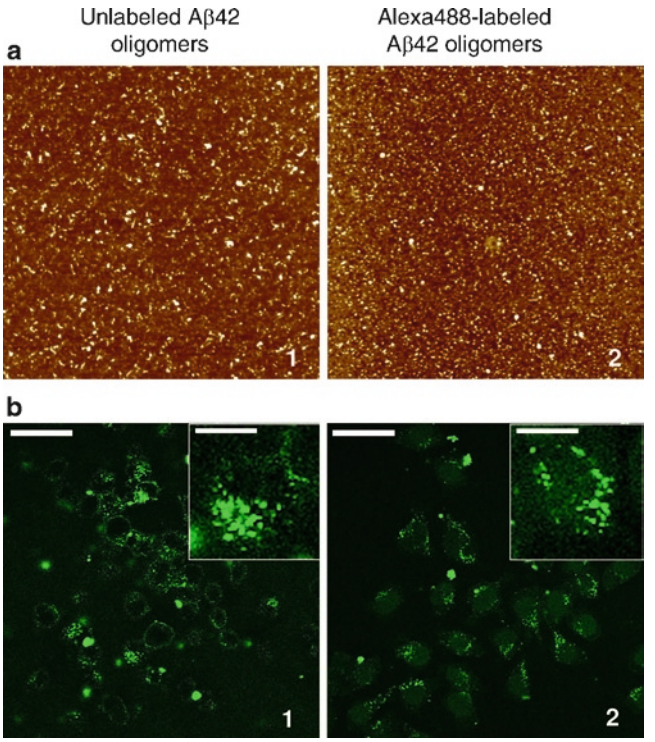

Fig. 6. Structure and neuronal uptake of Alexa Fluor® 488-labeled Aβ42 oligomers compared to unlabeled Aβ42 oligomers. (**a**) AFM analysis shows that oligomer assemblies are preserved after fluorophore-labeling. Aβ42 oligomers were prepared from unlabeled synthetic Aβ42 HFIP films (100 μM, PBS pH 7.4, 4°C) and analyzed by AFM (**a1**). Fluorophore-labeling of the oligomers with Alexa Fluor® 488 was performed using the Microscale Protein Labeling Kit and analyzed by AFM (**a2**). Unlabeled oligomers were diluted to 20 μM for analysis and Alexa-labeled oligomers were analyzed without dilution (estimated concentration of 25 μM). All AFM images shown are 2 × 2 μm x–y, 10 nm total z-range. (**b**) Following uptake, Alexa Fluor® 488-labeled oligomers (**b2**) appear as punctate fluorescence within the cell, similar to immunodetection of unlabeled Aβ42 oligomers (**b1**). Following 16 h treatment, Aβ uptake in N2A cells was analyzed using laser-scanning confocal microscopy. Panel B1 shows the image of cells treated with unlabeled Aβ42 oligomers, immunodetected with anti-Aβ monoclonal antibody 6E10 and Alexa488-rabbit-anti-mouse antibody. Panel B2 shows N2A cells treated for 16 h with 2 μM Alexa Fluor® 488-labeled Aβ42 oligomers. Scale bar = 44 μm. The insets show a single-cell magnification, scale bar = 12 μm. Reprinted from Jungbauer et al., Preparation of fluorescently labeled amyloid-beta peptide assemblies: the effect of fluorophore conjugation on structure and function, J. Mol. Recog., 2009, with permission from Wiley.

2. Materials

2.1. Preparation of HFIP-Treated Aβ Peptide Stocks

1. Chemical fume hood.
2. Synthetic human amyloid-β (1–42), (California Peptide Research, Inc., Napa, CA) (see Note 2).
3. 1,1,1,3,3,3-Hexafluoro-2-Propanol.

4. 2.5 mL glass Hamilton syringe with Teflon plunger and sharp non-coring needle tip (point style 5).
5. Bath sonicator, e.g., benchtop ultrasonic cleaner.
6. Needle, 16–18 gauge.
7. 0.65 mL and 1.7 mL microcentrifuge tubes, untreated (not siliconized).
8. Repeating Pipettor and tips.
9. SpeedVac.
10. Dessicant.
11. Plastic screw-top containers.

2.2. Unaggregated Aβ42 Preparation

1. Dimethylsulfoxide (DMSO) (see Note 3).
2. Ultrapure 18.2 MΩ H_2O.

2.3. Oligomeric Aβ42 Preparation

Ham's F-12, phenol red-free cell culture media, supplemented with 146 mg/L L-Glutamine (see Note 4).

2.4. Fibrillar Aβ42 Preparation

10 mM hydrochloric acid solution (prepared in ultrapure H_2O from a 1 M HCl stock).

2.5. "Plaques in a Dish" Preparation

10 mM HCl containing 150 mM NaCl.

2.6. Fluorophore-Labeled Aβ42 Oligomer Preparation

1. 1× PBS, pH 7.4.
2. Alexa Fluor® 488 TFP Ester Microscale Protein labeling kit (Invitrogen/Molecular Probes).

2.7. Structural Characterization of Aβ42 Preparations

2.7.1. Western Blot Analysis by SDS-PAGE

1. NuPAGE 4–12% BisTris gels, MES running buffer, LDS sample buffer, and Transfer Buffer.
2. Electrophoresis power supply.
3. Molecular weight standards.
4. PVDF membrane.
5. Filter paper packs.
6. Methanol.
7. Tween-20.
8. Tris-buffered saline (TBS): 25 mM Tris-HCl, pH 7.4, 137 mM NaCl, 2.7 mM KCl.
9. Carnation Instant Nonfat dry milk (NFDM).
10. Anti-Aβ antibodies 6E10 and 4G8 (Covance).
11. Rabbit anti-mouse IgG, HRP conjugate.
12. ECL Western blotting substrate.
13. Imaging system to detect chemiluminescence.

2.7.2. Atomic Force Microscopy Structural Analysis

1. Mica sheets (Ted Pella) die-punched into 7/16 in. to ½ in. discs using a punch and die set and mounted on 12 mm stainless steel pucks (Ted Pella) with 2-ton epoxy adhesive.
2. Adhesive tape.
3. Magnetic sample disc holder, sample disc grippers, and cantilever tweezers.
4. 1 M HCl.
5. 0.02 μm syringe filter.
6. 10 mL Luer lock non-siliconized syringe.
7. Ultrapure H_2O.
8. Tetrafluoroethane.
9. Veeco Multimode with NanoScope IIIa controller equipped with a MultiMode head using a Vertical Engage EV piezoceramic scanner.
10. Atomic force microscopy (AFM) probes: Al-coated Si cantilevers (42 N/m spring constant; ~300 kHz resonance frequency; tetrahedral tip with 7 nm radius).
11. NanoScope Software vs. 5.31R1.

2.8. Functional Characterization of Aβ42 Preparations

2.8.1. Neurotoxicity Assay (For Example, Figs. 1c, d and 2b). (See Note 5)

1. Neuro-2a (N2A) mouse neuroblastoma cells.
2. Opaque, white 96-well culture plates.
3. Earle's minimum essential medium (EMEM).
4. Liquid penicillin-streptomycin.
5. 0.05% trypsin solution with EDTA.
6. Fetal bovine serum (FBS).
7. N2 supplement.
8. Unaggregated (Subheading 3.2), oligomeric (Subheading 3.3), or fibrillar (Subheading 3.4) Aβ42.
9. Dulbecco's phosphase-buffered saline (DPBS).
10. CellTiter-Glo® Luminescent Cell Viability Assay (Promega).
11. 96-well luminescence plate reader.

2.8.2. Neuronal Uptake Assay (Fig. 6b)

1. Poly-D-Lysine 8-well culture slides.
2. 16% paraformaldehyde solution.
3. Blocking buffer: DPBS with 50 mM NH_4Cl, 10 mM glycine, 3% BSA.
4. Alexa Fluor® 488 donkey anti-mouse IgG.
5. VectaShield mounting medium for fluorescence.
6. Laser scanning confocal microscope.

3. Methods

3.1. Preparation of HFIP-Treated Aβ Peptide Stocks (Figs. 3 and 4)

Steps 1–7 need to be done in a fume hood.

1. Prepare a 1 mM Aβ solution by adding HFIP directly to the vial containing lyophilized powder through the rubber septum using a 2.5 mL glass Hamilton syringe with a Teflon plunger and sharp (not blunt-end) needle. For Aβ42, add 2.217 mL to 10 mg peptide (see Note 6).
2. After the peptide is completely dissolved, pierce the septum with a syringe needle to release the vacuum (see Note 7).
3. Incubate the Aβ – HFIP solution at room temperature (RT) for at least 30 min (see Note 8).
4. Decap the glass vial (pliers work well) and remove the rubber septum being careful not to allow the HFIP to come in contact with the septum. Have a rack of 0.5 mL or 1.7 mL microcentrifuge tubes ready.
5. Using a positive-displacement repeating pipette, aliquot the solution into 10 μL (0.045 mg for Aβ42) or 100 μL (0.45 mg for Aβ42) aliquots in either 0.5 mL or 1.7 mL microcentrifuge tubes (see Note 9).
6. Allow HFIP to evaporate in the open tubes overnight in the fume hood.
7. Transfer tubes to a SpeedVac and dry down for 1 h without heating to remove any remaining traces of HFIP and moisture.
8. Remove tubes from SpeedVac. The resulting peptide should be a thin clear film at the bottom of the tubes (see Note 10).
9. Store dried peptide films over desiccant in glass jars at −20°C (see Note 11).
10. Prior to use, remove peptide film from −20°C freezer and allow sample to come to RT.
11. Prepare a 5 mM Aβ DMSO stock by adding 20 μL fresh dry DMSO to 0.45 mg Aβ42 peptide (2 μL to 0.045 mg Aβ42). Pipette thoroughly, scraping down the sides of the tube near the bottom to ensure complete resuspension of peptide film (see Note 12).
12. Vortex well (~30 s) and pulse in a microcentrifuge to collect solution at the bottom of the tube (see Note 13).
13. Sonicate 5 mM Aβ DMSO solution for 10 min in a bath sonicator.
14. Use this preparation as the starting material for unaggregated Aβ (Subheading 3.2), oligomeric Aβ (Subheading 3.3), fibrillar Aβ (Subheading 3.4), “plaque in a dish” (Subheading 3.5), or fluorophore-labeled oligomeric Aβ (Subheading 3.6).

3.2. Unaggregated Aβ Preparation (see Note 14)

1. Start with a tube of freshly resuspended 5 mM Aβ42 in DMSO at RT (see Note 15).
2. To this Aβ aliquot, add ice-cold H_2O to a final concentration of 100 μM Aβ.
3. Vortex for 15 s and use immediately.
4. The expected AFM pattern for this preparation is shown in Fig. 1a, upper panels.

3.3. Oligomeric Aβ Preparation

1. Start with a tube of freshly resuspended 5 mM Aβ42 in DMSO at RT (see Note 15).
2. To this Aβ aliquot, add cold phenol-free F-12 cell culture media, diluting to a final concentration of 100 μM Aβ. For example, to 2 μL of 5 mM Aβ in DMSO, add 98 μL cold F-12. Remember to use proper sterile technique. When using F-12 media, avoid prolonged exposure to light and keep F-12 solutions on ice.
3. Vortex for 15 s, transfer to 4°C and incubate for 24 h.
4. The expected AFM pattern for this preparation is shown in Fig. 1a, lower left panel.

3.4. Fibrillar Aβ Preparation

1. Start with a tube of freshly resuspended 5 mM Aβ42 in DMSO at RT (see Note 15).
2. To this Aβ aliquot, add 10 mM HCl at RT, diluting to a final concentration of 100 μM Aβ. For example, to 2 μL of 5 mM Aβ in DMSO, add 98 μL of 10 mM HCl.
3. Vortex for 15 s, transfer to 37°C and incubate for 24 h.
4. The expected AFM pattern for this preparation is shown in Fig. 1a, lower right panel.

3.5. "Plaque in a Dish" Preparation

1. Start with a tube of freshly resuspended 5mM Aβ42 in DMSO at RT (see Note 15).
2. To this Aβ aliquot, add 10 mM HCl + 150 mM NaCl, diluting to a final concentration of 100 μM Aβ.
3. Vortex for 15 s, transfer to 37°C and incubate for 24 h.
4. The expected AFM pattern for this preparation is shown in Fig. 5a, panel 2.

3.6. Fluorophore-Labeled Aβ42 Oligomer Preparation (Fig. 6)

1. Start with a tube of freshly resuspended 5 mM Aβ42 in DMSO at RT (see Note 15).
2. To this Aβ aliquot, add cold 1× PBS buffer, pH 7.4, diluting to a final concentration of 100 μM Aβ.
3. Incubate under oligomer-forming conditions (4°C, 24 h as in Subheading 3.3).
4. Prepare solution for labeling using the Alexa Fluor® 488 Microscale Protein labeling kit (Molecular Probes/Invitrogen)

according to the manufacturer instructions by adding 10% volume of 1 M $NaHCO_3$.

5. Dissolve the provided Alexa Fluor® 488 TFP Ester into 10 μL ultrapure H_2O immediately before adding to Aβ oligomers. Use 8 μL dye for every 100 μL oligomer solution.
6. Incubate the labeling reaction for 15 min in the dark at RT.
7. In the meantime, prepare the spin columns by delivering 425 μL of the kit-provided Bio-Gel P-6 fine resin slurry into the provided spin column tubes. Prepare two spin columns for every 100 μL of oligomers. One minute before the end of the labeling incubation, centrifuge the spin columns at RT for 15 s at 16,000 × *g* per the manufacturer recommendations.
8. Add 55 μL of the crude labeling reaction to the top of the resin and centrifuge for 1 min at 16,000 × *g* to removed unincorporated fluorophore. The leftover crude reaction solution can be analyzed by gel.
9. Store the labeled product at 4°C protected from light. Avoid prolonged storage.

3.7. Structural Characterization of Aβ42 Preparations

3.7.1. Western Analysis by SDS-PAGE (see Note 16)

1. Prepare dilutions of Aβ solutions in LDS sample buffer without reducing agent to deliver 50–200 pmoles Aβ per lane.
2. Perform electrophoresis on NuPAGE 4–12% BisTris gels in 1× MES running buffer until the dye front reaches the bottom of the gel (see Note 17).
3. Prepare the gel for transfer to PVDF membrane in the transfer cassette using filter paper, pads, and membrane pre-equilibrated in chilled 1× transfer buffer containing 10% methanol.
4. Set power supply limits for the transfer for 20–30 min at very low current (such as 15 mA) followed by 25 V, 160 mA for 1 h.
5. After transfer, incubate the membrane in TBST for 5 min.
6. Block for 30–60 min in TBST + 5% NFDM.
7. Perform incubation with primary antibody (1:5,000 dilutions of mouse monoclonal antibody 4G8 (anti-Aβ 17–24) or 6E10 (anti-Aβ 1–16) prepared in TBST + 5% NFDM) overnight at 4°C.
8. Perform 3 × 10 min washes in TBST + 5% NFDM.
9. Incubate in secondary antibody for 1 h at RT (1:10,000 dilutions of rabbit anti-mouse IgG-HRP conjugate).
10. Wash 3 × 10 min in TBST + 5% NFDM.
11. Rinse in TBST.
12. Incubate in ECL substrate for 1 min followed by the immediate detection of chemiluminescence.
13. For representative example of expected results, see Fig. 5b.

3.7.2. Atomic Force Microscopy

1. Fill a 10 mL syringe with ultrapure water and equip with a 0.02 μm filter. Discard the initial 1–2 mL syringe filter output. All subsequent steps use 0.02 μm-filtered water.
2. Prepare samples for spotting on mica by diluting to final concentrations of 10–30 μM in water.
3. Immediately before sample delivery, cleave away the top one to four layers of mica using adhesive tape to reveal a clean, flat, featureless surface.
4. For mica pre-treatment, add ~3 μL (enough to cover the surface) of 1 M HCl to mica for 30 s and rinse with two drops of water by letting water out of the syringe filter roll over the mica, held at a 45° angle on a magnetic surface (see Note 18).
5. Immediately deliver sample onto mica and incubate for 3 min.
6. Rinse with three drops of water and blow dry with several gentle pulses of compressed air.
7. Incubate on benchtop for a few minutes to hours (covered to protect from dust) at RT until analysis (see Note 19).
8. When AFM tip engages, optimize instrument parameters for each scan keeping contact force at a minimum, with scan rates between 1 and 2 Hz, drive amplitude between 20 and100 mV (depending on cantilever), and amplitude set point between 1.4 and 1.5 V.
9. Process data to remove vertical offset between scan lines by applying zero order flattening polynomials using NanoScope Software vs. 5.31R1.
10. For representative examples of expected results, see Figs. 1–3, 5 and 6.

3.8. Functional Characterization of Aβ42 Preparations

3.8.1. Neurotoxicity/ Viability Assay (Figs. 1c, d and 2b) (see Note 5)

Cell Culture

1. Mouse neuroblastoma N2A cells are routinely grown in 100-mm tissue culture dishes containing 10 mL of complete growth medium, consisting of EMEM supplemented with 10% FBS and 1% penicillin/streptomycin. The cells are maintained in a humidified incubator at 37°C with a 5% CO_2 atmosphere.
2. Cells are split such that 0.5×10^6 cells were seeded in a new dish each time the cells reached 80–90% confluency. Briefly, when the cells reach this confluency (approximately once a week), the old growth medium is removed, and DPBS is used to wash cells. 1.5 mL of 0.05% Trypsin-EDTA solution is added to cells, and the dish is returned to the incubator for 2–5 min without disturbance. When cells are detached from the dish, 6 mL of the complete growth medium is added to halt the trypsinization of cells. Cells are collected in a sterile

15 mL conical tube, and pelleted in a clinical centrifuge with the setting of $168 \times g$ for 2 min. The supernatant is decanted and cells are resuspended in 6 mL of complete growth medium. The cell density in a 12 μL aliquot of this cell suspension is counted using a hemocytometer. Based on the counted cell density, an appropriate volume to deliver 0.5×10^6 cells is then added to a new 100 mm dish containing 10 mL of complete growth medium. The dishes are then placed back into the incubator.

Neurotoxicity Assay (see Note 5)

Day 1: Preparing Cells and Aβ

3. Start fresh oligomeric or fibrillar Aβ preparations so that they will be ready to use the next day.
4. Prepare a 96-well plate of N2A cells to be treated. N2A cells from a healthy growing dish are seeded at 5,000 cells/well on an all-white 96-well plate in complete growth medium. An accurate multichannel pipette is ideal to dispense cells. In experimental planning, calculate the minimal number of wells required. For example, within a 96-well plate, we typically perform five to six replicate treatments of the same dose of Aβ assembly (e.g., 10 μM oligomers). Do not use corner wells in the plate as these wells do not have consistent luminescence values. Also include control wells containing medium without cells to measure the background luminescence of the wells. Cells are allowed to grow for 24 h before the start of treatments for the neurotoxicity assay.

Day 2: Cell Treatment

5. Prepare the 96-well plate cultures for treatment. Cells are washed twice with 90 μL of prewarmed plain EMEM medium using a 12-channel pipette. Take care not to touch the well bottom to minimize cell loss during this washing step. 90 μL of fresh EMEM medium supplemented with 1% N2 Supplement is added to each well.
6. Add the appropriate volumes of prepared oligomeric or fibrillar Aβ to the wells being treated according to the desired experimental design (e.g., comparing oligomers versus fibrils at 10 μM Aβ concentration). The final volume of medium is 100 μL. Add the same volume of F-12 or 10 mM HCl + DMSO to other wells to serve as the vehicle control. Cells are returned to the incubator for 24 h.

Day 3: Measuring Toxicity

7. At the end of the 24-h treatment, leave the plate at the bench for 10 min to allow it to equilibrate to RT. The neurotoxicity assay is performed by measuring the cellular ATP value with

CellTiter-Glo® reagent according to the manufacturer's instruction. Briefly, the reagent is thawed to reach RT and an equal volume (100 μL) of the reagent is added directly to the cells. The plate is then gently rotated in an orbital shaker for 10 min. The luminescence intensity is then measured in a luminescent plate reader.

8. To calculate the neurotoxicity, the data set is normalized to the vehicle-treated cells, which is set to 100% for viability, and the relative values of treated cells versus control cells is calculated accordingly.

3.8.2. Neuronal Uptake Assay (Fig. 6b)

1. N2A cells are seeded at 30,000 cells/well on poly-D-lysine coated 8-well culture slides for 8 h in phenol red-free DMEM + 10% FBS.
2. Cells are washed with plain DMEM medium. Alexa Fluor® 488-labeled (1–2 μM) or unlabeled (10 μM) synthetic Aβ42 oligomers are added to cells in the fresh media of DMEM supplemented with 1% N2, and incubated for 2–16 h at 37°C.
3. At the end of the treatment, cells are washed extensively with blocking buffer without BSA, and then fixed in 4% paraformaldehyde for 20 min at RT.
4. Cells treated with unlabeled Aβ42 oligomers are permeabilized with 0.2% Triton X-100 in DPBS for 5 min, and then blocked for 15 min with 3% BSA in the blocking buffer. Cells are then incubated overnight with anti-Aβ(1–16) antibody 6E10 (1:500) at 4°C. After several washes with DPBS, cells are incubated 1 h at RT with Alexa488-labeled donkey anti-mouse IgG (1:500). Cells are further washed several rounds with DPBS. Wells are mounted with VectaShield mounting medium and covered with glass coverslips.
5. Immunofluorescence images are acquired on a laser scanning confocal microscope using a Plan-Apochromate Zeiss 40×/1.3 oil immersion objective. To visualize the 488 nm excited fluorophores from the directly fluorophore-labeled Aβ42 oligomers, or the Alexa488-immunolabeled Aβ42 oligomers, 488 nm laser light (krypton-argon laser), a 488/543 two notch dichroic excitation mirror, and a 505–530 nm bandpass emission filter are used with optimized PMT parameters.

4. Notes

1. Cellular uptake by neurons is reported only for oligomeric Aβ42, as treatment with fibrillar Aβ42 does not result in any detectable uptake in the model described (data not shown).

2. In-house synthetic peptide or peptide from other vendors will also work, but it must be of very high purity and quality. The TFA salt (as opposed to the acetate or ammonium salt) is preferred. In-house material should be accurately weighed in clean glass vials with a HFIP-resistant closure.
3. Dry DMSO stocks can be made by transferring DMSO from a freshly opened ampule to a 1–2 mL glass vial with a DMSO-resistant closure (such as Teflon – VWR, Cat. No. 66009-556). Store vials containing the dry DMSO in a dessicated glass jar in the dark at RT and discard after 2 weeks.
4. The glutamine supplementation is to match the composition of the Biosource phenol red-free F-12 media, which was described in the original oligomer protocol (10) but is no longer available.
5. Originally, we used the 3-[4,5-dimethylthiazol-2-yl]-2,5-diphenyl tetrazolium bromide (MTT) assay (Roche Molecular Biochemicals) as a measure of neurotoxicity (9, 11) (Figs. 1c, d and 2b). This method is based on the reduction of internalized MTT tetrazolium to a colored formazan compound by cellular redox potential. The formazan production is proportional to viable cells in culture. However, MTT reduction does not necessarily reflect cellular metabolic activity, as some Aβ assemblies may also enhance exocytosis of MTT formazan (32). This assay also requires relatively long staining and extraction times. Therefore, we now use the Promega CellTiter-Glo® Luminescent Cell Viability Assay as a measure of in vitro neurotoxicity. This has resulted, as one would predict, in lower toxicity for comparable doses of Aβ, and so higher doses of Aβ42 are now required to achieve the same toxicity (12).
6. HFIP is corrosive and very volatile. Avoid contact and work in the fume hood; take care not to contact septum or other surfaces during solubilization.
7. Peptide comes stored under vacuum, and the peptide in the bottom of the vial needs to be in solution before the vacuum is broken. After the peptide is in solution, pierce the septum with a syringe needle to release the vacuum. For other peptides, add enough HFIP such that the final peptide concentration is 1 mM. Use proper sterile technique to avoid any bacterial contamination when the peptide stocks are resuspended in culture media or buffer.
8. Solution should be clear and colorless. Any trace of yellow color or cloudy suspension indicates poor peptide quality and should not be used. Some peptides may require brief (~5 min) bath sonication.
9. Do not use siliconized tubes for the preparation of HFIP stocks. Be careful when dispensing HFIP solution and watch

for bubbles. Leave tubes open when evaporating HFIP overnight.

10. The peptide should not be white or chunky. An even clear film is a strong indicator of good peptide quality.
11. These stocks should be stable for several months to years.
12. DMSO stock should be clear and colorless. Remember to use proper sterile technique.
13. Do not store peptide as a DMSO stock for more than 1 h to avoid protofibril formation.
14. While the "unaggregated" prep is an ideal control for conformation, it is most useful in assays that require either a very low concentration of peptide (9) or a short incubation period (14). Prolonged incubation at higher concentrations result in the uncontrolled aggregation of the peptide and unpredictable functional activity.
15. Do not keep 5 mM Aβ stock on ice because the DMSO will solidify.
16. Western analysis by SDS-PAGE is not a method for assessing the conformation/assembly of Aβ42 (Fig. 5) (15). However, it is useful for visualizing the relative amount of peptide for comparison between samples.
17. Depending on the age of the electrode/power supply equipment, voltage, and current settings may affect the pattern and abundance of bands typically observed for Aβ (monomer, dimer, trimer, and tetramer). We have found that power supply limits set at 90–100 V, 80 mA for 80–90 min for electrophoresis yield consistent results.
18. For Aβ preparations in F-12, the HCl pretreatment of the mica improves consistent and uniform peptide adsorption to the mica. For Aβ preparations in HCl or PBS, including the Alexa Fluor® 488-labeled oligomers, no mica pretreatment is performed.
19. Dried sample disks can be stored in a helium-purged desiccator for several months.

Acknowledgments

We gratefully acknowledge financial support for these studies from NIH 1F32AG030256-01 (LMJ), Alzheimer's Association NIRG-06-26957 (CY), NIH R01 AG19121 (MJL), NIH PO1AG030128-A2 (MJL), Alzheimer's Association Zenith Award ZEN-08-89900 (MJL), and NIH (NIA) PO1AG021184 (MJL). We also gratefully acknowledge Kevin Laxton and Amy Pham for technical and intellectual contributions.

References

1. Roychaudhuri R, Yang M, Hoshi MM, Teplow DB (2009) Amyloid beta-protein assembly and Alzheimer disease. *The Journal of biological chemistry* **284**, 4749–53.
2. Rahimi, F., Shanmugam, A., and Bitan, G. (2008) Structure-function relationships of pre-fibrillar protein assemblies in Alzheimer's disease and related disorders. *Curr Alzheimer Res* **5**, 319–41.
3. Mastrangelo, I. A., Ahmed, M., Sato, T., Liu, W., Wang, C., Hough, P., and Smith, S. O. (2006) High-resolution atomic force microscopy of soluble Abeta42 oligomers. *J Mol Biol* **358**, 106–19.
4. Huang, T. H., Yang, D. S., Plaskos, N. P., Go, S., Yip, C. M., Fraser, P. E., and Chakrabartty, A. (2000) Structural studies of soluble oligomers of the Alzheimer beta-amyloid peptide. *J Mol Biol* **297**, 73–87.
5. Harper, J. D., Wong, S. S., Lieber, C. M., and Lansbury, P. T. (1997) Observation of metastable Abeta amyloid protofibrils by atomic force microscopy. *Chem Biol* **4**, 119–25.
6. Harper, J. D., Wong, S. S., Lieber, C. M., and Lansbury, P. T., Jr. (1999) Assembly of A beta amyloid protofibrils: an in vitro model for a possible early event in Alzheimer's disease. *Biochem* **38**, 8972–80.
7. Roher, A. E., Chaney, M. O., Kuo, Y. M., Webster, S. D., Stine, W. B., Haverkamp, L. J., Woods, A. S., Cotter, R. J., Tuohy, J. M., Krafft, G. A., Bonnell, B. S., and Emmerling, M. R. (1996) Morphology and toxicity of Abeta-(1-42) dimer derived from neuritic and vascular amyloid deposits of Alzheimer's disease. *J Biol Chem* **271**, 20631–35.
8. Legleiter, J., Czilli, D. L., Gitter, B., DeMattos, R. B., Holtzman, D. M., and Kowalewski, T. (2004) Effect of different anti-Abeta antibodies on Abeta fibrillogenesis as assessed by atomic force microscopy. *J Mol Biol* **335**, 997–1006.
9. Dahlgren, K. N., Manelli, A. M., Stine, W. B., Jr., Baker, L. K., Krafft, G. A., and LaDu, M. J. (2002) Oligomeric and fibrillar species of amyloid-beta peptides differentially affect neuronal viability. *J Biol Chem* **277**, 32046–53.
10. Stine, W. B., Jr., Dahlgren, K. N., Krafft, G. K., and LaDu, M. J. (2003) In vitro characterization of conditions for amyloid-beta peptide oligomerization and fibrillogenesis. *J Biol Chem* **278**, 11612–22.
11. Manelli, A. M., Stine, W. B., Van Eldik, L. J., and LaDu, M. J. (2004) ApoE and Abeta1-42 interactions: effects of isoform and conformation on structure and function. *J Mol Neurosci* **23**, 235–46.
12. Manelli, A. M., Bulfinch, L. C., Sullivan, P. M., and LaDu, M. J. (2007) Abeta42 neurotoxicity in primary co-cultures: effect of apoE isoform and Abeta conformation. *Neurobiol Aging* **28**, 1139–47.
13. White, J. A., Manelli, A. M., Holmberg, K. H., Van Eldik, L. J., and LaDu, M. J. (2005) Differential effects of oligomeric and fibrillar amyloid-beta1-42 on astrocyte-mediated inflammation. *Neurobiol Dis* **18**, 459–65.
14. Trommer, B. L., Shah, C., Yun, S. H., Gamkrelidze, G., Pasternak, E. S., Stine, W. B., Manelli, A., Sullivan, P., Pasternak, J. F., and LaDu, M. J. (2005) ApoE isoform-specific effects on LTP: blockade by oligomeric amyloid-beta1-42. *Neurobiol Dis* **18**, 75–82.
15. Bitan, G., Fradinger, E. A., Spring, S. M., and Teplow, D. B. (2005) Neurotoxic protein oligomers – what you see is not always what you get. *Amyloid* **12**, 88–95.
16. Jiang, Q., Lee, C. Y., Mandrekar, S., Wilkinson, B., Cramer, P., Zelcer, N., Mann, K., Lamb, B., Willson, T. M., Collins, J. L., Richardson, J. C., Smith, J. D., Comery, T. A., Riddell, D., Holtzman, D. M., Tontonoz, P., and Landreth, G. E. (2008) ApoE promotes the proteolytic degradation of Abeta. *Neuron* **58**, 681–93.
17. Hickman, S. E., Allison, E. K., and El Khoury, J. (2008) Microglial dysfunction and defective beta-amyloid clearance pathways in aging Alzheimer's disease mice. *J Neurosci* **28**, 8354–60.
18. El Khoury, J., Toft, M., Hickman, S. E., Means, T. K., Terada, K., Geula, C., and Luster, A. D. (2007) Ccr2 deficiency impairs microglial accumulation and accelerates progression of Alzheimer-like disease. *Nature Med* **13**, 432–8.
19. Giunta, B., Zhou, Y., Hou, H., Rrapo, E., Fernandez, F., and Tan, J. (2008) HIV-1 TAT inhibits microglial phagocytosis of Abeta peptide. *Int J Clin Exp Pathol* **1**, 260–75.
20. Majumdar A, Chung H, Dolios G, Wang R, Asamoah N, Lobel P, Maxfield FR (2008) Degradation of fibrillar forms of Alzheimer's amyloid beta-peptide by macrophages. *Neurobiology of aging* **29**, 707–15.
21. Chung, H., Brazil, M. I., Soe, T. T., and Maxfield, F. R. (1999) Uptake, degradation, and release of fibrillar and soluble forms of Alzheimer's amyloid beta-peptide by microglial cells. *J Biol Chem* **274**, 32301–8.

22. Brazil, M. I., Chung, H., and Maxfield, F. R. (2000) Effects of incorporation of immunoglobulin G and complement component C1q on uptake and degradation of Alzheimer's disease amyloid fibrils by microglia. *J Biol Chem* **275**, 16941–7.
23. Paresce, D. M., Ghosh, R. N., and Maxfield, F. R. (1996) Microglial cells internalize aggregates of the Alzheimer's disease amyloid beta-protein via a scavenger receptor. *Neuron* **17**, 553–65.
24. Parvathy S, Rajadas J, Ryan H, Vaziri S, Anderson L, Murphy GM, Jr. (2009) Abeta peptide conformation determines uptake and interleukin-1alpha expression by primary microglial cells. *Neurobiology of aging* **30**, 1792–1804.
25. Li, R., Shen, Y., Yang, L. B., Lue, L. F., Finch, C., and Rogers, J. (2000) Estrogen enhances uptake of amyloid beta-protein by microglia derived from the human cortex. *J Neurochem* **75**, 1447–54.
26. Chafekar, S. M., Baas, F., and Scheper, W. (2008) Oligomer-specific Abeta toxicity in cell models is mediated by selective uptake. *Biochim Biophys Acta* **1782**, 523–31.
27. Simakova, O., and Arispe, N. J. (2007) The cell-selective neurotoxicity of the Alzheimer's Abeta peptide is determined by surface phosphatidylserine and cytosolic ATP levels. Membrane binding is required for Abeta toxicity. *J Neurosci* **27**, 13719–29.
28. Saavedra, L., Mohamed, A., Ma, V., Kar, S., and de Chaves, E. P. (2007) Internalization of beta-amyloid peptide by primary neurons in the absence of apolipoprotein E. *J Biol Chem* **282**, 35722–32.
29. Clifford, P. M., Zarrabi, S., Siu, G., Kinsler, K. J., Kosciuk, M. C., Venkataraman, V., D'Andrea, M. R., Dinsmore, S., and Nagele, R. G. (2007) Abeta peptides can enter the brain through a defective blood-brain barrier and bind selectively to neurons. *Brain Res* **1142**, 223–36.
30. Smits, H. A., van Beelen, A. J., de Vos, N. M., Rijsmus, A., van der Bruggen, T., Verhoef, J., van Muiswinkel, F. L., and Nottet, H. S. (2001) Activation of human macrophages by amyloid-beta is attenuated by astrocytes. *J Immunol* **166**, 6869–76.
31. Kuhnke, D., Jedlitschky, G., Grube, M., Krohn, M., Jucker, M., Mosyagin, I., Cascorbi, I., Walker, L. C., Kroemer, H. K., Warzok, R. W., and Vogelgesang, S. (2007) MDR1-P-Glycoprotein (ABCB1) Mediates Transport of Alzheimer's amyloid-beta peptides – implications for the mechanisms of Abeta clearance at the blood-brain barrier. *Brain Pathol* **17**, 347–53.
32. Liu, Y., and Schubert, D. (1997) Cytotoxic amyloid peptides inhibit cellular 3-(4,5-dimethylthiazol-2-yl)-2,5-diphenyltetrazolium bromide (MTT) reduction by enhancing MTT formazan exocytosis. *J Neurochem* **69**, 2285–93.

Chapter 3

Isolation of Low-n Amyloid β-Protein Oligomers from Cultured Cells, CSF, and Brain

Ganesh M. Shankar, Alfred T. Welzel, Jessica M. McDonald, Dennis J. Selkoe, and Dominic M. Walsh

Abstract

Recent data suggest that soluble, non-fibrillar assemblies of the amyloid β-protein (Aβ) may mediate the synaptic deficits that characterize the early stages of Alzheimer's disease. Consequently, much effort has been expended in isolating and studying a variety of different Aβ assemblies. Here, we describe the use of immunoprecipitation/western blotting and size exclusion chromatography/western blotting to characterize Aβ present in conditioned medium from cultured cells, human cerebrospinal fluid, and human cortex extracted with aqueous buffer, detergent, and formic acid.

Key words: Aggregation, Alzheimer's disease, Amyloid β-protein, Brain, Cerebrospinal fluid, Oligomers

1. Introduction

Current biochemical and genomic evidence suggests that the cerebral accumulation of the amyloid β-protein (Aβ) is a proximal event in Alzheimer's disease pathogenesis (1). Although the molecular mechanisms by which Aβ mediates disease remain unclear, it seems to require Aβ self-association, oligomerization, and aggregation (2). While many investigators have used synthetic peptides to study Aβ aggregation and toxicity, we have chosen to focus on naturally produced Aβ. Using immunoprecipitation(IP)/autofluorography, IP/western blotting and size exclusion chromatography (SEC)/lyophilization/western blotting, we have detected Aβ species which migrate on SDS–polyacrylamide gels with molecular weights consistent with Aβ dimers and trimers — species that we refer to as SDS-stable low-n Aβ oligomers.

Erik D. Roberson (ed.), *Alzheimer's Disease and Frontotemporal Dementia*, Methods in Molecular Biology, vol. 670,
DOI 10.1007/978-1-60761-744-0_3,

Using these techniques, low-n oligomers have been detected in extracts of human brain (3), in human CSF (4, 5), and in a variety of cultured cells (4, 6, 7). Because of their easy maintenance and fast growth rate, much of our work has taken advantage of a particular Chinese hamster ovarian cell line, referred to as 7PA2, that stably expresses human APP_{751} bearing the familial Alzheimer's disease-associated V717F mutation (8).

2. Materials

2.1. Culture of 7PA2 Cells

1. 7PA2 cells (available from D. Selkoe, Center for Neurologic Diseases).
2. Dulbecco's modified Eagle's medium (DMEM) containing 10% bovine fetal calf serum, 50 µg/mL penicillin/streptomycin, 2 mM L-glutamine, and 200 µg/mL G418. The latter reagent is used to maintain stable expression of APP.
3. 10-cm tissue culture dishes.
4. 0.5% Trypsin–EDTA.
5. Plain DMEM lacking any additives.
6. Protease inhibitor 100× stock solutions:
   (a) Pefabloc, 100 mM in Milli-Q water.
   (b) Leupeptin, 10 mg/mL in Milli-Q water.
   (c) Aprotinin, 1 mg/mL in Milli-Q water.
   (d) Pepstatin, 1 mg/mL in methanol.
   (e) 1,10 phenanthroline, 200 mM in methanol.
   (f) EDTA, 0.5 M in Milli-Q water and adjusted to pH 8.0 with 1 M NaOH.
   (g) EGTA, 0.5 M in Milli-Q water.
7. Centriprep-YM3 centrifugal filtration device.

2.2. Serial Extraction of Human Brain Tissue

1. Tris-buffered saline (TBS): 15 mM Tris–HCl, pH 7.4, 140 mM NaCl, 3 mM KCl.
2. Protease inhibitors (see Subheading 2.1, item 6).
3. Phosphatase inhibitor cocktail (Sigma).
4. Mechanical dounce homogenizer.
5. TBS containing 1% Triton X-100 (TBS-TX): 1 mL TritonX-100 in 99 mL TBS.
6. 88% formic acid (FA): diluted from 99% formic acid stock using Milli-Q water.
7. Beckman TL 100 centrifuge with TLA100.2 rotor (or equivalent).

8. 11 × 34 polyallomer centrifuge tubes.
9. Bath sonicator.

2.3. Immunoprecipitation

1. 1 M Tris (unbuffered) containing 0.025% phenol red.
2. 2× STEN: 0.1 M Tris–HCl, pH 7.6, containing 0.3 M NaCl, 4 mM EDTA and 0.4% NP-40.
3. Protein A–Sepharose: 5 g suspended in 5 mL of 2× STEN plus 5 mL of 10 mg/mL BSA (Cohn Fraction V). Incubate on nutator for 1 h at 4°C. Store in 1 mL aliquots at –20°C.
4. Protein G–Sepharose suspension. Purchased as a slurry and used without further manipulation.
5. Microcentrifuge.
6. Anti-Aβ antibody (see Note 1).
7. 0.5 M STEN IP wash buffer: 0.05 M Tris–HCl, pH 7.6 containing *0.5 M NaCl*, 2 mM EDTA, 0.2% NP40. Prepare from 2× STEN by adding NaCl and diluting to 1×. Prepare in batches of 1 L and store in 50 mL aliquots at –20°C.
8. SDS-STEN IP wash buffer: 0.05 M Tris–HCl, pH 7.6 containing 0.15 M NaCl, 2 mM EDTA, 0.2% NP40, *0.1% SDS*. Prepare from 2× STEN by adding SDS and diluting to 1×. Prepare in batches of 1 L and store in 50 mL aliquots at –20°C.
9. STEN IP wash buffer: 0.05 M Tris–HCl, pH 7.6 containing 0.15 M NaCl, 2 mM EDTA, 0.2% NP40. Prepare from 2× STEN by diluting 1:1 with Milli-Q water. Prepare in batches of 1 L and store in 50 mL aliquots at –20°C.
10. 4× sample buffer: 450 mM Tris–HCl, pH 8.45, containing 12% glycerol, 4% SDS, 0.0025% Coomassie blue G, and 0.0025% phenol red. Store at room temperature and dilute as required with Milli-Q water.

2.4. Size Exclusion Chromatography

1. Elution buffer: 50 mM ammonium acetate, pH 8.5, in Milli-Q water. Adjust by dropwise addition of 28–30% ammonium hydroxide. Pass through a 0.2 μM filter before use. To avoid fluctuations in pH, the buffer is stored at 4°C and used within 1 week of preparation.
2. Superdex 75 10/300 column (GE Healthcare, Little Chalfont, UK) using an Äkta FPLC (GE Healthcare, Little Chalfont, UK) eluted at 0.8 mL/min.
3. Unbranched dextran standards of molecular masses: 123,600; 66,700; 43,800; 21,400; 9890; and 4440 (Pharmacosmos, Holbaek, Denmark), prepared in Milli-Q water containing 0.025% phenol red.
4. Mixed protein standards (BioRad): Thyroglobulin (670,000), γ-globulin (123,600), chicken ovalbumin (44,000), equine

myoglobin (17,000), and vitamin B12 (1,350). The lyophilized powder was reconstituted in Milli-Q water according to the supplier's recommendations.

5. Centriprep-YM3 centrifugal filtration device.
6. Freeze-drier (Labconc, Kansas city, MO).

2.5. SDS-Polyacrylamide Gel Electrophoresis and Western Blotting

1. Pre-cast 10–20% polyacrylamide tricine gels.
2. Electrophoresis running buffer: 0.1% SDS in 0.1 M Tris–tricine, pH 8.3 (the balance of Tris and tricine achieves a pH of 8.3).
3. BA-S 83 Optitran 0.2 μm nitrocellulose (GE Healthcare).
4. Transfer buffer: 25 mM Tris base, 0.192 M glycine, 10% methanol.
5. Phosphate buffered saline (PBS).
6. Blocking buffer: 5% (w/v) non-fat dry milk in PBS.
7. TBS containing 0.05% Tween-20 (TBS-T).
8. Appropriate primary antibody (see Note 1 and Table 1).
9. Horseradish peroxidase–conjugated donkey anti-mouse IgG or goat anti-mouse IgG conjugated with infrared dye 700 or infrared dye 800.
10. ECL+ reagent (GE Healthcare, Little Chalfont, UK) for blots probed with secondary antibody conjugated to HRP, or Li-Cor Odyssey Imaging System, for blots developed with the infrared dye-containing secondary antibody.

Table 1
Antibodies used for IP/western blotting

Antibody/source	Immunogen	Species	APP proteolytic fragments detected				
			APPs	C99	C83	Aß	p3
AW8/Walsh lab	Aβ1-40/42	Rabbit	X	X	X	X	X
1282/Selkoe lab	Aβ1-40	Rabbit	X	X	X	X	X
DW6/Walsh lab	Aβ1-40	Rabbit	X	X	X	X	X
3D6/Elan Pharma	Aβ1-5	Mouse		X		X	
82E1/Antibodies online	Aβ1-5	Mouse		X		X	
26D6/Merck Res Labs	Aβ1-5	Mouse	X	X		X	
6E10/Convance Inc.	Aβ1-17	Mouse	X	X		X	
6C6/Elan Pharma	Aβ1-16	Mouse	X	X	X		
4G8/Convance Inc.	Aβ17-24	Mouse		X	X	X	X
2G3/Elan Pharma	Aβx-40	Mouse				X	X
21F12/Elan Pharma	Aβx-42	Mouse				X	X

3. Methods

This section describes the preparation of Aβ species naturally secreted by cells or found in CSF or extracts of cerebral cortex. While the methods will predominantly describe the analysis of such samples by western blotting, we also indicate how samples are prepared for assessing the effects of these Aβ species on various physiologic readouts (see Note 2).

3.1. Culture of 7PA2 Cells and Generation of Oligomer-Containing Conditioned Medium

1. 7PA2 cells are cultured in DMEM containing 10% bovine fetal calf serum and grown in 10-cm dishes. Once cells form a uniform monolayer, they are passaged using 0.5% trypsin–EDTA at a dilution of 1:3, which will generate confluent cells within 24 h. Cells passaged at a dilution of 1:6 or 1:9 will reach confluency in 48 or 72 h, respectively.
2. Nearly confluent (95–100%) 10-cm dishes of 7PA2 cells are washed with serum-free medium (5 mL × 1) and incubated in 5 mL serum-free medium for ~15 h.
3. Conditioned Medium (CM) is removed and cleared of cells by centrifugation at 200 × *g* for 10 min at 4°C. Protease inhibitors (final concentration: 5 μg/mL leupeptin, 5 μg/mL aprotinin, 2 μg/mL pepstatin, 120 μg/mL Pefabloc, 0.2 mM 1,10 phenanthroline, 0.5 mM EDTA, 0.5 mM EGTA) are added to the supernatant (see Note 2).
4. The CM collected in step 3 can be used directly for IP or concentrated using Centriprep YM-3 centrifugal filtration devices. Prior to use with CM, YM-3 filters are rinsed twice with 15 mL Milli-Q water by centrifuging at 3,000 × *g* for 10 min. CM is subsequently added to the reservoir and concentrated by centrifugation at 3,000 × *g* to achieve the desired concentration. Tenfold concentration of CM by this method typically results in ~20% loss of Aβ species (see Note 3).

3.2. Preparation of Human Brain Extracts

1. Dice frozen human brain tissue with a clean razor and weigh (see Note 4). Add protease and phosphatase inhibitors to ice-cold TBS and homogenize the frozen cortex in five volumes of this buffer (i.e. 1 mL buffer/0.2 g brain) with 25 strokes at a setting of ~6,000 rpm on a mechanical Dounce homogenizer (Fisher, Ottawa, Canada). Centrifuge the homogenate at 175,000 × *g* in a TLA100.2 rotor on a Beckman TL 100 for 30 min. Aliquot the supernatant (called TBS extract) and store at –80°C.
2. Re-homogenize the pellet from step 1 in five volumes of TBS + 1% Triton X-100 containing protease and phosphatase inhibitors (TBS-TX) (i.e. 1 mL buffer/0.2 g brain used

above). For this step, we first reconstitute the pellet in 2.5 volumes (relative to original brain weight) of TBS-TX and transfer to a homogenizer tube. Any residual pellet left in the centrifuge tube is collected by washing with an additional 2.5 volumes TBS-TX and this suspension transferred to the homogenizer tube. The resulting suspension is homogenized as described in step 1 and then centrifuged at 175,000 × *g* as in step 1. The resultant supernatant (called TBS-TX extract) is aliquoted and store at −80°C.

3. To release the Aβ present in amyloid plaques that is not liberated by TBS or TBS-TX, the remaining brain material is extracted with 88% formic acid. Resuspend the pellet from step 2 in 0.5 volumes 88% formic acid (i.e. 100 µl/0.2 g). This is done by adding 50 µl of 88% formic acid and pipetting the sample up and down ten times using a 200 µl pipette tip (the bottom 2 mm of which has been cut off to provide a wider orifice), then adding another 50 µl of 88% formic acid and pipetting an additional ten times. Finally, the sample is sonicated in a bath sonicator at 485 W and 4°C for 5 min and gently agitated on a shaking platform for ~4 h. Aliquots of the FA extract are stored at −80°C.

3.3. Immunoprecipitation

1. To minimize detection of cross-reactive proteins that nonspecifically bind to protein A/G, samples are incubated with protein A/G before addition of antibody — a process we refer to as "pre-clearing". Two to four milliliters of CM or 300–500 µl TBS or TBS-TX extracts are incubated with 25 µl Protein A + 25 µl Protein G for 1 h at 4°C with gentle shaking on a nutator.
2. To pre-clear FA extracts, dilute FA extracts 1:27 with 1 M Tris (unbuffered) containing 0.025% phenol red (i.e. 25 µl FA extract + 650 µl 1 M Tris). The neutralized solution should be an orange/red color. Pre-clear 675 µl neutralized FA extract with 25 µl Protein A + 25 µl Protein G for 1 h at 4°C with gentle shaking on a nutator.
3. Centrifuge samples at 3,500 × *g* for 5 min and remove the supernatants to clean tubes.
4. Incubate pre-cleared samples with IP antibody (see Notes 5 and 6) plus 15 µL Protein A and 15 µL Protein G for 1 h at room temperature with gentle shaking.
5. Centrifuge samples at 3,500 × *g* for 5 min, aspirate the supernatant using a gel loading tip attached to a vacuum line (see Note 7), and transfer beads to 1.5 mL microfuge tubes via two sequential 0.5 mL additions of 0.5 M STEN wash buffer. Vortex briefly and wash with gentle shaking at 4°C for 20 min.

6. Centrifuge at 3,500 × *g* for 5 min, aspirate the supernatant, add 1 mL SDS-STEN buffer, vortex, and wash with gentle shaking for 20 min at 4°C.
7. Centrifuge at 3,500 × *g* for 5 min, aspirate the supernatant, add 1 mL STEN IP wash buffer, vortex, and wash with gentle shaking for 20 min at 4°C.
8. Following the STEN wash, centrifuge at 3,500 × *g* for 5 min, aspirate the supernatant, and add 10 µL appropriate sample buffer. Heat samples at 100°C for 10 min, cool to room temperature, and centrifuge at 15,000 × *g* for 5 min. Remove all of the retrievable liquid and use for SDS-Polyacrylamide Gel Electrophoresis (SDS-PAGE).

3.4. Size Exclusion Chromatography

1. Attach a Superdex 75 10/300 HR column to an Äkta FPLC system and elute with 50 mM ammonium acetate, pH 8.5 at a flow rate of 0.8 mL/min. The programmed parameters include: 0.1 column volume equilibration volume, 0.15 column volume to empty sample loop, and begin collecting fractions once the sample is fully loaded onto the column. For the 10/300 HR column, 0.5 or 1 mL fractions are collected.
2. Columns are calibrated using the unbranched dextran standards listed in the Subheading 2 (see Note 8). While the elution of most of the dextrans is recorded at 254 nm, the 9,890 and 4,440 Da standards are detected at 280 nm. The globular protein standards are not used for calibration, but provide an inexpensive reference to test the performance of the column. The partition coefficient (*Kav*) is given by the following equation:

$$Kav = \frac{Ve - Vo}{Vt - Vo},$$

where *Ve* represents the elution volume, *Vo* the void volume (given by the *Ve* of the largest standard in each group), and *Vt* the total volume of the Superdex 75 10/300 column is 24 mL. The relationship between the *Kav* and log(MW) for each standard is fit linearly, providing an equation that can be used to estimate the molecular weights of species contained within a given fraction.

3. Inject up to 1 mL sample (tenfold concentrated CM, tenfold concentrated CSF, or unconcentrated brain extract) onto the Superdex 75 10/300 (see Note 9) and elute at a flow rate of 0.8 mL/min. Aliquot each fraction into two equal portions, store one half at −80°C and place the other half on dry ice, freeze (it is important that samples are lyophilized in tubes the capacity of which is two times larger than the volume used), and then lyophilized.

4. In order to obtain reproducible fractionation of Aβ species on SEC, it is essential to thoroughly clean the column between runs (see Note 10).
5. Centrifuge lyophilates at 15,000 × *g* for 2 min, then resuspend in 15 μL 2× sample buffer, vortex, and heat at 100°C for 10 min. Cool to room temperature, then centrifuge at 15,000 × *g* for 5 min.

3.5. Denaturing PAGE and Western Blotting

This protocol will describe the western blotting analysis of the supernatant generated in Subheadings 3.3, step 8, or Subheading 3.4, step 5.

1. Load sample into the wells of a 15-well 10–20% polyacrylamide Tris–tricine mini-gel (see Note 11).
2. Electrophorese at 50 V until the sample dye front completely enters the gel, then increase to 120 V. While using SeeBlue molecular weight markers (Invitrogen), stop electrophoresis when the lowest marker reaches the bottom of the gel.
3. Transfer proteins from the gel onto 0.2 μm nitrocellulose at 400 mA for 2 h in Transfer Buffer.
4. Rinse the nitrocellulose quickly with Milli-Q water three times to remove residual transfer buffer, place in 200 mL PBS, and microwave at 800 W for 1.5 min (9). Let stand for 3.5 min, turn the filter over, microwave for a further 1.5 min, and leave in the boiling PBS for a further 3.5 min (i.e. total time in PBS = 10 min).
5. To reduce non-specific binding of primary and secondary antibodies to the nitrocellulose, the filter is blocked in 5% non-fat dried milk in TBS-T overnight at 4°C.
6. Wash the nitrocellulose once with TBS-T.
7. Incubate with primary antibody (see Note 1) prepared in 5% non-fat dried milk in TBS-T for 1 h at room temperature.
8. Wash filter 4 × 5 min with TBS-T.
9. Incubate with secondary antibody: 1:25,000 donkey anti-mouse-HRP in TBS-T or 1:5,000 goat anti-mouse 800 (or anti-mouse-700) in TBS-T containing 0.02% SDS.
10. Wash filter 4 × 5 min with TBS-T.
11. Develop with ECL+ or Li-Cor as per manufacturer instructions.

4. Notes

1. Antibodies raised to epitopes within Aβ can also recognize other proteolytic fragments of APP. Therefore, to ensure that proteins detected by western blotting are *bona fide* Aβ, several antibodies should be used. Please *see* Table 1 for further details.

2. Conditioned media from Subheading 3.1, step 3 or Subheading 3.1, step 4, TBS extract from Subheading 3.2, step 1, or SEC fractions from Subheading 3.4, step 3 can be used for physiologic assays, in which case protease inhibitors are not added to these preparations. Before their use in such paradigms, it is important to verify the nature of the sample by analyzing an aliquot by IP/western blotting as described in Subheadings 3.3 and 3.5. Supernatants from samples used for IP can also serve as a valuable negative control for physiologic experiments since they contain the same non-Aβ proteins as the non-immunoprecipitated samples, but are depleted of Aβ.
3. Minimizing Aβ loss. When concentrating CM, a portion of Aβ is inevitably lost onto the filter membrane and plastic container, and the degree of loss increases with fold-concentrations >10.
4. Handling and preparation of human CSF and brain extracts. Great care should be exercised when handling human fluids and tissues. All investigators should be vaccinated for hepatitis B before initiating experiments. Homogenizations should be conducted in a fume hood and the investigator should wear adequate safety protection (gloves, laboratory coat, and protective goggles). All waste should be incinerated and instruments and work area cleaned with bleach after use.
5. The concentration of IP antibody needs to be determined empirically. Generally, we find that 1:100 for polyclonal antisera and 5 μg/mL for monoclonal antibodies provide good starting dilutions. Dose–response curves should be generated for each antibody, as the efficiency of some antibodies can decrease at high concentrations. For routine analysis, samples are immunoprecipitated using polyclonal anti-Aβ antibodies.
6. Aβ monomer and dimer in the TBS brain extract are most efficiently immunoprecipitated by antibodies directed to the N-terminus of Aβ (e.g., 82E1 or 3D6), whereas such antibodies do not effectively immunoprecipitate 7PA2 low-n oligomers. Conversely C-terminal-specific antibodies (e.g. 2G3 and 21F12) effectively immunoprecipitate 7PA2 dimers and trimers, but not TBS brain-derived dimers.
7. Alternatively, the supernatant can be saved instead of aspirating to waste. The supernatant obtained following IP is now depleted of Aβ and can provide a useful immunodepleted control for activity studies.
8. The migration pattern of Aβ monomer on size exclusion chromatography is more accurately predicted by unbranched dextran standards than globular protein standards (10, 11). This likely reflects that under native conditions Aβ monomer is unfolded with an extended structure more similar to extended dextrans than globular proteins.

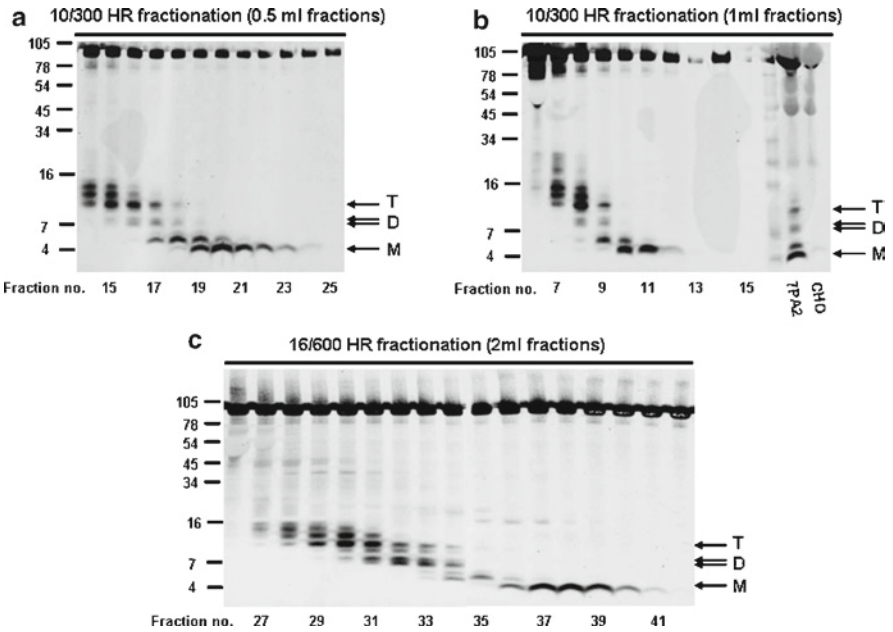

Fig. 1. Size exclusion fractionation of 7PA2 CM. (**a**, **b**) One milliliter of tenfold concentrated 7PA2 CM was loaded onto a 10/300 HR Superdex 75 column and separated at 0.8 mL/min. Either 0.5 mL (**a**) or 1 mL (**b**) fractions were collected, and half were lyophilized and analyzed by western blotting with the anti-Aβ monoclonal antibody, 6E10 (1 μg/mL). Lanes marked "7PA2" and "CHO" indicate AW8 (anti-Aβ polyclonal antibody) IPs from 3 mL 7PA2 CM or 3 mL CHO CM, respectively. (**c**) Five milliliter of tenfold concentrate 7PA2 CM was loaded onto a 16/600 HR Superdex 75 column and separated at a flow rate of 1 mL/min. Two milliliter fractions were collected, lyophilized, and used for western blot analysis with 6E10. Migration of molecular weight standards are indicated on the *left* and *arrows* indicating monomer (M), dimer (D), and trimer (T) are on the *right*. The fraction numbers of samples analyzed are on the *bottom.*

9. Depending on the volume of sample to be used or the level of separation required, a Superdex 75 16/600 HR column can be used. This column is longer than the 10/300 column and consequently allows more effective separation of the various Aβ species (Fig. 1).
10. We have developed a standard protocol that we employ after every third Aβ-containing sample is chromatographed. The column is washed with a series of solutions that have been 0.2-micron-filtered, in the following order: MQ water, at least 1 column volume (CV); 50% formic acid, at least 1 CV; MQ water, at least 2 CVs; 0.1 M NaOH, at least 1 CV; MQ water at least 2 CVs; 1 M Tris (unbuffered), at least 1 CV; MQ water, at least 2 CVs. At this stage, the column can be stored in 20% EtOH or re-equilibrated in 50 mM ammonium acetate, pH 8.5 to be ready for use.
11. We have also found that hand-prepared gels cast using the BioRad Mini-PROTEAN Tetra Electrophoresis System, and pre-cast 4–12% polyacrylamide Bis-Tris NuPAGE gels (Invitrogen) provide results similar to those obtained using

pre-cast 10–20% polyacrylamide Tris–tricine gels. Hand-poured 16% polyacrylamide tricine gels are prepared as described previously (12) and electrophoresed using 0.2 M Tris–HCl, pH 8.9 as the anode buffer and 0.1 M Tris, 0.1 M tricine, pH 8.25 containing 0.1% SDS as the cathode buffer. Four to twelve percent polyacrylamide Bis-Tris NuPAGE are electrophoresed using 3.5 mM SDS in 50 mM Tris, 50 mM 2-(N-morpholino) ethane sulfonic acid, pH 7.3 containing 1 mM EDTA.

Acknowledgments

This work was supported by grants from the Wellcome Trust (067660; DMW), European Union Framework Programme 7 (200611; DMW) and the National Institutes of Health (AG027443; DJS and DMW).

References

1. Hardy, J., and Selkoe, D. J. (2002) The amyloid hypothesis of Alzheimer's disease: progress and problems on the road to therapeutics. *Science* **297**, 353–6.
2. Walsh, D. M., Klyubin, I., Shankar, G. M., Townsend, M., Fadeeva, J. V., Betts, V., Podlisny, M. B., Cleary, J. P., Ashe, K. H., Rowan, M. J., and Selkoe, D. J. (2005) The role of cell-derived oligomers of Abeta in Alzheimer's disease and avenues for therapeutic intervention. *Biochem Soc Trans* **33**, 1087–90.
3. Shankar, G. M., Li, S., Mehta, T. H., Garcia-Munoz, A., Shepardson, N. E., Smith, I., Brett, F. M., Farrell, M. A., Rowan, M. J., Lemere, C. A., Regan, C. M., Walsh, D. M., Sabatini, B. L., and Selkoe, D. J. (2008) Amyloid-beta protein dimers isolated directly from Alzheimer's brains impair synaptic plasticity and memory. *Nat Med* **14**, 837–42.
4. Walsh, D. M., Tseng, B. P., Rydel, R. E., Podlisny, M. B., and Selkoe, D. J. (2000) Detection of intracellular oligomers of amyloid ß-protein in cells derived from human brain. *Biochemistry* **39**, 10831–39.
5. Klyubin, I., Betts, V., Welzel, A. T., Blennow, K., Zetterberg, H., Wallin, A., Lemere, C. A., Cullen, W. K., Peng, Y., Wisniewski, T., Selkoe, D. J., Anwyl, R., Walsh, D. M., and Rowan, M. J. (2008) Amyloid beta protein dimer-containing human CSF disrupts synaptic plasticity: prevention by systemic passive immunization. *J Neurosci* **28**, 4231–7.
6. Podlisny, M. B., Ostaszewski, B. L., Squazzo, S. L., Koo, E. H., Rydel, R. E., Teplow, D. B., and Selkoe, D. J. (1995) Aggregation of secreted amyloid β-protein into SDS-stable oligomers in cell culture. *J Biol Chem* **270**, 9564–70.
7. Morishima-Kawashima, M., and Ihara, Y. (1998) The presence of amyloid beta-protein in the detergent-insoluble membrane compartment of human neuroblastoma cells. *Biochemistry* **37**, 15247–53.
8. Koo, E. H., and Squazzo, S. (1994) Evidence that production and release of amyloid β-protein involves the endocytic pathway. *J Biol Chem* **269**, 17386–89.
9. Ida, N., Hartmann, T., Pantel, J., Schroder, J., Zerfass, R., Forstl, H., Sandbrink, R., Masters, C. L., and Beyreuther, K. (1996) Analysis of heterogeneous A4 peptides in human cerebrospinal fluid and blood by a newly developed sensitive Western blot assay. *J Biol Chem* **271**, 22908–14.
10. Paivio, A., Jarvet, J., Graslund, A., Lannfelt, L., and Westlind-Danielsson, A. (2004) Unique physicochemical profile of beta-amyloid peptide variant Abeta1-40E22G protofibrils: conceivable neuropathogen in arctic mutant carriers. *J Mol Biol* **339**, 145–59.

11. Walsh, D. M., Lomakin, A., Benedek, G. B., Condron, M. M., and Teplow, D. B. (1997) Amyloid β-protein fibrillogenesis: detection of a protofibrillar intermediate. *J Biol Chem* **272**, 22364–74.

12. Schagger, H., and von Jagow, G. (1987) Tricine-sodium dodecyl sulfate-polyacrylamide gel electrophoresis for the separation of proteins in the range from 1 to 100 kDa. *Anal Biochem* **166**, 368–79.

Chapter 4

Detecting Aβ*56 Oligomers in Brain Tissues

Mathew A. Sherman and Sylvain E. Lesné

Abstract

Since its original description in 1906 by Dr Alois Alzheimer, amyloid plaques and neurofibrillary tangles have remained the hypothetical cause of Alzheimer's disease. However, plaque burden poorly predicts cognitive status in humans, which led several groups to investigate the possibility that soluble species of amyloid-beta (Aβ) peptides could be playing an important pathological function in the aging brain. Through a multistep fractionation protocol, we identified a 56 kDa oligomer of Aβ, termed Aβ*56, the amount of which correlates with cognitive impairment. Here, we describe our biochemical approach to isolate this oligomeric Aβ species in brain tissue of transgenic mouse models of AD.

Key words: Alzheimer, Amyloid-beta (Aβ), Brain, SDS-PAGE, Western blotting, Transgenic mouse model

1. Introduction

Protein aggregation and protein misfolding appear to be responsible for multiple neurological diseases like Parkinson's disease, Huntington's disease, prion diseases, and Alzheimer's disease (AD). Due to increasing aging of the population, AD has been at the forefront of protein-misfolding research (1). The disease is neuropathologically characterized by the presence of two protein aggregates, amyloid plaques formed by amyloid-β peptides and neurofibrillary tangles composed of insoluble tau proteins.

Aβ is derived from its precursor protein, amyloid-β precursor protein (APP), following sequential cleavage by BACE (β-site APP cleaving enzyme) and the γ-secretase complex (1–3). Due to their protein sequence, Aβ peptides can adopt various intermediate states during the aggregation process. Although insoluble fibrillar Aβ as amyloid plaques was thought for nearly 100 years to be the culprit of AD, the relevance of plaques to AD pathogenesis

Erik D. Roberson (ed.), *Alzheimer's Disease and Frontotemporal Dementia*, Methods in Molecular Biology, vol. 670,
DOI 10.1007/978-1-60761-744-0_4,

still remains elusive. In contrast, soluble oligomeric Aβ species have been shown over the past decade to be deleterious, causing synaptic dysfunction and cognitive decline that may be critical for the development and progression of AD (4–10).

With growing interest in identifying Aβ oligomers in brain tissues to determine their relative function during the disease process, we developed a simple biochemical assay based on Sodium Dodecylsulfate-Polyacrylamide Gel Electrophoresis (SDS-PAGE), western blotting, and immunoprecipitation techniques.

2. Materials

2.1. Brain Tissues and Lysis

1. Brain tissues to be tested, microdissected into subregions of interest and stored at −80°C until use. The volume measures in this protocol are intended for 125–175 mg samples of wet brain tissue.
2. Micropipettors and tips (see Note 1).
3. NP40-lysis buffer: 50 mM Tris–HCl, pH 7.6, 0.01% NP-40, 150 mM NaCl, 2 mM EDTA, 0.1% SDS. Store at room temperature. Filter with a 0.2 μm membrane and add protease inhibitors (1 mM phenylmethylsulfonyl fluoride (PMSF), 2 mM 1,10-phenanthroline monohydrate, 1× Sigma protease inhibitor cocktail) before use (see Note 2). Keep on ice once inhibitors are added.
4. 1 mL syringes.
5. 20-gauge needles.
6. Refrigerated microcentrifuge with rotor for 1.5 mL tubes.
7. TNT-lysis buffer: 50 mM Tris–HCl, pH 7.4, 150 mM NaCl, 0.1% Triton X-100. Store at room temperature. Filter with a 0.2 μm membrane and add protease inhibitors (1 mM PMSF, 2 mM 1,10-phenanthroline monohydrate, 1× Sigma protease inhibitor cocktail) before use (see Note 2). Keep on ice once inhibitors are added.
8. RIPA-lysis buffer: 50 mM Tris–HCl, pH 7.4, 150 mM NaCl, 0.5% Triton X-100, 1 mM EDTA, 3% SDS, 1% deoxycholate. Store at room temperature. Filter with a 0.2 μm membrane and add protease inhibitors (1 mM PMSF, 2 mM 1,10-phenanthroline monohydrate, 1× Sigma protease inhibitor cocktail) before use (see Note 2). Keep on ice once inhibitors are added for no longer than 15 min (SDS will precipitate if kept longer).
9. Rotating platform mixer.
10. Mixing heat block or Thermomixer.

11. Formic Acid buffer: Freshly prepare a 70% formic acid solution. Store at room temperature for a maximum of 1 week.
12. Vacuum centrifuge.
13. BCA protein assay kit.

2.2. Sodium Dodecylsulfate-Polyacrylamide Gel Electrophoresis

1. Tricine anode buffer: 200 mM Tris–HCl, pH 8.9. Store at room temperature.
2. Tricine cathode buffer: 100 mM Tris base, 100 mM Tricine, 0.1% SDS. Do not adjust pH, which should be about 8.25. Store at room temperature.
3. Glycine running buffer: 25 mM Tris base, 192 mM glycine, 0.1% SDS. Adjust pH to 8.3 if necessary with HCl. Store at room temperature.
4. 4× Tricine Loading Buffer: 450 mM Tris–HCl, pH 8.0, 24% Glycerol, 80 g/L SDS, 0.1% Coomassie Blue G-250, 0.1% Phenol Red. Store at room temperature. Add 5% (v/v) β-mercaptoethanol (βME) just before use.
5. Pre-cast 10–20% polyacrylamide gels (see Note 3).
6. Prestained molecular weight marker.
7. Synthetic Aβ1-42 peptide: Resuspend 0.1 mg of synthetic peptide (Sigma) in 1 mL of deionized water and store at −20°C. Transfer 10 µL into a new Eppendorf tube and add 90 µL of 4× Tricine Loading Buffer to reach a concentration of 0.01 µg/µL.

2.3. Transfer and Western Blotting

1. Transfer buffer: 25 mM Tris base, 192 mM glycine, 10% methanol. Adjust pH to 8.3 if necessary with HCl. Place under agitation on stir-plate at 4°C until use or store at 4°C in a sealed container.
2. Nitrocellulose membrane (0.2 µm pore size). Cut membranes very carefully to 9 cm (height) × 14.5 cm (width), minimizing pressure points and folds. Store at room temperature.
3. Scotch bright pads and blotting paper, precut.
4. Phosphate buffered saline (PBS): 10 mM phosphate, pH 7.4, 2.7 mM KCl, and 137 mM NaCl. Add ten tablets (Sigma) to 2 L of deionized water. Stir and store at room temperature.
5. Tween-Tris buffered saline (TTBS): 10 mM Tris–HCl, pH 7.40, 200 mM NaCl, 0.1% Tween-20.
6. Blocking buffer: 5% (w/v) BSA in TTBS. Add 25 g of bovine serum albumin, 98% grade (Sigma) to 500 mL of TTBS. Store at −20°C in 40 mL aliquots using 50 mL tubes. Thaw frozen aliquots in 37°C water bath for 15 min.
7. Primary antibody: Mouse monoclonal 6E10 or biotinylated 6E10 (Covance). Other commercially available N-terminal anti-Aβ antibodies can also be used (e.g., BAM-10).

8. Secondary antibody: Antimouse IgG-Fc specific, biotin conjugated (Pierce).
9. Avidin-HRP conjugate. We use Neutravidin (Invitrogen).
10. SuperSignal® West Pico Enhanced Chemiluminescence (Pierce).

2.4. Immunoprecipitation

11. ImmunoPrecipitation Dilution Buffer (IPDB): 50 mM Tris–HCl, pH 7.4, 150 mM NaCl. Store at room temperature.
12. Wash buffer A: 50 mM Tris–HCl, pH 7.4, 300 mM NaCl, 0.1% Triton X-100 (v/v), 1 mM EDTA.
13. Wash buffer B: 50 mM Tris–HCl, pH 7.4, 150 mM NaCl, 0.1% Triton X-100 (v/v), 1 mM EDTA.
14. FastFlow® Protein A-sepharose beads (GE Life Sciences): 1:1 (v:v) slurry solution with IPDB. From the stock solution, vortex and quickly transfer 1 mL into a 1.5 mL tube. Centrifuge 5 min at 9,300 × *g* at 4°C and discard supernatant. Add 750 µL of ice-cold, 0.2µ-filtered IPDB and vortex for 5 s. Centrifuge 5 min at 9,300 × *g* at 4°C and discard supernatant. Repeat washes three more times and store washed beads at 4°C for up to 2–3 weeks.
15. FastFlow® Protein G-sepharose beads (GE Life Sciences): 1:1 (v:v) slurry solution with IPDB. From the stock solution, vortex and quickly transfer 1 mL into a 1.5 mL tube. Centrifuge 5 min at 9,300 × *g* at 4°C and discard supernatant. Add 750 µL of ice-cold, 0.2 µ-filtered IPDB and vortex for 5 s. Centrifuge 5 min at 9,300 × *g* at 4°C and discard supernatant. Repeat washes three more times and store washed beads at 4°C for up to 2–3 weeks.

3. Methods

3.1. Brain Tissue Lysis and Fractionation

The goal of this lysis process is to fractionate proteins based on their cellular compartmentalization. The separation allows a recovery of a predicted protein in its known compartment to 75–90% fidelity, 100% representing the total expression of a given protein across all compartments (4). Note that even the smallest deviations from this protocol (e.g., using different grade BSA in western protocol) can result in major differences downstream in terms of results.

Day 1

1. Precool refrigerated microcentrifuge to 4°C. All but the ultracentrifugation steps will be performed in this centrifuge.
2. Thaw frozen hemi-forebrains (~125–200 mg) on ice. Olfactory bulbs, midbrain and cerebellum are kept separately

as control structures since Aβ does not preferentially deposit in these brain regions.

3. Add 500 µL of ice-cold NP40-lysis buffer.
4. Dissociate the tissue using a 1 mL syringe without needle for three repeats.
5. With the syringe filled with grossly triturated tissue, add a 20-gauge needle and further dissociate for five repeats.
6. Centrifuge at 800 × *g* for 10 min at 4°C.
7. Collect supernatant 1, the fraction corresponding to soluble proteins – mostly extracellular (EC) and place in a new Eppendorf tube. Be careful not to aspirate the very loose pellet, which contains intact cells; save the pellet for step 12.
8. Centrifuge supernatant 1 at 16,100 × *g* for 90 min at 4°C.
9. Discard the small pellet (should be very small reflecting the amount of cells broken by steps 3–6), collect supernatant 2.
10. Centrifuge supernatant 2 at 16,100 × *g* for 90 min at 4°C.
11. Collect supernatants and store at –20°C overnight as EC-enriched fraction.
12. Resuspend pellet 1 from step 6 with 500 µL of ice-cold TNT-lysis buffer.
13. Dissociate with 1 mL pipette until tissues/cells are dissolved (8–10 repeats).
14. Centrifuge at 16,100 × *g* for 90 min at 4°C. Save pellets for step 18. They should be fairly large, ~400 µL in volume, reflecting the amount of lipids present in tissues/cells.
15. Collect supernatant 3, the fraction corresponding to soluble proteins – mostly intracellular (IC).
16. Centrifuge supernatant 3 at 16,100 × *g* for 90 min at 4°C.
17. Collect supernatants and store at –20°C overnight as IC-enriched fraction.
18. Resuspend pellet 2 from step 14 with 750 µL of RIPA lysis buffer to extract membrane-bound (MB) proteins.
19. Dissociate vigorously with 1 mL pipette (20 repeats), and vortex for 20 s. The mixture should be extremely viscous due to the high content of DNA and lipids.
20. Place the tube on a rotating platform for 15 min at 4°C to increase passive lysis.
21. Centrifuge at 16,100 × *g* for 90 min at 4°C. Save the pellets for step 25. (They should be fairly large, ~200 µL in volume, reflecting the amount of lipids/insoluble material present in tissues/cells).
22. Collect supernatant 4, the fraction corresponding to MB proteins.

23. Centrifuge supernatant 4 at 16,100×*g* for 90 min at 4°C.
24. Collect supernatants and store at –20°C overnight as MB-enriched fraction.
25. Resuspend pellet 3 from step 21 in 40 µL of freshly prepared 70% formic acid and dissociate pellets with 1 mL pipette (10 repeats minimum) followed by ten additional repeats using a 200 µL pipette. Samples must run smoothly in the pipette tips. Continue pipetting if the aspiration is uneven. Vortex thoroughly for 10 s and place in a thermomixer with agitation for 30 min at RT (1,200 rpm).
26. Add 760 µL of 1 M Tris-HCl (pH 8.0).
27. Dissociate with 1 mL pipette (20 repeats) until all material is fully resuspended.
28. Centrifuge at 16,100×*g* for 90 min at 4°C.
29. Save the pellets, which should be fairly small (~100 µL in volume), in case lysis was incomplete. Collect supernatant 4, the fraction corresponding to insoluble/aggregated proteins.
30. Centrifuge supernatant 4 at 16,100×*g* for 90 min at 4°C.
31. Concentrate samples (twofold) using a vacuum centrifuge set at room temperature for 150 min (see Note 4).
32. Collect supernatants and store at –20°C overnight as formic acid (FA)-enriched fraction.

Day 2

33. All saved fractions must be ultracentrifuged at 100,000×*g* for 30 min at 4°C (alternatively 16,100×*g* for 90 min). A faint pellet can be seen after overnight freezing depending on lipid raft contamination and DNA precipitation. Discard this pellet and save supernatants.
34. Once all fractions have been subjected to all necessary centrifugations, add 50 µL of IPDB-washed Fastflow® Protein G-sepharose beads (1:1 slurry) and agitate on a rotating platform for 1 h at 4°C. The purpose of this immunodepletion is to remove endogenous murine immunoglobulins that could cross-react with detection secondary antibodies or could be pulled down during the immunoprecipitation steps.
35. Centrifuge at 16,100×*g* for 5 min at 4°C.
36. Save supernatants and transfer into new 1.5 mL tubes. Add 50 µL of IPDB-washed Fastflow® Protein A-sepharose beads (1:1 slurry) and agitate on a rotating platform for 1 h at 4°C.
37. Centrifuge at 16,100×*g* for 5 min at 4°C.
38. Save supernatants and transfer into new 1.5 mL tubes. Now that samples have been immunodepleted, protein concentration can be assessed.
39. Determine protein concentration using a BCA protein assay.

3.2. Tris–Tricine SDS-PAGE and Western Blotting

Next, Aβ oligomers in the various fractions are separated by SDS-PAGE and detected by western blotting. Since Aβ monomers have a molecular weight lower than 20 kDa (4–4.5 kDa), tricine replaces glycine in the gel and appropriate buffers.

Day 1

1. Take sample out of the −20°C freezer and leave at room temperature until fully thawed. The time will depend on the volume of the aliquots, typically 15–20 min for 100 µL aliquots.
2. In a new 1.5 mL tubes, transfer 100 µg of proteins per sample.
3. Add 10 µL of 4× tricine loading buffer with βME into tubes
4. Place samples on thermomixer and boil at 95°C for 5 min under agitation (1,200 rpm).
5. Transfer tubes into a room temperature centrifuge and quick-spin for 10 s.
6. Load samples onto gel(s).
7. Load 3.5 µL of molecular weight marker standards and 0.1 µL of unboiled synthetic Aβ1-42 standard.
8. Run the gel under constant voltage of 80 V until the phenol red is running off, but the Coomassie brilliant blue is still visible, normally about 2 h and 45 min.
9. Thirty minutes before the end of the SDS-PAGE run, fill up the transfer tank (to two-third of the indicated maximum fill line, with a cold pack in place) with transfer buffer. Place magnetic stir-bar in the bottom of the Transfer tank (Fig. 1).
10. Carefully cut gel so that it can be laid onto the transfer sandwich properly. Cut off the stacking gel at the top with a sharp razor blade and remove the thicker lower part of the gel at the bottom of the gradient area in the same manner.
11. Assemble transfer sandwich on the black side of cassette in the following order:
    (a) one scotch bright pad
    (b) one blotting paper
    (c) gel with proteins
    (d) 0.2 µm nitrocellulose membrane
    (e) one blotting paper
    (f) one scotch bright pad.

    Preassemble your blotting pad and paper in a container filled with Transfer buffer to minimize air bubbles in the sandwich. Lay the gel on the pad already submerged into the container. Then, delicately remove all three from the container and place them on the black end of the cassette.

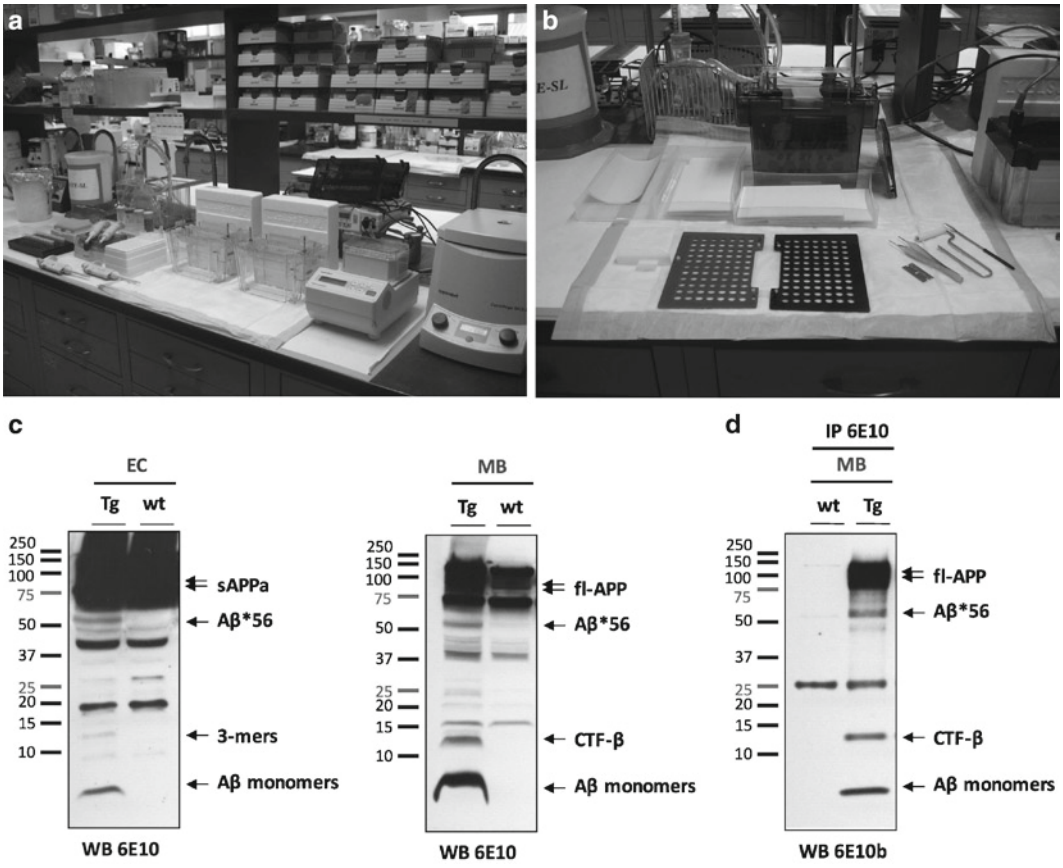

Fig. 1. *Preparation and expected results using the described method.* (**a**) SDS-PAGE setting using Criterion systems. (**b**) Layout of materials required for transferring proteins. (**c**) Representative western blot analyses of Aβ species using extracellular-enriched fractions (EC) or membrane-bound protein fractions (MB) from APP-over expressing mice and age-matched controls (J20 line). (**d**) Example of immunoprecipitation followed by western blot analysis using 6E10 as the capture antibody using the same MB extracts used in (**c**).

12. With forceps, place the prewet membrane (see Note 5) onto the preformed half-sandwich. Use roller to create appropriate contact (see Note 6). Finish forming the sandwich *layer by layer* and use a roller after creating each layer.
13. Close sandwich by locking the cassette, keeping pressure on left side, which minimizes chance that bubbles could be pushed back into the membrane area (see Note 7).
14. Place cassette/s in partially prefilled transfer system and finish filling with cold transfer buffer until your sandwiches are completely submerged.
15. Transfer proteins at constant current (400 mA) for 120–180 min at 4°C in a cold room on a stir plate (set at a spin rate of 3–4). Longer transfer times may be necessary for larger protein complexes while shorter durations will be appropriate for smaller proteins.

16. Before removing membrane(s) from the transfer unit, add 50 mL of PBS into an appropriately sized container.
17. Place 0.2 μm-nitrocellulose membrane(s) with the protein side facing up in the PBS.
18. Microwave for 25 s at maximum power (see Note 8).
19. Wait 3 min and flip the membrane over.
20. Microwave for 15 s at maximum power.
21. Wait 3 min.
22. Discard the PBS, add 20 mL of blocking buffer and agitate on orbital platform for 2 h at room temperature.
23. Add 8–10 μL of 6E10 (or biotinylated 6E10) antibody (1:2,000–2,500 final dilution) and probe overnight at 4°C in the cold room under agitation (see Note 9).

Day 2

24. Rinse membrane(s) with 20 mL of TTBS, gently agitate for 5 s and discard.
25. Wash membrane(s) with 20 mL of TTBS 5 × 5 min at room temperature. If using biotinylated primary antibody, proceed directly to step 29.
26. In 20 mL of blocking buffer, add antimouse IgG-biotinylated antibody (1:60,000–80,000 final dilution) and incubate for 60 min @ RT.
27. Rinse membrane(s) with 20 mL of TTBS, gently agitate for 5 s and discard.
28. Wash membrane(s) with 20 mL of TTBS 5 × 5 min at room temperature.
29. In 20 ml TTBS, add 4 μL of Neutravidin®-peroxidase conjugate (1:5,000 final dilution) and incubate for 10 min at room temperature under agitation.
30. Rinse membrane(s) with 20 mL of TTBS, gently agitate for 5 s and discard.
31. Wash membrane(s) with 20 mL of TTBS 5 × 5 min at room temperature.
32. Discard TTBS.
33. Add 10 ml of ECL reagent/membrane and incubate for 4 min under strong agitation, enough to entirely cover your membrane.
34. Using forceps, place membrane(s) in plastic sheet and place BioMax Kodak films for exposures of 1 s, 5 s, 15 s, 30 s, 1 min, 5 min, 15 min, 1 h (if necessary). When preparing for the 60 min exposure, stack two films to ensure that the signal of at least one of the films will not saturate.

3.3. Immunoprecipitation

In some cases, Aβ species may not be sufficiently abundant to be visible with the standard procedure described above. In the cases, it may be desirable to immunoprecipitate Aβ. Briefly, protein samples are incubated overnight with 6E10 and Protein-G sepharose beads, pulled down by centrifugation and washed under various conditions before loading denatured complexes onto SDS-PAGE. The correctly performed immunoprecipitations should result in increased sensitivity in the signal(s) detected.

Day 1

1. Thaw 100–250 μg of the protein extract of interest.
2. Add 0.2 μm-filtered IPBD buffer (plus protease inhibitors) to total volume of 1 mL.
3. Add 50 μL of IPDB-washed FastFlow® Protein-A sepharose beads (1:1 slurry) to ensure the absence of endogenous immunoglobulins in protein samples. It is important to repeat this immunodepletion step, even though it is performed as part of Subheading 3.2, to remove any remaining endogenous immunoglobulins, which would interfere with the IP.
4. Agitate on an orbital platform for 1 h at 4°C.
5. Centrifuge at 9,300 × *g* for 5 min at 4°C.
6. Save supernatants and transfer into a new 1.5 mL tube.
7. Add 5 μL of 6E10 antibody and 50 μL of IPDB-washed FastFlow® Protein-G sepharose beads (1:1 slurry).
8. Incubate overnight at 4°C on an orbital platform.

Day 2

9. Centrifuge at 9,300 × *g* for 5 min at 4°C.
10. Save supernatants and transfer into a new 1.5 mL tube. Store at –20°C until you have verified that all Aβ species were properly captured.
11. Add 1 mL of Wash Buffer A (plus protease inhibitors) into the tubes containing immune complexes and agitate on an orbital platform for 20 min at 4°C (see Note 10).
12. Centrifuge at 9,300 × *g* for 5 min at 4°C.
13. Aspirate supernatants manually or with a pump and add 1 mL of Wash Buffer B (plus protease inhibitors) into the tubes containing immune complexes and agitate on an orbital platform for 20 min at 4°C.
14. Centrifuge at 9,300 × *g* for 5 min at 4°C.
15. Aspirate supernatants manually or with a pump and add 25 μL of βME-containing 4×-tricine loading buffer.
16. Denature samples at 95°C for 7 min under agitation on a thermomixer.

17. Centrifuge denatured samples at 13,400 × *g* for 5 min at room temperature and load supernatants onto 10–20% Tricine SDS-PAGE gels, taking great care not to aspirate beads into the loading tips.
18. Follow the electrophoresis, transfer and western blot protocol as described above, but use 6E10-biotinylated to avoid cross-reactivity with the 6E10 antibodies used for the capture.

4. Notes

1. Use Eppendorf brand tips and pipettes for this protocol. Other brands will not have similar extremity tip sizes and could alter protein enrichment percentages.
2. Additionally, phosphatase inhibitor cocktails can be added if studies require phospho-dependent analyses.
3. We use Bio-Rad Criterion gels. These gels are 8.7 cm long and therefore allow a gain of 28% in length over a classic mini-gel. We prefer the 12 + 2 well format.
4. Make sure you do not concentrate your samples further. The duration of the concentration process must be tested by the user depending on the number of tubes processed (more tubes will translate into longer spin times because more solvent needs to be evaporated).
5. Nitrocellulose membranes (9 × 14.5 cm) should be prewetted for at least 2 min before laying it onto the gel in transfer buffer. If using a 0.2 μm PVDF membrane, activate your membrane by submersing it into 100% methanol.
6. As you create the sandwich, be sure to roll out any bubbles that might form. Use a roller and press gently each added layer of your sandwich alternating vertical and horizontal movement. Start vertically so that the upper and lower parts of your nitrocellulose membrane form a firm contact with the blotting paper below.
7. The sandwich should be tight. However, excessive pressure may compromise the gel/membrane interface.
8. Boiling the membrane will improve the detection of Aβ epitopes. Do not overheat as it will distort the nitrocellulose membrane.
9. First time users might want to use biotinylated 6E10. This will speed the protocol processing time and potentially lower background generated by secondary antibody. However, a drop in sensitivity will be observed (~2–3-fold).

10. Be extremely careful to not add Washing Buffers A or B directly onto the resin. Place your tip horizontally against the inside wall of the tubes before ejecting your solutions.

References

1. Haass, C., and Selkoe, D. J. (2007) Soluble protein oligomers in neurodegeneration: lessons from the Alzheimer's amyloid beta-peptide. *Nat Rev Mol Cell Biol* **8**, 101–12.
2. Walsh, D. M., Minogue, A. M., Sala Frigerio, C., Fadeeva, J. V., Wasco, W., and Selkoe, D. J. (2007) The APP family of proteins: similarities and differences. *Biochem Soc Trans* **35**, 416–20.
3. Selkoe, D. J., and Wolfe, M. S. (2007) Presenilin: running with scissors in the membrane. *Cell* **131**, 215–21.
4. Lesne, S., Koh, M. T., Kotilinek, L., Kayed, R., Glabe, C. G., Yang, A., Gallagher, M., and Ashe, K. H. (2006) A specific amyloid-beta protein assembly in the brain impairs memory. *Nature* **440**, 352–7.
5. Walsh, D. M., and Selkoe, D. J. (2007) A beta oligomers – a decade of discovery. *J Neurochem* **101**, 1172–84.
6. Cleary, J. P., Walsh, D. M., Hofmeister, J. J., Shankar, G. M., Kuskowski, M. A., Selkoe, D. J., and Ashe, K. H. (2005) Natural oligomers of the amyloid-beta protein specifically disrupt cognitive function. *Nat Neurosci* **8**, 79–84.
7. Walsh, D. M., Klyubin, I., Fadeeva, J. V., Cullen, W. K., Anwyl, R., Wolfe, M. S., Rowan, M. J., and Selkoe, D. J. (2002) Naturally secreted oligomers of amyloid beta protein potently inhibit hippocampal long-term potentiation in vivo. *Nature* **416**, 535–9.
8. Shankar, G. M., Li, S., Mehta, T. H., Garcia-Munoz, A., Shepardson, N. E., Smith, I., Brett, F. M., Farrell, M. A., Rowan, M. J., Lemere, C. A., Regan, C. M., Walsh, D. M., Sabatini, B. L., and Selkoe, D. J. (2008) Amyloid-beta protein dimers isolated directly from Alzheimer's brains impair synaptic plasticity and memory. *Nat Med* **14**, 837–42.
9. Cheng, I. H., Scearce-Levie, K., Legleiter, J., Palop, J. J., Gerstein, H., Bien-Ly, N., Puolivali, J., Lesne, S., Ashe, K. H., Muchowski, P. J., and Mucke, L. (2007) Accelerating amyloid-beta fibrillization reduces oligomer levels and functional deficits in Alzheimer disease mouse models. *J Biol Chem* **282**, 23818–28.
10. Lesne, S., Kotilinek, L., and Ashe, K. H. (2008) Plaque-bearing mice with reduced levels of oligomeric amyloid-beta assemblies have intact memory function. *Neuroscience* **151**, 745–9.

Chapter 5

Assessing Aβ Aggregation State by Atomic Force Microscopy

Justin Legleiter

Abstract

There has been a growing recognition of a wide variety of diseases commonly referred to as conformational diseases, which share the feature of specific disease-related proteins adopting nonnative conformation that promote their ordered aggregation and deposition on surfaces. Due to the nanoscale dimensions and the varied morphology of such aggregates, atomic force microscopy (AFM) has emerged as an ideal tool for distinguishing structural features of the numerous potential aggregate forms, ranging from small globular oligomers to large mature amyloid fibrils. Beyond the ability to morphologically distinguish aggregate forms, AFM also can dynamically track the aggregation process due to its unique ability to be operated not only in air (ex situ), but also in solution (in situ). This feature provides for tracking the fate of individual aggregates over time. This chapter describes the use of AFM in characterizing the aggregation of the amyloid-β peptide (Aβ), which is hypothesized to play a key role in Alzheimer's disease (AD), a late-onset neurodegenerative conformational disease.

Key words: Atomic force microscopy, Alzheimer's disease, Amyloid-β, Amyloid, Oligomers, Fibrils, Protofibrils

1. Introduction

A large and varied number of diseases, commonly classified as conformational diseases, involve the rearrangement of a specific protein to a nonnative conformation that promotes aggregation and deposition within tissues or cellular compartments. These conformational diseases include Alzheimer's disease (AD), Huntington's disease (HD), Parkinson's disease (PD), and many more (1, 2). A frequent emerging structural motif associated with the majority of these diseases is the formation of extended, β-sheet-rich, proteinaceous fibrillar aggregates, referred to as amyloids. Amyloid fibrils often comprise intertwined protofibrillar filaments.

Erik D. Roberson (ed.), *Alzheimer's Disease and Frontotemporal Dementia*, Methods in Molecular Biology, vol. 670,
DOI 10.1007/978-1-60761-744-0_5,

These protofibrils and fibrils have globular, soluble protein aggregate precursors, often termed oligomers (Fig. 1).

In the case of AD, the ordered aggregation of the β-amyloid peptide (Aβ) into fibrils and its subsequent deposition as extracellular neuritic plaques in the diseased brain is a major hallmark of the disease. Aβ is a cleavage product of the membrane-associated amyloid precursor protein (APP) (Fig. 2). Due to the progression of protein aggregates from globular precursors to mature fibrils,

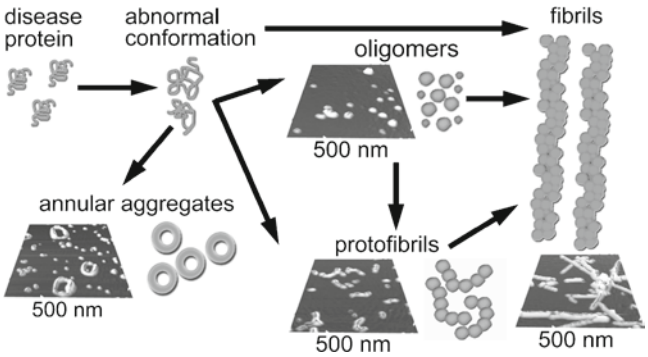

Fig. 1. Schematic potential pathway of neurodegenerative protein aggregation. Neurodegenerative protein aggregation begins with a disease protein that adopts an abnormal conformation and then proceeds through several aggregate intermediate stages that are characterized by distinct morphologies (i.e., oligomers, protofibrils, and annular structures) into mature fibrils that comprise inclusions commonly found in many diseases. Corresponding AFM images of different aggregate morphologies are from samples of Aβ.

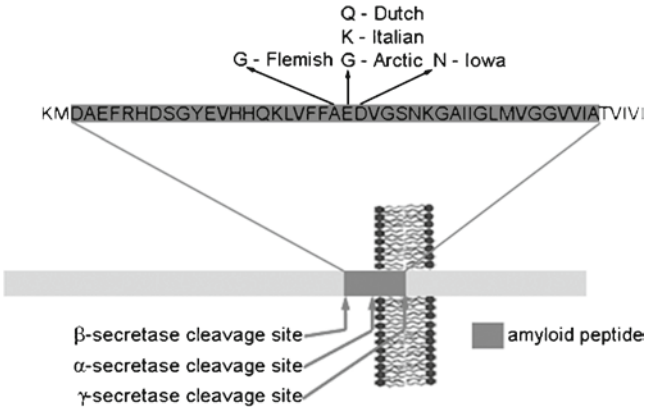

Fig. 2. Schematic representation of APP processing and point mutations in Aβ. α-secretase-mediated proteolytic cleavage of APP occurs after residue 687 of APP, β-secretase-mediated cleavage occurs after residue 671, and γ-secretase cleavage at position 711 or 713. Successive cleavage by β-secretase and γ-secretase results in the release of an intact Aβ peptide; whereas, the p3 fragment is a product of α-secretase and γ-secretase. Several point mutations in APP and Aβ are indicated.

there is an active debate as to which type of aggregate is the most relevant form of the misfolded peptide in disease progression. There is, therefore, a need for techniques that allow for distinguishing, both statically and dynamically, different morphological features of different aggregate species of Aβ. Atomic force microscopy (AFM) has emerged as a particularly useful technique to accomplish this task.

Since its invention in 1986 (3), AFM has become a standard technique in exploring nanoscale biophysical phenomena and has become an increasingly important technique in the study of disease-related protein aggregation. As AFM can be operated not only in air (ex situ), but also in solution (in situ), it has the unique ability to directly observe and track the behavior of individual Aβ aggregates on surfaces under physiological buffer conditions (4–6). The resolution of AFM when imaging Aβ aggregates is comparable to that achieved by transmission election microscopy (TEM); however, AFM does not require extensive sample preparations, such as staining, that prevent the applicability of TEM in kinetic studies. Furthermore, AFM provides three dimensional topography maps of surfaces, which can provide structural information that is not achievable from two dimensional cross-sectional profiles obtained by TEM.

The basic scheme and components of an AFM are shown in Fig. 3. In AFM, the force interaction between a sharp probe tip affixed to a flexible cantilever and surface is measured. A laser produced by a laser diode is reflected off the back of the cantilever and focused onto a position-sensitive photo detector, creating an optical lever capable of measuring the vertical deflection of the cantilever

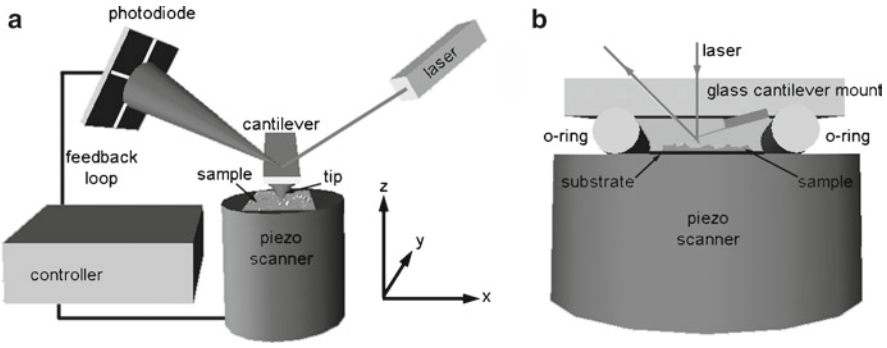

Fig. 3. Basic schematic of an atomic force microscope (AFM). (**a**) The laser beam produced by the laser diode is reflected off the back of a cantilever and then focused onto the position-sensitive photodetector, acting as an optical lever that can be used to determine the vertical displacement of the cantilever with subangstrom resolution. The cantilever is raster-scanned across the sample while monitoring the interaction between the surface and tip to reproduce topographical images. The feedback loop allows for the precise control of the force between the tip and sample, allowing for minimization of the interaction force and providing the ability to perform force-dependent experiments. (**b**) AFM can be easily implemented under liquids by use of a fluid cell.

with subangstrom resolution. Images are formed by raster-scanning the tip across the surface while using a feedback loop to monitor the force interactions between the tip and surface.

The three major operating modes of AFM are contact mode, tapping (or intermittent contact) mode, and noncontact mode. Owing to its ability to significantly minimize lateral forces associated with scanning, tapping mode is the most commonly applied of the three modes to study Aβ aggregates, and its basic operation is discussed here. During tapping mode operation, the cantilever is oscillated near its resonance frequency ω_o resulting in a "free" oscillation amplitude A_o. When the cantilever is placed in close proximity to the surface, the tip intermittently contacts (or taps) the surface, resulting in a decreased cantilever oscillation amplitude from the "free" amplitude to a "tapping" amplitude A. The image is acquired during raster-scanning over the sample by measuring the necessary adjustments to the vertical displacement of the scanner, via a feedback loop, to maintain the constant value of set-point ratio $s=A/A_o$. The feedback loop provides precise control over the cantilever amplitude minimizing the tapping force between the tip and surface.

2. Materials

1. Atomic force microscope system with in situ capabilities. Several systems have become commercially available from a variety of vendors (Veeco, Asylum Research, JEOL, Agilent, Omicron, Pacific Scanning, Quesant Instrument Corporation, and Accurion Scientific Instruments).
2. Standard fluid cell or fluid cell with piezoelectric actuator for your AFM system.
3. Low-spring-constant cantilever probes, e.g., silicon cantilevers with nominal spring constant of 40 N/m for ex situ AFM and 100-μm wide-legged silicon nitride cantilevers with nominal spring constant of 0.58 N/m for in situ tapping mode AFM (commercially available from several vendors: Veeco, Olympus, Asylume Research, BioForce, MikroMasch).
4. Hexafluoroisopropanol (HFIP).
5. Chemical fume hood.
6. Vacuum concentrator or similar to evaporate off organic solvents.
7. Dimethyl sulfoxide (DMSO).
8. Bath sonicator.
9. Phosphate-buffered saline (PBS) buffer of approx pH 7.4 or other appropriate buffer.

10. Mica.
11. Highly ordered pyrolitic graphite (HOPG).
12. Aβ(40, 42), or other fragments and mutant forms of Aβ that are commonly available from several vendors (see Note 1).
13. Nitrogen.
14. Ultra pure water.
15. Double-sided tape or other adhesive to immobilize substrates for imaging.
16. Support for substrates. This is dependent on the AFM system used. For some systems, this is simply a glass slide. Another commonly used support is metal pucks or discs that can be held in place on the AFM via a magnet.

3. Methods

Here, we describe protocols for synthetic Aβ sample preparation, handling, incubation, and deposition on substrates for both ex situ and in situ AFM characterization. Common methods for analyzing AFM data are also presented. Finally, incorporating other factors into AFM studies of Aβ is briefly discussed.

3.1. Preparation of Aβ Samples

A variety of solvents, such as HFIP, DMSO (4, 5), trifluoroacetic acid (TFA) (6), acetic acid (7), chloroform (8), physiological buffer (9, 10), and deionized water (11), have been used to for the initial solubilization of Aβ. Due to the structural heterogeneity contained in commercially available lyophilized stocks of Aβ peptide, organic solvents are commonly applied to remove any preexisting structures that can seed aggregation and to provide a reproducible starting point for aggregation reactions. Often, solvents are used in tandem to ensure complete disassociation of Aβ. Stock solutions of Aβ in organic solvents are then dissolved into a physiological buffer, e.g., PBS or Tris–HCl. A well-established procedure (12) that results in a reproducible preparation of predominately monomeric Aβ is described here.

1. As lyophilized Aβ is properly stored at −80°C in sealed glass vials, it is important to allow each vial to equilibrate to room temperature (~30 min) to prevent condensation upon opening the vial.
2. Once the vial has equilibrated to room temperature, the lyophilized Aβ is treated with 1,1,1,3,3,3-hexafluoro-2-propanol (HFIP), which has been shown to remove β-sheet structure, disrupt hydrophobic forces, and promotes α-helical secondary structure (13). When working with HFIP, a chemical fume

hood with adequate protection is required (refer to a material safety data sheet for HFIP for more information). Dilute the Aβ in HFIP to a final concentration of 1 mM. The resulting clear solution can be distributed between several microcentrifuge tubes, and the HFIP is then evaporated off in the fume hood. The clear peptide films that remain in the microcentrifuge tubes are further dried under vacuum in a SpeedVac to ensure complete removal of the HFIP. These peptide films can be stored desiccated for future use at −20°C.

3. Aβ peptide films are now easily dissolved in anhydrous DMSO with vigorous pipette mixing followed by ~10 min of bath sonication. As these stock solutions of Aβ in DMSO will be further diluted into a physiological aqueous buffer (see Note 2), it is important to prepare these stocks with a high enough concentration of Aβ (usually 2–10 mM but this can vary) so that the residual DMSO will be less than 0.5% of the total final volume. This will minimize the effects of residual DMSO in the final solution on Aβ.
4. Stock solutions of Aβ in DMSO can be diluted into the desired physiological buffer (PBS, Tris, etc.). To ensure the solubility of the Aβ into the physiological buffer, the buffer can be heated to 37°C before the addition of the DMSO Aβ stock solution. To ensure thorough mixing, the new solution should be gently vortexed for~1 min. This mixing initiates the aggregation process.
5. Freshly prepared solution can be sampled for AFM analysis (as described in Subheading 3.2) and should be relatively free of higher order aggregates.
6. Incubation of these solutions (at room, elevated, or cooler temperatures) results in aggregation into higher ordered structures such as oligomers, protofibrils, and fibrils. The time needed to form these different structures depends on concentration, temperature, and other buffer conditions. For example, lowering the pH of solution enhances the formation of fibrillar aggregates (12).

3.2. Ex Situ Studies of Aβ

Ex situ AFM experiments, i.e. imaging of dried Aβ samples in air, have provided many insights into the self-assembly of Aβ into higher ordered structures and is quickly becoming a standard technique for assessing Aβ aggregation state. A method for depositing samples of Aβ aggregates on a surface for AFM analysis is provided. As this procedure consists of deposition, washing, and drying steps, care must be taken in preparing samples to avoid perturbation or contamination of the original Aβ structures in solution. The major limitation of ex situ AFM is that it does not allow for the tracking of the same individual Aβ aggregate over

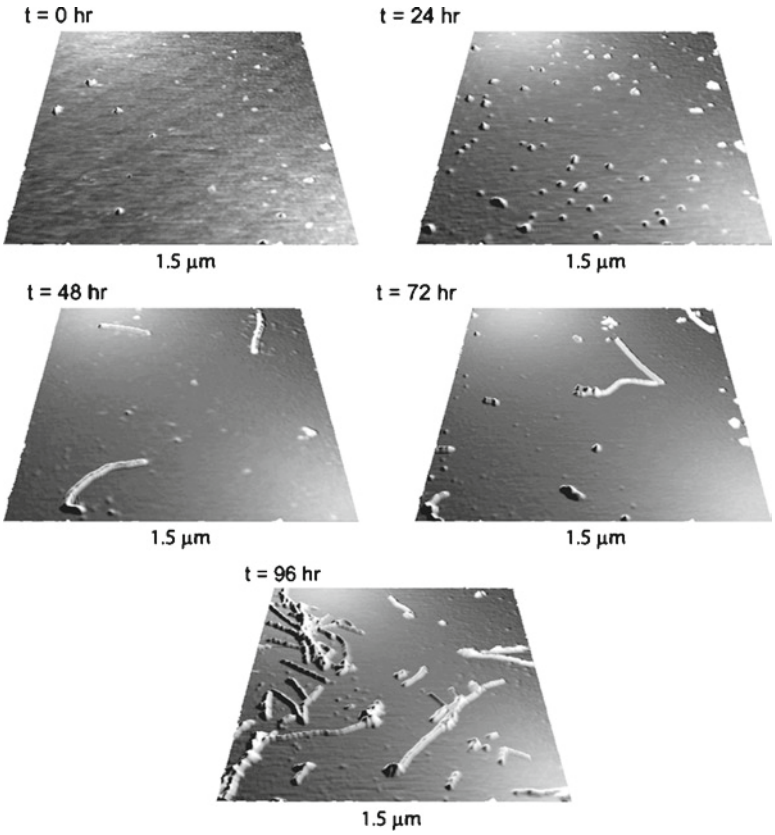

Fig. 4. A series of AFM height images of Aβ42 aggregates deposited on mica over a period of 96 h. Freshly prepared Aβ42 contained few small oligomers at 0 h of incubation. After 24 h, small oligomeric aggregates of Aβ42 were still present and appeared to be forming protofibrillar species. Short fibrils were evident after 48 h of incubation, and these fibrils increased in number and length through 72 and 96 h of incubation.

time (this is possible with in situ AFM); however, by sampling the same incubation at various time points, it is possible to determine the transition between different aggregate states over extended periods of time (days) (Fig. 4).

The key experimental component of ex situ AFM is deposition of Aβ onto a surface (substrate). To ensure reproducible results, a strict deposition protocol should be followed. Optimization of the deposition process for particular experimental conditions should be systematically carried out. Aβ concentrations can be adjusted to control the relative amount of deposited peptide on a surface. Practically speaking, sufficient bare substrate should be present between individual aggregates to provide a baseline for aggregate dimension measurements, such as height. The following is a brief protocol for Aβ deposition onto mica that can be easily adapted to other surfaces.

1. Using a brightly colored marker pen, mark the backside of a piece of rectangular piece of mica (~1 in. by 0.5 in.) with a

small dot near one end of the substrate to aid in aligning the cantilever over the deposited sample later. The colored marker is easier to distinguish from other spurious features on the surface from an overhead optical microscope view during alignment. Cleave the mica to expose a clean surface for deposition.

2. Take an aliquot of 2–5 μL from the incubating Aβ. solution with a pipettor and deposit it on the mica surface directly above the dot (make sure the actual marking is on the back of the mica and not on the side you are placing the sample). The deposited droplet is left on the substrate for ~30 s to 2 min based on the concentration of the Aβ solution and the desired coverage of aggregates on the mica.
3. Next, wash the sample with 200 μL of ultrapure water to remove excess salts and unbound peptide. To prevent damage to Aβ aggregates (broken fibrils) and other artifacts, tilt the substrate ~45°, apply the wash above the sample and allow it to gently flow over the deposited sample. It is also useful to place the bottom edge of the mica on a Kimwipe to absorb the excess wash and prevent it from flowing back onto the deposited sample. From this point on, only handle the mica substrate along its edges to prevent accidental contamination of the sample.
4. Gently blow the sample dry under a gentle stream of nitrogen to prevent contamination.
5. Using double-sided tape or a similar adhesive, the dry piece of mica can be mounted onto a substrate support with the sample exposed for imaging. If the AFM system requires round metal pucks as sample supports, the excess mica can be trimmed away using scissors. The sample is now ready to be imaged by ex situ tapping mode AFM.

3.3. In Situ Studies of Aβ

The use of in situ tapping mode AFM (TMAFM) offers the ability to dynamically observe the aggregation process on surfaces (see Note 3 and Fig. 5), and it has been successfully applied to the study of Aβ aggregation (5, 9, 14). Time lapse imaging of Aβ samples by in situ AFM can be used to study dynamic aggregation process and allows direct observation of the initial aggregation of Aβ into higher ordered structures.

1. Choose a substrate. A major issue in using in situ TMAFM to study Aβ aggregation is the choice of substrate. Different surface properties of the substrate can strongly influence the aggregation rate and morphology of resulting aggregates. Surface interactions can play an important role in both aggregation and deposition of Aβ. Two commonly used model surfaces are mica and HOPG, both of which are easily cleaved

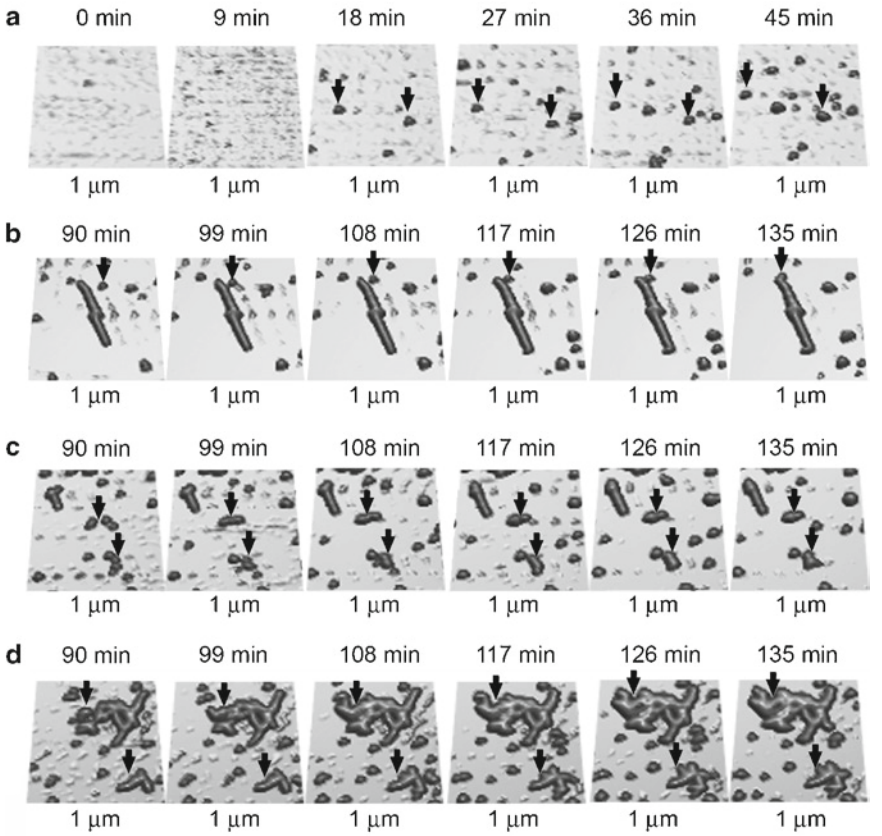

Fig. 5. In situ tapping mode AFM makes it possible to track the fate of individual Aβ aggregates. (**a**) The *arrows* indicate the appearance and relative stability of discrete oligomeric aggregates. (**b**) *Arrows* point out the movement of an oligomeric aggregate and its eventual incorporation into a growing fibril structure. (**c**) *Arrows* show groups of oligomers that coalesce to form putative protofibrillar aggregates. (**d**) The *arrows* highlight the growth of intertwined fibrillar structures as a function of time.

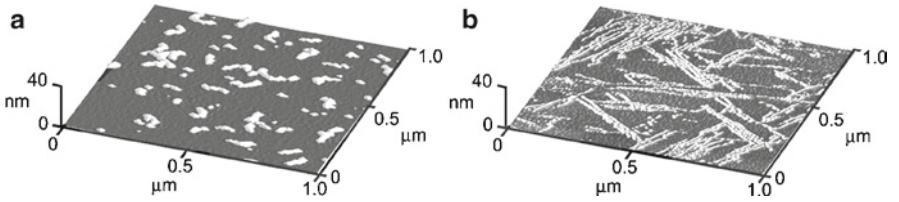

Fig. 6. Comparison of Aβ42 aggregates observed by in situ AFM on (**a**) mica and (**b**) graphite. (**a**) On mica, Aβ42 forms discrete globular species that coalesce to form extended protofibrillar structures. (**b**) When imaged on graphite, Aβ42 forms extended ribbon-like structures that preferentially align along the graphite lattice.

to provide clean flat surfaces. Aβ forms morphologically distinct aggregates on the charged hydrophilic mica compared to hydrophobic HOPG (Fig. 6) (5, 14). A more physiologically relevant surface for in situ AFM experiments can be provided by various supported lipid bilayers (6, 15–17).

2. Obtain a background image of neat buffer to ensure the cleanliness of the AFM fluid cell.
3. Then, inject a freshly prepared Aβ sample (as described in Subheading 3.1) directly into the fluid cell.
4. Image the same area continuously for the duration of the experiment. Care must be taken not to use too high a concentration of Aβ to prevent completely covering the surface.

3.4. Quantitative Analysis of AFM Images

Quantitative analysis of AFM images can easily be carried out with the aid of computer programs designed for image analysis. Common measurements used to study Aβ aggregates are height, diameter, volume, and contour length. Often, these measurements will be indicative of specific types of aggregates (Fig. 7) and can be used to determine the relative amounts of aggregate types in heterogeneous mixtures of Aβ aggregates (see Notes 4 and 5).

As the finite size and shape if the tip always contributes to the lateral dimensions of aggregates observed in AFM images (Fig. 8), it is important to take this into account when interpreting AFM results, especially when different cantilevers or imaging conditions were used. Damaged or contaminated tips can lead to several artifacts, such as double images.

There are several methods for characterizing and estimating the contribution due to the finite size and shape of the tip. These include the use of tip characterizers (18) and blind tip reconstruction (19).

A simple, yet useful, quantitative measurement is the number of specific aggregates, defined by a morphological characteristic, per unit area appearing on the surface as a function of time (4, 5, 9). This type of analysis has been used to show that smaller aggregates disappear as protofibrils and fibrils form (4, 5, 9). This method has also been useful in determining the effect of different agents (i.e., small molecules, lipoproteins, and antibodies) on the Aβ aggregation process (10, 20, 21) as well as the effect of specific point mutations in Aβ (22).

Changes in physical attributes of Aβ aggregates over time can provide insight into the aggregation process. For instance, rate of fibril elongation can be determined by measuring the change in length of individual fibrils over time by in situ AFM (4, 9).

3.5. Incorporating Other Factors into AFM Studies of Aβ

AFM can also provide the direct observation of interactions of Aβ aggregates with other biologically relevant agents, which potentially inhibit or reverse disease-related aggregation. In this regard, AFM has been used to study the interaction of Aβ with anti-Aβ antibodies, lipid bilayers, glycerol and trimethylamine *N*-oxide (which act as chemical chaperones) (6, 8, 10, 15–17, 21–23).

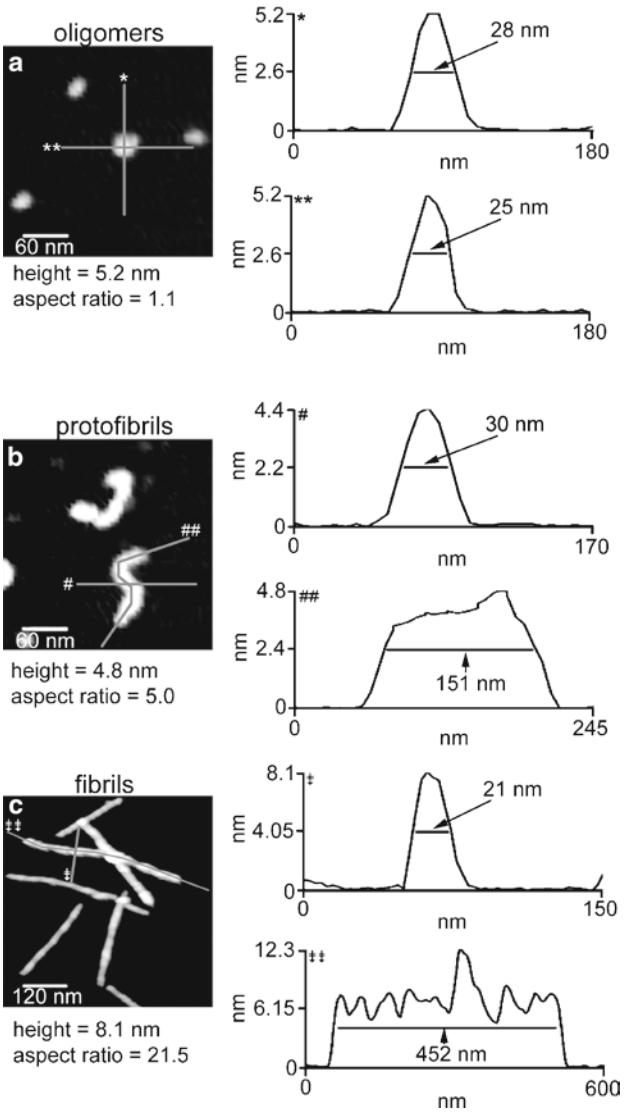

Fig. 7. AFM images and aggregate profiles that compare basic dimensions of (**a**) oligomers, (**b**) protofibrils, and (**c**) fibrils of Aβ42. Profiles on the *right* are indicated in each AFM image. By using a combination of height and aspect ratio, it is possible to distinguish relative populations of these aggregates from a heterogeneous mixture.

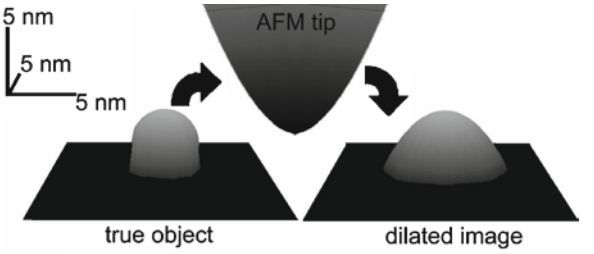

Fig. 8. Due to the finite size and shape of the AFM probe tip, the lateral dimensions observed in AFM are larger than the true dimensions of the nanosized particles being imaged.

AFM has proven useful in determining the effects of Aβ on cells (8, 11). Although Aβ was not directly observed in images of endothelial cells, the vitality of individual cells based on mechanical and morphological cellular properties can be explored.

4. Notes

1. Aβ40 aggregates at a slower rate than Aβ42 (24), and these different aggregation rates could prove useful for experimental design. Furthermore, several point mutations in Aβ have also been shown to alter aggregation rates (25–31).
2. Whenever performing AFM experiments, it is a good idea to check the cleanliness of your buffer by preparing a blank sample of buffer alone by the same deposition protocol. Often times if a buffer contains spurious particles when deposited on a substrate, filtering your buffers will alleviate this problem.
3. When using in situ AFM, the imaging forces (tapping forces) are much higher in comparison to operation in air. This is due to the viscous damping of the cantilever motion in solution. These higher imaging forces have the potential to damage or sweep away loosely bound fragile aggregates of Aβ. Care must be taken to minimize imaging forces, which is most often accomplished using low excitation amplitudes and set points. An alternative strategy is to use active resonance *Q*-control (32–35).
4. Dimensions used to distinguish aggregate types in a heterogeneous mix of aggregates include height and aspect ratio (length/width). Oligomer structures are often shorter than fibrils. Although oligomers are often similar in height to protofibrils, the two aggregate types have different aspect ratios.
5. There are several options available for software to analyze AFM images. Most commercially available AFMs come with some type of software package. There are also other software packages available such as the Scanning Probe Image Processor (SPIP) from Image Metrology and the freeware WSxM software from Nanotec Electronica. MatLab from Mathworks can be used with their image processing toolbox to custom write routines to quickly analyze AFM images based on your specific needs. To get started, code that can be used to open and import data into MatLab from several commercially available AFM systems can be found on the MatLab Central user community web forum.

Acknowledgments

Financial support from West Virginia University (start-up grant) is gratefully acknowledged.

References

1. Žerovnik, E. (2002) Amyloid-fibril formation: proposed mechanisms and relevance to conformationl disease. *Eur. J. Biochem.* **269**, 3362–71.
2. Chiti, F., and Dobson, C. M. (2006) Protein misfolding, functional amyloid, and human disease. *Annu. Rev. Biochem.* **75**, 333–66.
3. Binnig, G., Quate, C. F., and Gerber, C. (1986) Atomic force microscope. *Phys. Rev. Lett.* **56**, 930–33.
4. Harper, J. D., Wong, S. S., Lieber, C. M., and Lansbury, P. T., Jr. (1999) Assembly of Aβ amyloid protofibrils: an in vitro model for a possible early event in Alzheimer's disease. *Biochemistry* **38**, 8972–80.
5. Kowalewski, T., and Holtzman, D. M. (1999) In situ atomic force microscopy study of Alzheimer's β-amyloid peptide on different substrates: new insights into mechanism of beta-sheet formation. *Proc. Natl. Acad. Sci. U S A.* **96**, 3688–93.
6. Yip, C. M., Elton, E. A., Darabie, A. A., Morrison, M. R., and McLaurin, J. (2001) Cholesterol, a modulator of membrane-associated Aβ-fibrillogenesis and neurotoxicity. *J. Mol. Biol.* **311**, 723–34.
7. Blackley, H. K., Patel, N., Davies, M. C., Roberts, C. J., Tendler, S. J., Wilkinson, M. J., and Williams, P. M. (1999) Morphological development of Aβ(1-40) amyloid fibrils. *Exp. Neurol.* **158**, 437–43.
8. Lin, H., Bhatia, R., and Lal, R. (2001) Amyloid β protein forms ion channels: implications for Alzheimer's disease pathophysiology. *FASEB J.* **15**, 2433–44.
9. Blackley, H. K. L., Sanders, G. H. W., Davies, M. C., Roberts, C. J., Tendler, S. J. B., and Wilkinson, M. J. (2000) In-situ atomic force microscopy study of β-amyloid fibrillization. *J. Mol. Biol.* **298**, 833–40.
10. Yang, D. S., Yip, C. M., Huang, T. H., Chakrabartty, A., and Fraser, P. E. (1999) Manipulating the amyloid-β aggregation pathway with chemical chaperones. *J. Bio. Chem.* **274**, 32970–4.
11. Bhatia, R., Lin, H., and Lal, R. (2000) Fresh and nonfibrillar amyloid β protein(1-42) induces rapid cellular degeneration in aged human fibroblasts: evidence for AβP-channel-mediated cellular toxicity. *FASEB J.* **14**, 1233–43.
12. Stine Jr., W. B., Dahlgren, K. N., Krafft, G. A. and LaDu, M. J. (2003) In vitro characterization of conditions for amyloid-β peptide oligomerization and fibrillogenesis. *J. Bio. Chem.* **278**, 11612–22.
13. Barrow, C. J., Yasuda, A., Kenny, P. T. M., and Zagorski, M. G. (1992) Solution conformations and aggregational properties of synthetic amyloid β-peptides of Alzheimer's disease: analysis of circular dichroism spectra. *J. Mol. Biol.* **225**, 1075–93.
14. Wang, Z., Zhou, C., Wang, C., Wan, L., Fang, X., and Bai, C. (2003) AFM and STM study of β-amyloid aggregation on graphite. *Ultramicroscopy.* **97**, 73–79.
15. Yip, C. M., Darabie, A. A., and McLaurin, J. (2002) Aβ42-peptide assembly on lipid bilayers. *J. Mol. Biol.* **318**, 97–107.
16. Yip, C. M., and McLaurin, J. (2001) Amyloid-β assembly: a critical step in fibrillogensis and membrane disruption. *Biophys. J.* **80**, 1359–71.
17. Choucair, A., Chakrapani, M., Chakravarthy, B., Katsaras, J., and Johnston, L. J. (2007) Preferential accumulation of Aβ(1-42) on gel phase domains of lipid bilayers: an AFM and fluorescence study. *Biochim. Biophys. Acta* **1768**, 146–54.
18. Xu, S., and Ansdorf, M. F. (1994) Calibration of scanning (atomic) force microscope with gold particles. *J. Microsc.* **173**, 199–210.
19. Villarrubia, J. S. (1997) Algorithms for scanned probe microscope image simulation, surface reconstruction, and tip estimation. *Natl. Inst. Stand. Technol.* **102**, 425.
20. Lambert, M. P., Barlow, A. K., Chromy, B. A., Edwards, C., Freed, R., Liosatos, M., Morgan, T. E., Rozovsky, I., Trommer, B., Viola, K. L., Wals, P., Zhang, C., Finch, C. E., Krafft, G. A., and Klein, W. L. (1998) Diffusible, nonfibrillar ligands derived from Aβ1-42 are potent central nervous system neurotoxins. *Proc. Natl. Acad. Sci. U S A.* **95**, 6448–53.
21. Legleiter, J., Czilli, D., Dematttos, R., Gitter, B., Holtzman, D., and Kowalewski, T. (2004)

Effect of different anti-Aβ antibodies on Aβ fibrillogenesis as assessed by atomic force microscopy. *J. Mol. Biol.* **335**, 997–1006.

22. Rhee, S. K., Quist, A. P., and Lal, R. (1998) Amyloid β protein-(1-42) forms calcium-permeable, Zn^{2+}-sensitive channel. *J. Biol. Chem.* **273**, 13379–82.
23. Lin, H., Zhu, Y. J., and Lal, R. (1999) Amyloid-β protein (1-40) forms calcium-permeable, Zn2 + -sensitive channel in reconstituted lipid vesicles. *Biochemistry.* **38**, 11189–96.
24. Cai, X. D., Golde, T. E., and Younkin, S. G. (1993) Release of excess amyloid β protein from a mutant amyloid β protein precursor. *Science* **259**, 514–16.
25. Cheng, I. H., Scearce-Levie, K., Legleiter, J., Palop, J. J., Gerstein, H., Bien-Ly, N., Puolivali, J., Lesne, S., Ashe, K. H., Muchowski, P. J., and Mucke, L. (2007) Accelerating amyloid-β fibrillization reduces oligomer levels and functional deficits in Alzheimer disease mouse models. *J. Biol. Chem.* **282**, 23818–28.
26. De Jonghe, C., Zehr, C., Yager, D., Prada, C. M., Younkin, S., Hendriks. L., Van Broeckhoven, C., and Eckman, C. B. (1998) Flemish and Dutch mutations in amyloid β precursor protein have different effects on amyloid β secretion. *Neurobiol. Dis.* **5**, 281–86.
27. Miravalle, L., Tokuda, T., Chiarle, R., Giaccone, G., Bugiani, O., Tagliavini, F., Frangione, B., and Ghiso, J. (2000) Substitutions at codon 22 of Alzheimer's Aβ peptide induce diverse conformational changes and apoptotic effects in human cerebral endothelial cells. *J. Biol. Chem.* **275**, 27110–16.
28. Watson, D. J., Selkoe, D. J., and Teplow, D. B. (1999) Effects of the amyloid precursor protein Glu693Gln "Dutch" mutation on the production and stability of amyloid β-protein. *Biochem. J.* **340**, 703–9.
29. Sian, A. K., Frears, E. R., El-Agnaf, O. M., Patel, B. P., Manca, M. F., Siligardi, G., Hussain, R., and Austen, B. M. (2000) Oligomerization of β-amyloid of the Alzheimer's and the Dutch-cerebral-haemorrhage types. *Biochem. J.* **349**, 299–308.
30. Nilsberth, C., Westlind-Danielsson, A., Eckman, C. B., Condron, M. M., Axelman, K., Forsell, C., Stenh, C., Luthman, J., Teplow, D. B., Younkin, S. G., Naslund, J., and Lannfelt, L. (2001) The "Arctic" APP mutation (E693G) causes Alzheimer's disease by enhanced Abeta protofibril formation. *Nat. Neurosci.* **4**, 887–93.
31. Van Nostrand, W. E., Melchor, J. P., Cho, H. S., Greenberg, S. M., and Rebeck, G. W. (2001) Pathogenic effects of D23N Iowa mutant amyloid β – protein. *J. Biol. Chem.* **376**, 32680–3266.
32. Humphris, A., Tamayo, J., and Miles, M. (2000) Active quality factor control in liquids for force spectroscopy. *Langmuir* **16**, 7891–94.
33. Humphris, A. D. L., Round, A. N., and Miles, M. J. (2001) Enhanced imaging of DNA via active quality factor control. *Surf. Sci.* **491**, 468–72.
34. Tamayo, J., Humphris, A., and Miles, M. (2000) Piconewton regime dynamic force microscopy in liquid. *Appl. Phys. Lett.* **77**, 582–84.
35. Tamayo, J., Humphris, A. D. L., and Miles, M. J. (2001) High-Q dynamic force microscopy in liquid and its application to living cells. *Biophys. J.* **81**, 526–37.

Chapter 6

Measuring APP Carboxy-Terminal Fragments

Luke A. Esposito

Abstract

The accumulation of the amyloid-β (Aβ) peptide in the form of insoluble fibrillar deposits and soluble oligomeric aggregates is widely believed to play a causal role in Alzheimer's disease (AD). Proteolytic cleavage of APP by the β-site APP cleaving enzyme (BACE1) near the C-terminus results in the formation of the APP C-terminal fragment (CTF) C99, a substrate for subsequent cleavage by γ-secretase to generate Aβ. Alternatively, APP cleavage by α-secretase to generate the APP CTF C83 occurs within the Aβ region, precluding its formation. Therefore, modulation of β- and/or γ-secretase activity represents important therapeutic targets. Transgenic mice overexpressing human APP generate detectable levels of APP CTFs and Aβ. We have shown that highly sensitive and specific methods for determining levels of APP CTFs and Aβ are useful for understanding how genetic manipulation of APP processing impacts Aβ generation and accumulation.

Key words: Amyloid precursor protein, APP C-terminal fragments, Aβ, Western blot, Alzheimer's disease, BACE

1. Introduction

The amyloid precursor protein (APP) undergoes serial proteolysis by β-secretase (β-site APP cleaving enzyme, BACE1) and γ-secretase to generate the 4 kDa amyloid-β peptide (Aβ) (reviewed in (1)). BACE1 first cleaves APP to generate a 99-amino acid membrane-associated C-terminal fragment (CTF) known as APP-C99 (C99). C99 then undergoes regulated intramembrane proteolysis by γ-secretase to release Aβ and the APP intracellular domain (AICD). An alternative nonamyloidogenic APP processing pathway precludes Aβ formation by substituting α-secretase cleavage, which cuts within the Aβ region and generates APP-C83 (C83), for β-secretase cleavage (reviewed in (2)). The imprecise cleavage sites of BACE1 and γ-secretase result in a heterogeneous collection of

Erik D. Roberson (ed.), *Alzheimer's Disease and Frontotemporal Dementia*, Methods in Molecular Biology, vol. 670,
DOI 10.1007/978-1-60761-744-0_6,

N- and C-terminally truncated Aβ peptides. The most common Aβ isoform is $A\beta_{1-40}$, whereas the more aggregation prone $A\beta_{1-42}$ is less prevalent under normal conditions. However, the production of $A\beta_{1-42}$ is enhanced in certain forms of familial AD by mutations in either APP or presenilin proteins (a primary component of the γ-secretase complex), thus increasing its proportion relative to $A\beta_{1-40}$ (reviewed in (2, 3)). APP is phosphorylated at sites near the C-terminus, and it is believed that phosphorylated APP and/or C99 are preferred substrates for β- and/or γ-secretase (4, 5). Since pharmacological, dietary, or genetic manipulations that are designed to limit Aβ production or accumulation may do so by altering α-, β- or γ-secretase activity, the measurement of APP CTF levels (an indirect measure of secretase activity), along with corresponding Aβ levels, may provide mechanistic resolve on their course of action (6–8). Therefore, we present methods for measuring the levels of APP CTFs and Aβ using high-resolution gel electrophoresis and Western blotting as a tool to elucidate the effects of genetic or pharmacological manipulations targeting APP processing and Aβ generation.

To measure APP CTFs, brain samples are lysed in a suitable detergent-free buffer and subjected to differential centrifugation to enrich for membrane-bound proteins. Electrophoretic separation of APP CTFs is facilitated with large (15 × 15 cm) Tris/Tricine/SDS-polyacrylamide gels, which offer superior resolution to commercially available mini-gels. APP CTFs and their phosphorylated forms are detected on Western blots with an appropriate APP C-terminal antibody. The ability to detect CTFs is dependent on the level of APP expression. For medium-to-high expressing APP mouse lines, such as J20 (APP_{FAD}) and I5 (APP_{WT}) lines (9) or the APP_{FAD} line 41 (10), 50–75 μg of protein per lane is sufficient, but in transgenic lines that express less APP, 100 μg or more protein per lane is necessary. APP CTFs are not readily available as standards, therefore, brains or cells expressing hAPP with mutations that elicit predictable patterns of APP CTFs (for example, APP_{WT} yields predominantly α-secretase-derived C83 whereas APP_{Swe} would result in a shift toward more β-secretase-derived C99 and a reduction in C83) are used to aid in establishing the molecular identity of Western blot bands (10).

For the examination of Aβ peptides from brain tissue, formic acid denaturation allows complete separation of Aβ from any known binding proteins that may have adverse effects on Aβ detection and quantification. Furthermore, formic acid denaturation facilitates electrophoresis and quantitation by Western blot by fully reducing aggregated Aβ to its monomeric form. Separation of the Aβ species by acetic acid urea polyacrylamide gel electrophoresis has three distinct advantages over traditional SDS/PAGE for the analysis of Aβ. First, it allows for the detection of low abundance Aβ because large amounts of protein (up to 3 mg) can

be loaded in a single lane. Second, its high resolution separates a variety of Aβ species (for example $A\beta_{1-38}$ vs $A\beta_{1-40}$ vs. $A\beta_{1-42}$ or N-terminally truncated Aβs). Finally, it is run in acidic conditions that allow formic acid-extracted Aβ to be loaded without prior neutralization.

The following protocol (adapted from (11)) is used here to detect human Aβ from transgenic mouse brain, although it is also suitable for human brain as well as systems where Aβ levels may be low, such as intracellular Aβ in cultured cells (12). This method also allows electrophoretic separation of rodent Aβs from human Aβs due to primary sequence changes at three amino acids that affect the overall size to charge ratio of the peptide. As such, rodent Aβ is distinguishable from human Aβ using an antibody that cross-reacts with both.

2. Materials

2.1. Brain Lysis and Fractionation for APP CTFs

1. Sucrose/HEPES lysis buffer (50 mL): 320 mM sucrose, 5 mM HEPES, 5 mM benzamidine, 3 mM EGTA, 500 μM $MgSO_4$, 500 μM $ZnSO_4$, adjust to pH 7.4 with 1.0 N NaOH, filter sterilize, add 0.0156% (vol/vol) 2-mercaptoethanol, store up to 1 month at 4°C. On day of use, add complete protease inhibitor (Roche) + pepstatin at 1 μg/mL final.
2. Kontes tissue grinder, size 18.

2.2. Tris/Tricine SDS-Polyacrylamide Gel Electrophoresis for APP C-Terminal Fragments

1. Gel apparatus for running large (15 × 15 cm) gels.
2. Rinsable detergent for cleaning glass plates, such as Alconox.
3. 4× Tris/Cl/SDS buffer: 0.50 M Tris base, adjust pH to 6.8 with HCl, filter with 0.45 μm pore size filter, add SDS to 0.4% (w/vol). Store at 4°C up to 1 month.
4. 2× Tricine sample buffer: Mix 2.0 mL 4× Tris/Cl/SDS buffer pH 6.8 with 2.4 mL glycerol (24%; vol/vol), 0.8 g SDS (8%; w/vol), 0.31 g dithiothreitol (20 mM), and 2 mg Coomassie G-250 (0.02%; w/vol). Add water to 10 mL final and store at room temperature.
5. Tris/Cl/SDS pH 8.45: 3 M Tris base, adjust the pH to 8.45 with HCl and adjust volume to 500 mL final. Pass through 0.45 μm pore size filter, add 1.5 g SDS (0.3%; w/vol) and store at 4°C for up to 1 month.
6. Cathode buffer (top chamber): 100 mM Tris base, 100 mM Tricine, and 0.1% (w/vol) SDS (do not adjust pH). Store at 4°C.
7. 10× Anode buffer (bottom chamber): 2 M Tris base, adjust pH to 8.9 with HCl. Store at 4°C.

8. 40% Acrylamide/Bis solution (37.5:1).
9. Ammonium persulfate (APS), 10% (w/vol) solution in water. Prepare fresh for each experiment.
10. TEMED solution. Once opened, store at room temperature up to 2 months.
11. Water-saturated N-butanol. Shake equal volumes of water and N-butanol in a glass bottle and allow separation. Use the top layer. Store at room temperature.
12. Glycerol.
13. Prestained molecular weight markers: Precision Plus molecular weight markers (Bio-Rad).

2.3. Western Blot for APP C-Terminal Fragments

1. 20× transfer buffer (1 L): 200 mM Tris base, 2 M glycine (do not adjust pH).
2. 1× transfer buffer: 200 mL 20× stock, 3 L water, and 800 mL methanol (20% vol/vol). Prepare day before use and store at 4°C.
3. 10× Tris-buffered saline (10× TBS): 248 mM Tris base, 1.37 M NaCl, 27 mM KCl, and adjust pH to 7.4 with concentrated HCl. Store at room temperature.
4. 1× Tris-buffered saline/Tween-20 (0.05%; vol/vol) (TBS-T): 200 mL 10× TBS, 1.8 L distilled water, and 1 mL Tween-20 (Bio-Rad). Store at room temperature up to 1 week.
5. Ponceau S solution.
6. Blocking buffer and primary antibody dilution buffer: 5% (w/vol) nonfat dry milk (Bio-Rad) in TBS-T.
7. Primary antibodies: CT-15 (generous gift of Dr. Eddie Koo, U. California San Diego) (see Note 1); 22C11 (Roche Biochemicals); 8E5 (generous gift of Elan Pharmaceuticals); α-tubulin (Sigma); Phospho-APP Thr 668 antibody (Cell Signaling Technology).
8. Secondary antibody: anti-rabbit IgG conjugated to horseradish peroxidase (GE Healthcare/Amersham Biosciences), anti-mouse IgG conjugated to horseradish peroxidase (Cell Signaling Technology).
9. SuperSignal West Pico chemiluminescent (ECL) substrate (Pierce Biochemicals) and Bio-Max ML film (Kodak).

2.4. Brain Lysis for Measurement of Aβ Peptides

1. Formic Acid (>97%) (MP Biochemicals).
2. Wheaton Dounce style homogenizer with "tight" pestle.
3. Polyallomer ultracentrifuge tube.
4. Human $A\beta_{1-40}$ and $A\beta_{1-42}$ (BioPeptide, San Diego, CA) and mouse $A\beta_{1-40}$ (AnaSpec, San Jose, CA) at 1 mg/mL in fresh

80% (vol/vol) formic acid. Aliquot and store at −80°C. 10 ng/μL and 1 ng/μL solutions in 80% (vol/vol) formic acid, store up to 1 month at −80°C.

2.5. Acetic Acid Urea PAGE for Measurement of Aβ Peptides

1. 40% Acrylamide/Bis (37.5:1).
2. APS and TEMED (see Subheading 2.2, items 9 and 10).
3. Glacial acetic acid.
4. Urea.
5. 6× sample loading buffer: 80% (vol/vol) formic acid, 60% (w/vol) sucrose, 0.03% (w/vol) methyl green. Heat and vortex >1 h to completely solubilize. Store at room temperature.
6. 2-mercaptoethanol.
7. 5% (w/vol) bovine serum albumin (BSA) in water (for blank lanes).
8. Molecular weight markers, M.W. range 2,512–16,949 Da (GE Healthcare/Amersham Biosciences). Markers are reconstituted in 1 mL phosphate-buffered saline pH 7.4 (and not according to manufacturer's recommendations). Prepare 10 μL aliquots and store at −20°C.
9. Running buffer: 6.25% (vol/vol) glacial acetic acid in water.
10. Phosphate-buffered saline (PBS), pH 7.4: reconstitute from preweighed powder (Sigma).
11. Acrylamide solutions: 6 M urea, 10% (vol/vol) glacial acetic acid, and the following concentrations of acrylamide/bis from the 40% stock solution: 22%, 10%, and 4% (vol/vol). Prepare 32 mL of the 22% solution, 8 mL of the 10% solution, and 16 mL of the 4% solution (per gel).
12. Blocking solution: 5% (w/vol) nonfat milk in TBS-T.
13. Antibody dilution buffer : 1% (w/vol) nonfat milk in TBS-T.
14. Primary antibody: 1.0 μg/mL m266; 1.6–3.0 μg/mL 3D6 (generous gifts of Elan Pharmaceuticals); 1.0 μg/mL 4G8 (Covance, Madison, WI); 1.0 μg/mL 6E10 (Covance); 20 μg/mL Bam 10 (Sigma).
15. Primary antibody wash solution: 1% (w/vol) BSA in TBS-T.
16. Secondary antibody: anti-mouse IgG conjugated to horseradish peroxidase (Cell Signaling).
17. Transfer buffer (4L): 25 mM Tris base, 0.2 M glycine, 20% (vol/vol) methanol, make up the day before use, and store at 4°C.
18. ECL reagent (see Subheading 2.3, item 9).

3. Methods

The best resolution of APP CTFs and Aβ is obtained using a gel electrophoresis system designed to run 15 × 15 cm (1.5 mm thickness) gels. These instructions assume the use of the Hoefer SE600 system and the Bio-Rad Trans Blot transfer system. Perform everything in the cold room.

The transfer conditions are optimized for smaller MW species (APP CTFs are approximately 10–15 kDa). The membrane can be cut horizontally near the 25 kDa marker, and the top can be probed simultaneously with an APP N-terminal antibody (such as 22C11 or 8E5) and/or anti-tubulin as a loading control. Since frequently the goal is to determine relative levels of the various CTFs and thus each sample serves as its own internal control, this may not be necessary, although it is desirable if between group differences in holo-APP levels are expected. Also, the cytosolic fraction, which would also contain abundant APP and α-tubulin, can be probed.

3.1. Brain Lysis and Fractionation for APP CTFs

1. Determine and record the weight of each brain sample to be analyzed (do not thaw).
2. On ice, homogenize the sample in nine volumes of Sucrose/HEPES lysis buffer with protease inhibitors, using just enough strokes (15–20) to break up the tissue.
3. Spin at 2,500 × *g*, 8 min, 4°C.
4. Transfer supernatant to a small ultracentrifuge tube (such as Beckman tubes for the TLA 100.2 rotor).
5. Spin at 100,000 × *g*, 1 h, 4°C (53,000 rpm in TLA 100.2 rotor).
6. Save the supernatant (cytosolic fraction) and freeze at –80°C.
7. Resuspend the pellet with 2.5 volumes (relative to original tissue weight) of lysis buffer.
8. Sonicate 5 × 1 s on ice, medium setting, with 5 s pause between pulses.
9. Determine protein concentration using an appropriate assay, such as the microLowry. The approximate expected protein concentration is 4–8 mg/mL.
10. Aliquot and store the particulate fraction at –80°C.

3.2. Tris/Tricine SDS-Polyacrylamide Gel Electrophoresis for Measurement of APP C-Terminal Fragments

1. Carefully clean the glass plates with a rinsable detergent, rinse thoroughly and allow to air dry, or use an acetone rinse to speed up drying time.
2. Use a marking pen to note 11 cm from the bottom of the glass plates.

3. Prepare a 14% (w/vol) gel by mixing 14 mL of 40% acrylamide/bis (37.5:1), 13.3 mL Tris/Cl/SDS buffer, 4.2 mL glycerol, and 8.5 mL distilled water.
4. Degas this solution for 15 min by placing the flask inside a sealed desiccator connected to a vacuum pump. Once the vacuum is initiated, a brief period of bubbling (10–30 s) will occur.
5. Add 67 µL fresh 10% APS and 14 µL TEMED. Immediately pour the gel up to the 11 cm mark, and then gently add N-butanol overlay (750 µL). Allow to polymerize for 2 h (do not leave the N-butanol overlay longer than 2 h).
6. Prepare a 4.3% (w/vol) stacking gel by mixing 1.35 mL 40% acrylamide/bis (37.5:1), 3.1 mL Tris/Cl/SDS buffer, and 8.0 mL distilled water. Degas as above.
7. Prewarm the degassed 4.3% solution by placing at 37°C for 15 min.
8. Remove the N-butanol overlay, rinse with Tris/Cl/SDS buffer to remove all of the N-butanol.
9. Add 40 µL 10% APS and 12 µL TEMED to the stacking gel solution, pour to the top of the glass plates, add the comb, and place at 37°C for 15 min, then room temperature for at least 30 additional minutes.
10. Prerun the gel for 45–60 min at 150 V at 4°C with constant stirring.
11. On ice, combine 75 µg of the particulate fraction with the appropriate volume of 2× Tricine sample buffer. Dilute all samples to the same volume using HEPES/sucrose lysis buffer but be sure that the final volume of loading buffer is 1×.
12. Heat the samples to 90°C for 5 min.
13. Place at 40°C for 20–30 min until loading onto the gel.
14. Run the gel at 30 V for 15 min, 75 V for 15 min, and 185 V overnight (approximately 14–16 h or until the 10 kDa molecular weight marker is 2–3 cm from the bottom of the gel) at 4°C with constant stirring.

3.3. Western Blot for APP C-Terminal Fragments

1. Separate the glass plates, remove the gel, and incubate for 15 min in 1× transfer buffer at 4°C with gentle agitation.
2. Transfer to nitrocellulose membrane for 2.5 h at 250 mA constant current.
3. Incubate the membrane for 5 min in Ponceau S stain, destain briefly (3–5 rinses) in water. Image using a flatbed scanner.
4. Block for 1 h at room temperature and incubate in primary antibody. To assess phospho-CTF levels, probe first with Phospho-APP Thr 668 antibody, then CT-15 or equivalent.

Table 1
Anti-APP and anti-Aβ antibodies: APP fragments recognized by various anti-APP and anti-Aβ antibodies

Antibody	Recognizes	Full length APP	sAPP-β	sAPP-α	Aβ	CTF-β (C99)	CTF-α (C83)	AICD
22C11	APP 66–81	✓	✓	✓				
8E5	APP 444–592	✓	✓	✓				
3D6	Aβ 1–5[a]				✓	✓		
Bam-10	Aβ 1–12	✓		✓	✓	✓		
6E10	Aβ 1–17	✓		✓	✓	✓		
m266	Aβ 13–28	✓			✓	✓	✓	
4G8	Aβ 17–24	✓			✓	✓	✓	
CT-15	APP 756–770	✓				✓	✓	✓

[a]3D6 recognizes a neo epitope produced by β-secretase cleavage, i.e., the amino-terminus of CTF-β and Aβ and thus does not recognize full-length APP or sAPP-α

Incubate overnight at 4°C. Other primary antibodies can be used, depending on which fragments are of interest (Table 1).

5. Wash 3 × 10 min in TBS-T.
6. Incubate in secondary antibody for 1 h at room temperature.
7. Wash 3 × 10 min in TBS-T.
8. During the final wash, combine 7.5 mL of each portion of the ECL reagent. Once the final wash is removed from the blot, add the ECL reagents to the blot, cover to protect from light, and incubate for 5 min.
9. Remove the blot from the ECL reagents, blot dry, and then place between the leaves of an acetate sheet protector that has been cut to the size of an X-ray film cassette.
10. Place the acetate/membrane/acetate sandwich in an X-ray film cassette and expose to film for a suitable exposure time, typically 5–30 min, depending on the expression levels of APP and nonspecific background signal.
11. An example result is shown in Fig. 1. The phospho-CTF bands should be confirmed using the phospho-specific APP antibody described above. Probe first with the phospho-specific antibody, then probe with CT-15 or equivalent, and overlay the films to identify the bands. If enough protein is loaded, six bands are detectable and most likely include holo- and phospho-forms of C83, C99, and C89.

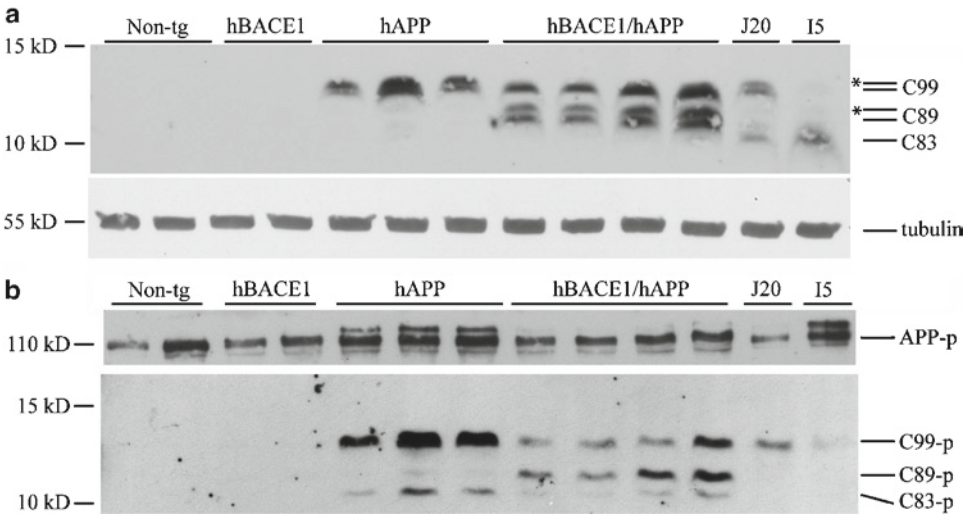

Fig. 1. Accumulation of APP CTFs in hAPP and hBACE1/hAPP doubly tg mice. Western blot of homogenates of frontal cortex from 3- to 5-month-old singly transgenic mice from hBACE1 (line 1), hAPP (FAD mutant APP, line 41), J20 (FAD mutant APP; 8-months-old), I5 (wild-type hAPP; 14-months-old), doubly tg hBACE1/hAPP mice (3–5-months-old), and Non-tg (nontransgenic) controls. (**a**) Western blotting for APP CTFs was performed with CT-15 antibody. Overexpression of hBACE1 increased APP CTFs in hAPP mice. Comparison of J20 and I5 shows that the Swedish mutation had a predictable effect on APP cleavage by endogenous mouse BACE1, as the J20 mice had more C99 whereas the I5 mice had mostly C83. Note also that the N-terminally truncated APP CTF C89, a product of β′ cleavage of APP at residue 10, is detected in hBACE1/hAPP mice. * indicates putatively phosphorylated forms of C99 and C89 (**b**) Analysis of phosphorylated full length APP (APP-p) and phosphorylated APP CTFs (C99-p, C89-p, and C83-p). Western blotting for phosphorylated APP and CTFs was performed with the Phospho-APP Thr 668 antibody. Note that APP-p, C99-p, and C83-p were reduced in the hBACE1/hAPP mice relative to hAPP (line 41) mice. (Adapted and reproduced from (10) with permission from Humana Press).

3.4. Brain Lysis for Measurement of Aβ Peptides

The brain region of interest (e.g., cortex or hippocampus) should be flash-frozen on dry ice and stored at −80°C. When handling human tissue, appropriate biohazard safety precautions and decontamination protocols should be followed.

1. Determine and record the weight of each brain sample to be analyzed (do not thaw).
2. On ice, homogenize the sample in 4.4× volumes of 98% formic acid (80% v/v final concentration of formic acid) using the tight pestle, with 15–20 strokes, or until completely homogenized (see Note 2). Transfer to an ultracentrifuge tube and carefully balance.
3. Ultracentrifuge at 50,000 × *g* for 30 min at 4°C.
4. Transfer the supernatant to an eppendorf tube, avoiding the lipid layer on top and the small pellet.
5. In a separate tube, dilute 2 µl of formic acid extract in 800 µl 0.1 N NaOH and determine protein concentration using an appropriate assay such as microLowry assay.

6. Load as little as 12 μg of total protein per lane, depending on the age of the animal and the application. For mice from the J20 line of hAPP transgenics, the following guidelines are used: 3–4-months-old, 1 mg; 6–8-months-old, 150–300 μg; 22–24-months-old, 12–15 μg (see Note 3).
7. Load from 0.5 ng to 5 ng human Aβ (and mouse Aβ if desired) as controls, with the amount depending on the abundance of Aβ in the samples.

3.5. Acetic Acid Urea PAGE for Measurement of Aβ Peptides

1. Clean the glass plates, comb, and 1.5 mm spacers as above except include a final rinse with 100% ethanol.
2. Mark the outside of the outward-facing plate with a black marker at 10 cm (22% separating gel) and 11.75 cm (10% step gel) from the bottom.
3. For each acrylamide solution (22%, 10%, and 4%), add urea, acrylamide, glacial acetic acid (GAA), and water into 50 mL conical tubes. Vortex briefly and incubate in a 55°C water bath. Vortex every few minutes until the urea is completely dissolved.
4. Degas all solutions for 15 min (see Subheading 3.2, step 4) and place the 10% and 22% solutions on ice (leave the 4% solution at room temperature and return to 55°C approximately 30 min before use).
5. Add 600 μL TEMED to the 22% solution and gently invert several times to mix. Next, add 100 μL 10% APS and invert several times. Using a 25 mL pipette, immediately pour the solution between the plates until it reaches the 10 cm mark.
6. Carefully add a 750 μL overlay of 5% GAA. Allow the gel to polymerize at room temperature for at least 1 h.
7. Add 200 μL TEMED and 100 μL 10% APS to the 10% acrylamide solution in the same manner as the 22% solution. Remove the overlay, and add the solution up to the second mark at 11.75 cm. Again, carefully pour a 750 μL overlay of 5% GAA. Allow the gel to polymerize at room temperature for 30 min.
8. Prior to adding the 4% stacker solution, place the gel stand in a 37°C incubator for 15 min. Return the 4% stacker solution to 55°C water bath. Remove the GAA overlay.
9. Add 450 μL TEMED, invert several times, and then add 100 μL 10% APS. Immediately pour this solution and insert a clean, dry comb. After pouring the stacker, place the stand back in the 37°C incubator for 15 min then remove and allow to polymerize at room temperature. The 4% stacking gel will take at least 1.5 h to polymerize completely (see Note 4).
10. Combine the appropriate amount of formic acid extract (12 μg–3 mg per lane) with 80% formic acid such that the total

volume is 75 µL. Then, add 24 µL 98% formic acid, 20 µL 6× loading buffer, and 1 µL 2-mercaptoethanol (120 µl/lane total for 15 well combs). For any empty lanes, make BSA blanks by using 1 µL of 5% BSA (50 µg) (see Note 5).

11. Assemble the gel apparatus in the cold room. Fill the bottom chamber three-fourths full with prechilled running buffer (~3 L). Add 1 L of buffer to the top reservoir. Prerun the gel Anode to Cathode (+ to –) (see Note 6) at 250 V for 30 min with constant stirring at 4°C. If necessary, remove any air bubbles at the bottom of the gel and verify that the buffer has not leaked from the top reservoir.
12. Flush wells with running buffer prior to loading samples to remove excess urea and load samples.
13. Run anode (+) to cathode (–) with constant stirring at 4°C as follows: 15 min each at 25 V, 50 V, 100 V, and 200 V, then approximately 15 h at 275 V or until the dye front (green) is 2–2.5 cm from the bottom of the gel.
14. Disassemble the glass plates and carefully transfer the gel to a large glass dish, cover with cold transfer buffer (200 mL) rock gently for 15 min. Repeat this wash step a total of five times (75 min).
15. Transfer to 0.2 µm nitrocellulose membrane for 2.5 h at 100 V constant. Transfer back (–) to front (+) (see Note 7). Use a power supply with the capacity for high current, such as the Bio-Rad PowerPac HC (3 A), perform on ice, in a 4°C cold room since high current will increase temperature (see Note 8).
16. After transfer, visualize the molecular weight markers by Ponceau-S staining for 5 min. After destaining the membrane with water (3–5 short washes), digitally scan the membrane and mark the ladders with a dull pencil (see Note 9).
17. Prior to probing, cut the membrane horizontally at the top MW marker. Boil membrane in 700 mL PBS, pH 7.4 for 5 min in a glass dish large enough so that part of the dish extends over the edge of the heating element. Place the membrane here so that it is not directly over the heating element. This avoids the bubbles that are present in this area and reduces background. Quickly place the membrane in 300 mL room temperature PBS prior to blocking.
18. Block the membrane for 60 min at room temperature.
19. Incubate in primary antibody overnight at 4°C (see Table 1 and Notes 10 and 11).
20. Wash the membrane 3 × 15 min in TBS-T.
21. Incubate in secondary antibody for 3 h at room temperature.
22. Wash the membrane 3 × 15 min in TBS-T.

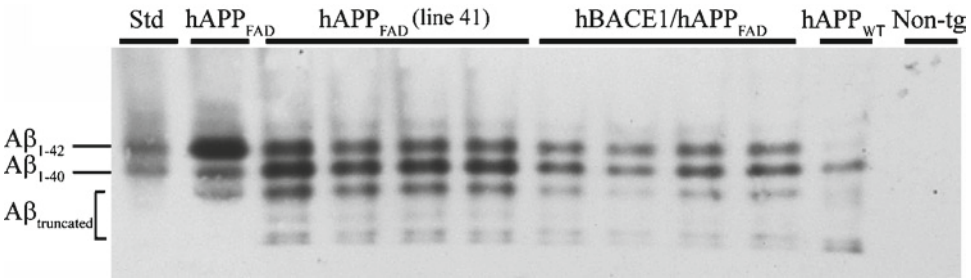

Fig. 2. Aβ$_{1–42}$, Aβ$_{1–40}$, and truncated Aβs detected by high resolution acetic acid urea PAGE and western blot analysis with the m266 antibody. Each lane contained proteins extracted from the neocortex (1 mg/lane) of a different mouse. Note that there are reduced levels of Aβ peptides in the hBACE1/hAPP doubly tg mice, consistent with reduced C99-p, relative to hAPP$_{FAD}$ singly transgenic mice (Fig. 1). Also, because of the Swedish and London mutations in hAPP$_{FAD}$ line 41 and the Swedish and Indiana mutations in hAPP$_{FAD}$ line J20, the proportion of Aβ$_{1–42}$, and total Aβ levels, are increased, relative to hAPP$_{WT}$ (l5) mice. As a positive control, a mixture of synthetic Aβ$_{1–42}$ and Aβ$_{1–40}$ are included (Std). As a negative control, a non-tg (nontransgenic) mouse brain is included and shows that under these conditions, only human Aβ species are detected (Adapted and reproduced from (10) with permission from Humana Press).

23. Perform ECL as in Subheading 3.2, step 22 and develop as in steps 23 and 24.
24. An example result is shown in Fig. 2.

4. Notes

1. Other commercially available antibodies can be used, such as the anti-amyloid precursor protein C-terminal antibody (Sigma).
2. For small brain regions, such as hippocampus, it is better to use a disposable pellet mixer and 1.5 mL microtube with a cordless pestle motor (VWR).
3. It may be best to run a pilot experiment with different amounts of protein per lane to determine optimal amounts.
4. During polymerization, you may notice what appear to be air pockets forming in the resolving gel. These pockets form because of the change in temperature of the gel during and after polymerization. These spaces do not affect the performance of the gel.
5. Final volumes can be adjusted as per need, but the final formic acid concentration should always be 70–90%. Distortion (smiling) occurs for the outside two lanes of every gel run. To help minimize the negative effects of this distortion, load BSA blanks in the outside lanes.
6. The Aβ peptides are positively charged at this acidic pH and thus run from the (+) to the (–) electrode, the opposite of

SDS-Polyacrylamide Gel Electrophoresis (SDS-PAGE). Therefore, it is critical to reverse the electrodes in the power supply to run (+) top to (−) bottom.

7. Following neutralization, the Aβ peptides are now negatively charged, so transfer (−) to (+) as described.
8. Expect the temperature inside the chamber to rise to >25°C. Exchange transfer buffer midway through transfer if necessary to avoid overheating (>30°C). Do not completely fill the transfer chamber as more buffer creates higher current. Place the bottom of gel toward the bottom of chamber.
9. Note that all bands from the peptide standard ladder do not transfer. This ladder should be used solely for alignment purposes. This technique separates peptides according to their molecular weight (size) and charge. For example, two peptides of the same molecular weight but with differing charges will likely not have the same net mobility. Because of these issues, we always run Aβ peptide standards in at least one well to enable accurate Aβ peptide identification.
10. Mouse Aβ migrates more slowly than human Aβ on acetic acid urea PAGE. Note that the antibody affinity for rodent Aβ may be less, so given equal amounts of human and rodent Aβ standards, the rodent bands are weaker. You may need to load up to 10 ng per lane of rodent Aβ standards.
11. Note that any Aβ antibody or antibodies can be used, although 3D6 has proven to be the most sensitive. Using 3D6, the lower range of sensitivity is approximately 75–150 pg of Aβ peptide, a range that is adequate for cerebrospinal fluid (CSF) and tissue analysis, although detection from human plasma may require the addition of other more sensitive methods, such as immunoprecipitation. Antibody m266 can be used to detect N-terminally-truncated Aβ species.

Acknowledgments

The author would like to thank Dr. Ron DeMattos for the development of the acetic acid urea PAGE protocol and for his advice on the use of the technique, Dr. Eliezer Masliah for providing the opportunity to collaborate on the hAPP/BACE1 project, Dr. Lennart Mucke for his mentorship, advice, and encouragement, and Dr. Judy Cam for reviewing the manuscript.

References

1. Haass, C. (2004) Take five – BACE and the gamma-secretase quartet conduct Alzheimer's amyloid beta-peptide generation. *EMBO J.* **23**, 483–8.
2. Tanzi, R., and Bertram, L. (2005) Twenty years of the Alzheimer's disease amyloid hypothesis: A genetic perspective. *Cell* **120**, 545–55.
3. Selkoe, D. J. (2001) Alzheimer's disease: Genes, proteins, and therapy. *Physiol. Rev.* **81**, 741–66.
4. Lee, M. S., Kao, S. C., Lemere, C. A., Xia, W., Tseng, H. C., Zhou, Y., Neve, R., Ahlijanian, M. K., and Tsai, L. H. (2003) APP processing is regulated by cytoplasmic phosphorylation. *J. Cell Biol.* **163**, 83–95.
5. Lee, E. B., Zhang, B., Liu, K., Greenbaum, E. A., Doms, R. W., Trojanowski, J. Q., and Lee, V. M. (2005) BACE overexpression alters the subcellular processing of APP and inhibits Aβ deposition in vivo. *J. Cell Biol.* **168**, 291–302.
6. Abramowski, D., Wiederhold, K. H., Furrer, U., Jaton, A. L., Neuenschwander, A., Runser, M. J., Danner, S., Reichwald, J., Ammaturo, D., Staab, D., Stoeckli, M., Rueeger, H., Neumann, U., and Staufenbiel, M. (2008) Dynamics of Aβ turnover and deposition in different APP transgenic mouse models following gamma-secretase inhibition. *J. Pharmacol. Exp. Ther* **327**, 411–24.
7. Lim, G. P., Calon, F., Morihara, T., Yang, F., Teter, B., Ubeda, O., Salem, N., Jr., Frautschy, S. A., and Cole, G. M. (2005) A diet enriched with the omega-3 fatty acid docosahexaenoic acid reduces amyloid burden in an aged Alzheimer mouse model. *J. Neurosci.* **25**, 3032–40.
8. Sano, Y., Syuzo-Takabatake, A., Nakaya, T., Saito, Y., Tomita, S., Itohara, S., and Suzuki, T. (2006) Enhanced amyloidogenic metabolism of the amyloid beta-protein precursor in the X11L-deficient mouse brain. *J. Biol. Chem.* **281**, 37853–60.
9. Mucke, L., Masliah, E., Yu, G.-Q., Mallory, M., Rockenstein, E. M., Tatsuno, G., Hu, K., Kholodenko, D., Johnson-Wood, K., and McConlogue, L. (2000) High-level neuronal expression of $A\beta_{1-42}$ in wild-type human amyloid protein precursor transgenic mice: Synaptotoxicity without plaque formation. *J. Neurosci.* **20**, 4050–58.
10. Rockenstein, E., Mante, M., Alford, M., Adame, A., Crews, L., Hashimoto, M., Esposito, L., Mucke, L., and Masliah, E. (2005) High β-Secretase activity elicits neurodegeneration in transgenic mice despite reductions in amyloid-β levels: Implications for the treatment of Alzheimer's disease. *J. Biol. Chem.* **280**, 32957–67.
11. DeMattos, R. B., Bales, K. R., Cummins, D. J., Dodart, J.-C., Paul, S. M., and Holtzman, D. M. (2001) Peripheral anti-Aβ antibody alters CNS and plasma Aβ clearance and decreases brain Aβ burden in a mouse model of Alzheimer's disease. *Proc. Natl. Acad. Sci. U.S.A.* **98**, 8850–55.
12. Esposito, L., Gan, L., Yu, G.-Q., Essrich, C., and Mucke, L. (2004) Intracellulary generated Aβ counteracts the antiapoptotic function of its precursor protein and primes proapoptotic pathways for activation by other insults in neuroblastoma cells. *J. Neurochem.* **91**, 1260–74.

Chapter 7

Detection of APP Intracellular Domain in Brain Tissue

Sanjay W. Pimplikar and Anupama Suryanarayana

Abstract

The cleavage of amyloid precursor protein (APP) by γ-secretase produces Aβ peptides, which are prominent features in Alzheimer's disease and have been extensively studied. By contrast, APP intracellular domain (AICD), also a product of this cleavage event, has received little or no investigative attention. A major reason for this is that AICD is generally not detected in tissue lysates and, therefore, is neglected as a non-relevant product of APP metabolism. However, recent studies have shown that AICD regulates a number of important cellular events. Furthermore, we found that contrary to previous assertions, AICD can be detected in brain lysates using Western blotting if an antigen retrieval protocol is employed. Here we describe the protocol for AICD detection and note the biological relevance of AICD in physiological and pathological conditions.

Key words: Amyloid precursor protein, APP Intracellular domain, Western blotting, Antigen retrieval, Alzheimer's disease

1. Introduction

Amyloid precursor protein (APP) is a neuronally enriched, transmembrane protein of unknown function. During its lifespan, APP is proteolytically processed, giving rise to a number of smaller fragments. Of these, Aβ peptides have garnered the most attention because they form senile plaques (1), a pathological hallmark of Alzheimer's disease (AD), and are considered to be a primary cause of AD (2). Full-length APP is initially "shaved off" near the outer surface of the membrane, leaving the membrane-associated stubs, which become substrates for presenilin-mediated intramembrane cleavage. A combination of β-secretase and γ-secretase cleavage of APP results in the formation of Aβ peptides. The intra-membrane cleavage by γ-secretase should also result in the obligatory release of APP intracellular domain (AICD). However, AICD had traditionally eluded detection and as a result

Erik D. Roberson (ed.), *Alzheimer's Disease and Frontotemporal Dementia*, Methods in Molecular Biology, vol. 670,
DOI 10.1007/978-1-60761-744-0_7, © Springer Science+Business Media, LLC 2011

has been regarded as an unimportant by-product of APP processing that is rapidly degraded. As described below, it is becoming clear that both of these assumptions are incorrect.

Several recent studies have established that AICD is an important regulator of a number of biological processes. Despite a contrary report (3), a vast number of studies have shown AICD to regulate gene expression in non-neuronal and neuronal cells (4). AICD also perturbs signaling pathways, including those mediated by glycogen synthase kinase 3-β (GSK-3β) (5). Expression of AICD has been shown to induce apoptosis (6) and to produce a number of other harmful effects. AICD has also been implicated in altering the cytoskeletal network (4). A recent study has also suggested that AICD is involved in neurogenesis (7). Thus, the biological significance of AICD is being elucidated, and AICD is clearly important in a variety of cellular processes. We can now show that endogenous AICD is present in low but detectable levels (see Note 1) and becomes detectable by Western blotting after the antigen retrieval protocol (Fig. 1). Endogenous AICD mostly fractionates with the membrane and nuclear fraction (Fig. 2), with no AICD detected in the cytoplasm (5, 8).

Here we describe a protocol of "antigen retrieval" and show that by using this procedure, endogenous AICD can be detected using C-terminal APP antibodies. The protocol of antigen retrieval is not specific only for AICD detection, but can be applied universally to other proteins. In our experience, one needs 10- to 50-fold less primary antibody to get the same level of band intensity for holo-APP or tubulin.

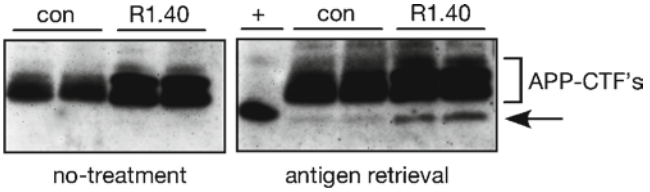

Fig. 1. AICD is detected upon antigen retrieval. PNS proteins (40 μg) from brains of two C57Bl6 mice (con) or transgenic mice overexpressing APPswe (R1.40) were loaded in duplicate lanes (*left* panel and *right* panel), separated by SDS-Polyacrylamide Gel Electrophoresis (SDS-PAGE), and electrophoretically transferred on to a nitrocellulose membrane. The membrane was cut in the middle, and the right half was subjected to the antigen retrieval protocol (antigen retrieval) and the left half was left untreated (no treatment). The membranes were blocked and probed with APP-C terminal antibody and developed using ECL. Note that the AICD band (*arrow*) is detected only after antigen retrieval and that AICD levels are higher in a transgenic mouse model of AD compared to that in wild-type controls. The AICD signal in control mice can be enhanced by loading more protein (up to 80 μg) per lane or by reducing the dilution of primary antibody from 1:1,000 to 1:250. Lane indicated "+" represents cell lysates from COS cells transfected with AICD59. ©Ryan, K. A., Pimplikar, S. W., 2005. Originally published in *Journal of Cell Biology*, 171(2):327–335.

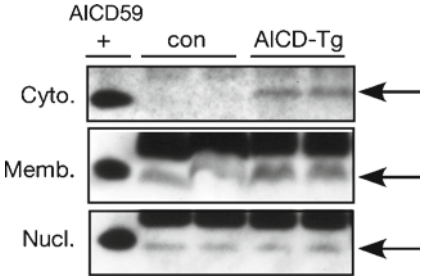

Fig. 2. AICD is present in the membrane and nuclear fraction, but not in free cytosolic proteins. Brain homogenates from two C57Bl6 (con) or transgenic mice overexpressing AICD59 and Fe65 (AICD-Tg) were fractionated into cytosolic, membrane, or nuclear fractions and Western blotted as above. Note that AICD is completely absent from the cytosol of control animals but is present in the membrane and nuclear fraction, whereas AICD-Tg mice show AICD in the cytosol as well as moderately elevated levels in the membrane fraction. ©Ryan, K. A., Pimplikar, S. W., 2005. Originally published in *Journal of Cell Biology*, 171(2):327–335.

2. Materials

2.1. Brain Tissue and Homogenization

1. Homogenizing buffer (HB): 50 mM Tris-HCl, pH 7.4, 150 mM NaCl, 1 mM EDTA.
2. Protease inhibitor cocktail (Sigma).
3. Phosphatase inhibitor cocktail (Sigma).
4. Polytron steel homogenizer, e.g., PowerGen 125.
5. Refrigerated tabletop microcentrifuge.
6. BCA Protein Assay Kit (Pierce).

2.2. SDS-Polyacrylamide Gel Electrophoresis

1. Nu PAGE Novex gel 4–12% Bis–Tris (Invitrogen), LDS sample buffer, reducing agent, and MES running buffer.
2. Ponceau S stain, 0.1%. Mix 100 mg of Ponceau S in 100 mL of 5% glacial acetic acid.

2.3. Western Blotting

1. Transfer buffer. Prepare from 20× stock (Invitrogen).
2. Nitrocellulose membrane.
3. Tris-buffered saline with Tween-20 (TBS-T): 137 mM of NaCl, 27 mM of KCl, 25 mM of Tris-HCl, pH 7.4, and 0.1% Tween-20.
4. Blocking buffer (BB): 10% newborn calf serum in TBS-T.
5. Primary antibody: Anti-APP-C-terminal antibody 0443 (Calbiochem).
6. Secondary antibody: Donkey Anti-Rabbit Ig-HRP conjugated to horseradish peroxidase.
7. Enhanced chemiluminescence (ECL) reagents.

3. Methods

Upon cleavage by γ-secretase within the bilipid layer, AICD is released from the membrane and translocates to the nucleus. A number of in vitro assays for AICD detection have been published (9) that are based on incubation of broken membranes at 37°C in the presence of protease inhibitors (to prevent AICD breakdown). The membranes are pelleted and AICD released in the supernatant is detected by Western blotting. Using such in vitro assays, it has been concluded that AICD is cleaved at the ε-site and remains free and soluble in the cytoplasm (10).

Previous investigations could not detect endogenous AICD in mouse or human brains. As described below, endogenous AICD is present at low but detectable levels and can be detected by Western blotting after "Antigen Retrieval Treatment" (ART) (see Fig. 1). Interestingly, endogenous AICD is present in the membrane and nuclear compartment, but not in the free cytosolic fraction (5, 8) (see also Fig. 2). It is possible that previous investigations failed to detect the presence of endogenous AICD in tissue lysates because they did not perform antigen retrieval and did not probe the membrane (or nuclear fractions), where most of AICD can be detected at steady state. The specificity of the AICD detection after antigen retrieval can be checked by analyzing brain lysates from APP knock-out mice (Fig. 3).

3.1. Brain Tissue Sample Preparation

1. Sacrifice mice by cervical dislocation and quickly dissect the brain from the skull.
2. Cut and discard the cerebellum. If necessary, microdissect the brain into separate cortex and hippocampus.
3. Place the tissue on aluminum foil on dry ice to ensure quick freezing and to minimize post-mortem changes. The tissue can be left frozen in 1.5-mL Eppendorf tubes at –80°C until further use.

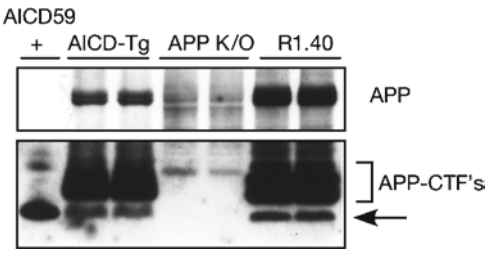

Fig. 3. Specificity of AICD detection following antigen retrieval. PNS proteins from two animals (each from AICD-Tg, APP knock-out, and R.40) were Western blotted using 0443 antibody. Note that holo-APP, APP-CTF, and AICD bands are absent from APP knock-out animals. ©Ryan, K. A., Pimplikar, S. W., 2005. Originally published in *Journal of Cell Biology*, 171(2):327–335.

4. Weigh the frozen brain and add 5 vol (w/v) of homogenizing buffer (HB) containing protease and phosphatase inhibitor cocktails.
5. Homogenize the tissue in a Polytron at medium speed for 10 s with ten strokes.
6. Centrifuge the homogenate at 700×*g* for 10 min in a refrigerated tabletop Eppendorf centrifuge (~3,000 rpm). Remove the post-nuclear supernatant (PNS), carefully leaving the nuclear pellet undisturbed. A significant amount of AICD appears in the nuclear fraction. If increased yields are required, suspend the nuclear pellet with 2.5 vol of HB, vortex briefly, and centrifuge as above. Pool both PNS fractions (see Note 2).
7. If necessary, purified nuclear fraction can be obtained from the pellet by using a Pierce kit (NE-PER nuclear and cytoplasmic extraction reagent kit).
8. The PNS can be directly analyzed by Western blot or can centrifuged at 150,000×*g* for 30 min to separate total membranes and cytoplasm. The membrane pellet is suspended in HB at 0.5 vol of PNS.
9. Determine protein concentration in each fraction using the BCA protein assay kit.

3.2. SDS-PAGE

1. Load between 60 and 90 μg of protein onto a 4–12% Bis–Tris Novex NuPAGE gel according to the manufacturer's instructions. We routinely load 75 μg of protein in a volume of 32 μl.
2. Perform electrophoresis at 150 V for 45 min.
3. Transfer proteins onto 0.2 μm Optitran nitrocellulose membranes at 350 mA for 90 min in a Bio-Rad transfer cell.
4. Quickly rinse nitrocellulose membranes in water.
5. Optional: At this stage, the membranes can be stained with Ponceau S with gentle agitation for 1 min and several washes of water for 3 min. We routinely scan the membrane at this stage. Destain membranes by washing in PBS until the color disappears (1–2 min).

3.3. Antigen Retrieval

1. Rinse membrane briefly in PBS and blot dry by gently patting between two Kimwipes.
2. Allow the Membrane to air dry for 5 min (see Note 3).
3. Place the membrane in a plastic tray and add boiling PBS, making sure that PBS is not poured directly over the membrane but rather in a corner of the tray, away from the membrane.
4. Gently agitate on a rocking platform for 5 min at RT.
5. Discard the buffer and wash with TBS for 2–3 min (×2).

3.4. Western Blotting

1. Block membranes in blocking buffer (BB) for 1–2 h at RT.
2. Incubate the membranes in anti-APP C-terminus antibody 0443 (1:250–1:1,000 dilution) overnight at 4°C.
3. Remove the antibody and refrigerate. It can be stored with 0.02% azide and reused several times.
4. Wash the membrane in TBS-T thoroughly with six washes (10 min each) at RT.
5. Incubate the membrane with an anti-rabbit secondary antibody conjugated to HRP in BB at 1:10,000 dilution.
6. Remove and discard the secondary antibody and wash the membrane with TBS-T 6 times (10 min each).
7. Rinse briefly with water, remove the excess water by patting dry, and visualize the protein bands using ECL (see Note 4).

4. Notes

1. Endogenous AICD levels are detectable by Western blotting after the antigen retrieval protocol (Fig. 1). Such procedures are routinely applied to immunohistochemistry to make the antigenic epitopes "accessible." It is not entirely clear why incubating the membranes in boiling PBS increases the detectability of AICD. One possibility is that exposure to boiling buffer denatures AICD completely, which then refolds as the buffer returns to RT. It is also possible that boiling PBS removes residual SDS and allows better protein folding.
2. Total homogenate cannot be separated cleanly since the presence of DNA interferes with the proper migration protein bands near the tracking dye (5–10 kDa range). This problem can be somewhat mitigated by sonicating the homogenates and incubating them with DNAse prior to addition of sample buffer. The problem of DNA interference can also be avoided by analyzing the PNS. However, in our experience, we lose a significant fraction of membrane vesicles in the nuclear pellet. This can be prevented by re-washing the nuclear pellet to recover membrane vesicles, or by gently homogenizing the brain in handheld or motorized Teflon glass homogenizers.
3. It is extremely important that the nitrocellulose membrane is dried completely before adding boiling PBS. After electrophoretic transfer, proteins are mostly held on the membrane by hydrophobic interactions. After drying, the proteins on the nitrocellulose bind the membrane extremely tightly (almost covalently) and do not come off when boiling PBS is added.

4. Under the conditions described above, we generally expose the film twice; once for a short time (5–30 s) to see spatially resolved α- and β-CTF, and again to expose the membrane to a fresh film for 15–60 min when the AICD band begins to appear. An important consideration for the exposure time is that it should be long enough such that both α- and β-CTF bands merge into one band. AICD levels are low enough that they will not be detected as long as α- and β-CTF bands are visibly resolved.

Acknowledgments

The work in author's laboratory is supported by grants from the NIH (R01-AG026146), Alzheimer's Association, and Rotary-CART funds. We thank Dr. Chris Nelson for his comments on this manuscript.

References

1. Glenner, G. G., and Wong, C. W. (1984) Alzheimer's disease and Down's syndrome: sharing of a unique cerebrovascular amyloid fibril protein. *Biochem Biophys Res Commun* **122**, 1131–5.
2. Hardy, J., and Selkoe, D. J. (2002) The amyloid hypothesis of Alzheimer's disease: progress and problems on the road to therapeutics. *Science* **297**, 353–6.
3. Hebert, S. S., Serneels, L., Tolia, A., Craessaerts, K., Derks, C., Filippov, M. A., Muller, U., and De Strooper, B. (2006) Regulated intramembrane proteolysis of amyloid precursor protein and regulation of expression of putative target genes. *EMBO Rep* **7**, 739–45.
4. Muller, T., Meyer, H. E., Egensperger, R., and Marcus, K. (2008) The amyloid precursor protein intracellular domain (AICD) as modulator of gene expression, apoptosis, and cytoskeletal dynamics-relevance for Alzheimer's disease. *Prog Neurobiol* **85**, 393–406.
5. Ryan, K. A., and Pimplikar, S. W. (2005) *J Cell Biol* **171**, 327–35.
6. Passer, B., Pellegrini, L., Russo, C., Siegel, R. M., Lenardo, M. J., Schettini, G., Bachmann, M., Tabaton, M., and D'Adamio, L. (2000) *J Alzheimers Dis* **2**, 289–301.
7. Ma, Q. H., Futagawa, T., Yang, W. L., Jiang, X. D., Zeng, L., Takeda, Y., Xu, R. X., Bagnard, D., Schachner, M., Furley, A. J., Karagogeos, D., Watanabe, K., Dawe, G. S., and Xiao, Z. C. (2008) A TAG1-APP signalling pathway through Fe65 negatively modulates neurogenesis. *Nat Cell Biol* **10**, 283–94.
8. Nakaya, T., and Suzuki, T. (2006) Role of APP phosphorylation in FE65-dependent gene transactivation mediated by AICD. *Genes Cells* **11**, 633–45.
9. Pinnix, I., Musunuru, U., Tun, H., Sridharan, A., Golde, T., Eckman, C., Ziani-Cherif, C., Onstead, L., and Sambamurti, K. (2001) A novel gamma -secretase assay based on detection of the putative C-terminal fragment-gamma of amyloid beta protein precursor. *J Biol Chem* **276**, 481–7.
10. Yu, C., Kim, S. H., Ikeuchi, T., Xu, H., Gasparini, L., Wang, R., and Sisodia, S. S. (2001) Characterization of a presenilin-mediated amyloid precursor protein carboxyl-terminal fragment gamma. Evidence for distinct mechanisms involved in gamma -secretase processing of the APP and Notch1 transmembrane domains. *J Biol Chem* **276**, 43756–60.

Chapter 8

Cell-Based Assays for Regulators of Tau Biology

Umesh K. Jinwal and Chad A. Dickey

Abstract

Understanding the molecular mechanisms of Alzheimer's disease (AD) is a challenging endeavor, namely, due to the fact that the disease only occurs in the central nervous system of elderly humans. Thus, model systems simply do not accurately portray this cellular landscape. While we cannot ask many mechanistic questions using the human brain as our test subject, cell culture techniques that have emerged at least provide us with the ability to pose fundamental biochemical questions, which may ultimately lead to translational outcomes for AD. In particular, the intracellular microtubule-associated protein tau that accumulates in AD is found in normal cells. Manipulating these cells may allow us to address basic questions about tau biology that would provide novel therapeutic strategies down the road. Here, we describe several techniques to explore tau cell biology using the Odyssey® Infrared Imaging system (Odyssey system) from LI-COR Biosciences. We provide a detailed protocol on how to perform a scalable drug screening assay called the In-Cell Western and follow-up these screens with standard Western analysis to confirm whether "hits" are valid by more traditional means. We provide some tips on where mistakes are most likely to occur, and we interpret our standard Western data, providing some estimation as to the composition of the banding pattern that is typical for this enigmatic protein.

Key words: Odyssey, Tau, In-Cell Western, Near-infrared, Fluorescence, Cell culture

1. Introduction

For most neurodegenerative protein aggregation disorders, intracellular accumulation of an aberrant form of the parent protein initiates the cascade that ultimately culminates in the presentation of a pathological marker detected by histochemistry in post-mortem tissue. While these postmortem analyses have been critical to establish the foundation of these diseases, it is the early events that seed the pathology that will likely be the best targets for therapeutic design. The microtubule-associated protein tau accumulates into tangles in Alzheimer's disease (AD), although the pathogenic process leading up to this is still largely unclear.

Erik D. Roberson (ed.), *Alzheimer's Disease and Frontotemporal Dementia*, Methods in Molecular Biology, vol. 670,
DOI 10.1007/978-1-60761-744-0_8,

While mouse modeling has furthered our understanding of the disease process, these studies carry a high cost, both in time and resources. Therefore, the emergence of cell culture models has been critical for understanding the mechanisms at play in tau pathogenicity. With these models, we have been able to take advantage of a number of emerging technologies that are helping us define our understanding of the mechanisms involved with tau biology (1–3). Moreover, we are continuing to discover therapeutic targets that might prove most effective in our fight against AD and other tauopathies. In this chapter, we describe the methods using the Odyssey® Infrared Imaging system from LI-COR Biosciences, which has allowed us to begin to address questions in a semi-high throughput quantitative format previously not achievable for the tau protein. Screening the effects of small molecules, siRNAs and even biological agents, such as growth factors and cytokines, can be done in a high volume within a two-day protocol. The dual-color capability provides an option for greater control and reliability of the assay in a single run. Herein, we provide basic protocols to analyze total tau levels relative to GAPDH; however, this technique can be applied to any number of intracellular targets, provided antibody specificity is high. We also describe validation studies using the Odyssey system for more traditional Western blotting.

1.1. In-Cell Western

The LI-COR Biosciences In-Cell Western (ICW) assay is suited for drug discovery assay development where protein quantification is important in the cellular environment. It incorporates the use of near infrared-labeled secondary antibodies, which can be independently detected with the dual laser Odyssey system at 680 nm and 800 nm, to detect any combination of two proteins, provided species-specific antibodies are available. The assay can quantify proteins within a monolayer of fixed cells in 96 or 384-well microplates, making this platform a cross between high-throughput immunofluorescent chemistry and Western blotting; however, with this increased throughput, resolution is lost, making follow-up validation studies critical. This procedure is unique from typical plate reader-based applications and other biological system applications, such as the Typhoon from GE, because of the use of near-infrared laser scanning. Near-infrared light has a longer wavelength than light in the visible range. Therefore, near-infrared light can travel farther and pass through certain surfaces without losing intensity. Thus, the Odyssey system is the most affordable of a handful of devices that allows for this type of application. The signal from the Odyssey system is linear and, thus, the values provided by the system software allow for relative quantitation within each plate scanned. Moreover, a normalization template can be used for variance across plates, allowing for multiplate assay analyses. Here, we describe a protocol specific for analyzing

tau levels relative to GAPDH; however, this application could be applied to a number of other proteins. That being said, a large amount of effort went into optimizing the conditions described herein to specifically develop our assay around the tau protein; specifically, cell line and antibody selections.

1.2. Western Blotting with the Odyssey System

Protein blotting has become the most routine tool to detect specific proteins in a given sample of tissue homogenate or extract. Recent advances in chemiluminescent technologies have greatly increased the ease-of-use and rapidity for this procedure. Now, with the advent of the Odyssey system, Western blotting for two individual proteins can be performed simultaneously without the need of film or a dark room. Moreover, as opposed to signals produced by enzymatic labeling reactions, this latest technology uses linear fluorescent chemistry, allowing for true quantitative analyses to be done. Here, we describe Western blotting using the Odyssey system since standard Western analysis is a very common laboratory practice. Nevertheless, in Fig. 3c, we have utilized standard Western blotting for comparison with near-infrared detection.

2. Materials

2.1. In-Cell Western

2.1.1. Cell Culture and Treatment

1. Cell line: H4 neuroglioma highly adherent cell line.
2. Cell culture facility.
3. 96-well tissue culture plates, black shell, optically clear bottom (see Note 3).
4. Tissue culture flasks (T-75).
5. 25 ml Reagent reservoirs.
6. Sterile filtered pipette tips.
7. 12-Channel multichannel pipetter.
8. Trypsin/EDTA solution.
9. DMEM + 10% Fetal Bovine Serum (FBS).
10. Opti-MEM, no additives.
11. Compounds from a chemical library (10 mM stocks; Prestwick Chemical or Microsource, Gaylordsville, CT).
12. Standard 96-well tissue culture plates.
13. 17-AAG (17-(Allylamino)-17-demethoxygeldanamycin), (A.G. Scientific, San Diego, CA).

2.1.2. In-Cell Western Assay

1. Fixing solution: 3.7% formaldehyde in PBS.
2. Triton washing solution: 0.1% Triton X-100 in PBS.

3. Odyssey blocking buffer, neat.
4. Orbital shaker.
5. 96-well plate automatic washer (recommended).
6. Mouse monoclonal anti-GAPDH antibody (Biodesign, Saco, ME).
7. Rabbit polyclonal antitotal tau antibody (Dako, Carpinteria, CA).
8. Primary dilution buffer: 1:1 mixture of Odyssey blocking buffer and 1× PBS + 0.2% Tween-20 (see Note 1).
9. Goat antirabbit antibody labeled with Alexa-Fluor 680 (Molecular Probes).
10. Goat antimouse antibody labeled with IRDye 800 (Rockland Laboratories).
11. Secondary dilution buffer: 1:1 mixture of Odyssey blocking buffer and 1× PBS + 0.4% Tween-20.
12. Tween washing solution: 0.1% Tween-20 in PBS.
13. Aluminum foil or black boxes.
14. Odyssey Infrared Imaging system (LI-COR Biosciences, Nebraska USA).

2.2. Western Validation of Hits

2.2.1. Cell Lysis

1. 6-well tissue culture plates.
2. Vacuum source connected to a tube and a pasteur glass pipette for aspiration of media.
3. 1× Dulbecco's phosphate-buffered saline (DPBS).
4. Cell lifters.
5. Pipettes and tips from 10 µl to 1,000 µl.
6. Microcentrifuge tubes, 1.5 ml.
7. Sonicator.
8. Lysis Buffer: 50 mM Tris–HCl pH 7.5, 100 mM NaCl, 15 mM EDTA, 0.1% Triton X-100, 1%SDS, 1× Protease Inhibitor (CalBiochem, Gibbstown, NJ), Phosphatase Inhibitor cocktail 1 and 2 (Sigma, St. Louis, MO), 1 mM PMSF.

2.2.2. Protein Estimation

1. BCA Protein Assay Reagents A and B.
2. 1 µg/µl Bovine Serum Albumin (BSA).
3. 37°C Incubator.
4. Clear 96-well plate.
5. Spectrophotometer to read protein at 562 nm.

2.2.3. Western Blotting with the Odyssey System

1. Square plastic Petri dishes.
2. 10% Tris-Glycine, 1.0 mm Precast Gels, 12-well.

3. Thick blot papers, 1 cm larger than the membrane.
4. Immobilon-FL-PVDF membrane (see Note 11), cut 1 mm larger than the gel size.
5. Saran wrap.
6. Protein gel apparatus.
7. Western Transfer apparatus.
8. Power supply.
9. Heating block for heating samples at 95°C.
10. Rotary shaker.
11. Rocking mixer.
12. Odyssey Infrared Imaging system (LI-COR Biosciences).
13. 2× Laemmli sample buffer.
14. 2-Mercaptoethanol.
15. PBST: 0.2% Tween-20 in PBS.
16. Mouse monoclonal anti-GAPDH antibody (Biodesign).
17. Rabbit polyclonal antitotal tau antibody (Dako).
18. Goat antirabbit antibody labeled with Alexa-Fluor 680 (Molecular Probes).
19. Goat antimouse antibody labeled with IRDye 800 (Rockland Laboratories).
20. Odyssey blocking buffer, neat (LI-COR Biosciences).

3. Methods

3.1. In-Cell Western

3.1.1. Cell Culture and Treatments

Ensure that all cell culture work prior to fixation is performed in a Biological safety cabinet under sterile conditions. Do not forget to turn on airflow before starting work.

1. Grow H4 neuroglioma cells in DMEM containing 10% FBS (complete media) in a T75 tissue culture flask until confluency is reached (see Note 2).
2. Aspirate media and add 5 ml of Trypsin-EDTA solution to your flask. Once cells detach, remove 4 ml of this suspension and dispense 1 ml of cells into each of four individual 50 ml tubes. Replace media in flask.
3. Add 20 ml of complete media to each of the four 50 ml tubes. Cover and invert to distribute suspension.
4. Decant the contents of one tube into a sterile 25 ml reagent reservoir, and using a multichannel pipetter, dispense 200 µl/well into a sterile 96-well tissue culture treated plate (Black shell, optically clear bottom; see Note 3). Repeat with three

additional 96-well plates. During distribution, ensure that the cell suspension is evenly disbursed by triturating with the multichannel pipetter (see Note 4).

5. Incubate cells at 37°C in 5% CO_2 until they reach 95–100% confluency.
6. Remove the complete media from each well using a multichannel vacuum manifold and replace with 200 µl of serum-free Opti-MEM media.
7. In a standard 96-well assay plate, prepare 1 mM compound stocks from one plate of a commercially available library (we have used the GenesisPlus library from Microsource and the Prestwick Chemical library) by diluting in Opti-MEM. As a positive control, prepare a 100 µM stock of the Hsp90 inhibitor, 17-(Allylamino)-17-demethoxygeldanamycin (17-AAG). A vehicle control of DMSO should also be prepared using a volume equivalent to the highest concentration of drug. Most libraries come with the first and last columns empty to add controls. Add the 17-AAG stock to wells A, C, E, and G to the first column; add vehicle to wells B, D, F, and H of the first column.
8. Using a multichannel pipetter, add 2 µl from row A of the drug dilution plate to rows B, C, and D of the cell culture plates, creating triplicates for each compound in row A of the compound library (Fig. 1). Add 2 µl from row B of the drug dilution plate to rows E, F, and G of the cell culture plates, creating triplicates for each compound in row B of the compound library. Repeat for rows C–H in other culture plates (see Note 5). Incubate at 37°C for 24 h.

3.1.2. In-Cell Western Assay (Per Four Plates)

1. Prepare fresh 3.7% fixing solution by adding 5 ml of 37% formaldehyde to 45 ml of PBS.
2. Remove media from the cells using a multichannel vacuum manifold. Wash three times with 1× PBS.
3. Immediately and carefully add 150 µl of fixing solution by pipetting down the side of the wells to avoid detaching the cells. Incubate for 20 min at room temperature (RT) with no shaking.
4. Prepare Triton washing solution by adding 5 ml of 10% Triton X-100 into 495 ml of PBS.
5. Remove the fixing solution from cells using a multichannel vacuum manifold.
6. Wash cells with 200 µl of Triton washing solution for 5 min, with gentle shaking on a rotary shaker to permeabilize the cells. Repeat wash step three more times (see Note 4). Do not allow cells to dry out.

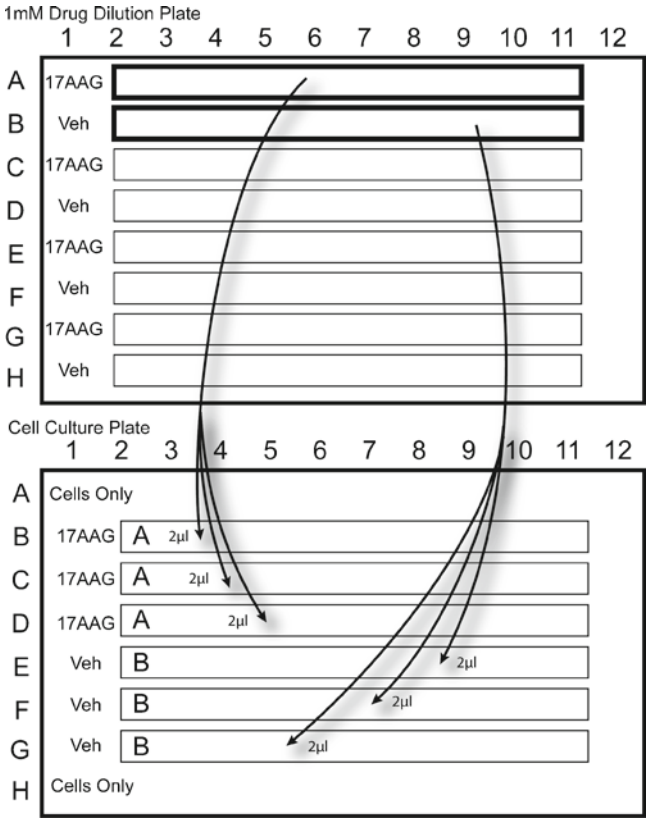

Fig. 1. Procedure for diluting drugs from a 1 mM stock drug dilution plate directly into cell culture plates. In a standard 96-well assay plate, prepare 1 mM compound stocks from one plate of a commercially available library by diluting in Opti-MEM. As a positive control, prepare a 100 μM stock of the Hsp90 inhibitor, 17-(Allylamino)-17-demethoxygeldanamycin (17-AAG). A vehicle control (Veh) of DMSO should also be prepared using a volume equivalent to the highest concentration of drug. Most libraries come with the first and last columns empty to add controls. Add the 17-AAG stock to wells A, C, E, and G to the first column; add vehicle to wells B, D, F, and H of the first column. Using a multichannel pipetter, add 2 μl from row A of the drug dilution plate to rows B, C, and D of the cell culture plates, creating triplicates for each compound in row A of the compound library. Add 2 μl from row B of the drug dilution plate to rows E, F, and G of the cell culture plates, creating triplicates for each compound in row B of the compound library. Repeat for rows C–H in other culture plates.

7. Remove the Triton Washing Solution using an automated plate washer.
8. Carefully, add 150 μl of Odyssey blocking buffer down the side of the wells into each well. Incubate at RT for 1.5 h with gentle shaking on a rotary shaker.
9. Dilute mouse anti-GAPDH at 1:1,000 and rabbit antitau at 1:1,000 in primary dilution buffer (8 ml of blocking buffer and 8 ml of PBS + 0.2% Tween-20). Remove the blocking buffer from the cell-containing wells using vacuum, and add

50 µl of this antibody mixture to rows B–G of all plates (see Note 6).

10. Add 50 µl of Odyssey blocking buffer to the top row of empty wells to control for evaporation due to overnight incubation.
11. Cover the plates and incubate overnight at 4°C with no shaking.
12. Prepare Tween washing solution by adding 1 ml 20% Tween-20 to 999 ml of PBS.
13. Wash the plates five times, incubating for 5 min between each wash at RT with gentle shaking on a rotator.
14. Dilute goat antirabbit Alexa Fluor 680 (1:500 dilution) and Goat/sheep antimouse IRDye 800CW (1:500 dilution) in secondary dilution buffer (10 ml of blocking buffer and 10 ml of 1× PBS + 0.4% Tween-20). Preparations should be made for low-light applications from this point forward.
15. Add 50 µl of this secondary antibody solution to all 96 wells of each of the four plates, wrap the plates with aluminum foil or store in black box to protect from light.
16. Incubate at RT for 60 min with gentle rotational shaking.
17. Wash the plates five times, incubating for 5 min between each wash at RT with gentle shaking on a rotator. Protect from light by wrapping the plate with aluminum foil.
18. Perform one final wash with 1× PBS without any detergent.
19. After this final wash, plates can be gently blotted dry using a Kimwipe or sterile towel.
20. Wipe the bottom plate surface and Odyssey imager scanning bed with lint-free paper. Scan plate immediately or wrap the plate with aluminum foil and store at 4°C for several weeks. Plates can also be stored long term at –20°C, although some signal intensity will be lost.
21. Adjust the settings of Odyssey Imager: use medium quality, 169 µm resolution, 3.0 mm focus offset, and intensity settings of five for both 700 nm and 800 nm channel. Start scanning simultaneously at 700 nm and 800 nm. These intensity settings may vary; however, plates can be scanned multiple times without consequence (see Note 7).
22. Once scanned, refer to the Odyssey application software manual for detailed methodology regarding data analysis (see Notes 8 and 9).
23. Figure 2 provides a detailed flow diagram for this procedure.

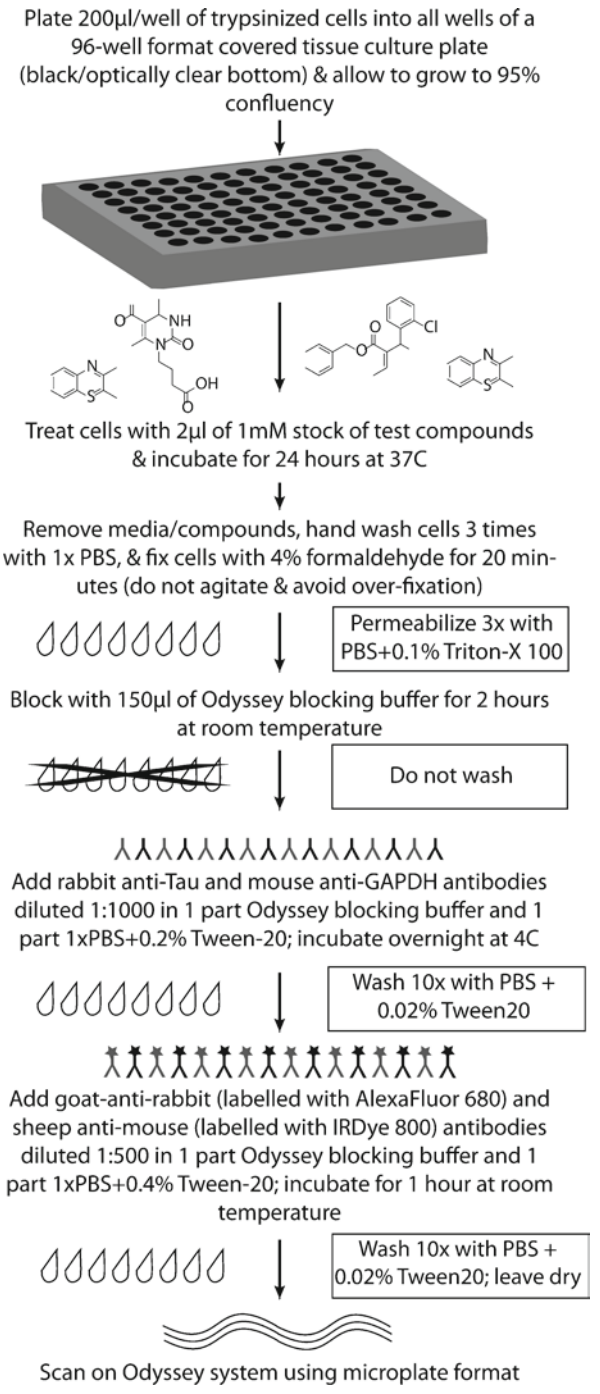

Fig. 2. Flow diagram of the In-Cell Western procedure. This diagram provides the minimal basics for the In-Cell Western procedure in a schematic single-page format.

3.2. Western Validation of Hits

3.2.1. Cell Culture and Treatment

1. Maintain H4 cells in complete media.
2. Remove media from the flask containing 95% confluent cells and add 5 ml of trypsin-EDTA to the flask and incubate for 2–5 min in the 37°C incubator.
3. Dispense 0.5 ml of suspended cells into a 15 ml conical tube and add 12 ml of complete media. Mix by tituration. Dispense 2 ml of cells into each well of a 6-well plate. Repeat two more times.
4. Incubate cells at 37°C in 5% CO_2 until 95% confluency is reached.
5. Prepare dilutions of the two hits and the toxic compound. Use the following concentrations: 10, 3, 1, 0.3, and 0 μM. Prepare each of these in 2 ml of Opti-MEM. Thus, there should be 15 tubes with 2 ml drug suspensions (see Note 10).
6. Remove complete media from cells and replace with these drug suspensions, one tube per well. Incubate cells at 37°C in 5% CO_2 for 24 h.

3.2.2. Cell Lysis

1. Remove media from the wells by vacuum aspiration and rinse cells gently with 1 ml of PBS.
2. Add 50 μl of Lysis buffer in the well and scrape cells using a cell lifter.
3. Transfer the lysed cells into 1.5 ml tubes and pulse sonicate for 30 s at 4°C.
4. Centrifuge at 13,500 × *g* for 10 min at 4°C and transfer supernatant into a new 1.5 ml tube. Discard pellet.
5. Perform BCA protein assay or store supernatant at –20°C.

3.2.3. Protein Estimation

1. Use a clear 96-well plate to do protein estimation.
2. Prepare BCA reagent by diluting Reagent B 1:50 in reagent A (e.g., add 200 μl of reagent B in to 9.8 ml of Reagent A.) BSA is provided as a standard protein to establish a standard curve.
3. All standards, samples and blanks should be run in triplicate.
4. The standard curve should be as follows for cell culture studies: dilute a 1 mg/ml stock of BSA with water to final concentrations of 1, 2, 5, 10, 15, 20, and 25 μg/ml. 25 μl water as a blank control should also be included for normalization.
5. 1 μl of each sample should then be added to other wells containing 24 μl of water.
6. Add 175 μl of BCA reagent to each well, mix by gentle rotation and incubate for 30 min at 37°C.
7. Measure optical density at 562 nm using a visible light spectrophotometer and use these values to generate a standard curve and determine protein concentrations.

3.2.4. Western Blotting with the Odyssey System

1. To investigate total tau levels by Western blot, a high amount of protein is typically required. Therefore, prepare 50 μg of total protein from H4 lysates and mix with equal volumes of 2× Laemmli sample buffer containing β-mercaptoethanol.
2. Heat denature these samples at 95°C for 10 min.
3. Centrifuge at 16,000 × *g* for 1 min at RT.
4. Load either the first or sixth lane of a 12-well 10% SDS-PAGE gel with a molecular weight ladder containing at least three standards in the 65–35 kDa range.
5. Load the samples in order from highest drug concentration to lowest drug concentration. Group samples by specific treatments, not concentrations. For example 10, 3, 1, 0.3, and 0 μM for Hit 1, followed by 10, 3, 1, 0.3, and 0 μM for the toxic hit.
6. Run the gel and transfer per standard procedures. The only caveat for running an Odyssey Western blot is to use PVDF-FL from Millipore in lieu of other membrane materials (see Note 11).
7. Following transfer, place the membrane in a square petri dish and block the membrane with Odyssey blocking buffer for 2 h at RT.
8. Dilute mouse anti-GAPDH at 1:5,000 and rabbit antitau at 1:5,000 in primary dilution buffer (5 ml of blocking buffer and 5 ml of PBS + 0.2% Tween-20). Decant the blocking buffer from the membrane and add the antibody mixture. Wrap with foil and incubate overnight at 4°C on a platform rocker.
9. Remove antibody mixture and wash the membrane with PBST (PBS with 0.2% Tween-20) for 10 min, repeating three times.
10. Dilute goat antirabbit Alexa Fluor 680 (1:1,000 dilution) and Goat/sheep antimouse IRDye 800CW (1:1,000 dilution) in secondary dilution buffer (5 ml of blocking buffer and 5 ml of 1× PBS + 0.4% Tween-20).
11. Decant wash buffer and add the secondary antibody mixture. Preparations should be made for low-light applications from this point forward (i.e., cover dish with foil).
12. Remove antibody mixture and wash the membrane with PBST for 10 min, repeating three times.
13. Remove PBST and replace with 1× PBS. Membrane can be scanned immediately or stored at 4°C for later (see Notes 12–17).

4. Notes

1. The most important note for this assay is the adherence to the reagents and supplies specified. In particular, it is important to use PBS and not TBS.
2. It is important to test the properties of your cell line with regard to adherence. We have utilized a number of cell lines and some work well while others do not. H4, CHO, and HeLa seem to be the most suitable for this assay.
3. Plate selection is important. The optically clear plates work great, but they are costly. Some plastics have less autofluorescence than others. These can be tested if the cost becomes prohibitive.
4. Automation is a central key for the reproducibility of this assay. Multichannel pipetters, plate washers, etc., where possible, dramatically improves the results.
5. It is essential that only the inner 60 wells of the tissue culture plate be used for your test samples, but that the outer wells contain cells and media.
6. The near-infrared channel corresponding to 800 nm/green fluorescence exhibits slightly lower intensity than the 680 nm/red channel. Thus, our loading control, GAPDH, was always used with the 800 nm dye.
7. Saturation is a problem with the fluorescent detection of the Odyssey system. When antibody concentrations are too high, saturation will occur, which manifests as a white signal. The scanning intensity can be adjusted before the scan, reducing this phenomenon; however, it may require that the entire experiment be rerun if it cannot be corrected. Therefore, it is very important that antibodies be titrated carefully to avoid this problem at the end of a large experiment.
8. Once the data has been collected from the In-Cell Western assay, we must begin the process of validating whether these compounds directly affect tau biology. We have summarized an example of results in Fig. 3a. One main concern with this type of assay is controlling for toxicity. By using GAPDH as one of our proteins, its levels can be used to estimate this. If GAPDH levels are significantly decreased, irrespective of tau levels, it suggests to us that this agent is simply killing cells (Fig. 3a). In this same assay, we considered two compounds to be "hits" because they appear to reduced tau (red) without reducing GAPDH (green). The overlay of the screen shows this contrast more clearly (yellow). These would be the best lead molecules for further testing. We also have internal

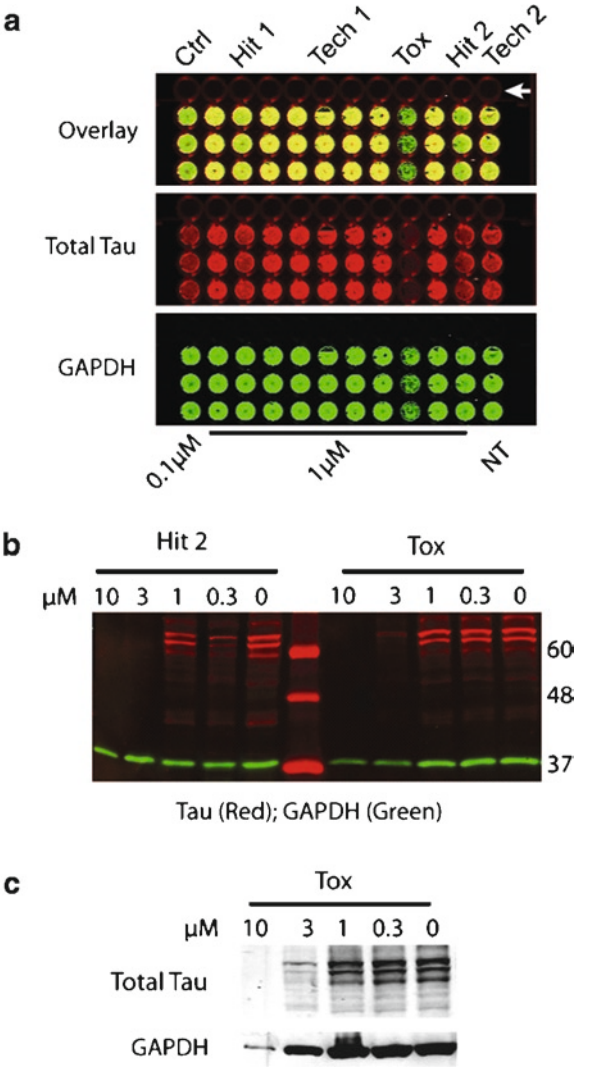

Fig. 3. Tau and GAPDH levels from drug-treated H4 cells following In-Cell and Odyssey Western analysis. (**a**) Images for one row of compounds run in triplicate with 17-AAG as a control (column 1, *indicated as Ctrl*) and untreated controls (column 12, indicated as Tech 2 at *top* and NT at *bottom*). Total tau is shown in *red*, GAPDH in *green*, and the overlay in *yellow*. The *white arrow* indicates *row A* of the plate showing no signal despite the presence of cells. This controls for autofluorescence. Presumptively effective drugs are designated as Hit 1 and Hit 2, showing reduced *red fluorescence* (Tau) with minimal loss of *green fluorescence* (GAPDH). Tox indicates that a toxic effect was observed, where GAPDH and Tau levels were both reduced. Tech1 demonstrates a common technical problem associated with cell adhesion. Tech2 demonstrates a common technical problem with nonuniform fluorescence across plates, particularly in the outer wells. (**b**) Dose response to Hit 2 and Tox as determined by standard Odyssey Western analysis. *Green bands* indicate GAPDH signal; *red bands* indicate Total tau signal. The molecular weight ladder in the *Sixth lane* fluoresces *red* and molecular weights are indicated on the *right*. (**c**) Dose response to Tox by Western blot using chemiluminscent detection.

validation within each plate because of the use of 17AAG as a positive control (Ctrl; Fig. 3a). Our vehicle control was in the bottom half of the plate (not shown). Now that we have hits to analyze, the next step in the process will be concentration optimization and validation by Western blot.

9. Figure 3a also illustrates two important technical challenges with the In-Cell Western; cell adhesion and signal distribution across plates. These are indicated as Tech 1 and Tech 2. Tech 1 shows that even extremely hearty cells like H4 can become detached during the In-Cell Western process despite fastidious care being taken. Thus, other less adherent cell lines can pose significant problems for assay development. Tech 2 shows perhaps the most difficult challenge with these assays; that being the growth kinetics of cells across 96-well plates. Gas exchange and heat properties vary for the outer wells relative to the inner core of 60 wells in a 96-well plate. While we have not been able to prevent this, we have adapted to the problem. For every assay, we include a control plate with no treatment across wells. Following the In-Cell Western protocol, we can then use this control plate as a normalization template for the growth dynamics of cells in that given run.

10. Toxicity with any compound is a concern for cell culture. Prior to preparing the samples and performing the Odyssey Western, toxicity assessment can be performed on the supernatant from cells 4 h after drug treatment using a CytoTox LDH analysis kit.
11. Always use the PVDF-FL membrane for Odyssey Westerns. This particular polymer has been specially designed to demonstrate extremely low autofluorescence.
12. Remove air bubbles between the membrane and scanning surface prior to scanning.
13. Use flat forceps to move membrane, particularly when applying the membrane to the scanning surface; never touch membrane with bare hands.
14. If signals are intense, there may be “bleed through” of the 800 nm signal with the 680 nm laser such that green signal shows up as a red signal, or vice versa. This can be titrated out using the appropriate concentration of antibody. This is particularly important if the proteins being investigated have a similar molecular weight.
15. If signals are too intense, wash the membrane with PBS containing up to 0.5% Tween-20 for 1 h and scan again.
16. If signals are not clear, reimmerse the membrane in methanol, wash with 1× PBS, and reapply a second round of secondary

antibodies at higher concentrations while reducing the stringency of the dilution buffer.

17. Tau biochemical analyses by Western blot can also be a challenge, and understanding these nuances is critical for interpretation of results. By Western blot, tau manifests not as a single band, but as multiple bands anywhere between 70 and 30 kDa. This can make analysis of tau Western blots difficult; however, a large amount of effort has been taken to understand why these bands emerge, and we will clarify some of those reasons here. First, tau is alternatively spliced into six isoforms (4). In cell culture, the species predominantly produced lack exon 10, leaving three primary isoforms ranging from 65 to 50 kDa (5). Some treatments may influence splicing factors that could change this pattern, allowing the other three isoforms to emerge. Tau is also heavily modified post-translationally. Each isoform can be differentially phosphorylated at any number of its >20 phosphorylation sites (6), dramatically altering its migration through a gel. It can be nitrated (7), glycosylated (8) and ubiquitinated (9). Tau can also be cleaved by proteases to produce smaller fragments that can range anywhere between 40 and 17 kDa (10). Therefore, it is critical to try and develop a mechanistic model for each test compound based on its known mechanism of action, which will help direct future experimental design.

Acknowledgments

This work was supported by the Alzheimer's Association and the NIA K99/R00AG031291.

References

1. Dickey, C. A., Eriksen, J., Kamal, A., Burrows, F., Kasibhatla, S., Eckman, C. B., Hutton, M., and Petrucelli, L. (2005) Development of a high throughput drug screening assay for the detection of changes in tau levels – proof of concept with HSP90 inhibitors. *Curr Alzheimer Res* **2**, 231–8.
2. Dickey, C. A., Ash, P., Klosak, N., Lee, W. C., Petrucelli, L., Hutton, M., and Eckman, C. B. (2006) Pharmacologic reductions of total tau levels; implications for the role of microtubule dynamics in regulating tau expression. *Mol Neurodegener* **1**, 6.
3. Dickey, C. A., Dunmore, J., Lu, B., Wang, J. W., Lee, W. C., Kamal, A., Burrows, F., Eckman, C., Hutton, M., and Petrucelli, L. (2006) HSP induction mediates selective clearance of tau phosphorylated at proline-directed Ser/Thr sites but not KXGS (MARK) sites. *Faseb J* **20**, 753–5.
4. Goedert, M., Spillantini, M. G., Jakes, R., Rutherford, D., and Crowther, R. A. (1989) Multiple isoforms of human microtubule-associated protein tau: sequences and localization in neurofibrillary tangles of Alzheimer's disease. *Neuron* **3**, 519–26.
5. Ko, L. W., DeTure, M., Sahara, N., Chihab, R., and Yen, S. H. (2002) Cellular models for tau filament assembly. *J Mol Neurosci* **19**, 311–6.
6. Mandelkow, E. M., Biernat, J., Drewes, G., Gustke, N., Trinczek, B., and Mandelkow, E. (1995) Tau domains, phosphorylation, and

interactions with microtubules. *Neurobiol Aging* **16**, 355–62; discussion 62–3.

7. Reynolds, M. R., Berry, R. W., and Binder, L. I. (2005) Site-specific nitration differentially influences tau assembly in vitro. *Biochemistry* **44**, 13997–4009.
8. Arnold, C. S., Johnson, G. V., Cole, R. N., Dong, D. L., Lee, M., and Hart, G. W. (1996) The microtubule-associated protein tau is extensively modified with O-linked N-acetylglucosamine. *J Biol Chem* **271**, 28741–4.
9. Dickey, C. A., Yue, M., Lin, W. L., Dickson, D. W., Dunmore, J. H., Lee, W. C., Zehr, C., West, G., Cao, S., Clark, A. M., Caldwell, G. A., Caldwell, K. A., Eckman, C., Patterson, C., Hutton, M., and Petrucelli, L. (2006) Deletion of the ubiquitin ligase CHIP leads to the accumulation, but not the aggregation, of both endogenous phospho- and caspase-3-cleaved tau species. *J Neurosci* **26**, 6985–96.
10. Gamblin, T. C., Chen, F., Zambrano, A., Abraha, A., Lagalwar, S., Guillozet, A. L., Lu, M., Fu, Y., Garcia-Sierra, F., LaPointe, N., Miller, R., Berry, R. W., Binder, L. I., and Cryns, V. L. (2003) Caspase cleavage of tau: linking amyloid and neurofibrillary tangles in Alzheimer's disease. *Proc Natl Acad Sci U S A* **100**, 10032–7.

Chapter 9

Split GFP Complementation Assay for Quantitative Measurement of Tau Aggregation In Situ

Wanjoo Chun, Geoffrey S. Waldo, and Gail V.W. Johnson

Abstract

A primary pathological hallmark of Alzheimer disease brain is the presence of neurofibrillary tangles, which are highly aggregated and insoluble accumulations of the microtubule-associated protein tau. Although it is becoming increasingly apparent that the mature neurofibrillary tangles are not the toxic species, intermediates between soluble tau and the neurofibrillary tangles likely play key roles in the neurodegenerative process. Therefore, it is critically important to be able to quantitatively monitor the process of tau aggregation in living cells in order to understand the evolution of tau from its physiological to its pathological forms. To detect and quantitate the aggregation of tau in cells, we established a split green fluorescent protein (GFP) complementation assay. In this assay, GFP is separated into two spontaneously associating fragments that form the fluorescent fluorophore. The smaller GFP fragment, GFP_{11}, is fused to tau and coexpressed in cells with the larger fragment $GFP_{1–10}$ leading to the association and reconstitution of the active fluorophore. However, if tau becomes partitioned into aggregates, the GFP_{11} tag will be less accessible for interactions with $GFP_{1–10}$ resulting in a decrease in GFP complementation and fluorescence which can be monitored either using fluorescence microscopy or with a fluorescence plate reader. Thus, this assay is a valuable tool for measuring tau aggregation in living cells and evaluating factors that modulate this process.

Key words: Split GFP complementation, Tau, Aggregation, GSK3β

1. Introduction

Tau is a soluble, neuronally enriched, alternatively spliced, microtubule-associated protein that is involved in regulating microtubule function, intracellular transport mechanisms and cellular signaling processes (1, 2). Tau is also a pivotal player in the pathogenic mechanisms underlying Alzheimer disease (AD), as well as other "tauopathies" (3). In these diseases, tau is abnormally modified and processed resulting in a loss of normal function, as well as a gain

Erik D. Roberson (ed.), *Alzheimer's Disease and Frontotemporal Dementia*, Methods in Molecular Biology, vol. 670,
DOI 10.1007/978-1-60761-744-0_9, © Springer Science+Business Media, LLC 2011

of toxic properties. One of the primary features of pathological tau is its increased propensity to self-associate and eventually form large, insoluble intracellular aggregates (neurofibrillary tangles, NFTs) (4, 5). Although the NFTs are unlikely to be the primary pathological species, intermediate forms, including soluble tau oligomers, are likely to be the contributors to neuronal dysfunction and death (6, 7). Therefore, it is of fundamental importance to be able to analyze the process of tau aggregation in living cells.

In this chapter, we describe a protocol to quantitatively detect the aggregation of tau in cells using a split green fluorescent protein (GFP) complementation assay (8). This assay was originally developed for in vitro use or in bacteria (9); however, we have now modified and adapted it for use in mammalian cells. In this assay, GFP is separated into two spontaneously associating fragments that form the fluorescent fluorophore. The smaller GFP fragment, GFP_{11}, is fused to tau and coexpressed in mammalian with the larger fragment $GFP_{1–10}$, which leads to association and reconstitution of the active fluorophore. However, if tau becomes partitioned into aggregates the GFP_{11} tag will be less accessible for interactions with $GFP_{1–10}$ resulting in a decrease in GFP complementation and fluorescence which can be monitored either using fluorescence microscopy or with a fluorescence plate reader (8, 9).

2. Materials

2.1. Preparation of Tau–GFP_{11} Constructs

1. Plasmid containing the desired tau construct.
2. PCR thermocycler.
3. Deoxynucleotide triphosphate (dNTP) mix for PCR.
4. Taq polymerase for PCR.
5. PCR product purification kit.
6. Mammalian Optimized Split GFP Detection System (Sandia BioTech), containing $GFP_{1–10}$ and GFP_{11} vectors.
7. XbaI and KpnI restriction enzymes, with their 10× reaction buffers.
8. Agarose gel electrophoresis apparatus with power supply.
9. Gel extraction kit (such as QIAquick gel extraction kit from Qiagen).
10. DNA ligase with 10× reaction buffer.
11. DH5α competent cells.
12. Plasmid purification kit (such as QIAprep spin miniprep kit from Qiagen).

2.2. Qualitative Imaging of In Situ GFP Complementation

1. Tissue culture facility with hood and incubators.
2. 60 mm tissue culture plates.
3. HEK293 cells (ATCC).
4. Dulbecco's Modified Eagle's Medium/F-12 Medium (DMEM/F-12). Add l-glutamine (20 mM final), penicillin (100 U/mL final) and streptomycin (100 U/mL final) from commercially available 100× stocks.
5. Fetal bovine serum (FBS).
6. DMEM/F-12 without phenol red. This is used to avoid interference of phenol red when measuring the intensity of GFP fluorescence (see Note 1).
7. FuGENE 6 transfection reagent (Roche).
8. Tau-GFP_{11} construct, produced as described in Subheading 3.1.
9. Epifluorescence microscope with digital camera.

2.3. Identify Optimal Amounts of Tau-GFP_{11} to Transfect

1. Flat- and clear-bottom, opaque white-walled 96-well plates (see Note 2).
2. Microplate reader capable of detecting GFP (excitation and emission wavelengths of 488 nm and 530 nm, respectively).

2.4. Confirm Sensitivity of the Assay to Changes in Tau Aggregation

1. K18-GFP_{11} construct (expressing tau microtubule binding domain, wild type sequence) (10).
2. K18/Δ280-GFP_{11} construct (expressing K18 with a deletion of lysine residue at the position of 280; proaggregation mutant) (10).
3. K18/Δ280/2P-GFP_{11} construct (expressing K18/Δ280 with substitutions of isoleucine residues at positions 277 and 308 to proline; antiaggregation mutant) (10).

2.5. Using Split GFP Complementation to Examine Changes in Tau Aggregation

1. Plasmid expressing constructs whose effect on tau aggregation is to be tested.
2. For the example in Subheading 3.5, we used the following GSK3β constructs: GSK3β-S9A-HA is a constitutively active form of GSK3β (11). The kinase-dead (kd)-GSK3β-HA construct, in which lysine residues at 85 and 86 were mutated to alanines leading to the significantly decreased activity compared to wild type, was a generous gift of G. Meares at the University of Alabama at Birmingham (12).

2.6. Western Blotting for Tau Expression

1. Phosphate buffered saline (PBS): 137 mM NaCl, 10 mM phosphate, 2.7 mM KCl, pH 7.4.
2. Lysis buffer: 150 mM NaCl, 10 mM Tris–HCl, 1 mM EGTA, 1 mM EDTA, 0.2 mM sodium vanadate, and 0.5% Nonidet p-40, 1 mM phenylmethylsulfonyl fluoride and 10 μg/mL

each of leupeptin, aprotinin, and pepstatin. Add protease inhibitors right before use.

3. Cell scrapers.
4. Sonicator.
5. Microfuge.
6. Bicinchoninic acid (BCA) protein assay kit for microplates.
7. 2× SDS Stop: 10% SDS, 100 mM EGTA, 100 mM EDTA, 25 mM DTT, 10% glycerol, 0.5 M Tris–HCl, pH 6.8.
8. Protein electrophoresis apparatus with power supply.
9. Separating gel buffer (4×): 1.5 M Tris–HCl, pH 8.8.
10. Stacking gel buffer (4×): 0.5 M Tris–HCl, pH 6.8.
11. 30% acrylamide/0.8% bisacrylamide solution (37.5:1). Acrylamide is a neurotoxin when unpolymerized, so care should be taken to reduce exposure.
12. 10% ammonium persulfate (APS). Prepare by diluting APS in water and immediately freeze in single use (200 µL) aliquots at –20°C.
13. *N*,*N*,*N*,*N*′-Tetramethyl-ethylenediamine (TEMED).
14. Separating gel solution: 8% acrylamide:bis (37.5:1), 375 mM Tris–HCl, pH 8.8, 0.08% APS, and 0.08% TEMED. To make 24 mL, mix 6.4 mL of 30% acrylamide:bis, 6 mL of 1.5 M Tris–HCl, pH 8.8, 11.4 mL water, 200 µL of 10% APS, and 20 µL of TEMED.
15. Stacking gel solution: 3% acrylamide:bis (37.5:1), 125 mM Tris–HCl, pH 6.8, 0.2% APS, and 0.1% TEMED. Mix 1.0 mL of 30% acrylamide:bis, 2.5 mL of 0.5 M Tris–HCl (pH 6.8), 6.3 mL water, 200 µL of 10% APS solution, and 10 µL of TEMED.
16. Electrode buffer (10×): 0.25 M Tris base, 1.9 M glycine.
17. Running buffer: 25 mM Tris, 190 mM glycine, 0.1% SDS. Mix 100 mL of 10× electrode buffer, 10 mL of 10% SDS, and add water to 1 L.
18. Prestained protein molecular weight markers.
19. Transfer buffer: 25 mM Tris, 190 mM glycine, 10% methanol. Mix 100 mL of 10× electrode buffer and 100 mL of methanol, then add water to 1 L.
20. Nitrocellulose membrane, 0.2 µm.
21. 10× Tris-buffered saline with Tween (10× TBS-T): 1.37 M NaCl, 27 mM KCl, 250 mM Tris–HCl, pH 7.4, 1% Tween-20.
22. Blocking buffer: 5% (w/v) nonfat dry milk in 1× TBS-T.
23. Primary antibodies.

- For tau: Either Tau5 (Abcam, 1:10,000), 5A6 (University of Iowa Developmental Studies Hybridoma Bank; 1:10,000), or polyclonal rabbit antihuman tau (Dako, 1:5,000).
- For GFP: Anti-GFP, N-terminal antibody (Sigma; 1:5,000).
- For GSK3β: The construct described here has an HA tag, and we use 16B12 monoclonal HA.11 antibody (Covance, 1:5,000).

24. Secondary antibodies
    - Antimouse IgG conjugated to horse radish peroxidase (HRP).
    - Antirabbit IgG conjugated to HRP.
25. Enhanced chemiluminescent (ECL) reagents (Amersham Biosciences) and Bio-Max ML film (Kodak, Rochester, NY).
26. Film and film developer.

3. Methods

The split GFP complementation assay was originally created to detect the aggregated state of proteins in vitro or in prokaryotes (9); however, we have now adapted it to measure tau aggregation in mammalian cells. GFP has been separated into two soluble and spontaneously associating fragments, GFP_{11} and $GFP_{1–10}$, using DNA shuffling techniques and with a variety of point mutations. When mixed together, the two GFP fragments spontaneously complement resulting in GFP folding and the formation of the fluorophore (8, 9). However, the aggregation of the protein to which the GFP_{11} fragment is fused results in a decrease in accessibility of this part of GFP and a loss of fluorescence.

3.1. Preparation of Tau–GFP_{11} Constructs

The first step is to produce the desired tau-GFP_{11} constructs. As an example, we provide here the protocol we used to produce the wild type 4R0N tau fusion with GFP_{11} (T4-GFP_{11}).

1. Design primers to amplify tau from its parent vector, with KpnI and XbaI sites engineered at the ends. It is important to design the primers so that the tau construct is inserted in frame (Fig. 1). To amplify T4 from its expression vector, we used the following primers:
    - Forward primer: GGG GTA CCA TGG CTG AGC CCC GCC AGG AGT T
    - Reverse primer: GCT CTA GAT CCC AAA CCC TGC TTG GCC AGG GAG G

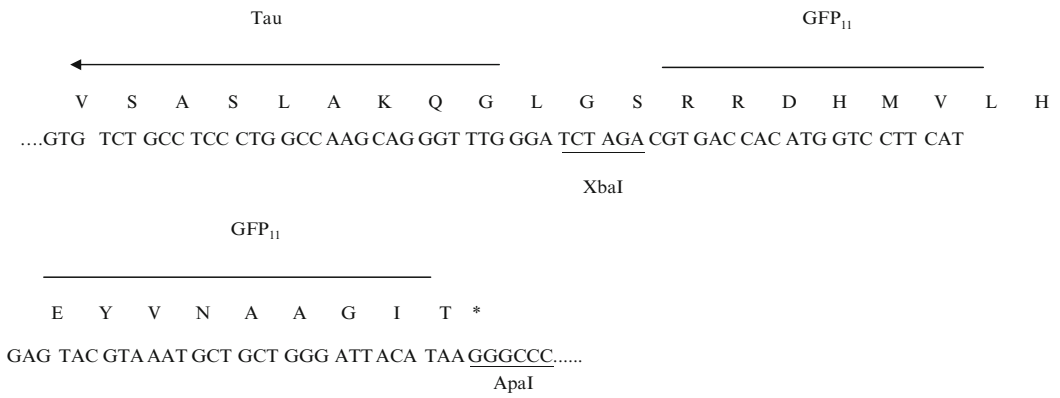

Fig. 1. Diagram showing the T4-GFP_{11} construct in pcDNA3.1(+) where T4 (Tau) and GFP are fused. Note that the original linker domain between the protein and the GFP_{11} tag was removed to increase the sensitivity of the assay.

2. Use these primers to amplify the tau fragment by PCR. In a 50 µL reaction, mix 5 µL 10× reaction buffer, 1 µL dNTPs, 1 µg of tau DNA template, 1 µL of each primer (1 mg/mL stock), and 1 µL Taq polymerase. Amplify for 30 cycles.
3. Purify the amplified fragment using a commercial PCR product purification kit, according to the manufacturer's instructions.
4. Digest the PCR products and the GFP_{11}-pcDNA 3.1(+) vector with KpnI and XbaI. In 20 µL reactions, mix 2 µL 10× reaction buffer, 1 µg of DNA (either from the PCR reaction or supercoiled GFP_{11}-pcDNA3.1(+) vector), 1 µL of KpnI and 1 µL of Xba I. Incubate at 37°C for 3 h for vector digestion and overnight for PCR products.
5. Isolate the digested fragments by agarose gel electrophoresis and purify with a gel extraction kit according to the manufacturer's instructions.
6. Ligate the PCR fragment into the linearized GFP_{11}-pcDNA3.1(+) vector. In a 20 µL reaction, mix 2 µL 10× reaction buffer, 2.5 ng of purified tau PCR fragment in 5 µL, 40 ng of linearized GFP_{11}-pcDNA3.1(+) in 2 µL, and 1 µL of ligase. Incubate at room temperature for 2 h.
7. Transform into DH5α competent cells according the manufacturer's instructions and plate on ampicillin agarose plates.
8. Pick bacterial colonies and inoculate in 5 mL of ampicillin-containing LB broth. Incubate with shaking at 37°C overnight.
9. Purify plasmids using a plasmid miniprep purification kit.
10. Verify clone by sequencing.

3.2. Qualitative Imaging of In Situ GFP Complementation

Before proceeding with quantitative measurements, it is important to confirm the ability of the constructs to produce GFP complementation and fluorescence. This is achieved by transient transfection in HEK cells and routine fluorescence microscopy.

1. Plate 6×10^5 HEK cells onto each 60 mm dish and incubate in 5% FBS/DMEM/F-12 medium without phenol red at 37°C for 24 h. This will result in about 70% confluency.
2. Dilute 6 μL FuGENE 6 transfection reagent in 100 μL serum-free DMEM-F12 without phenol red. Incubate 5 min at RT.
3. Prepare transfection reagent for three conditions: tau-GFP_{11} alone, $GFP_{1–10}$ alone, and tau-GFP_{11} with $GFP_{1–10}$. For each condition, mix 100 μL of diluted FuGENE and 2 μL of DNA containing either 2 μg of tau-GFP_{11} or 2 μg of $GFP_{1–10}$ or both. Tap to mix, and incubate 15 min at RT.
4. Remove the medium and add fresh medium containing 5% FBS right before the transfection.
5. Add 100 μL of DNA/FuGENE complex to the 60 mm dish. Swirl gently to mix.
6. Incubate cells at 37°C for 48 h.
7. Examine the complementation of tau-GFP_{11} and $GFP_{1–10}$ proteins under a fluorescence microscope (see Note 3). No fluorescence should be observed with either tau-GFP_{11} or $GFP_{1–10}$ alone (see Note 4).

3.3. Identify Optimal Amounts of Tau-GFP_{11} to Transfect

Before utilizing the assay to determine the effects of various manipulations on tau aggregation, it is important to identify a concentration of tau-GFP_{11} at which the assay exhibits first-order kinetics of complementation. To do this, transfect cells with increasing amounts of tau-GFP_{11}, and fixed amounts of $GFP_{1–10}$, and determine the resulting fluorescence (see Note 5). The graph of fluorescence versus tau-GFP_{11} amount should be linear (Fig. 2).

1. Seed 1×10^4 HEK cells per well in DMEM/F-12 with 2% FBS, without phenol red. For this experiment, you will test seven different amounts of tau-GFP_{11}, with six replicate wells for each concentration.
2. Incubate 24 h at 37°C.
3. For each tau-GFP_{11} concentration, prepare transfection reagent by diluting 9 μL FuGENE 6 transfection reagent in 100 μL serum-free DMEM-F12 without phenol red. Incubate 5 min at RT.
4. Add DNA to transfection reagent. Each condition will have 2 μg of $GFP_{1–10}$ and from 0–4 μg of tau-GFP_{11}. Tap to mix, and incubate 15 min at RT.

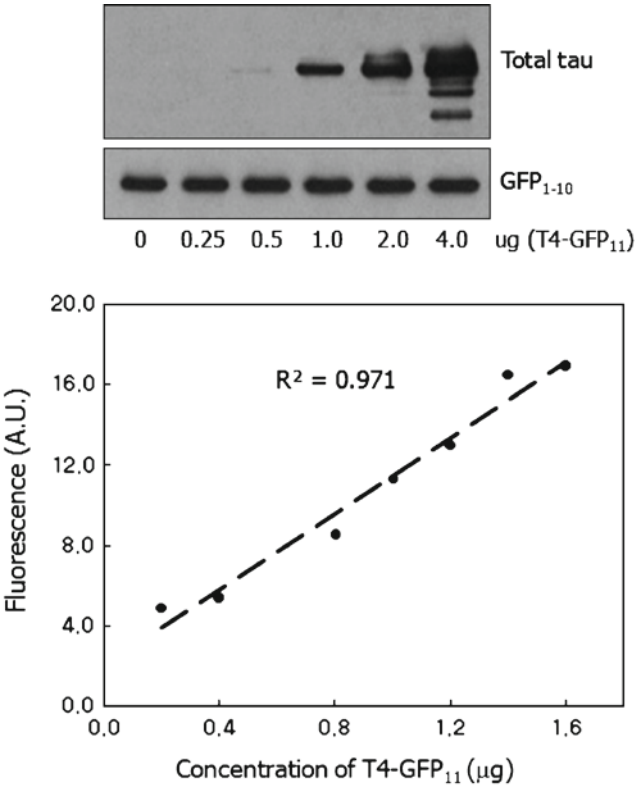

Fig. 2. Quantification in situ split GFP complementation. *Top*: immunoblots of increasing amount of T4-GFP_{11} (0–4.0 μg) and constant amount of $GFP_{1–10}$ (2 μg). Indicated the amount of T4-GFP_{11} and $GFP_{1–10}$ constructs were transiently cotransfected into 60 mm dishes of HEK cells. Five micrograms of protein were run in each lane and immunoblots of T4-GFP_{11} was probed with the 5A6 tau antibody and $GFP_{1–10}$ blot with a polyclonal GFP antibody (Sigma). *Bottom*: Quantitative analysis of in situ complementation of T4-GFP_{11} and $GFP_{1–10}$. Indicated amount of T4-GFP_{11} and 2 μg of $GFP_{1–10}$ and 9 μL of Fugene were mixed with 100 μL of serum free media and 16 μL were added to each well of HEK cells on a 96-well microtiter plate. Forty-eight hours after transfection, the intensity of GFP fluorescence was measured using a fluorescence reader. (Reproduced from (8) with permission from John Wiley & Sons Ltd.).

5. Remove the medium and add fresh medium containing 2% FBS right before the transfection.
6. Add 16 μL of DNA/FuGENE complex to each well. Swirl to mix.
7. Incubate 48 h at 37°C.
8. Measure the intensity of GFP fluorescence using a 96-well microplate reader.
9. Plot the amount of GFP intensity to obtain the linear quantitative ranges of complementation of the two GFP fragments (Fig. 2).

10. Select the appropriate amount of tau-GFP_{11} and $GFP_{1–10}$ constructs based on these preliminary studies to examine the effects of modulators that affect the propensity of aggregation of tau. We chose to use an amount of $GFP_{1–10}$ that was double the amount of tau-GFP_{11}.

3.4. Confirm Sensitivity of the Assay to Changes in Tau Aggregation

Before examining the effects of various manipulations on the propensity for tau aggregation, the sensitivity of the split GFP complementation assay for detecting tau aggregation should be confirmed. This is done using constructs expressing the tau microtubule-binding domain (MBD) with mutations that have previously been shown to affect aggregation. Compared to the wild type tau MBD (K18 construct), the tau ΔK280 mutation (K18/ΔK construct) is highly prone to aggregation, whereas additional mutation of two isoleucine residues (I277 and I308) to proline (K18/ΔK/2P construct) produces resistance to aggregation (10).

1. Seed 1×10^4 HEK cells per well in 2% FBS-DMEM/F-12 without phenol red and grow for 24 h at 37°C. Plan on six replicate wells for each construct.
2. Prepare tubes for each condition (K18, K18/ΔK, and K18/ΔK/2P, plus K18-GFP_{11} alone and $GFP_{1–10}$ alone), each with 9 μL FuGENE 6 transfection reagent in 100 μL serum-free DMEM-F12 without phenol red. Incubate 5 min at RT.
3. Add 2 μg of $GFP_{1–10}$ and 1 μg of the appropriate K18-GFP_{11} construct to each tube. Tap to mix, and incubate 15 min at RT.
4. Remove the medium and add fresh medium containing 2% FBS right before the transfection.
5. Add 16 μL of DNA/FuGENE complex to each well. Swirl to mix.
6. Incubate 24 h at 37°C.
7. Measure the intensity of GFP fluorescence on a microplate reader.
8. Return the cells to the 37°C incubator, and repeat the fluorescence measurements every 24 h up to 5 days after transfection (see Note 6).
9. Emission of GFP fluorescence should not be observed in cells with either each microtubule-binding domain-GFP_{11} or $GFP_{1–10}$ alone.
10. Plot the amount of the split GFP complementation in terms of intensity of GFP fluorescence to confirm the sensitivity of the assay (Fig. 3).

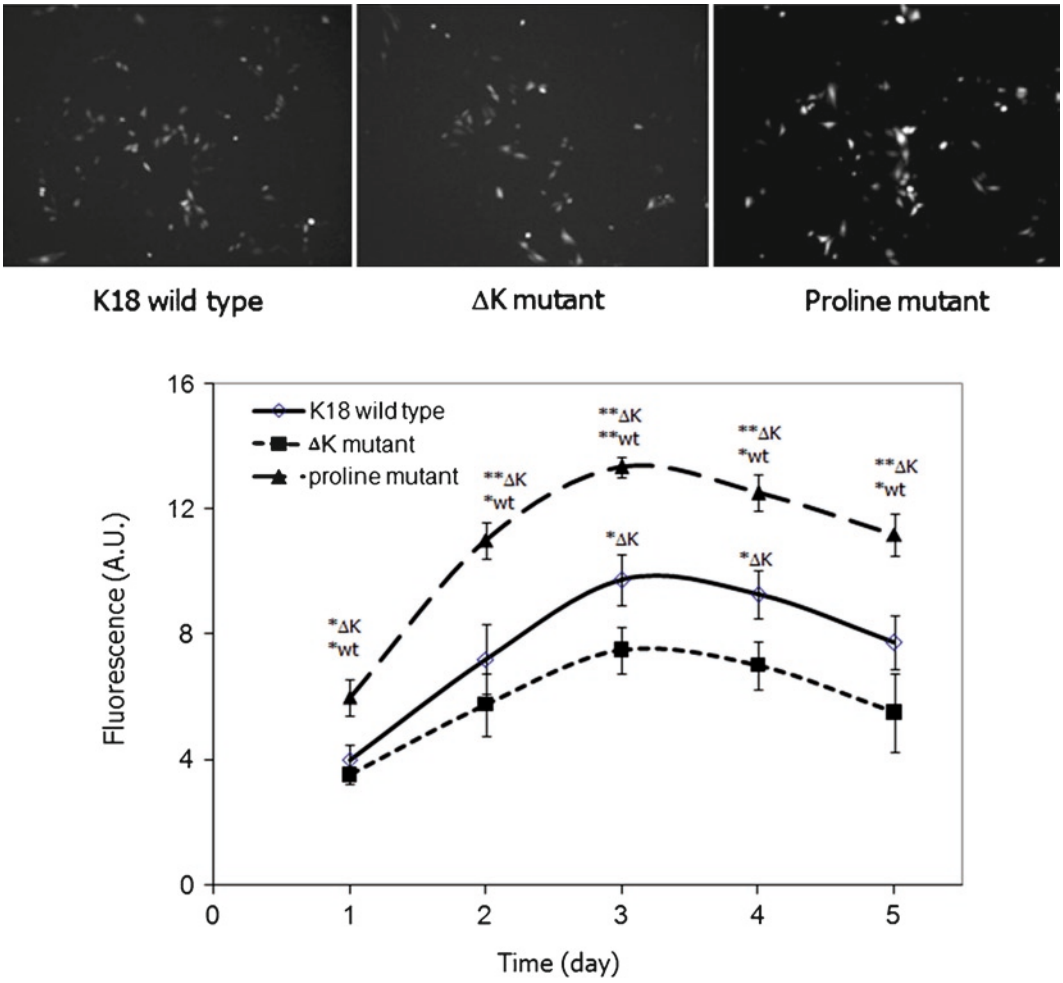

Fig. 3. Quantitative analysis of in situ split GFP complementation of microtubule-binding domain constructs. HEK cells were transfected with 1 μg of the respective microtubule-binding domain-GFP_{11} construct and 2 μg of $GFP_{1–10}$ construct. Top: representative images of split GFP complementation in each group 48 h after transfection. Cells on culture plates were examined using fluorescence microscopy. Bottom: quantitative analysis of in situ complementation of microtubule-binding domain-GFP_{11} proteins. The GFP intensity was quantitatively measured every 24 h up to 5 days ($\lambda_{exe} = 488$ nm/$\lambda_{em} = 530$ nm) and plotted as mean ± SE from three independent experiments ($n = 3$). There was no detectable GFP emission right after transfection; therefore, day 0 was not included in the graph. *$p < 0.05$; **$p < 0.01$. (Reproduced from (8) with permission from John Wiley & Sons Ltd.).

3.5. Using Split GFP Complementation to Examine Changes in Tau Aggregation

At this point, the assay is ready for use in determining the effect of various manipulations on tau aggregation. The assay should be amenable to cotransfection with plasmids expressing other gene products or siRNAs, or pharmacologic agents. As an example, we detail the protocol by which we examined the effects of the GSK3β protein kinase on tau aggregation (8).

1. Seed 1×10^4 HEK cells per well in 2% FBS-DMEM/F-12 without phenol red and grow for 24 h at 37°C. Plan on six wells for each construct.

2. Prepare FuGENE reagent for each condition, each with 9 μL FuGENE 6 transfection reagent in 100 μL serum-free DMEM-F12 without phenol red. Incubate 5 min at RT.
3. Add 1.6 μg of $GFP_{1–10}$, 0.8 μg of tau-GFP_{11} construct, and 0.6 μg of GSK construct (either the constitutively active S9A form, or the kinase-dead from with K85A/K86A mutations) to each tube (see Note 7). Tap to mix, and incubate 15 min at RT.
4. Remove the medium and add fresh medium containing 2% FBS right before the transfection.
5. Add 16 μL of DNA/FuGENE complex to each well. Swirl to mix.
6. Twenty-four hours after transfection, measure the intensity of GFP fluorescence every 24 h up to 5 days.
7. Emission of GFP fluorescence should be not observed in cells with either each tau-GFP_{11} or $GFP_{1–10}$ alone.
8. Measure the amount of the split GFP complementation in terms of intensity of GFP fluorescence to examine the role of GSK3β-mediated phosphorylation and caspase-3-mediated cleavage on the aggregate formation of tau (Fig. 4; see Note 8).

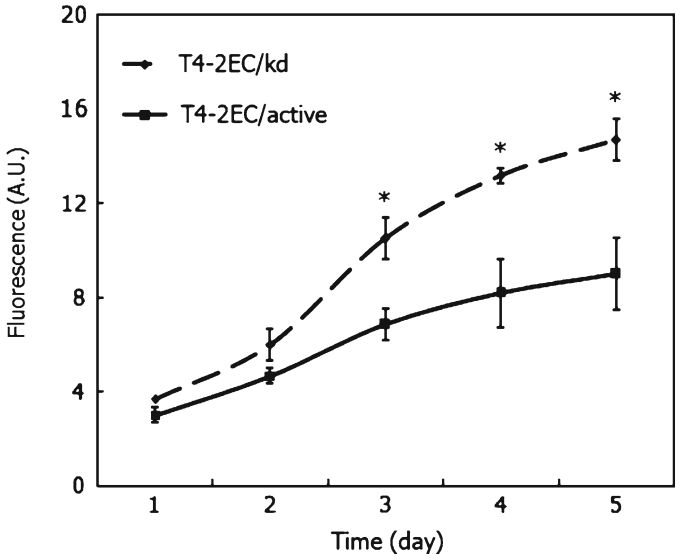

Fig. 4. Effects of GSK3β activation on the aggregation of T4-2EC in situ split GFP complementation. A master mix of T-2EC-GFP_{11} (0.8 μg), $GFP_{1–10}$ (1.6 μg) and kd-GSK3β (kd) (0.6 μg) or active GSK3β (active) (0.6 μg) was prepared in with 9 μL of Fugene in 100 μL of serum-free media. Sixteen microliters of the master mix was used in each well of HEK cells in a 96-well microtiter plate. The GFP intensity was quantitatively measured every 24 h up to 5 days ($\lambda_{exe} = 488$ nm/$\lambda_{em} = 530$ nm) and plotted as mean ± SE from three independent experiments ($n = 3$). There was no detectable GFP emission right after transfection; therefore, day 0 was not included in the graph. *$p < 0.05$. (Reproduced from (8) with permission from John Wiley & Sons Ltd.).

3.6. Western Blotting for Tau Expression

Immunoblotting for analysis of tau-GFP_{11} construct expression is an essential control to show that any changes in fluorescence induced by your experimental manipulation are truly due to altered tau aggregation, and not to changes in expression of tau-GFP_{11}. Because the 96-well format does not produce enough material for western blotting, this experiment is done in 60 mm dishes.

1. Plate 6×10^5 HEK cells onto each 60 mm dish and incubate in 5% FBS/DMEM/F-12 medium with phenol red at 37°C for 24 h.
2. For each condition, dilute 9 µL FuGENE 6 transfection reagent in 100 µL serum-free DMEM-F12 with phenol red. Incubate 5 min at RT.
3. Prepare transfection reagent by adding 1 µg of tau-GFP_{11} and 2 µg of $GFP_{1–10}$ DNA or 0.8 µg of tau-GFP_{11} + 1.6 µg of $GFP_{1–10}$ + 0.6 µg of GSK3β (active or kinase dead). Tap to mix, and incubate 15 min at RT.
4. Remove the medium and add fresh medium containing 5% FBS right before the transfection.
5. Add 100 µL of DNA/FuGENE complex to the 60 mm dish. Swirl gently to mix.
6. Incubate cells at 37°C for 48 h.
7. Remove medium and rinse cells twice with cold PBS.
8. Add 100 µL lysis buffer with protease inhibitors, scrape cells and transfer to a 1.5 mL microfuge tube.
9. Sonicate 3×2 s on ice.
10. Spin briefly at $10{,}000 \times g$ and transfer supernatants to clean tubes.
11. Measure protein concentrations of supernatants using the BCA assay in a microplate format according to manufacturer's instructions.
12. Dilute samples with 2× SDS Stop to a final concentration of 1 µg/µL.
13. Incubate in a boiling water bath for 5 min.
14. Assemble a 1.0-mm thick mini-gel casting apparatus.
15. Pour an 8% running gel, leaving space for a stacking gel, and overlay with water. The gel should polymerize in about 30 min.
16. Pour off the water.
17. Pour the stacking gel and insert the comb. The stacking gel should polymerize within 30 min.
18. Once the stacking gel has set, carefully remove the comb and wash the wells with running buffer.
19. Add the running buffer to the upper and lower chambers of the gel unit and load 5 µL (=5 µg protein) of each sample in a well. Add prestained molecular weight markers to a well on each gel.

20. Run the gels at 20 mA per each gel until the dye fronts are near the bottom of the gel.
21. Disconnect the gel unit from the power supply and disassemble. Discard the stacking gel. Transfer the separating gel to the top of a filter paper, cover the gel with nitrocellulose membrane, and then put a filter paper on top of them. Make them a sandwich with two sheets of sponges to complete the transfer cassettes.
22. Place the cassettes and an ice pack into the transfer tank. It is important to ensure correct orientation so that proteins are transferred to the nitrocellulose rather than lost into the buffer.
23. Transfer at 100 V for 1 h.
24. Once the transfer is complete, block the nitrocellulose in 5 mL blocking buffer for 1 h at room temperature on a rocking platform.
25. Discard the blocking buffer and rinse the membrane briefly prior to addition of primary antibodies in blocking buffer. Incubate overnight at 4°C on a rocking platform.
26. Remove the primary antibody and wash the membrane three times for 5 min each with 5 mL TBST.
27. Incubate the membranes with the appropriate secondary antibody at 1:5,000 in blocking buffer for 2 h at room temperature on a rocking platform.
28. Remove the secondary antibody and wash the membrane three times for 5 min each with 5 mL TBST.
29. Prepare the ECL reagents by mixing the solution A and B at 1:1 ratio and add immediately to the blot. Rotate by hand for 1 min to ensure even coverage.
30. Discard the ECL reagents. Place blot between the leaves of an acetate sheet protector in an X-ray film cassette.
31. Expose to film and develop.

4. Notes

1. Phenol red in DMEM/F-12 medium interferes with the measurement of intensity of GFP florescence. Therefore, use DMEM/F-12 without phenol red to quantitatively measure the intensity of GFP fluorescence.
2. HEK cells should be seeded in white clear-bottom 96-well microtiter plates to minimize the interference from neighboring wells.

3. Although microscopy is used to validate the constructs, this assay could be adapted such that fluorescence could be quantitated microscopically if the necessary equipment were available (e.g., an inverted confocal microscope with a mark and find function).
4. Either GFP fragment alone GFP_{11} or $GFP_{1–10}$, would result in an incomplete fluorophore, therefore no fluorescence should be observed when each fragment is expressed individually.
5. To quantitate the amount of tau complementation, an excessive amount of $GFP_{1–10}$ construct should be transfected compared to that of tau-GFP_{11} construct so that the tau-GFP_{11} is the limiting factor.
6. Intensity of GFP fluorescence should be measured every 24 h for 5 days. Be aware of any bacterial contamination that may occur and affect the outcome of the measures.
7. The total amount of DNA transfected is kept constant at 3 μg. In Subheadings 3.2–3.4, we used 2 μg of $GFP_{1–10}$ and 1 μg of the appropriate tau-$GFP_{11.}$ In Subheading 3.5, because we are also transfecting GSK plasmid, the amounts of the GFP plasmids are reduced somewhat, maintaining the same ratio as before.
8. Sarkosyl fractionation can be used to confirm the results from the split GFP complementation assay (8, 13).

Acknowledgments

This work was supported by NIH grant NS051279 and a grant from the Alzheimer Association.

References

1. Johnson, G. V., and Bailey, C. D. (2002) Tau, where are we now? *J Alzheimers Dis* 4, 375–98.
2. Stoothoff, W. H., and Johnson, G. V. (2005) Tau phosphorylation: physiological and pathological consequences. *Biochim Biophys Acta* 1739, 280–97.
3. Ding, H., and Johnson, G. V. (2008) The last tangle of tau. *J Alzheimers Dis* 14, 441–7.
4. Grundke-Iqbal, I., Iqbal, K., Quinlan, M., Tung, Y. C., Zaidi, M. S., and Wisniewski, H. M. (1986) Microtubule-associated protein tau. A component of Alzheimer paired helical filaments. *J Biol Chem* 261, 6084–9.
5. Kosik, K. S., Joachim, C. L., and Selkoe, D. J. (1986) Microtubule-associated protein tau (tau) is a major antigenic component of paired helical filaments in Alzheimer disease. *Proc Natl Acad Sci U S A* 83, 4044–8.
6. Roberson, E. D., Scearce-Levie, K., Palop, J. J., Yan, F., Cheng, I. H., Wu, T., Gerstein, H., Yu, G. Q., and Mucke, L. (2007) Reducing endogenous tau ameliorates amyloid beta-induced deficits in an Alzheimer's disease mouse model. *Science* 316, 750–4.
7. Santacruz, K., Lewis, J., Spires, T., Paulson, J., Kotilinek, L., Ingelsson, M., Guimaraes, A., DeTure, M., Ramsden, M., McGowan, E., Forster, C., Yue, M., Orne, J., Janus, C., Mariash, A., Kuskowski, M., Hyman, B., Hutton, M., and Ashe, K. H. (2005) Tau suppression in a neurodegenerative mouse model improves memory function. *Science* 309, 476–81.

8. Chun, W., Waldo, G. S., and Johnson, G. V. (2007) Split GFP complementation assay: a novel approach to quantitatively measure aggregation of tau in situ: effects of GSK3beta activation and caspase 3 cleavage. *J Neurochem* 103, 2529–39.
9. Cabantous, S., Terwilliger, T. C., and Waldo, G. S. (2005) Protein tagging and detection with engineered self-assembling fragments of green fluorescent protein. *Nat Biotechnol* 23, 102–7.
10. Khlistunova, I., Biernat, J., Wang, Y., Pickhardt, M., von Bergen, M., Gazova, Z., Mandelkow, E., and Mandelkow, E. M. (2006) Inducible expression of Tau repeat domain in cell models of tauopathy: aggregation is toxic to cells but can be reversed by inhibitor drugs. *J Biol Chem* 281, 1205–14.
11. Cho, J. H., and Johnson, G. V. (2003) Glycogen synthase kinase 3beta phosphorylates tau at both primed and unprimed sites. Differential impact on microtubule binding. *J Biol Chem* 278, 187–93.
12. Meares, G. P., and Jope, R. S. (2007) Resolution of the nuclear localization mechanism of glycogen synthase kinase-3: functional effects in apoptosis. *J Biol Chem* 282, 16989–7001.
13. Cho, J. H., and Johnson, G. V. (2004) Glycogen synthase kinase 3 beta induces caspase-cleaved tau aggregation in situ. *J Biol Chem* 279, 54716–23.

Chapter 10

Apolipoprotein E Expression and Purification

Yvonne Newhouse and Karl H. Weisgraber

Abstract

Since the discovery of the association of apolipoprotein E (apoE) 4 with Alzheimer's disease 17 years ago, numerous in vitro experiments with the apoE isoforms (apoE2, apoE3, and apoE4) have been performed to try to understand the basis for this association. The majority of these studies used commercial sources for apoE, but some used recombinant protein. In either case, these studies were most often conducted without considering the ramifications of the structural and biophysical differences among the three isoforms or without adequate quality control of the preparations.

Here, we present a protocol for producing recombinant apoE that we have used successfully in our laboratory for the last 20 years. We also review the considerations that are critical for obtaining reliable and interpretable results with the end product.

Key words: Apolipoprotein E, Alzheimer's disease, Recombinant protein expression, Gel filtration, apoE structure

1. Introduction

ApoE4 is the major genetic risk factor for Alzheimer's disease (AD) (1–4). Since this discovery in 1993, many studies have attempted to establish the basis for this association. They were performed in vivo with various apoE transgenic and knock-in mouse models or in vitro with apoE preparations.

A basic understanding of the apoE isoform structural and biophysical differences is helpful for conducting studies with apoE. ApoE contains two structural domains, an N- and C-terminal domain, separated by a hinge region (Fig. 1). The three common apoE isoforms result from cysteine and arginine differences at positions 112 and 158: apoE3 contains arginine at position 158 and cysteine at 112; apoE2 and apoE4 contain cysteine and arginine at both sites, respectively (5).

Erik D. Roberson (ed.), *Alzheimer's Disease and Frontotemporal Dementia*, Methods in Molecular Biology, vol. 670,
DOI 10.1007/978-1-60761-744-0_10,

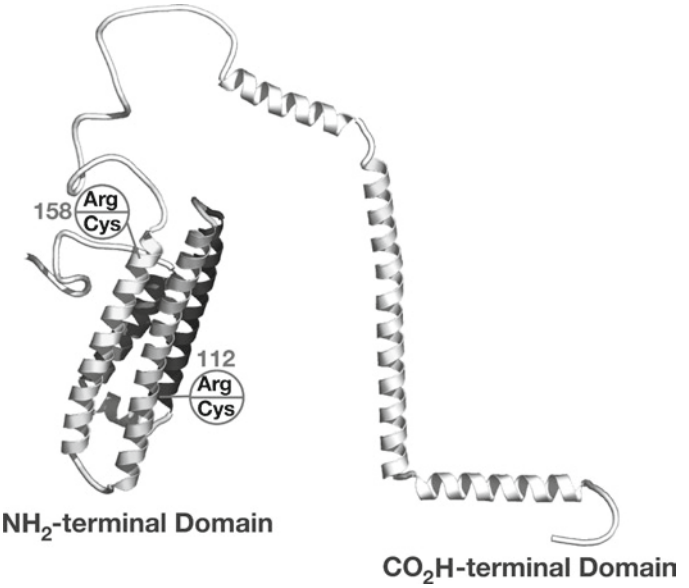

Fig. 1. Model of apoE structural domains. Residues 112 and 158 in the amino-terminal domain are the polymorphic sites where cysteine and arginine differences distinguish the three common apoE isoforms apoE2, apoE3, and apoE4.

These seemingly small structural differences have a significant effect on the structure and function of apoE in normal physiology and in pathophysiology. ApoE2 binds defectively to members of the low-density lipoprotein (LDL) receptor family, whereas apoE3 and apoE4 bind with high affinity. ApoE2 in combination with genetic and environment factors is associated with the lipoprotein disorder type III hyperlipoproteinemia and with accelerated atherosclerosis (6). ApoE4 is also associated with a modest increase in the risk for cardiovascular disease (7).

Structurally, apoE4 differs from apoE2 and apoE3 in three important aspects. ApoE4 does not contain cysteine. It exhibits "domain interaction." The N- and C-terminal domains interact through a salt bridge, which results from the influence of Arg-112 on Arg-61, causing an interaction with Glu-255 and a more compact structure than apoE3 (Fig. 2). Domain interaction was hypothesized to contribute to the association of apoE4 with AD (8). The third apoE4 difference is that apoE4 is the least stable of the three isoforms to unfold and has a propensity to form a molten globule structure, also suggested to contribute to the apoE4 association with AD (9). The relative instability of apoE4 results in its tendency to form soluble aggregates that have increased β structure and are neurotoxic (10).

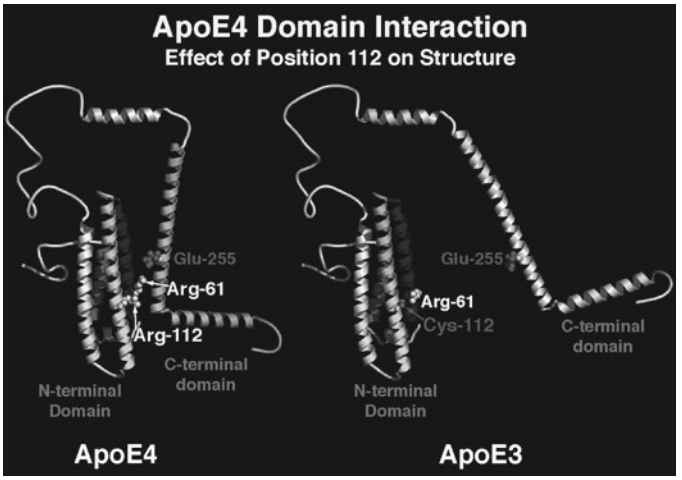

Fig. 2. The effect of the cysteine–arginine difference at position 112 on structure. In apoE4, arginine-112 affects the conformation of arginine-61 so that it interacts with glutamic acid-255, resulting in an interaction of the two structural domains and a compact structure. In apoE3, cysteine-112 does not have the same effect on argininie-61, resulting a reduced interaction of the domains and a more open structure.

2. Materials

2.1. Transform Bacteria with ApoE Construct

1. Plasmids containing cDNA for the desired isoform(s) of full-length human apoE. The parent vector is pET32a (Novagen), which includes a thioredoxin (TRX) tag, a 6× histidine (His) tag, and an engineered thrombin site at the fusion junction that generates an amino-terminal sequence addition of Gly-Ser (see Note 1). Available upon request from Dr. Karl Weisgraber.
2. One Shot BL21 (DE3) chemically competent *Escherichia coli* stored at –80°C (Invitrogen, see Note 2).
3. Water bath with variable temperature control.
4. Super Optimal broth with catabolite supression (S.O.C. medium, Invitrogen).
5. Luria broth (LB) agar plates containing ampicillin.
6. Glass rod for spreading colonies on agar plate.
7. Incubator with temperature control.
8. 500-mL flasks.
9. 2-L flask.
10. LB medium. We purchase large capsules (Q-Biogene) and reconstitute four per liter of water.
11. Autoclave.

12. Ampicillin stock: 100 mg/mL in water. Can be stored at –20°C in aliquots for single use. Do not freeze thaw.
13. Shaking incubator with temperature control.
14. Centrifuge.
15. Spectrophotometer.
16. 80% glycerol.
17. Isopropyl β-D-thiogalactopyranoside (IPTG): 500 mM stock in water, prepared fresh just before use.
18. Bug Buster extraction reagent (Novagen) with 0.05% benzonase (Novagen) (see Note 9).

2.2. Protein Production, Induction, Harvest and Cell Lysis

1. 2,700-mL Fernbach flasks (Sigma).
2. Inoculating loops.
3. Tris-buffered saline (TBS): 10 mM Tris–HCl, pH 7.4, 150 mM NaCl.
4. Ultracentrifuge with rotor and accessories.
5. Cell disruptor/sonicator, such as Branson Sonifier 450.

2.3. Lipidation and Thrombin Cleavage

1. 1,2-Dimyristoyl-*sn*-glycero-3-phosphocholine (DMPC, powder form; Avanti Polar Lipids).
2. Tris-buffered saline (TBS) with azide: 10 mM Tris–HCl, pH 7.4, 150 mM NaCl, 0.005% NaN_3.
3. 10 mM Tris–HCl, pH 7.4 or 10 mM ammonium bicarbonate.
4. Bovine α-thrombin (Haematological Technologies, Inc.).
5. $d = 1.006$ solution: 200 mM NaCl, 1 mM EDTA, pH 7.0. Stock is stable at RT.
6. $d = 1.10$ solution: 200 mM NaC1, 1 mM EDTA, pH 7.0, 140.5 g/L potassium bromide. Stock is stable at RT.
7. $d = 1.19$ solution: 200 mM NaCl, 1 mM EDTA, pH 7.0, 289.9 g/L potassium bromide. Stock is stable at RT.
8. Quick-Seal, polyallomer, 39 mL, 25 × 89 mm tubes (Beckman).
9. Long blunt needle, such as Popper 14 gauge, 6-in. pipetting needle.
10. SW 60 Ti rotor for ultracentrifuge.
11. Tube slicer.
12. Dialysis membrane with 6–8,000 MW cutoff.

2.4. Lyophilization and Delipidation

1. 50-mL, glass, conical-bottom centrifuge tubes, 28 × 76 mm, with pennyhead stopper (Fisher).
2. Dry ice or liquid nitrogen.

3. Methanol (Fisher).
4. Lyophilizer.

2.5. Chromatographic Purification

1. Sephacryl S-300 High Resolution chromatography medium (GE Life Sciences).
2. 4 M guanidine buffer: 4 M guanidine, 10 mM Tris–HCl, 7.4, 1 mM EDTA, 0.005% NaN_3, 0.1% beta-mercaptoethanol (βME).
3. Chromaflex column (120 cm length) with flow adapter (Kontes). Size will depend on the amount of protein being purified, either 4.8 cm I.D./2,172 mL volume or 2.5 cm I.D./589 mL volume.
4. Chromatography system with fraction collector, pump, and UV monitor.
5. 6 M guanidine buffer: 6 M guanidine, 10 mM Tris–HCl, 1 mM EDTA, 1% βME.
6. 100 mM ammonium bicarbonate.
7. Centriprep YM10 centrifugal filter unit with ultracel-10 membrane (Millipore; see Note 5).

2.6. SDS-PAGE and Coomassie Staining

1. SDS-PAGE minigel system, such as from Bio-Rad or Invitrogen.
2. Power supply.
3. Precast 10–20% gels.
4. Molecular weight markers.
5. Coomassie stain.
6. Destain.

3. Methods

The protocol described here assumes that one is starting with a sample of the supercoiled apoE expression vector. We provide a protocol for the various steps in producing purified apoE from this vector, including transforming this plasmid into *E. coli* and making glycerol stocks for storage of the vector (Subheading 3.1), producing and harvesting apoE from the bacterial expression system (Subheading 3.2), lipidation and cleavage of the thioredoxin tag (Subheading 3.3), delipidation (Subheading 3.4), and column purification (Subheading 3.5). Sodium dodecyl sulfate–polyacrylamide gel electrophoresis (SDS-PAGE) with Coommassie staining is utilized at various stages of the procedure to monitor purity, and is described in Subheading 3.6.

3.1. Transform Bacteria with the ApoE Construct

1. Thaw one vial of One Shot BL21(DE3) chemically competent *E. coli* (see Note 2) on ice for 30 min.
2. Add 5–10 ng of DNA in 1–5 μL to the thawed cells.
3. Mix by tapping. Do not pipet up and down. Leave the vial on ice for 30 min.
4. Incubate the vial for exactly 30 s in a 42°C water bath. Do not mix or shake. Return the vial to the ice, and add 250 μL of SOC rich medium by sterile technique.
5. Place the vial in a larger tube and tape it to a rack, laying the tube on its side in a shaking incubator. Shake for 1 h at 225 rpm at 37°C.
6. Have ready two LB agar plates containing 100 μg/mL ampicillin at room temperature. Plate the transformed cells at two levels to ensure a good distribution of colonies (e.g., 20 μL to one plate and 200 μL to the other plate). Spread the cells evenly with a sterile glass rod. Invert the plates and incubate overnight at 37°C. Look for a moderate number of well-distributed colonies.
7. Colonies from these plates can be used for several weeks, but a new transformation must be prepared after that time. Store the plates at 4°C for future use or proceed to the next step to make glycerol stocks that can be used for a longer period when stored at –80°C.
8. Prepare four 500-mL flasks containing 250 mL each of LB, and one 2-L flask containing one liter of LB, then autoclave.
9. When cool, add ampicillin to a final concentration 100 μg/mL from the 10 mg/mL stock (250 μL/250 mL).
10. Pick single colonies from the newly transformed plated cells and inoculate half of the 500-mL flasks.
11. Incubate these flasks overnight at 37°C in a shaking incubator at 200–250 rpm. Good aeration is necessary for rapid growth so a small volume in a large flask is ideal.
12. After overnight growth, collect the contents of the 250-mL flask by centrifugation at 1,000 × *g* and discard the supernatant. Refresh the cell pellet with sterile LB medium and resuspend the cells from each of the flasks. Use 5 mL of this cell suspension to inoculate each of the remaining flasks containing new medium.
13. Incubate these flasks at 37°C in a shaking incubator until the O.D. = 0.400–0.600. Monitor the O.D. by taking an aliquot every 30 min and reading on a spectrophotometer at 600 nm against a medium blank. The culture will be in log-phase in 2–3 h when it doubles O.D. in 20–30 min. Take a 1-mL aliquot as the preinduction sample for gel analysis.

14. Take a 5-mL sample from each of the flasks for glycerol stock. Pipet 150 µL of 80% glycerol into several microfuge tubes. Add 850 µL of the cultured cells to the glycerol. Mix by pipetting up and down several times and place them on dry ice immediately or freeze at –80°C.
15. Induce the remaining cells with IPTG at a final concentration 0.5 mM (250 µL of 500 mM IPTG). Continue to shake the flasks for 2–3 h, taking a 1-mL aliquot every hour to determine the best time to harvest the cells when doing a large-scale prep.
16. To evaluate the expression level of the various samples and to determine the optimal induction time, spin the preinduction and postinduction time course samples briefly and discard the supernatant. Resuspend the pellets in 1-mL Bug Buster containing 0.05% benzonase. Take 10–20 µL for SDS-PAGE analysis, as described in Subheading 3.6.
17. Compare the preinduced cell pellet to the time-course pellet by SDS-PAGE with Coomassie staining. Look for high expressers for long-term storage at –80°C. It is a sound practice to make new glycerol stocks every year to maintain high expression.

3.2. Protein Production, Induction, Harvest, and Cell Lysis

1. Prepare two 500-mL flasks containing 250 mL of sterile LB medium for overnight culture and refreshing media and 1 L in each 2,700-mL Fernbach flask, depending on your protein needs.
2. When the medium is cool, add ampicillin to a final concentration 100 µg/mL from the 100-mg/mL stock (250 µL/250 mL for the overnight culture medium and 1 mL/L for the Fernbach flasks).
3. Scrape the glycerol stock with a sterile inoculating loop while maintaining the glycerol stock at –80°C or on dry ice and inoculate the overnight culture media with the glycerol stock. Place in a shaking incubator overnight at 37°C.
4. Spin the heavy overnight growth at low speed (1,000 × *g*), discard the supernatant, refresh the pellet with the remaining 250 mL LB media, and gently resuspend. Use 10 mL of these cells to inoculate each of the Fernbach flasks.
5. Incubate in the shaking incubator at 37°C until the growth is in log phase at O.D. 0.400–0.600. Monitor the O.D. by taking an aliquot every 30 min and reading on a spectrophotometer at 600 nm against a media blank. The culture will be in log phase in 2–3 h when it doubles O.D. in 20–30 min.
6. Induce the cells by adding IPTG at a final concentration 0.5 mM (1 mL of 500 mM IPTG per liter of cells). Continue to shake the flasks for the induction time determined in Subheading 3.1 to yield optimal expression of apoE.

7. Harvest the cells by centrifugation at 1,000 × *g*. Discard the supernatant and resuspend the pellet in 6–8 mL of TBS/liter and place the cells on ice. It is important to keep cells and protein cold after this point.
8. Cell pellets can be stored frozen or the cells can be disrupted by sonication. Combine the cell pellets in a small beaker and place on ice. Using a sonicator with a large probe on high setting, sonicate on continuous mode for 30 s, then rest, cool for 2 min, and repeat four times. There should be a slight clearing of the thick slurry as the cell membranes disrupt.
9. Spin at high speed (35,000 × *g*) for 15 min. The apoE–thioredoxin fusion will be in the supernatant.

3.3. Lipidation and Thrombin Cleavage

The thrombin cleavage site preceding the start of the protein allows the removal of the thioredoxin fusion partner. However, it is necessary to protect the hinge region of apoE from also being cleaved. Combining apoE with the phospholipid DMPC before adding thrombin not only protects the hinge region, but also allows for an additional purification step. "Floating" the complex on a potassium bromide (KBr) gradient after ultracentrifugation results in a purer product.

1. Estimate the amount of apoE in the sonicate supernatant by SDS-PAGE analysis. DMPC is added at 3.75:1 w/w ratio (DMPC:apoE). It is better to add too much DMPC, which will just float, than too little, which will cause apoE cleavage by thrombin.
2. Weigh out the DMPC and add TBS with azide to a concentration of 20 mg/mL. Sonicate the solution until the DMPC clears, using the large probe on a high setting. Ensure that the sample does not overheat by placing it in the center of a 1-L water bath at room temperature while sonicating. Spin the solution briefly to remove any titanium that may have come off the tip.
3. Add the DMPC to the sonicate supernatant and incubate overnight at the transition temperature of DMPC (23.8°C) in a circulating water bath. Alternatively, the mixture can be passed through the transition temperature three times, allowing 15 min equilibration at each temperature (i.e., 18–30°C).
4. Thrombin cleaves well in low salt. Over the course of one day, dialyze apoE•DMPC three times against 4 L of 10 mM Tris, pH 7.4, or 10 mM ammonium bicarbonate.
5. Add thrombin at a 100:1 ratio (apoE:thrombin) and incubate at 37°C for 1 h. Leave digestion at 37°C while an aliquot is checked in the next step; the DMPC is very protective and it is impossible to "over-digest."

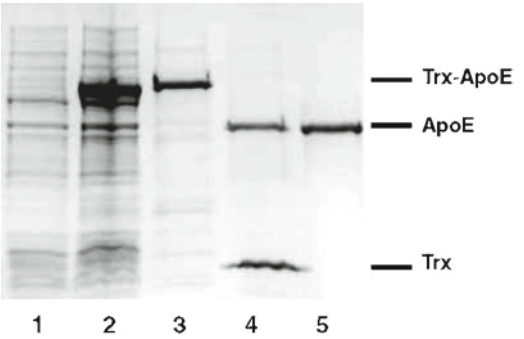

Fig. 3. Bacterial expression and purification of apoE. SDS-PAGE of stages of protein and purification: *lane 1,* uninduced cells; *lane 2*, induced cells, *lane 3*; isolated thioredoxin fusion protein; *lane 4*, thrombin cleavage of thioredoxin fusion protein; *lane 5*, purified apoE.

6. Check for complete cleavage by running about 5 µL of the digestion on SDS-PAGE with Coomassie staining (Fig. 3). If cleavage is incomplete, add more thrombin and incubate longer.
7. Add 1% βME to inactivate thrombin.
8. A KBr step gradient is used for isolation of the apoE•DMPC complexes. Prepare density solutions as described in Subheading 2.3.
9. Prepare the step gradient by underlaying each of the density solutions in ultracentrifuge tubes, starting with the least dense. A syringe with a long, large-bore blunt-end needle placed at the bottom of the Quick-seal tube allows for underlaying with minimal disturbance.
10. Raise the density of the sonicate supernatant containing the apoE•DMPC complexes to $d = 1.21$ by adding KBr. Calculate the needed amount according to the following formula:

    Volume of the sonicate supernatant in mL × 0.3265 = g of KBr.
11. Underlay the sample to the bottom of the tube. Fill any remaining space with $d = 1.006$ solution. Heat-seal and cap the tubes.
12. Centrifuge in a 60Ti rotor for 16 h, 215,000 × *g* at 15°C. The apoE•DMPC complexes will float to $d = 1.009$.
13. Recover the complexes by tube slicing, keeping the top third of the gradient.
14. Dialyze the complexes against 3 × 4 L (a couple hours each) of cold 5 mM ammonium bicarbonate before lyophilizing.

3.4. Lyophilization and Delipidation

1. Distribute the dialyzed sample among several 50-mL glass conicals so that they are approximately half full.
2. Using dry ice or liquid nitrogen, shell freeze by laying the tubes on their side and rotating them to cover the walls of the tubes so they are evenly distributed.
3. Lyophilize. This method increases the surface area of the material and speeds the drying. A soft pellet will remain when the material is dry.
4. To delipidate, add cold methanol and vortex the pellet to form a slurry (see Note 3). Fill the conical with cold methanol and let sit at 4°C for 30 min before centrifugation at low speed (1,000 × *g*) for 10 min.
5. Decant the supernatant to chemical waste and repeat the methanol wash. Vortex and spin at 1,000 × *g* for 10 min.
6. Decant the methanol, and add 6 M guanidine buffer while vortexing. The protein will go into solution in a small amount of guanidine buffer. Reduce with 1% βME. Keep the volume small so that it can be easily loaded on the Sephacryl column.

3.5. Chromatographic Purification

ApoE is purified in the denatured monomeric state making it easier to isolate the protein from the column void volume.

1. Equilibrate the Sephacryl by pouring off the ethanol used for shipping and storage, and replacing it with 4 M guanidine buffer. Repeat three times allowing the matrix to settle each time.
2. Form a thick slurry and pour the column. Using a packing reservoir, pack the column at twice the flow rate, depending on the size of the column, for several hours. Attach the flow adapter leaving no space between the matrix and the adapter.
3. Pump on the apoE in 6 M guanidine reducing buffer (1% βME). Run the column in 4 M guanidine buffer containing 0.1% βME.
4. Using a chromatography system with fraction collector and UV monitor, collect the apoE peak. With our columns, the void volume is ~750 mL and the apoE peak is ~1,000 mL.
5. Dialyze five times against a large volume of cold 0.1 M ammonium bicarbonate. Dialysis into ammonium bicarbonate readily accomplishes refolding to the tetrameric form.
6. Concentrate the protein to ~1 mg/mL with a Centriprep YM10 (see Note 5).
7. Assess the quality of resulting products. The primary method is by SDS-PAGE with Coomassie staining (Fig. 3; see Note 6). Using a reducing SDS gel buffer, a single band should be seen, regardless of the isoform, whereas the same sample in a nonreducing SDS buffer will contain dimers with apoE3 and

multimers with apoE2 because of their cysteine content, while apoE4 remains monomeric (Fig. 4) (see Note 4). Aggregation of apoE, especially with apoE4 is problematic (see Note 7). ApoE4 has a higher tendency to form aggregates than apoE3 (Fig. 5).

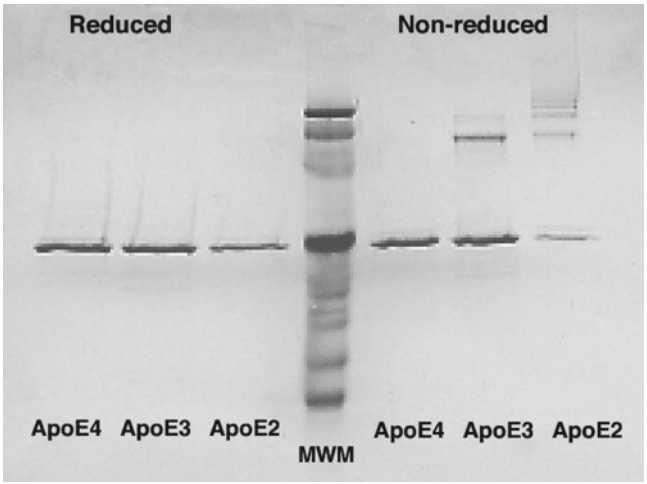

Fig. 4. SDS-PAGE of apoE isoforms. Nonreduced samples of cysteine-containing apoE3 and apoE2 display higher molecular weight disulfide-linked forms.

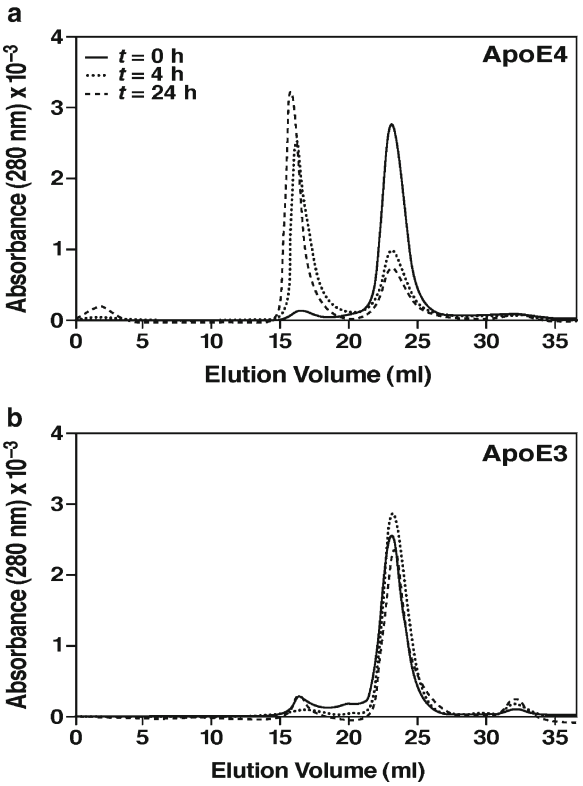

Fig. 5. Time-course incubation of apoE4 and apoE3 at 37°C. **a**, apoE4; **b**, apoE3.

8. For long-term storage, snap-freeze in small aliquots in Eppendorf tubes (see Note 8). Immersing tubes in liquid nitrogen allows for rapid freezing, preventing apoE from concentrating in the bottom of the tube. Storage at room temperature jeopardizes the quality of the protein. Avoid multiple freeze–thaw cycles.

3.6. SDS-PAGE and Coomassie Staining

1. Assemble the electrophoresis apparatus with a 10–20% gel according to the manufacturer's instructions.
2. Load samples and run until the dye front reaches the bottom of the gel.
3. Remove gel from plates, and place into Coomassie staining solution.
4. Transfer gel to destaining solution with gentle agitation. Replace destain periodically until bands are clear.

4. Notes

1. The His-Tag option in the expression vector has been used for initial purification as it does provide a relatively pure product; however, there is evidence of oxidation of apoE with this option so its use is not recommended. The addition of Gly-Ser to the amino terminus does not affect the properties of the protein (11).
2. Yields are ~20 mg/L when transformed into the BL21(DE3) expression vector in the T7 strain of *E. coli*.
3. For the delipidation step, fresh cold methanol is essential to avoid oxidation of the lipid.
4. For use in experiments, it is important to ensure that apoE3 and apoE2 are monomeric for full biological activity. This can be accomplished by using them in with reducing agent. βME and dithiothreitol can interfere with some biochemical reactions. For reducing disulfides, tris(2carboxyethyl)phosphine is a good alternative.
5. When concentrating the protein after gel filtration and dialysis, the concentrator of choice is Centriprep. Other devices concentrate the protein to high levels next to the membrane, levels well above its ideal concentration that will promote aggregation.
6. An additional assessment of biological activity is to determine LDL receptor binding activity (12).
7. Assessment of the aggregation state by chromatographic analysis by Superdex 200 gel filtration is a critical quality

control check to ensure that apoE4 is not aggregated before proceeding with experiments, unless one is interested in the effects of apoE4 aggregates (10). The aggregated apoE elutes in the void volume ahead of the natural tetrameric peak.

8. The ideal storage concentration for apoE is 0.5–1 mg/mL. The storage buffer of choice for apoE is fresh, cold, 100 mM NH_4HCO_3 with 1% NaN_3. If another buffer is needed for experiments, exchange the buffer by dialysis rather than by lyophilization and reconstitution.
9. Benzonase, an endonuclease, will digest the DNA and vastly improve the quality of gel analysis.

Acknowledgments

This work was supported in part by the National Institutes of Health/National Institute of Aging R01 AG028793; and The J. David Gladstone Institutes. The authors thank Gary Howard for editorial assistance, Linda Turney for manuscript preparation, and John Carroll for graphics assistance.

References

1. Corder, E. H., Saunders, A. M., Strittmatter, W. J., Schmechel, D. E., Gaskell, P. C., Small, G. W., Roses, A. D., Haines, J. L., and Pericak-Vance, M. A. (1993) Gene dose of apolipoprotein E type 4 allele and the risk of Alzheimer's disease in late onset families. *Science* **261,** 921–23.
2. Strittmatter, W. J., Saunders, A. M., Schmechel, D., Pericak-Vance, M., Enghild, J., Salvesen, G. S., and Roses, A. D. (1993) Apolipoprotein E: High-avidity binding to β-amyloid and increased frequency of type 4 allele in late-onset familial Alzheimer disease. *Proc. Natl. Acad. Sci. USA* **90,** 1977–81.
3. Saunders, A. M., Strittmatter, W. J., Schmechel, D., St George-Hyslop, P. H., Pericak-Vance, M. A., Joo, S. H., Rosi, B. L., Gusella, J. F., Crapper-MacLachlan, D. R., Alberts, M. J., Hulette, C., Crain, B., Goldgaber, D., and Roses, A. D. (1993) Association of apolipoprotein E allele ε4 with late-onset familial and sporadic Alzheimer's disease. *Neurology* **43,** 1467–72.
4. Roses, A. D. (1996) Apolipoprotein E alleles as risk factors in Alzheimer's disease. *Annu. Rev. Med.* **47,** 387–400.
5. Hatters, D. M., Peters-Libeu, C. A., and Weisgraber, K. H. (2006) Apolipoprotein E structure: Insights into function. *Trends Biochem. Sci.* **31,** 445–54.
6. Mahley, R. W., and Rall, S. C., Jr. (2001) Type III hyperlipoproteinemia (dysbetalipoproteinemia): The role of apolipoprotein E in normal and abnormal lipoprotein metabolism. In *The Metabolic and Molecular Bases of Inherited Disease* (Scriver, C. R., Beaudet, A. L., Sly, W. S., Valle, D., Childs, B., Kinzler, K. W., and Vogelstein, B., Eds.), Vol. 2, pp. 2835–62, McGraw-Hill, New York.
7. Davignon, J., Gregg, R. E., and Sing, C. F. (1988) Apolipoprotein E polymorphism and atherosclerosis. *Arteriosclerosis* **8,** 1–21.
8. Dong, L.-M., and Weisgraber, K. H. (1996) Human apolipoprotein E4 domain interaction. Arginine 61 and glutamic acid 255 interact to direct the preference for very low density lipoproteins. *J. Biol. Chem.* **271,** 19053–57.
9. Morrow, J. A., Hatters, D. M., Lu, B., Höchtl, P., Oberg, K. A., Rupp, B., and Weisgraber, K. H. (2002) Apolipoprotein E4 forms a molten globule: A potential basis for its association with disease. *J. Biol. Chem.* **277,** 50380–85.
10. Hatters, D. M., Zhong, N., Rutenber, E., and Weisgraber, K. H. (2006) Amino-terminal

domain stability mediates apolipoprotein E aggregation into neurotoxic fibrils. *J. Mol. Biol.* **361,** 932–44.

11. Arnold, K. S., Innerarity, T. L., Pitas, R. E., and Mahley, R. W. (1992) Lipoprotein–receptor interactions. In *Lipoprotein Analysis. A Practical Approach* (Converse, C. A., and Skinner, E. R., Eds.), pp. 145–68, Oxford University Press, Oxford.
12. Morrow, J. A., Arnold, K. S., and Weisgraber, K. H. (1999) Functional characterization of apolipoprotein E isoforms overexpressed in *Escherichia coli*. *Protein Expr. Purif.* **16,** 224–30.

Chapter 11

Aβ Toxicity in Primary Cultured Neurons

Adriana Ferreira, Roxana C. Sinjoanu, Alexandra Nicholson, and Sara Kleinschmidt

Abstract

The aggregation of beta-amyloid (Aβ) into soluble oligomers is considered an early event in Alzheimer's disease. Furthermore, the presence of these aggregates seems to lead to neurodegeneration in the context of this disease. However, the mechanisms underlying Aβ-induced neurotoxicity are not completely understood. Primary cultures of pyramidal neurons have proven to be an excellent model system for the study of such mechanisms. These cultures provide a homogenous population of neurons that extend and differentiate axons and dendrites and that establish functional synapses among them. In addition, the neurotoxic effects of preaggregated Aβ can be easily analyzed both morphologically and biochemically. Here, we describe in detail the materials and methods used for the preparation and maintenance of primary cultures of hippocampal pyramidal neurons, as well as for the aggregation of and treatment with Aβ.

Key words: Cultured hippocampal neurons, Glia-conditioned medium, Preaggregated Aβ, Neurodegeneration, Cell death

1. Introduction

Alzheimer's disease (AD), the most common cause of dementia among people age 65 and older, is characterized by the progressive and irreversible degeneration of neuronal processes and the consequent loss of synaptic connections (1–8). Post mortem studies have identified two hallmark lesions, senile plaques and neurofibrillary tangles, in brain samples of AD patients. These hallmark lesions are the result of the pathological deposition of beta-amyloid (Aβ) and hyperphosphorylated tau, respectively (9–16). A growing body of evidence suggests that the aggregation of Aβ is an early event in the pathobiology of this disease (17–23). In the past 10 years, part of the research effort in the AD field has been focused on the mechanisms underlying Aβ toxicity. Most of

Erik D. Roberson (ed.), *Alzheimer's Disease and Frontotemporal Dementia*, Methods in Molecular Biology, vol. 670,
DOI 10.1007/978-1-60761-744-0_11, © Springer Science+Business Media, LLC 2011

these studies have been performed using primary neuronal cultures because they provide a particularly amenable model system for both morphological and biochemical assessment of neurodegeneration (24–47). Cultured pyramidal neurons obtained from either the hippocampal region or the cortex have been chosen for these types of studies since these neurons are the ones affected the most in AD. In addition, when placed in culture, pyramidal neurons extend two types of processes, axons and dendrites, with morphological characteristics, molecular composition, and function that resemble those of their counterparts in situ (reviewed in (48)). In our own laboratory, we have adopted long-term primary cultured hippocampal neurons as our model system for the study of Aβ-mediated toxicity for two additional reasons. First, cultures prepared from the embryonic hippocampal region are more homogeneous than the ones prepared from the cortex. This feature facilitates the interpretation of the results obtained. Second, hippocampal pyramidal neurons express adult tau isoforms when kept in culture for at least 3 weeks. Furthermore, the adult tau isoforms expressed in mature hippocampal neurons are less phosphorylated than their fetal counterparts, reproducing the phosphorylation state observed in situ (26). Combined, these features make the mature hippocampal culture an ideal model system to study of Aβ-induced neurotoxicity. In this chapter, we have described the methods used for the preparation of primary hippocampal neurons. In addition, we have included methods for aggregating Aβ as well as for the treatment of cultures with this peptide.

2. Materials

2.1. Coverslip and Culture Dish Preparations

1. Carolina™ Assistant-Brand Cover Glasses, 12 mm in diameter and 0.13–0.17 mm in thickness (Carolina Biological Supply; see Note 1).
2. Porcelain staining racks.
3. Tissue culture grade dishes 60 mm in diameter.
4. Concentrated nitric acid, 70% (v/v).
5. Paraplast (Sigma).
6. Poly-L-lysine hydrobromide (see Note 2).
7. Borate buffer: 50 mM boric acid and 12.5 mM Borax (Sigma), pH 8.5. Store solution at 4°C.
8. Small utility oven.

2.2. Cell Culture and Media

1. Calcium and magnesium-free Hank's balanced salt solution (CMF-HBSS): 10× HBSS (Invitrogen), 9.9 mM HEPES,

and 1 U/100 µg of penicillin/streptomycin in water (see Note 3). Store solution at 4°C.

2. 2.5% Trypsin. Store at –20°C
3. Glial and neuronal plating medium (MEM 10): Minimum essential medium (1× MEM, Invitrogen), 10% heat inactivated horse serum (Invitrogen, see Note 4), 0.6% D-glucose, and 1 U/100 µg penicillin/streptomycin. Store solution at 4°C.
4. Neuronal maintenance medium (N2): 1× MEM (Invitrogen), 0.6% D-glucose, 0.1% ovalbumin, 1 mM sodium pyruvate, 5 µg/mL insulin, 20 nM progesterone, 100 µM putrescine, 30 nM selenium dioxide, and 100 µg/mL apo-transferrin. Filter-sterilize and store at 4°C. Keep component stock solutions at –20°C.
5. Paraplast (Sigma).
6. Sterile plasticware: 35, 60, and 100 mm tissue culture dishes (see Note 5).
7. Surgical instruments, including scissors, tissue forceps, and Dumont #3 and #5 forceps.
8. Sterile plastic transfer pipets (1 mL).
9. Sterile 15 and 50 mL conical tubes.

2.3. Aβ Aggregation

1. N2 medium (see Subheading 2.1.4).
2. Lyophilized $A\beta_{1-40}$ or $A\beta_{1-42}$ peptide (American Peptide, Sunnyvale, CA; see Note 6).

3. Methods

We routinely assay Aβ toxicity in hippocampal neurons that have been cultured 21 days in astrocyte-conditioned medium, for the reasons described above. Below we present two methods for culturing such neurons, depending on the planned outcome measures. For morphological and immunocytochemical analyses, neurons can be cultured at low density on coverslips, inverted over a monolayer of astrocytes. For biochemical analyses, neurons can be cultured at high density in plastic dishes, fed with astrocyte-conditioned medium.

3.1. Preparation of Coverslips

The following steps are for preparing coverslips for low density cultures intended for morphological and immunocytochemical analyses. For biochemical analyses in neurons cultures in dishes, skip to Subheading 3.2.

1. Five days before culturing, place coverslips in porcelain staining racks in such a manner that they do not overlap (see Note 7).
2. Place the coverslip-containing racks into concentrated nitric acid for 36 h to make the coverslip surface more porous for the poly-L-lysine coating (see step 3.2.2; see Note 8).
3. Wash the coverslips in three changes of sterile water over 3 h.
4. Transfer the coverslip racks to a beaker, cover with aluminum foil, heat-sterilize (225°C) in a small utility oven for at least 8 h, and let cool to room temperature.

The subsequent steps should be performed in a laminar flow hood.

5. Two days before culturing, arrange the coverslips in 60 mm dishes with minimal overlapping, 11–12 coverslips per dish.
6. To provide support for the coverslips during coculturing with glia, place three equidistant drops of melted sterile paraplast at the edge of each coverslip using a glass Pasteur pipette.
7. Proceed to Subheading 3.2.

3.2. Coating of Culture Dishes and Coverslips with Poly-L-Lysine

The subsequent steps should be performed in a laminar flow hood.

1. Immediately before use, dissolve poly-L-lysine hydrobromide to 1 mg/mL in borate buffer and sterilize by filtration.
2. To enable the cells to adhere to plastic or glass surfaces, cover the bottom of each 60 mm dish and coverslips with 4 mL of the poly-L-lysine solution and incubate at room temperature overnight (see Notes 9 and 10).
3. Remove the poly-L-lysine and wash with three changes of sterile water, 1 h each.
4. After removing the final wash, add 5 mL of MEM 10 and store the dishes in an incubator (37°C, 5% CO_2) 24 h before plating.

3.3. Cortical Astroglia Cell Culture

3.3.1. Dissection

1. Sacrifice a pregnant Sprague–Dawley rat, embryonic day 18 (E18; see Notes 11 and 12) using an approved method of euthanasia.
2. Saturate the abdomen of the rat with 75% ethanol before making an incision.
3. Using sterile forceps and scissors, remove the skin to expose the muscular abdominal wall by making a vertical incision from pelvis to thorax.
4. Soak the used instruments with ethanol to remove any hair (see Note 13).

5. Cutting through the abdominal wall, expose the uterus.
6. Remove the uterus of the rat and place it in a sterile 100 mm dish (see Note 14).

Continue to work in a laminar flow hood.

7. Remove the fetuses from the uteri using sterile scissors and forceps (Dumont #3).
8. Decapitate the fetuses and transfer the heads to a 60 mm dish containing 3–4 mL CMF-HBSS.
9. To remove the brains, place a Dumont #3 forceps into the orbits to stabilize the head. Using a Dumont #5 forceps, peel away the skin and the skull to expose the brain.
10. Remove the brains and place them onto a drop of CMF-HBSS in the center of a 35 mm sterile dish coated with sterile paraplast (see Note 15).
11. Remove the meninges from each hemisphere (see Note 16).
12. After the dissection of the hippocampus (see step 3.4.1), cut a quarter of each hemisphere's cortex. Use approximately 6–8 hemispheres (24–36 quarters).
13. Transfer the cortical sections to a sterile 60 mm dish containing 3–4 mL of CMF-HBSS.

3.3.2. Dissociation and Plating

1. Aspirate the tissue using a sterile transfer pipette and transfer it to a 15 mL sterile conical tube that contains 15 mL 0.25% trypsin solution in CMF-HBSS. Invert the tube to mix.
2. Incubate in a water bath at 37°C for 30–35 min for digestion.
3. Using a sterile transfer pipette, aspirate the tissue from the 15 mL conical tube and transfer it to a 50 mL sterile conical tube.
4. Pipette up and down 10–12 times with a Pasteur pipette to triturate the tissue.
5. In the same tube, add 30 mL of glial plating medium (MEM 10) to inactivate the trypsin.
6. Spin this mixture for 10 min at $800 \times g$ to pellet the cells.
7. Discard the supernatant and add 20 mL of fresh MEM 10 to the pellet.
8. Using a Pasteur pipette, dissociate the tissue 10–15 times. Then, use a fire-polished Pasteur pipette (the tip diameter of which should be half of the regular diameter) and dissociate until the solution becomes homogenous.
9. Increase the total volume of MEM 10–50 mL before plating.

10. Determine the cell density using a hemocytometer and dilute the cell suspension to approximately 200,000 cells/mL and plate them into 60 mm dishes (see Notes 17 and 18).
11. Complete the volume in each dish up to 4 mL using MEM 10.
12. Swirl the dishes to spread cells evenly.
13. Incubate cultures at 37°C with 5% CO_2.

3.3.3. Maintenance

Four days later, remove all media and dead cells from the dishes and add 4 mL fresh MEM 10. The glial cultures should be fed once a week with fresh MEM 10 (see Notes 19 and 20).

3.4. Neuronal Culture

Proceed from step 11 of Subheading 3.3.1.

3.4.1. Dissection

1. Under a dissecting microscope, remove the meninges of each hemisphere and dissect the hippocampi (48).
2. Place the hippocampi in a sterile 60 mm dish containing 3–4 mL CMF-HBSS. Make sure that the tissue is submerged in CMF-HBSS at all times.

3.4.2. Dissociation and Plating

1. Gently aspirate all dissected hippocampi with a sterile transfer pipette and transfer to a 15-mL sterile conical tube containing 5-mL freshly prepared 0.25% trypsin in CMF-HBSS.
2. Incubate in a water bath at 37°C for 15 min. Do not invert or mix the tube's contents.
3. After the incubation, gently remove the trypsin solution and add 5 mL of CMF-HBSS and let stand for 5 min at room temperature. Do not invert or mix the tube's contents.
4. Repeat the wash in step 3 twice more and finally add 0.5 mL of CMF-HBSS per embryo dissected. Do not invert or mix the tube's contents.
5. Using a Pasteur pipette followed by a fire-polished pipette, gently dissociate the cells. To prevent foaming, pipette against the tube wall.
6. Determine the density of the cells using a hemacytometer. The yield should be around 500,000 cells per hippocampus.
7. Add the desired number of cells to prepared coverslips or dishes. We plate the cells at high-density (500,000 cells/60 mm dish) and low-density (150,000 cells/60 mm dish containing coverslips).
8. Swirl the dishes to disperse the cells evenly.
9. Incubate the cells at 37°C with 5% CO_2.
10. After 2–4 h, examine the dishes to ensure that the neurons have attached.

3.4.3. Maintenance

After the neurons have attached (usually 2–4 h), change the media of high density-plated dishes to glia-conditioned N2 media. Transfer low density-plated coverslips, cell-side down, into dishes containing a monolayer of astrocytes that have been conditioned with N2 media (see Notes 19 and 20). Keep the neurons for as long as 4 weeks without changing the media.

3.5. Aβ Aggregation

1. Dissolve the peptide in N2 medium to a concentration of 0.5 mg/mL.
2. Incubate this mixture for 3 days in a 37°C water bath to pre-aggregate the peptide.
3. After use, the Aβ should be flash frozen in liquid nitrogen before storing at –20°C (see Notes 21–23).

3.6. Separation of Oligomeric and Fibrillar Aβ

1. After aggregating the Aβ, the N2-peptide solution will contain a complex mixture of oligomeric and fibrillar peptide. Centrifuge this mixture at 100,000 × *g* for 1 h.
2. Remove the supernatant, which contains the soluble oligomers.
3. Resuspend the pellet (fibrillar fraction) in a volume of N2 medium equivalent to the supernatant (see Note 24).

3.7. Aβ Treatment

1. After pipetting up and down to mix, add preaggregated Aβ (mixed, oligomeric, or fibrillar fractions) directly to the culture medium of 21 days-in-culture hippocampal neurons at final concentrations ranging from 2 to 20 μM. Both the mixed and oligomeric fractions induce neurotoxicity in cultured central neurons.
2. Assess the presence of morphological features of neurodegeneration (tortuous processes, presence of axonal varicosities, and/or neurite retraction) by light microscopy as early as 8 h after the addition of mixed or oligomeric Aβ (Fig. 1).
3. Neuronal survival can be assessed by trypan blue exclusion.
4. Prepare the cultures for light or electron microscopy (coverslips) and biochemical (hippocampal neurons plated directly onto culture dishes) analysis according to routinely used protocols.

4. Notes

1. These coverslips, manufactured specifically from a Deutsche Spiegelglass micro sheet, have been shown to support neuronal growth in culture.

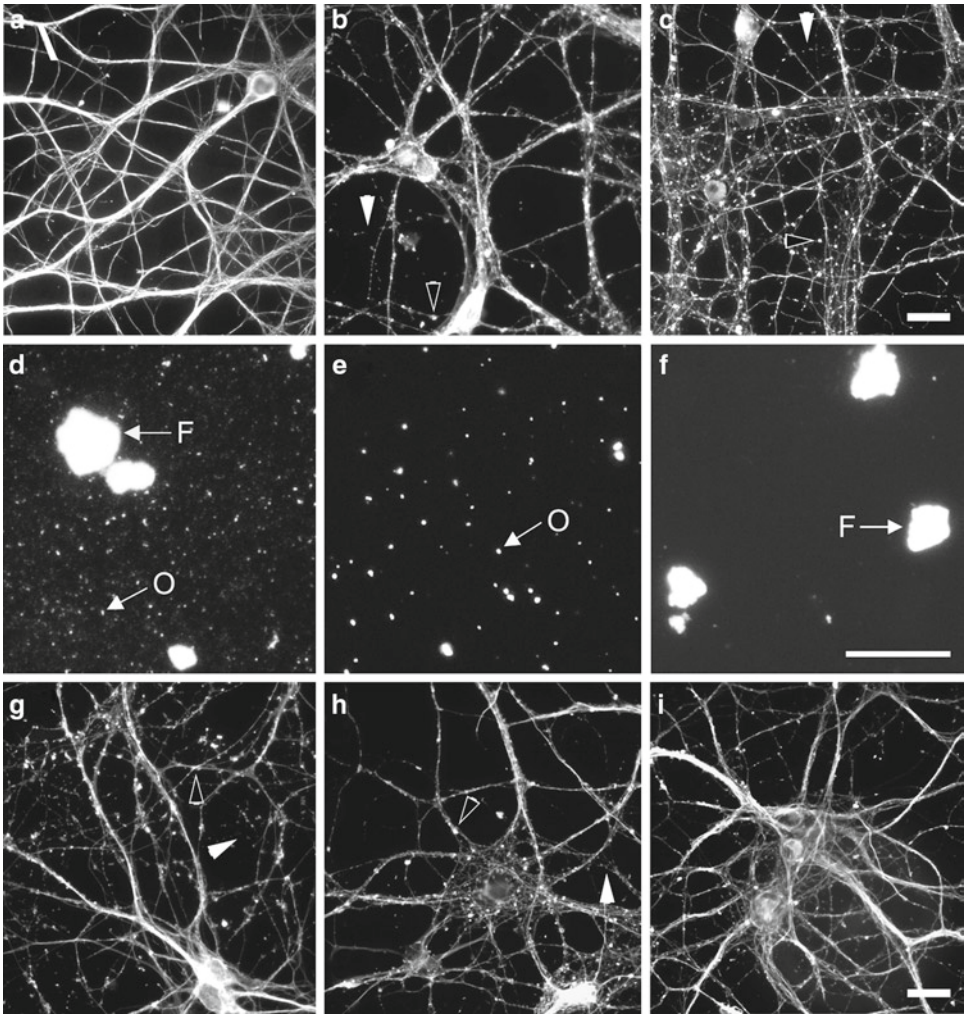

Fig. 1. Preaggregated Aβ induced neuronal degeneration in cultured hippocampal neurons. (**a**–**c**) Twenty-one days-in-culture hippocampal neurons treated with 0 μM (**a**), 2 μM (**b**), and 20 μM (**c**) preaggregated Aβ for 24 h were fixed and labeled with a tubulin antibody. Neurons treated with preaggregated Aβ displayed signs of degeneration, including the formation of varicosities (*black arrowheads* in **b**, **c**) and retraction of neurites (*white arrowheads* in **b**, **c**). (**d**–**f**) Light fluorescence microscopy picture of aggregated Aβ labeled with an Aβ antibody. The mixture contains oligomers (O) and fibrils (F) (panel **d**). High-speed centrifugation was used to separate oligomeric Aβ (**e**) from the fibrillar form (**f**). (**g**–**i**) Twenty-one days in culture hippocampal neurons treated with 2 μM mixed (**g**), oligomeric (**h**), and fibrillar Aβ (**i**) were fixed and labeled with a tubulin antibody. Only neurons treated with mixed (**g**) or oligomeric Aβ (**h**) displayed signs of degeneration (*black and white arrowheads* in **g**, **h**). *Scale bars*, 20 μm.

2. Poly-D-lysine hydrobromide may also be used for dish and coverslip preparations.
3. All solutions should be prepared in water that has resistivity of 18.2 MΩ-cm and has been filter-sterilized. We use sterile Milli-Q water at a temperature of 25°C.

4. For both glial and neuronal plating medium (MEM 10), we use heat-inactivated horse serum. We found that this serum has comparable effects with heat-inactivated fetal bovine serum in our culture system.
5. Culture dishes should be sterile and tissue culture grade in order to be suitable for the neuron and glial cultures. We prefer dishes purchased from BD Falcon, but other companies offer the same dishes.
6. In cultured hippocampal neurons, our lab has observed similar results using preparations of both $A\beta_{1-40}$ and $A\beta_{1-42}$ (27, 28).
7. Coverslips are best handled using a Dumont-style forceps at the edges so as to minimize potential breaking and scratching.
8. Coverslips can also be prepared for poly-lysine coating by transferring the racks into 95% ethanol overnight before washing.
9. Keep the dishes covered to ensure that the poly-lysine solution does not dry.
10. Exposing poly-lysine to UV light results in cross-linking of the polylysine, hindering the attachment of the cells to the surface. Therefore, after the polylysine has been applied to the dishes, do not expose them to UV light.
11. We use E18 rat embryos because at this stage, the neuronal migration is complete and the hippocampus is formed. For mouse neuronal hippocampal cultures, we follow the same protocol, except the age of the embryos is 16 days.
12. For glial culture, we use the cortex from the E18 rats to be used for hippocampal culture preparations, so as to minimize the number of animals sacrificed for each culture. The same culture can be done using postnatal rat pups (1 or 2 days old; (27, 28)).
13. Hair and skin are a source of fungal and bacterial contamination.
14. When removing the uterus, be cautious as not to pinch the nearby intestine, which is a source of bacterial contamination.
15. The 35 mm dishes used for the dissection of the hippocampi are coated with sterile paraplast to better stabilize the brain hemispheres and to protect the delicate tips of our surgical instruments. We coat each dish with the same volume of paraplast in order to minimize changes in the focal plane of the dissecting microscope.
16. Meninges are a source of contamination with different cell types, which secrete toxins that do not support neuronal survival.

17. We plate the cells at two different densities, so as to have cultures ready at different times.
18. We plate and grow the glial culture in sterile 60 mm dishes for easier use in coculturing with neurons. Glial cell suspension can be plated and expanded in T-flasks, harvested and then replated.
19. Use the glial cultures for the conditioning of the N2 media once the cultures reach 40–60% confluence, usually in 10–14 days.
20. For the long-term survival of neurons, we use N2 media that has been glia-conditioned for 24 h.
21. To use again, the Aβ should be quickly thawed in a 37°C water bath and flash frozen again prior to storage.
22. The aggregated peptide can be stored for up to 1 month.
23. Alternative methods of Aβ aggregation:
    (a) Aβ can be dissolved in double-distilled sterile water at a concentration of 200 μM (0.9 mg/mL) and stored at 4°C. This preparation will result in primarily the oligomeric moiety if it is incubated for 1 h at 37°C (49).
    (b) Aβ can be dissolved in double-distilled water at a concentration of 700 μM (3.0 mg/mL), then immediately diluted in PBS to 350 μM (1.5 mg/mL), and incubated at 37°C for 5 days (50).
    (c) Aβ can also be dissolved in 50 mM sodium borate buffer (pH 7.8, 4°C) at a concentration of 1 mg/mL and incubated for 4 days (51).
    (d) Aβ can be dissolved in anhydrous dimethyl sulfoxide (DMSO) to make 10 mg/mL stock solutions. After incubation for 30–60 min at 25°C, stock solutions of Aβ can be diluted into sterile cell culture medium and incubated at 25°C with agitation for 1 day (52). This method is not commonly used with primary cultures of hippocampal neurons due to the toxicity of DMSO.
24. The success of fractionation can be confirmed by:
    (a) Immunocytochemistry using an anti-Aβ antibody (Fig. 1).
    (b) Electron microscopy.
    (c) Immunoblot.

Acknowledgments

Research in our laboratory is supported by grants from the National Institutes of Health (NS39080), Alzheimer's Association, and The Amyotrophic Lateral Sclerosis Association to A.F.

References

1. Ropper, A.H., Adams, R.D., Victor, M., Brown, R.H., Victor, M., and Ebrary Inc. (2005) Adams and Victor's principles of neurology, 8th ed., McGraw-Hill Medical Pub. Division, New York.
2. Ferri, C.P., Prince, M., Brayne, C., Brodaty, H., Fratiglioni, L., Ganguli, M., Hall, K., Hasegawa, K., Hendrie, H., Huang, Y., Jorm, A., Mathers, C., Menezes, P.R., Rimmer, E., and Scazufca, M. (2005) Global prevalence of dementia: a Delphi consensus study. *Lancet* **366**, 2112–2117.
3. Blennow, K., de Leon, M.J., and Zetterberg, H. (2006) Alzheimer's disease. *Lancet* **368**, 387–403.
4. Parihar, M.S., and Hemnani, T. (2004) Alzheimer's disease pathogenesis and therapeutic interventions. *J. Clin. Neurosci.* **11**, 456–467.
5. Honer, W.G. (2003) Pathology of presynaptic proteins in Alzheimer's disease: more than simple loss of terminals. *Neurobiol. Aging* **24**, 1047–1062.
6. Scheff, S.W., Price, D.A., Schmitt, F.A., and Mufson, E.J. (2006) Hippocampal synaptic loss in early Alzheimer's disease and mild cognitive impairment. *Neurobiol. Aging* **27**, 1372–1384.
7. Selkoe, D.J. (2002) Alzheimer's disease is a synaptic failure. *Science* **298**, 789–791.
8. Tanzi, R.E. (2005) The synaptic Abeta hypothesis of Alzheimer disease. *Nat. Neurosci.* **8**, 977–979.
9. Roberson, E.D., and Mucke, L. (2006) 100 years and counting: prospects for defeating Alzheimer's disease. *Science* **314**, 781–784.
10. Glenner, G.G., and Wong, C.W. (1984) Alzheimer's disease: initial report of the purification and characterization of a novel cerebrovascular amyloid protein. *Biochem. Biophys. Res. Commun.* **120**, 885–890.
11. Kondo, J., Honda, T., Mori, H., Hamada, Y., Miura, R., Ogawara, M., and Ihara, Y. (1988) The carboxyl third of tau is tightly bound to paired helical filaments. *Neuron* **1**, 827–834.
12. Kosik, K.S., Joachim, C.L., and Selkoe, D.J. (1986) Microtubule-associated protein tau (tau) is a major antigenic component of paired helical filaments in Alzheimer disease. *Proc. Natl. Acad. Sci. USA* **83**, 4044–4048.
13. Arriagada, P.V., Growdon, J.H., Hedley-Whyte, E.T., and Hyman, B.T. (1992) Neurofibrillary tangles but not senile plaques parallel duration and severity of Alzheimer's disease. *Neurology* **42**, 631–639.
14. Morishima-Kawashima, M., and Ihara, Y. (2002) Alzheimer's disease: beta-amyloid protein and tau. *J. Neurosci. Res.* **70**, 392–401.
15. Holzer, M., Holzapfel, H.P., Zedlick, D., Bruckner, M.K., and Arendt, T. (1994) Abnormally phosphorylated tau protein in Alzheimer's disease: heterogeneity of individual regional distribution and relationship to clinical severity. *Neuroscience* **63**, 499–516.
16. Wood, J.G., Mirra, S.S., Pollock, N.J., and Binder, L.I. (1986) Neurofibrillary tangles of Alzheimer disease share antigenic determinants with the axonal microtubule-associated protein tau (tau). *Proc .Natl. Acad. Sci. USA* **83**, 4040–4043.
17. Yankner, B.A., Mesulam, M.M. (1991) Seminars in medicine of the Beth Israel Hospital, Boston. Beta-amyloid and the pathogenesis of Alzheimer's disease. *N. Engl. J. Med.* **325**, 1849–1857.
18. Cleary, J.P., Walsh, D.M., Hofmeister, J.J., Shankar, G.M., Kuskowski, M.A., Selkoe, D.J., and Ashe, K.H. (2005) Natural oligomers of the amyloid-beta protein specifically disrupt cognitive function. *Nat. Neurosci.* **8**, 79–84.
19. Hardy, J.A., and Higgins, G.A. (1992) Alzheimer's disease: the amyloid cascade hypothesis. *Science* **256**, 184–185.
20. Selkoe, D.J. (2001) Clearing the brain's amyloid cobwebs. *Neuron* **32**, 177–180.
21. Klein, W.L., Krafft, G.A., and Finch, C.E. (2001) Targeting small Abeta oligomers: the solution to an Alzheimer's disease conundrum? *Trends Neurosci.* **24**, 219–224.
22. Oddo, S., Caccamo, A., Tran, L., Lambert, M.P., Glabe, C.G., Klein, W.L., and Laferla, F.M. (2005) Temporal profile of Abeta oligomerization in an in vivo model of Alzheimer's disease: A link between Abeta and tau pathology. *J. Biol. Chem.* **281**, 1599–1604.
23. Pike, C.J., Walencewicz, A.J., Glabe, C.G., and Cotman, C.W. (1991) In vitro aging of beta-amyloid protein causes peptide aggregation and neurotoxicity. *Brain Res.* **563**, 311–314.
24. Anderson, K.L. and Ferreira, A. (2004) Alpha 1 integrin activation: a link between beta-amyloid deposition and neuronal death in aging hippocampal neurons. *J. Neurosci. Res.* **75**, 688–697.
25. Ferreira, A., Caceres, A., and Kosik, K.S. (1993) Intraneuronal compartments of the amyloid precursor protein. *J. Neurosci.* **13**, 3112–3123.

26. Ferreira, A., Lu, Q., Orecchio, L., and Kosik, K.S. (1997) Selective phosphorylation of adult tau isoforms in mature hippocampal neurons exposed to fibrillar Aβ. *Mol. Cell. Neurosci.* **9**, 220–234.
27. Kelly, B.L., Vassar, R., and Ferreira, A. (2005) Beta-amyloid-induced dynamin 1 depletion in hippocampal neurons. A potential mechanism for early cognitive decline in Alzheimer disease. *J. Biol. Chem.* **280**, 31746–31753.
28. Kelly, B.L, and Ferreira, A. (2006) Beta-amyloid-induced dynamin 1 degradation is mediated by NMDA receptors in hippocampal neurons. *J. Biol. Chem.* **281**, 28079–28089.
29. Kelly, B., and Ferreira, A. (2007) Beta-amyloid disrupted synaptic vesicle endocytosis in cultured hippocampal neurons. *Neuroscience* **146**, 60–70.
30. Park, S.Y., and Ferreira, A. (2005) The generation of a 17 kDa neurotoxic fragment: an alternative mechanism by which tau mediates beta-amyloid-induced neurodegeneration. *J. Neurosci.* **25**, 5365–5375.
31. Park, S.Y., Tournell, C.E., Sinjoanu, R.C., and Ferreira, A. (2007) Caspase 3- and calpain-mediated tau cleavage are differentially prevented by estrogen and testosterone in beta-amyloid-treated hippocampal neurons. *Neuroscience* **144**, 119–127.
32. Rapoport, M. and Ferreira, A. (2000) PD98059 prevents neurite degeneration induced by fibrillar beta-amyloid in mature hippocampal neurons. *J. Neurochem.* **74**, 125–133.
33. Rapoport, M., Dawson, H.N., Binder, L.I., Vitek, M. and Ferreira, A. (2002) Tau is essential for beta-amyloid induced neurotoxicity. *Proc. Natl. Acad. Sci. USA* **99**, 6364–6369.
34. Shah, R.D., Anderson, K.L., Rapoport, M. and Ferreira, A. (2003) Estrogen-induced changes in the microtubular system correlate with a decreased susceptibility of aging neurons to beta-amyloid neurotoxicity. *Mol. Cell. Neurosci.* **24**, 503–516.
35. Sinjoanu, R.C., Kleinschmidt, S., Bitner, R.S., Brioni, J., Moeller, A., and Ferreira, A. (2008) The novel calpain inhibitor A-705253 potently inhibits oligomeric beta-amyloid-induced dynamin 1 and tau cleavage in hippocampal neurons. *Neurochem. Intl.* **53**, 79–88.
36. Alvarez, A., Toro, R., Caceres, A., and Maccioni, R.B. (1999) Inhibition of tau phosphorylating protein kinase cdk5 prevents beta-amyloid-induced neuronal death. *FEBS Lett.* **459**, 421–426.
37. Boland, B., and Campbell, V. (2003) Beta-amyloid (1-40)-induced apoptosis of cultured cortical neurones involves calpain-mediated cleavage of poly-ADP-ribose polymerase. *Neurobiol. Aging* **24**, 179–186.
38. Busciglio, J., Lorenzo, A., Yeh, J., and Yankner, B.A. (1995) Beta-amyloid fibrils induce tau phosphorylation and loss of microtubule binding. *Neuron* **14**, 879–888.
39. Copani, A., Bruno, V., Battaglia, G., Leanza, G., Pellitteri, R., Russo, A., Stanzani, S., and Nicoletti, F. (1995) Activation of metabotropic glutamate receptors protects cultured neurons against apoptosis induced by beta-amyloid peptide. *Mol. Pharmacol.* **47**, 890–897.
40. Ekinci, F.J., Malik, K.U., and Shea, T.B. (1999) Activation of the L voltage-sensitive calcium channel by mitogen-activated protein (MAP) kinase following exposure of neuronal cells to beta-amyloid. MAP kinase mediates beta-amyloid-induced neurodegeneration. *J. Biol Chem.* **274**, 30322–30327.
41. Estus, S., Tucker, H.M., van Rooyen, C., Wright, S., Brigham, E.F., Wogulis, M., and Rydel, R.E. (1997) Aggregated amyloid-beta protein induces cortical neuronal apoptosis and concomitant "apoptotic" pattern of gene induction. *J. Neurosci.* **17**, 7736–7745.
42. Gamblin, T.C., Chen, F., Zambrano, A., Abraha, A., Lagalwar, S., Guillozet, A.L., Lu, M., Fu, Y., Garcia-Sierra, F., LaPointe, N., Miller, R., Berry, R.W., Binder, L.I., and Cryns, V.L. (2003) Caspase cleavage of tau: linking amyloid and neurofibrillary tangles in Alzheimer's disease. *Proc. Natl. Acad. Sci. USA* **100**, 10032–10037.
43. Harada, J., and Sugimoto, M. (1999) Acti vation of caspase-3 in beta-amyloid-induced apoptosis of cultured rat cortical neurons. *Brain Res.* **842**, 311–323.
44. Lee, M.S., Kwon, Y,T., Li, M., Peng, J., Friedlander, R.M., and Tsai, L.H. (2000) Neurotoxicity induces cleavage of p35 to p25 by calpain. *Nature* **405**, 360–364.
45. Loo, D.T., Copani, A., Pike, C.J., Whittemore, E.R., Walencewicz, A.J., and Cotman, C.W. (1993) Apoptosis is induced by β-amyloid in cultured central nervous system neurons. *Proc. Natl. Acad. Sci .USA* **90**, 7951–7955.
46. Marin, N., Romero, B., Bosch-Morell, F., Llansola, M., Felipo, V., Roma, J., and Romero, F.J. (2000) Beta-amyloid-induced activation of caspase-3 in primary cultures of rat neurons. *Mech. Ageing Dev.* **119**, 63–67.
47. Takashima, A., Noguchi, K., Sato, K., Hoshino, T., and Imahori, K. (1993) Tau protein kinase I is essential for amyloid beta-protein-induced neurotoxicity. *Proc. Natl. Acad. Sci. USA* **90**, 7789–7793.

48. Goslin, K., and Banker, G.A. (1991) Rat hippocampal neurons in low-density culture. In: Culturing Nerve Cells (Banker, G.A. and Goslin, K, ed.), pp. 251–281. Cambridge: MIT Press.
49. Sotthibundhu, A., Sykes, A.M., Fox, B., Underwood, C.K., Thangnipon, W., and Coulson, E.J. (2008) Beta-amyloid (1-42) induces neuronal death through the p75 neurotrophin receptor. *J Neurosci.* **28**, 3941–3946.
50. Lorenzo, A. and Yankner, B.A. (1994) Beta-amyloid neurotoxicity requires fibril formation and is inhibited by Congo Red. *Proc. Natl. Acad. Sci. USA.* **91**, 12243–12247.
51. Sachse, C., Fandrich, M., and N. Grigorieff, N. (2008) Paired beta-sheet structure of an Abeta(1-40) amyloid fibril revealed by electron microscopy. *Proc. Natl. Acad. Sci. USA.* **105**, 7462–7466.
52. Patel, D.A., Henry,J.E., and Good, T.A. (2007) Attenuation of beta-amyloid-induced toxicity by sialic-acid-conjugated dendrimers: role of sialic acid attachment. *Brain Res.* **1161**, 95–105.

Chapter 12

Manipulation of Gene Expression in the Central Nervous System with Lentiviral Vectors

Binggui Sun and Li Gan

Abstract

Viral vector-mediated gene transfer is widely used to manipulate gene expression (overexpression or knock down) in cultures and in different tissues of animals. Vectors based on lentiviruses have particularly useful features. Lentiviral vectors mediate gene transfer into any neuronal cell types and induce sustained expression without significant immune responses after delivery into the nervous system. Lentivirus-mediated expression of therapeutic genes has led to long-term treatment of animal models of neurological disorders, such as spinal injury, Parkinson's disease, Huntington's disease, and Alzheimer's disease. Here, we describe the preparation and purification of lentiviral vectors and methods of lentiviral infection in primary neural cultures and in brain regions of interest by stereotaxic injection.

Key words: Lentiviral vector, Gene expression, Primary neural culture, Stereotaxic injection, Central nervous system

1. Introduction

To modify gene expression in specific cell types in the central nervous system (CNS), the gene products must be efficiently delivered to cells in such a way that the genes are expressed at the appropriate level and for a sufficient duration. The development of viral vectors made it possible to manipulate gene expression in the CNS. Viruses tend to be very efficient at delivering their own DNA into the host cell. By replacing nonessential genes of the viral genome with foreign genes of interest, one can use recombinant viral vectors to overexpress genes in living organisms. Part of the viral genome can also be replaced with small hairpin RNAs, which can be processed into double-stranded RNA to induce gene silencing. Several kinds of viral vectors have been used extensively

Erik D. Roberson (ed.), *Alzheimer's Disease and Frontotemporal Dementia*, Methods in Molecular Biology, vol. 670,
DOI 10.1007/978-1-60761-744-0_12,

to manipulate genes, including retroviral vectors, adenoviruses, adeno-associated viruses, and herpes simplex virus type 1.

Lentiviruses are a subclass of retroviruses that can infect both proliferating and nonproliferating cells (1), including neurons (2). Lentiviral vectors hold great promise in the treatment of neurological diseases, as demonstrated in a rhesus monkey model of Parkinson's disease (3). Here, we describe methods for using lentiviral vectors to manipulate gene expression in the CNS.

2. Materials

2.1. Preparation of HEK293T Cells

1. Tissue culture facility with hood and incubators (see Note 1).
2. Poly-ornithine (PO) stock, 100×: Dissolve PO (Sigma) to 0.3 mg/ml in sterile deionized H_2O. Pass PO solution through a 0.22-μm filter to remove any crystals that may have formed, which are toxic to cells, aliquot in 1.5-ml/tubes, and store at –20°C.
3. 100-mm sterile tissue culture dishes.
4. T25 or T75 sterile tissue culture flasks.
5. HEK293 cells. Available from repositories such as ATCC.
6. 37°C water bath.
7. 10,000 U/ml penicillin (100×) and 10,000 μg/ml (100×) streptomycin (Invitrogen). Thaw at 37°C in a water bath, aliquot 10 ml/tube, and store at –20°C.
8. 200 mM (100×) L-glutamine (Invitrogen). Thaw at 37°C in a water bath, aliquot 10-ml/tube, and store at –20°C.
9. Heat-inactivated fetal bovine serum (FBS; Invitrogen): Thaw in 37°C water bath, aliquot in 50-ml tubes, and store at –20°C.
10. Dulbecco's modified Eagle's medium (DMEM): High-glucose DMEM with Glutamax, 100 U/ml penicillin, 100 μg/ml streptomycin, and 2 mM glutamine. Store at 4°C.
11. DMEM + 10% FBS. Add 10% FBS to DMEM.

2.2. Transfection of Lentivirus-Encoding Plasmids

1. FUGW-derived lentivirus backbone plasmid, into which you have cloned your gene or shRNA of interest. FUGW is available from Addgene.
2. Delta 8.9 packaging vector.
3. VSVG pseudotyping vector.
4. Calphos mammalian transfection kit (Clontech). This kit includes the 2 M calcium solution used to make Solution A and 2× HEPES-buffered saline (HBS or Solution B).

2.3. Virus Concentration/ Purification

1. 0.45-μm filter units.
2. Thinwall Ultra-Clear centrifuge tubes for SW-41Ti (Beckman).
3. 75% Ethanol.
4. Balance for weighing tubes.
5. SW-41Ti rotor with buckets and caps (kept in 4°C refrigerator in centrifuge room).
6. Ultracentrifuge.
7. Bleach.
8. 1× Dubecco's phosphate-buffered solution (DPBS) with calcium and magnesium (Invitrogen). Store at room temperature (RT), but chill before use for resuspending virus.
9. Parafilm.

2.4. Virus Titration

1. Epifluorescence microscope.
2. p24 HIV ELISA assay kit (PerkinElmer or Cell BioLabs).

2.5. Primary Neuronal Cultures

1. 1× DPBS without calcium and magnesium (Invitrogen). Store at RT.
2. Papain solution: For every 10–12 pups, add 200 units of papain (Worthington Biochemical Co.) to 20 ml of DPBS without Ca^{2+} and Mg^{2+}. Add 3.2 mg of L-cysteine (optional).
3. Earle's balanced salt solution (EBSS) without calcium and magnesium, 1× (Invitrogen).
4. Dissecting microscope.
5. Surgical tools and razor blades.
6. 0.22-μm filters.
7. 10× Low ovomucoid stock solution: 1.5% bovine serum albumin (BSA) and 1.5% ovomucoid in DPBS without calcium and magnesium. Dissolve 750 mg of BSA (Sigma) and 750 mg of ovomucoid (Boehringer Mannheim) in 50 ml of DPBS, adjust pH to 7.4, pass through a 0.22-μm syringe filter, place 1-ml aliquots in 1.5-ml centrifuge tubes, and store at –20°C.
8. 6× High ovomucoid stock solution: 6% BSA and 6% ovomucoid in DPBS without calcium and magnesium. Dissolve 3,000 mg of BSA and 3,000 mg of ovomucoid in 50 ml of DPBS, adjust pH to 7.4, pass through a 0.22-μm filter, place 1-ml aliquots in 1.5-ml centrifuge tubes, and store at –20°C.
9. 10 U/μl DNase stock solution. Add 15 ml of DPBS to 150,000 U DNase A (Sigma). Aliquot 0.4 ml/tube and store at –20°C.
10. 1× Low ovomucoid solution: 0.15% BSA, 0.15% ovomucoid, and 0.067 U/μl DNase in DPBS without calcium and magnesium.

Mix 27 ml of DPBS, 3 ml of 10× low ovomucoid stock, and 200 µl of 10 U/µl DNase stock.

11. 1× High ovomucoid solution: 1% BSA and 1% ovomucoid in DPBS. Mix 10 ml of DPBS and 2 ml of 6× Hi ovomucoid stock.
12. 70-µm Cell strainer nylon filter.
13. Centrifuge for 15- and 50-ml tubes.
14. NBA-B27 medium: Neurobasal A medium, including 2% B27 supplement, 100 U/ml penicillin, 100 µg/ml streptomycin, and 500 µM glutamine. Store at 4°C.
15. NBA-N2 medium: Neurobasal A medium, including 1% N2 supplement, 100 U/ml penicillin, 100 µg/ml streptomycin, and 500 µM glutamine. Store at 4°C.
16. Hemocytometer.
17. Teflon cell scrapers.

2.6. Stereotaxic Injection

1. Avertin (tribromoethanol) stock solution, 100%. In 20 ml glass vial, dissolve 10 g of 2,2,2,-tribromoethanol (99%) with 10 ml of tert-amyl alcohol. Wrap in foil and store in a glass jar at RT for up to 6 months.
2. Avertin working solution, 2.5%. Dilute Avertin stock solution 40 times with PBS by adding dropwise with constant stirring in PBS. Avoid the formation of crystals in the final solution as this will cause death in mice via intestinal necrosis. Store at room temperature. Inject (i.p.) 200 µl of the working solution per 10 g of mouse body weight.
3. Puralube Vet Ointment (Pharmaderm Animal Health).
4. Tissue glue or suture.
5. Surgical tools: Scissors, forceps, bulldog type homeostatic clamps (Fine Science Tools).
6. 70% Ethanol.
7. Stereotaxic apparatus.
8. Dissecting microscope.
9. Light source.
10. Drill.
11. Motorized infusion syringe pump.
12. Hamilton syringe (10 µl).

3. Methods

The procedure outlined here includes the preparation of cultured human embryonic kidney (HEK) cells, in which the virus is produced (Subheading 3.1), transfection of lentivirus-encoding

plasmids (Subheading 3.2), purification of the virus by high-speed centrifugation (Subheading 3.3), quantification of viral titer (Subheading 3.4), and use in primary cells (Subheading 3.5) or by stereotaxic injection into brain (Subheading 3.6).

3.1. Preparation of HEK293T Cells

1. Dilute PO stock solution (100×) to 1× solution with distilled water (DW).
2. Coat each 100-mm dish with 5 ml of 1× PO solution.
3. Allow plates to sit undisturbed for more than 3 h at RT or 1 h at 37°C.
4. Remove the PO solution by aspiration and wash plates twice with DW.
5. Let plates dry completely (lids on) in a tissue culture hood for at least 2 h.
6. Wrap plates with parafilm and store at 4°C.
7. Take a frozen vial of HEK293T cells with low passage number (see Note 2) from the liquid nitrogen container, and put it on dry ice.
8. Thaw cells quickly by incubating the vial in a 37°C water bath.
9. Add 1 ml of cell suspension to 5 ml (T25 flask) or 15 ml (T75 flask) of prewarmed (37°C) DMEM and resuspend the cells by gently pipetting up and down four to five times.
10. Shake the flask gently and put it into a tissue culture incubator (37°C with 5% CO_2).
11. Split cells when they are close to confluent: Seed 10^6 HEK 293 T cells in a 100-mm dish coated with PO and add 10 ml of DMEM supplemented with 10% FBS. Swirl the cells thoroughly to distribute them evenly across the surface of the dish. Incubate the cells for 24 h at 37°C.

3.2. Transfection of Lentivirus-Encoding Plasmids

Lentiviral vectors are produced in HEK cells by transfecting with three plasmids containing the component parts (4). The first will be some derivative of FUGW, the backbone into which you have cloned your gene of interest. FUGW, in its unmodified form, encodes enhanced green fluorescent protein (eGFP) driven by the human ubiquitin-C promoter. This vector also contains the woodchuck hepatitis virus posttranscriptional regulatory element (WRE) between cytomegalovirus long terminal repeats (LTRs) to increase protein production and the HIV-1 flap sequence to increase titer. FUGW is replication-deficient because it does not contain packaging proteins. The packaging proteins are provided by cotransfecting with the delta 8.9 packaging vector, which contains the gag, pol, and rev genes. A third plasmid mediates pseudotyping and expresses the vesicular stomatitis virus glycoprotein (VSVG).

The calcium-phosphate transfection procedure described here has been modified from the Calphos Mammalian Transfection Protocol (Clontech). Our standard procedure, described here, is to prepare virus from six 100-mm dishes at a time. This yields 300 µl of lentivirus, with titers of ~10^7 transducing units per µl.

1. The cells should be 70–80% confluent on the day of transfection.
2. Replace the medium with 10 ml of prewarmed DMEM + 10% FBS 0.5–3 h before transfection.
3. Prepare solution A for six 100-mm dishes: Sequentially add 60 µg of transfer vector (e.g., FUGW) (4), 45.0 µg of delta 8.9 plasmid, 30 µg of VSVG plasmid, sterile H_2O to a volume of 3,679.2 µl, and 520.8 µl of 2 M calcium solution. The total volume should be 4,200 µl.
4. Mix solution A and solution 4,200 µl of Solution B (2× HBS). Carefully and gently vortex solution B while adding solution A dropwise. This is the transfection solution. The total volume is 8.4 ml.
5. Incubate the mixed transfection solution at room temperature for 20 min.
6. Gently vortex transfection solution and then add 1.4 ml dropwise to each plate with a 5-ml serological pipette.
7. Gently move plates back and forth to distribute transfection solution evenly.
8. Incubate plates at 37°C in a tissue culture incubator overnight.
9. Wash cells with PBS the next morning. Add 10 ml of DMEM + 10% FBS and incubate for 48 h.
10. Collect culture medium containing virus from the plates at ~60 h after transfection. The viral medium can be processed immediately for concentration or stored at –80°C.

3.3. Virus Concentration/ Purification

1. In the tissue culture hood, prewet a 0.45 µm filter by pouring 20 ml of DMEM through it to prevent nonspecific binding of virus to the filter.
2. Filter the virus-containing medium.
3. Sterilize Ultra-Clear centrifuge tubes by soaking in 75% ETOH and then wash them with PBS in the tissue culture hood to remove any remaining ETOH.
4. Load the filtered, virus-containing medium into the sterilized tubes. Balance the tubes carefully with a scale; centrifuge the supernatant at 77,000×*g* for 2 h at 4°C using a swinging bucket rotor. We generally use a Beckman SW41Ti rotor. Beckman SW28 rotors can also be used.

5. Gently remove the tubes from the rotor buckets and place into a tube rack.
6. Tilt the tube and aspirate the medium (see Note 3). Add bleach (final concentration ~10%) to the aspirated medium before discarding to inactivate any remaining virus.
7. Invert tube over a Kimwipe tissue to absorb the moisture. Air dry.
8. Add 50 µl of cold 1× DPBS with Ca^{2+} and Mg^{2+} in each tube.
9. Seal tubes with parafilm to prevent evaporation. Keep the tube at 4°C at least 12 h to dissolve the pellet.
10. Pipette up and down at least 20 times to dissolve the pellets. Avoid air bubbles.
11. Combine the viral solution (for six 100-mm dishes, 6×50 µl = 300 µl). Aliquot the virus and store at –80°C.

3.4. Virus Titration

It is important to measure the titer of each virus prep to ensure sufficient quality and to determine how much virus to use for subsequent experiments. Two methods are provided. One is based on determining the biological activity of the virus, namely, its ability to transduce cells and express a fluorescent marker (Subheading 3.4.1). This is considered to be the gold standard. However, some vectors may not express a fluorescent marker; with such vectors, the immunocytochemistry required to identify transduced colonies is highly labor intensive. In these situations, biochemically quantifying the amount of HIV protein p24 (Subheading 3.4.2) provides an alternative method for titering virus.

Titers of at least 10^6 should be expected, and preps with titers of 10^5 or below are not sufficient for use in experiments. In our hands, the protocol above typically produces titers of 10^7 TU (transduction units)/µl.

Titers determined with these methods are useful for estimating how much virus to use for a given experiment. For example, if an experiment calls for comparing the effects of two viruses, and virus A has a titer of 2×10^7 while virus B has a titer of 1×10^7, then one should use twice as much virus B (by volume) for the experiment. Ideally, however, this estimation should be validated by directly measuring the expression of the gene of interest in the cell type of interest. In other words, if the experiment is being done in primary neurons, then infect some wells with virus A, other wells with twice the volume of virus B, and then measure the expression of the protein of interest by quantitative PCR or western blotting to ensure that the expression is equivalent.

3.4.1. Biological Transduction Units (TU)

1. Resuspend HEK293T cells (or other rapidly dividing cells, such as HeLa, see Note 4) at 5×10^4/ml 24 h before titration and add 100 µl of cell suspension to each well of a 96-well plate.

2. Prepare eight Eppendorf tubes for virus dilution. Add 54 µl of DMEM to each tube. Add 6 µl of virus solution to the first tube. Mix thoroughly, change tip, and take 6 µl to mix with the next tube. Repeat the procedure until the eighth tube. This produces a serial dilution ranging from 10^1- to 10^8-fold.
3. Aspirate medium from the wells of the 96-well plate. Add 50 µl of viral dilution per well, and incubate at 37°C in a tissue culture incubator with 5% CO_2.
4. For vectors expressing GFP, check for GFP fluorescence 3 days after infection. Count the number of green colonies in each well, and determine the titer of virus according to the following equation:

$$\left(\frac{\#\ \text{Colonies}}{50\mu\text{l}}\right) \times \text{Dilution Factor} = \text{TU}/\mu\text{l}.$$

For example, if five green colonies were counted in the last dilution, the titer should be:

$$\left(\frac{5}{50\mu\text{l}}\right) \times 10^8 = 1\times10^7\ \text{TU}/\mu\text{l}.$$

3.4.2. Quantification of p24

1. Titer the virus according to the manufactures' instructions using a p24 HIV-1 ELISA kit (Cell Biolabs or PerkinElmer) to determine the TU/ml and calculate the amount of virus to add to your target cells depending on the number of cells to infect and the multiplicity of infection (MOI).

3.5. Virus-Mediated Gene Transfer in Primary Neural Cultures

3.5.1. Neuronal Culture of P0 Rat Cortex

1. Prepare papain solution in a tissue culture hood, as directed in Subheading 2.5, and warm in a 37°C water bath.
2. Dissect postnatal day 0 (p0) rat cortices in EBSS without Ca^{2+} and Mg^{2+}. Remove EBSS from the tissue. Mince the tissue into about 1-mm blocks with razor blades in a 100-mm dish.
3. Filter papain through a 0.22-µm filter, and add the papain solution to the tissues in the dish.
4. Transfer tissue into a 50-ml tube and incubate the tissue at 37°C for 30 min.
5. Make 1× low and high ovomucoid solutions from 10× and 6× stocks during the papain digestion. Ovomucoid is a protease inhibitor found in egg whites.
6. Pipette the digested tissues into a 50-ml tube. Add 8 ml of low ovomucoid and let it sit for 5 min at RT or until the tissue chunks can move freely (which means all DNA was digested).

7. Aspirate the liquid to waste, add 10 ml of low ovomucoid, and triturate with a 10-ml pipette. Allow the tissue chunks to settle (without centrifugation) for 2–3 min until cell debris has settled to the bottom, and transfer the supernatant to a new 50-ml tube.
8. Repeat step 7 until all cells are dissociated (a 1-ml pipette can be used for these steps).
9. Filter the cells through a 70-μm nylon filter.
10. Split cells into two 15-ml tubes and spin at 1,000 × *g* for 10 min at room temperature.
11. Remove the supernatant. The tube will have red blood cells (RBC) and cell debris at the bottom, with your neuronal cells above. Tap the tube with your finger to loosen the upper part of the pellet.
12. Resuspend the upper cells in 5 ml of high ovomucoid, without disturbing the RBC and debris at the bottom, and transfer to a new tube.
13. Spin again at 1,000 × *g* for 10 min.
14. Repeat step 11 and resuspend the cells in 20 ml of NBA + B27 medium.
15. Split cells into two 15-ml tubes and centrifuge at 1,000 × *g* for 5 min.
16. For pure neuronal cultures, resuspend cells in 10 ml of NBA + B27 medium. For mixed neuronal-glial cultures, wash cells once with 10 ml of DMEM plus 10% FBS by spinning at 1,000 × *g* for 5 min, and resuspend cells in 20 ml of DMEM + 10% FBS.
17. Count cells and dilute with culture medium to $5–8 \times 10^5$ cells/ml.
18. Add cells to the PO-coated plates: 100 μl/well for 96-well plates and 500 μl/well for 24-well plates
19. Change to fresh medium 1–2 h after plating cells (see Note 5).

3.5.2. Viral Infection of Primary Neural Cells

1. Add viral solutions (1–5 μl, according to viral titers, see Note 6) to the medium of primary neural cultures on day 5–7 after plating. Rock the plates to distribute the viral solution evenly in the medium and return the plates to the culture incubator (37°C with 5% CO_2).
2. Depending on the applications, primary neural cells can be analyzed 5–10 days after the infection. To analyze secreted proteins, medium can be collected starting 2–3 days after the infection (see Note 7).
3. On the day of harvest, carefully aspirate the medium and inactivate any remaining viral particles with 10% bleach.

4. Wash cells with PBS. Fix cells with 4% paraformaldehyde (PFA) for 15 min at room temperature for immunocytochemical analysis (see Note 8), or collect cell lysates for Western blot, RT-PCR, or other analyses.

3.6. Virus-Mediated Gene Transfer in Special Brain Regions

3.6.1. Stereotaxic Injection

1. Inject anesthetics (we use avertin, see Note 9) into mice of interest. Wait for a couple of minutes until mice do not respond to pinching of tails or toes with tweezers.
2. Shave or cut the fur on the skull, clean the skin with 70% ethanol, and apply Puralube ophthalmic ointment to prevent eyes from overdrying.
3. Mount the animal onto a stereotactic apparatus. To place the animal in the apparatus, fix the head of the animal with an ear bar adaptor first, and then fix the adaptor with the animal onto the apparatus by using two ear bars.
4. Insert the animal's incisor into an incisor adaptor. Pull down the lower jaw of the animal with a forceps, move the adaptor into the mouth of the animal and let the animal's incisor fit into the opening of the adaptor, and then pull back slowly and fix the incisor adaptor in place.
5. Use nose clamp to fix the animal's nose.
6. Adjust the dissecting microscope so that you can visualize the top of the animal's skull. Cut the skin along the midline over the skull with a small scissors, keep the area open by using bulldog type homeostatic clamps, and clean the open area with sterile swabs.
7. Mount a drill onto the stereotaxic apparatus and place the tip of the drill at the location of lambda. Measure the *z* coordinate of lambda. Move the tip of the drill to the bregma, and measure the *z* coordinate of the bregma.
8. Adjust the adjustment screw at the incisor adaptor if the *z* coordinate of the bregma is different from that of the lambda. Make sure the two *z* coordinates of bregma and lambda have the same value to ensure the head is level in the frame, anterior–posterior.
9. Measure and record the *x* and *y* coordinates of the bregma.
10. Move the tip of the drill 1 mm lateral to the bregma on both sides, and measure the *z* coordinates of these two locations. Adjust the frame until they have the same value to ensure that the left side and the right side of the head are on the same level.
11. Calculate the *x* and *y* coordinates of the target injection position, as determined from a stereotaxic brain atlas, using the measured *x* and *y* coordinates of bregma as a reference.
12. Drill hole(s). Be careful not to damage the brain tissue.

13. Remove drill from the stereotaxic apparatus and mount the syringe drive motor of the injector to the apparatus.
14. Mount a 10-µl Hamilton syringe on the syringe drive motor, and fill the syringe with virus.
15. Move the tip of the syringe to the bregma, and measure the *z* coordinate. Determine the vertical depth of injection according to a stereotaxic brain atlas (5), and calculate it from this *z* coordinate.
16. Push the Run/Start button of the injector slowly to make sure that the solution can come out from the syringe.
17. Set up the injector. Select volume, syringe type, and injection rate.
18. Move the tip of the syringe to the hole(s), lower the syringe slowly to the desired depth.
19. Inject virus into the brain regions of interest.
20. Keep the needle in place for 5 min after the injection to prevent the injected solution from flowing back through the needle track.
21. Pull the needle out of the brain slowly and gently.
22. Close the skin with suture and/or tissue glue. Place the animal in a new cage with autoclaved Alpha Dry (see Note 10). Transfer the animal back to the holding room.
23. Rinse syringe sequentially with distilled water, acetone, and distilled water.
24. Clean the bench after surgery with 0.025% bleach and 70% ethanol.

3.6.2. Analysis of Gene Expression in the Brain

1. At desired time points after surgery (see Note 11), anesthetize animals with avertin and perfuse transcardially with saline.
2. Dissected brains quickly, and cut sagitally along the midline. One hemibrain can be snap frozen with dry ice and stored at –80°C for further analysis (e.g., Western blot, RT-PCR, or ELISA). Immerse the other hemibrain in 4% PFA and store at 4°C for 24 – 48 h. Transfer brains to PBS with 0.05% NaN_3 for long-term storage or 30% sucrose in 1× PBS for microtome sectioning within 1 week.
3. Measure gene expression by immunohistochemical staining (Fig. 1), Western blot, or RT-PCR analyses.

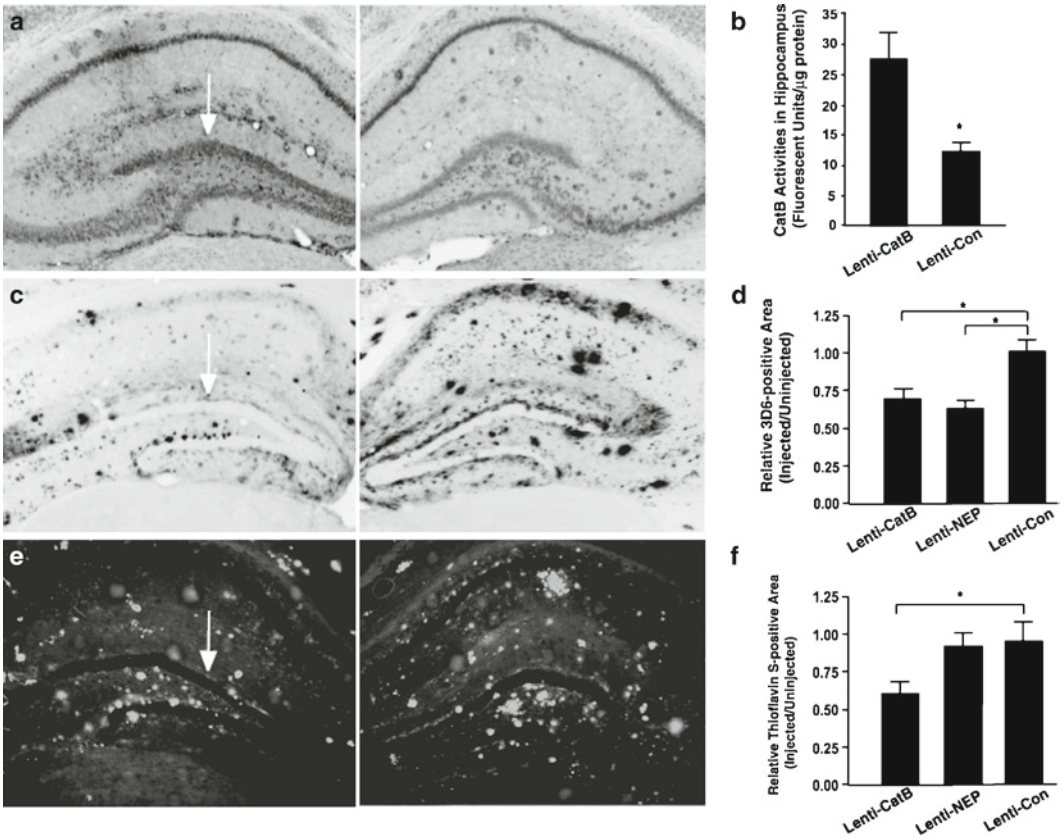

Fig. 1. Cathepsin B (CatB) gene transfer reduces amyloid plaques in aged hAPP mice. (**a**) Representative CatB immunostaining of the Lenti-CatB injected (*left*) and uninjected (*right*) hippocampus in a 12–15-month-old hAPP mouse. (**b**) CatB enzymatic activity in the hippocampus of $CatB^{+/-}$ mice after injection of Lenti-CatB or Lenti-control ($n=3$ mice/group, $^*P<0.05$, unpaired *t* test). (**c** and **e**) Photomicrographs of 3D6 immunostaining (**c**) and thioflavin-S-positive labeling (**e**) of the Lenti-CatB-injected (*left*) and uninjected (*right*) hippocampus. (**d**) Injection of Lenti-CatB (12 mice) or Lenti-NEP (7 mice), but not Lenti-control (5 mice), reduced 3D6-immunoreactive Aβ deposits in the hippocampus of 12–15-month-old hAPP mice. (**f**) Injection of Lenti-CatB (12 mice), but not Lenti-NEP (7 mice) or Lenti-control (5 mice), reduced thioflavin-S-positive plaques in the hippocampus of 12–15-month-old hAPP mice. $^*P<0.05$, Tukey Kramer post hoc test. Reproduced from Mueller-steiner et al. (7) with permission.

4. Notes

1. Lentivirus is a modified human immunodeficiency virus and although unable to replicate in a host, it must be handled with caution. When working with these viruses, work only in a BL2+ designated hood or a viral vector room. All handling,

storage, and disposal of biohazard waste must be in accordance with institute/university rules and OSHA and EPA regulations.

2. The HEK293T cells used for the lentiviral preparation should be within 15 generations.
3. During the viral preparation, after the ultracentrifugation, the pellet will be invisible, but will be stuck in the bottom and should not move with the supernatant as you tilt. When tilting to aspirate, be sure you never tilt back. Tilting back can cause the supernatant to splash back into the bottom of the tube and disrupt the pellet.
4. The titer of a lentiviral construct may vary depending on which cell line is chosen. We generally use HEK293T cells for titering. If you have more than one lentiviral construct, we recommend that you titer all of the lentiviral constructs using the same mammalian cell line.
5. Change culture medium to NBA-N2 before any drug treatments (around 7 days of culture).
6. When transducing a lentiviral construct into primary neural cells for the first time, a range of volumes or multiplicities of infection (MOIs) should be tested. 2, 5, 10, and 15 μl of lentiviral particles per 1.6×10^4 cells or MOIs of 0.5, 1, and 5 should be used to determine the optimal transduction efficiency to induce overexpressing or knockdown for each viral preparation.
7. Depending on the applications, different promoters could be used to target the viruses to different kinds of tissues or cell types (6).
8. Depending on the antigens you want to detect, different fixatives (e.g., acetone, alcohol, or a mixture of acetone and alcohol) could be used.
9. During the stereotaxic surgery, we use Avertin. However, ketamine/xylazine mixture, ketamine/meditomidine mixture, and other anesthetics are also widely used. Please keep in mind that recovery drug(s) are needed sometimes. For example, antipomezole could be injected after surgery if ketamine/meditomidine mixture is used.
10. To help animals recover after the surgery, it is critical to keep them warm and prevent dehydration. You can put a heat lamp on the cage for warmth and put a gel pack to provide easier access to water and nutrition.
11. In general, it takes at least 5 days for lentiviral vector-mediated gene expression to reach significant levels in the brain. In general, analyses should be performed no sooner than 10–14 days after infection to avoid possible acute inflammatory responses associated with the procedure.

Acknowledgments

The authors thank Yungui Zhou for discussion and advice on this chapter. This work was supported in part by NIH grant (AG024447) and a pilot project grant from the UCSF Alzheimer's Disease Research Center (to L.G.).

References

1. Zufferey, R., Dull, T., Mandel, R. J., Bukovsky, A., Quiroz, D., Naldini, L., et al. (1998) Self-inactivating lentivirus vector for safe and efficient in vivo gene delivery. *J. Virol.* **72**, 9873–9880.
2. Baekelandt, V., Claeys, A., Eggermont, K., Lauwers, E., De Strooper, B., Nuttin, B., et al. (2002) Characterization of lentiviral vector-mediated gene transfer in adult mouse brain. *Hum. Gene Ther.* **13**, 841–853.
3. Palfi, S., Leventhal, L., Chu, Y., Ma, S. Y., Emborg, M., Bakay, R., et al. (2002) Lentivirally delivered glial cell line-derived neurotrophic factor increases the number of striatal dopaminergic neurons in primate models of nigrostriatal degeneration. *J. Neurosci.* **22**, 4942–4954.
4. Lois, C., Hong, E. J., Pease, S., Brown, E. J., Baltimore, D. (2002) Germline transmission and tissue-specific expression of transgenes delivered by lentiviral vectors. *Science* **295**, 868–872.
5. Paxinos, G. and Franklin, K. B. J. (ed.) (2001) *The mouse brain in stereotaxic coordinates.* Academic Press, San Diego, CA.
6. Chen, J., Zhou, Y., Mueller-Steiner, S., Chen, L. F., Kwon, H., Yi, S., et al. (2005) SIRT1 Protects against microglia-dependent amyloid-beta toxicity through inhibiting NF-kappaB signaling. *J. Biol. Chem.* **280**, 40364–40374.
7. Mueller-Steiner, S., Zhou, Y., Arai, H., Roberson, E. D., Sun, B., Chen, J., et al. (2006) Antiamyloidogenic and neuroprotective functions of cathepsin B: Implications for Alzheimer's disease. *Neuron* **51**, 703–714.

Chapter 13

Selecting a Mouse Model of Alzheimer's Disease

Jeannie Chin

Abstract

Alzheimer's disease (AD) is the most common neurodegenerative disease and cause of dementia. Significant strides toward understanding and developing therapies for AD have been supported by the use of transgenic mouse models of AD. Over the last two decades, a number of mouse models have been created to recapitulate the major neuropathological hallmarks of the disease, namely amyloid plaques and neurofibrillary tangles. These mice recapitulate many, although not all, of the key features of AD, and have been widely used in AD research. At the present time, there are numerous types of transgenic mice available for the study of AD, many of which have been characterized to some extent in terms of neuronal, neuropathological, and/or behavioral abnormalities. This repository of transgenic mice offers a wealth of opportunity to investigate the cellular mechanisms underlying AD, and the choice of mouse model for research should be guided by the specific questions to be answered. We provide here some considerations for selecting a mouse model of AD best suited to particular lines of investigation.

Key words: Alzheimer's disease, Mouse model, Transgenic, Neuropathology, Behavior, APP, Presenilin, Tau, Amyloid plaques, Neurofibrillary tangles, Cognitive deficit

1. Introduction

Alzheimer's disease (AD) is characterized by progressive loss of memory and other cognitive functions (1, 2). Neuropathological hallmarks of the disease are amyloid plaques and neurofibrillary tangles, which are accompanied by synaptic and neuronal loss as well as astrocytic gliosis. Although it has been over a century since the first description of AD, progress in understanding the cellular basis of the disease has only been made in the last 25 years, spurred on by the discovery that the principal constituents of the extracellular, proteinaceous amyloid plaques are amyloid beta (Aβ) peptides (3, 4). Aβ is a peptide sequence within the amyloid precursor protein (APP) that is released by sequential cleavage of APP by a beta-site cleaving enzyme (BACE) and a gamma-site

Erik D. Roberson (ed.), *Alzheimer's Disease and Frontotemporal Dementia*, Methods in Molecular Biology, vol. 670,
DOI 10.1007/978-1-60761-744-0_13,

cleaving enzyme (gamma-secretase). This finding led to the hypothesis that altered processing of APP may be a causal factor in the disease ((5), reviewed in (6)). This hypothesis was supported by the identification of mutations in the APP *gene* that increase Aβ production and lead to early-onset autosomal dominant familial AD, FAD (6–8). Mutations in presenilin 1 and 2 genes, which encode components of the gamma-secretase complex that cleaves APP, also increase Aβ production and lead to early-onset familial AD (reviewed in (9)). Notably, while familial forms of AD have a much earlier onset than sporadic AD, the neuropathology associated with both forms of AD is identical.

A number of transgenic mice have been created over the last two decades that overexpress APP and/or presenilin containing one or more mutations linked to familial AD. These mice recapitulate many key aspects of AD, including amyloid neuropathology, cerebral amyloid angiopathy, synaptic loss, dystrophic neurites, and reactive gliosis, as well as impairments in synaptic plasticity and learning and memory. Such mouse models exhibit these characteristics to varying extents, and are widely used to investigate the roles of APP, Aβ, and amyloid pathology in the pathogenesis of AD.

Although APP transgenic mice exhibit many of the key features of AD, neurofibrillary tangles (NFTs) are notably absent. NFTs are primarily made up of hyperphosphorylated tau, a microtubule-binding protein that is highly expressed in neurons. Although NFT counts correlate with the severity of clinical dementia, no mutations in tau have been linked to AD (10, 11). However mutations in tau do result in inclusions and tangles in an inherited form of frontal temporal dementia with Parkinsonism (FTDP-17), a familial dementia related to AD, as well as other clinical syndromes (12, 13). These findings demonstrate that tau dysfunction can lead to neurodegeneration and dementia. In an effort to recapitulate both neuropathological hallmarks of AD, several laboratories have created transgenic mice expressing various combinations of mutant APP, presenilin, and tau.

A number of genes have also been identified that modulate risk for AD. Notably, the functions of many of these genes impact APP processing, Aβ fibrillization, deposition, and/or clearance, as well as tau phosphorylation, further supporting the importance of Aβ and tau in AD pathogenesis (see Fig. 1, and (14)). Knockout, knock-in, and transgenic mice with altered expression of these genes have been useful for investigating their roles in AD pathogenesis, particularly when crossed with APP and/or tau transgenic mice. However, because of space limitations, this chapter is limited to discussion of APP and tau transgenic mice.

The multitude of transgenic mice designed for AD research can be overwhelming at first glance. However, the vast array of AD pathologies and neuronal alterations manifest in each mouse model to different degrees, and the choice of mouse model for

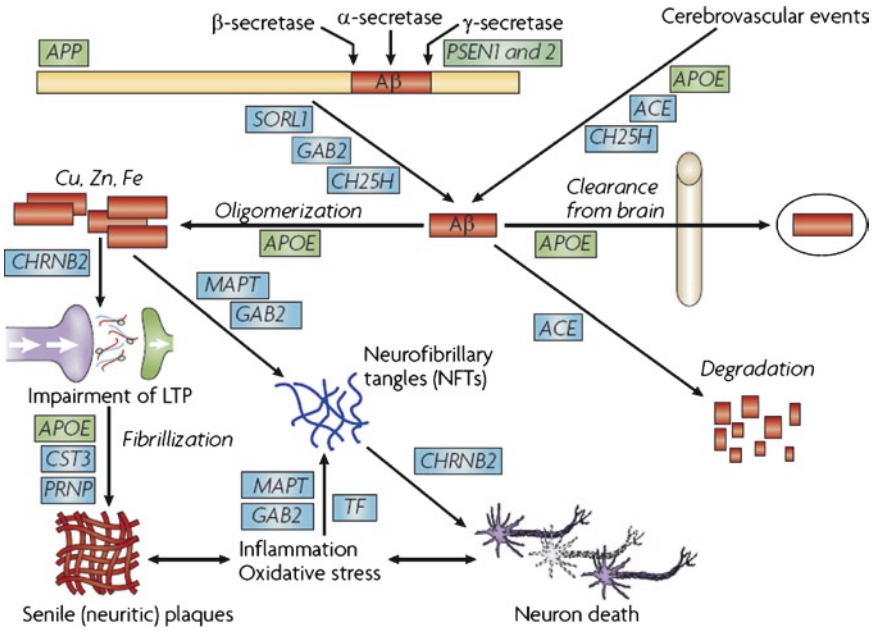

Fig. 1. Schematic depicting possible pathogenic roles for genes associated with Alzheimer's disease (AD). Many candidates for early-onset familial AD genes have been identified in the last 30 years that appear to contribute to or exacerbate AD pathogenesis. Notably, many of the proteins encoded by these genes can modulate Aβ generation, oligomerization, degradation, or clearance, while others can influence tau function and development of neurofibrillary pathology. The identification of such genes supports the pathogenic roles of Aβ and tau in AD pathophysiology. For a description of these genes and their functions, please see (14). (Reprinted by permission from Macmillan Publishers Ltd: Nature Reviews Neuroscience (14)).

research is guided by the questions to be addressed. In this chapter we describe the key features of several of these transgenic mouse models that make them particularly suitable for studying specific aspects of AD pathophysiology.

2. Major Mouse Models of AD

It is important to bear in mind that none of the current genetically-engineered mouse models of AD fully recapitulate the comprehensive neuropathology of the human AD brain. However, although incomplete in this aspect, individual AD mouse models offer great advantage toward the understanding of particular proteins, pathologies, and lesions in the pathogenesis of AD (15). Moreover, cross-breeding of these mice enables the study of pathogenic interactions between different proteins and pathways and their contributions to the disease.

With that in mind, there are a number of important considerations to take into account when selecting a transgenic mouse model of AD. First, the particular aspect of AD to be studied must be chosen. Mouse models of the amyloid hypothesis

(primarily APP and APP/presenilin mice) produce high levels of neurotoxic Aβ, develop amyloid pathology, and exhibit many of the key features of AD as discussed below. However, neurofibrillary tangles are not obvious in these mice. To investigate the role of tau dysfunction and tangles in AD, a mouse model that overexpresses tau, or a mutant form of tau with greater propensity for tangle formation, is often chosen. A few mouse models also exist that overexpress combinations of mutant APP, presenilin, and tau and exhibit both amyloid and tau pathology. Such mice are useful for investigating pathogenic interactions between Aβ and tau. Neuronal loss, another key aspect of AD, is not robustly evident in any mouse model, but is observed to some extent in a few mouse models, which is discussed below.

Second, the scope of research investigation must be considered. Will the focus of the investigation be limited to cellular/biochemical aspects of the disease, cognitive/behavioral impairments associated with the disease, or a combination? Some mouse models are more amenable to behavioral assessment than others, for various reasons including transgene expression patterns, age of onset of pathology, and background strain.

2.1. Evaluating APP and APP/PS1 Transgenic Mice

Sporadic AD, which constitutes >95% of all AD cases, is not associated with any known mutations in APP or the enzymes that cleave it to release Aβ. However, the neuropathology observed in sporadic AD is essentially identical to that observed in familial AD caused by mutations in APP that increase Aβ production or that increase the relative proportion of the particularly neurotoxic 42 amino acid form of Aβ, which has a higher propensity to aggregate than the 40 amino acid form (reviewed in (1)). Seventeen amino acids differ between human and mouse APP, three of which reside within the Aβ sequence (amino acids 3, 10, and 13 of the Aβ sequence). Murine Aβ does not accumulate to high levels nor does it form deposits, even when overexpressed (16).

Transgenic mice overexpressing wild-type human APP exhibit subtle increases in Aβ and little amyloid pathology. However, transgenic mice overexpressing human APP carrying at least one familial mutation exhibit robust age-dependent increases in Aβ levels and amyloid pathology similar to that observed in human AD brains, as shown in Fig. 2 (17, 18). Moreover, they exhibit both parenchymal and vascular amyloid pathology, plaque-associated dystrophic neurites and microglial activation, synaptic impairments, and deficits in synaptic plasticity and learning and memory. Therefore such mice have been widely used for AD research and have advanced the current understanding of the role of Aβ in AD. Space is insufficient to discuss all models that have been developed, but several models that are widely used are highlighted below. The primary reference describing each mouse line is provided.

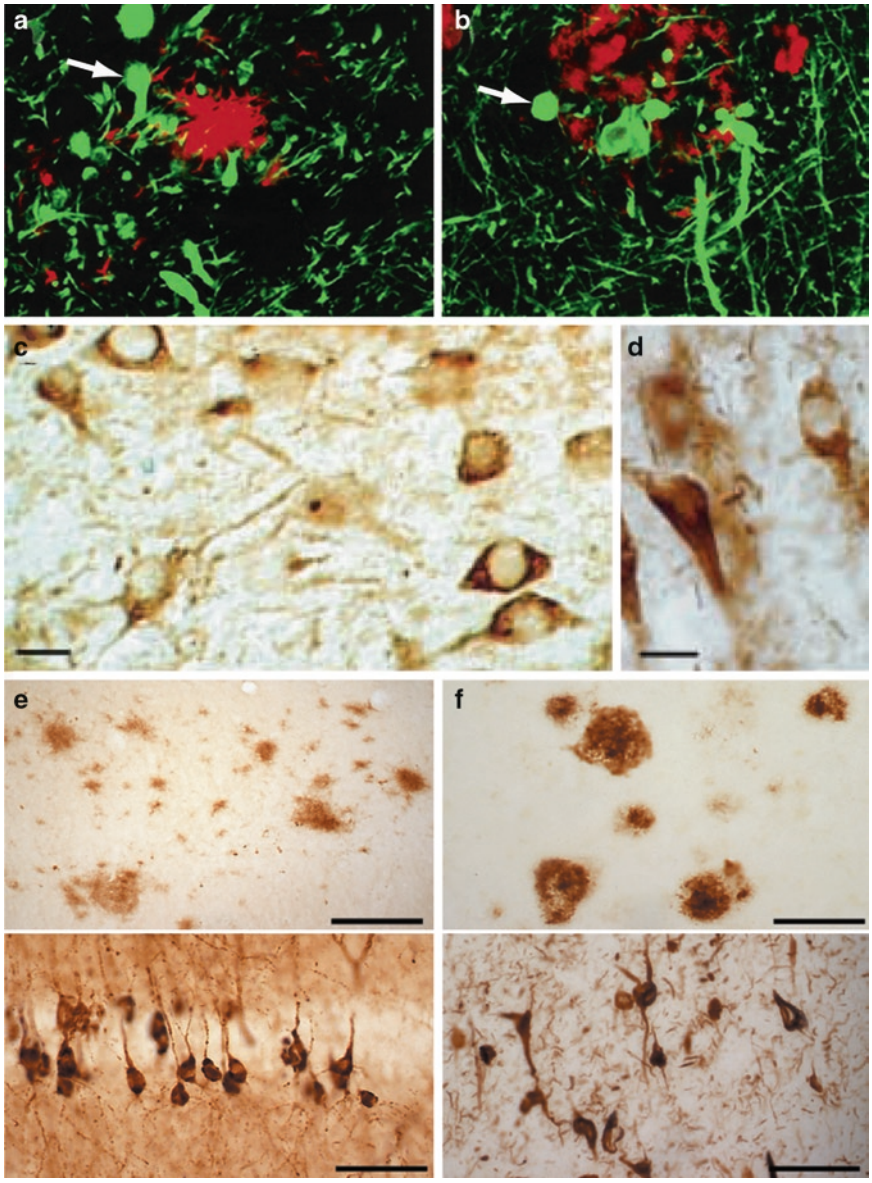

Fig. 2. Pathological hallmarks of AD in transgenic mouse models and in AD brains. (**a**, **b**), Amyloid plaques (*red*) and dystrophic neurites (*green*, see *arrows*) are similar in an APP_{Ind} transgenic mouse brain (**a**) and in an AD brain (**b**). Sections were double-labeled with antibodies against Aβ and phosphorylated neurofilaments. (Reprinted from (23) with permission from *The Journal of Neuroscience*). (**c**, **d**), pre-tangle pathology is observed both in Htau transgenic mice (**c**) as well as in AD brain (**d**). Tau pathology and NFTs develop progressively in Htau mice. Sections were stained with antibody CP13, which recognizes tau phosphorylated at serine 202, and is commonly used to detect tau pathology in early and advanced stages of NFT accumulation. Scale bars represent 5 μm. (Reproduced from (47) with permission from Blackwell Publishing Ltd). (**e**, **f**) Both amyloid plaques (*top panels*) and NFTs (*lower panels*) develop in 3XTG mouse brains (**e**) and are similar to those observed in AD brains (**f**). Amyloid plaques were visualized with antibodies against Aβ; tangles were visualized with the hyperphosphorylated tau-specific antibody AT-8 (**e**, *lower panel*) or with a conformation-specific antibody against paired-helical filaments (PHFs; F, *lower panel*). Scale bars represent 125 μm (*upper panels*) or 62.5 μm (*lower panels*). (Reprinted from (62) with permission from Elsevier).

To facilitate the review of APP transgenic mice and to clarify the differences between the various transgenes used, it is useful to have a few points in mind:

- There is a single human APP gene from which three major isoforms are produced by alternative splicing. These isoforms contain 770, 751, or 695 amino acids; the two longer forms contain a protease inhibitor domain homologous to the Kunitz type of serine protease inhibitors. The brain produces predominantly the 695 form; APP mRNA ratios are 1:10:20 for 770:751:695 (reviewed in (19)).
- The mutations in the APP gene that have been linked to autosomal dominant familial AD have been named by the geographic area in which they were identified. The most common APP mutations used for creating AD mouse models include the following (numbering corresponds to the longest APP isoform, APP770):
  - Swedish double mutation (K670N and M671L), which renders APP a more favorable substrate for BACE cleavage and increases Aβ production.
  - London (V717I) or Indiana (V717F) mutations, both of which increase gamma-secretase processing of the 42 amino acid form of Aβ relative to the 40 amino acid form.
  - Arctic mutation (E693G), which affects amino acid 22 within the Aβ peptide, decreases alpha-secretase processing of APP (the non-amyloidogenic processing pathway) and also increases the aggregation propensity of Aβ.
  - Dutch mutation (E693Q), which affects amino acid 22 within the Aβ peptide, increases production of Aβ40 and increases the Aβ40/Aβ42 ratio.
- Promoters commonly used to drive transgene expression include platelet-derived growth factor (PDGF) and Thy-1 or Thy-1.2, all of which are neuron-specific, and the hamster prion (PrP) promoter that is preferentially expressed in neurons but is also expressed in many cell and tissue types.

1. *PDAPP*: The PDAPP mouse line was the first transgenic mouse model of AD to exhibit significant Aβ accumulation and amyloid deposition (20). The transgene is a cDNA minigene bearing the human APP (APP) sequence with the Indiana mutation. The minigene construct allows alternative splicing for expression of the 695, 751, and 770 isoforms of APP, driven by the PDGF promoter. APP expression is roughly four- to sixfold increased over endogenous mouse APP. Amyloid deposition begins between 6–9 months, and both parenchymal and vascular deposition is observed. Parenchymal plaques are associated with dystrophic neurites and microgliosis and astrocytosis. Synaptic loss and impairments

in synaptic plasticity are observed in young mice before plaque deposition, implicating a role of soluble Aβ in these deficits. Cytoskeletal abnormalities including accumulation of hyperphosphorylated tau have been documented, although neurofibrillary tangles are absent.

2. *Tg2576*: This mouse line expresses APP695 carrying the Swedish double mutation, under the control of the hamster PrP promoter (21). Tg2576 mice exhibit amyloid deposition beginning around 9 months, which is also accompanied by neuritic dystrophy and gliosis. Hyperphosphorylated tau is present, but no neurofibrillary tangles develop. Progressive behavioral deficits in a variety of behavioral tasks have been described; such deficits can be observed as early as 6 months – before amyloid deposition occurs, again implicating soluble Aβ species in neuronal dysfunction. However, cognitive deficits are not robust before 12 months. In the search for the specific assembly state of soluble Aβ that most closely correlates with memory impairments, the first culprit, named Aβ*56 because it ran on an SDS-PAGE gel with an apparent molecular weight of 56 kDa, was identified using the Tg2576 line (22). Tg2576 mice are one of the most widely used APP transgenic mouse lines, and have been well-characterized in many parameters, including alterations in neuronal structure, neuronal transmission/plasticity deficits, cognitive/behavioral deficits, and cerebrovascular deficits.
3. *J20*: The J20 line was developed based on the PDAPP mouse (*see* above). The Swedish double mutation was introduced into the same minigene construct, creating a mouse that expresses APP with both Swedish and Indiana mutations (23). Aβ accumulation is more aggressive in these mice than in PDAPP or Tg2576 mice, resulting in an earlier age of onset of neuronal and behavioral deficits. For this reason, the use of J20 mice for AD research has increased in recent years. These mice produce high levels of Aβ, with plaque deposition beginning around 6 months. Neuritic dystrophy and gliosis are also observed. J20 mice exhibit synaptic loss and impairments in synaptic plasticity as early as 2–4 months. Progressive cognitive and behavioral impairments beginning around 3–4 months have been documented, and cerebrovascular abnormalities have also been reported. Notably, chronic EEG recordings in J20 mice revealed global epileptiform activity associated with compensatory inhibition in the hippocampus, which correlated with learning and memory deficits in these mice (24). Although seizures have been documented in a number of APP transgenic mice (as well as in AD patients), this study highlighted the relevance of epileptiform activity to AD-related cognitive impairments (25). Similar epileptiform activity has since been described in both Tg2576 and PSAPP mice.

4. *APP23*: The APP23 mouse line expresses APP751 with the Swedish mutation under control of the Thy-1 promoter (26). These mice exhibit plaque deposition beginning around 6 months, also associated with neuritic dystrophy and gliosis. Hyperphosphorylated tau, but not tangles, is present. APP23 mice exhibit predominant and severe vascular amyloid deposition, called cerebral amyloid angiopathy. Neuronal loss correlating with plaque load in 14–18-month-old mice has been documented in area CA1 of the hippocampus (up to 25% cell loss in mice with high levels of plaque load), and more subtle cell loss in the neocortex has been recently reported (27). Behavioral and cognitive deficits are first observed at 3 months and progress with aging.
5. *TgCRND8*: This mouse line expresses APP695 with Swedish and Indiana mutations under control of the PrP promoter, and is a very aggressive model of amyloidosis (28). Cerebral amyloid deposition is evident by 3 months, starting in the hippocampus and neocortex as in other mouse models, but also spreading to the cerebellum and brainstem by 8 months. Gliosis and neuritic dystrophy is marked at 5 months. Vascular deposition has been documented at around 6 months. Cognitive/behavioral deficits are evident by 3 months and robust at 5–6 months. TgCRND8 mice exhibit marked premature mortality, with only approximately 50% of mice reaching 9–10 months. Increased mortality has also been reported for many APP transgenic lines, although to a more subtle extent (10–20%). Premature mortality in TgCRND8 mice has been linked to increased susceptibility to spontaneous seizures.
6. *mThy1-hAPP751*: These transgenic mice express APP751 with Swedish and London mutations driven by the mouse Thy-1 promoter (29). Several transgenic lines were created, and Line 41 exhibits the highest expression of the transgene. This line is also sometimes referred to as TASD-41. These mice produce high levels of Aβ42 and develop mature plaques in the frontal cortex as early as 3–4 months, and by 5–7 months exhibit plaques in other brain regions including hippocampus, thalamus, and olfactory regions. Development of dystrophic neurites, gliosis, and loss of presynaptic terminals follows a similar time course. Amyloid deposition in the vasculature, or cerebral amyloid angiopathy, is evident at 7 months and progresses with age. mThy1-hAPP751 transgenic mice exhibit robust behavioral deficits by 6 months.
7. *APPDutch*: This mouse line expresses APP751 with the Dutch mutation driven by the Thy-1 promoter, and is a mouse model of hereditary cerebral amyloid angiopathy (30). This disease is

characterized by recurrent cerebral hemorrhages due to extensive vascular amyloid deposition, with onset usually occurring in the fifth decade of life in patients. Unlike AD, few parenchymal plaques accumulate in the disease and in the mouse model, although diffuse parenchymal Aβ is present. The human disease and the mouse model thus offer an opportunity to investigate the cerebral amyloid angiopathy that accompanies AD. In APPDutch mice, vascular amyloid deposition begins around 22 months, and is accompanied by perivascular microgliosis and astrocyte activation, as well as a severe loss of smooth muscle cells and increased hemorrhage incidence. The Dutch mutation appears to increase the production of vasculotropic Aβ40, and the ratio of Aβ40/Aβ42 is greatly enhanced in APPDutch mice. Notably, cross-breeding of these mice to mice expressing a mutant form of presenilin associated with AD increases the production of Aβ42 and redistributes the amyloid pathology to the parenchyma. Thus, the combination of APPDutch mice and APPDutch mice with presenilin mutations allows the study of the mechanisms that modulate Aβ production, distribution, deposition, and clearance.

8. *ARC6 and ARC48*: These lines were created by introducing the Arctic mutation into the minigene used to create the J20 line (*see* above), resulting in a transgenic mouse expressing APP containing the Swedish, Indiana, and Arctic mutations driven by the PDGF promoter (31). The ARC lines produce Aβ peptides with the Artic E22G mutation in the middle of the peptide, which causes Aβ-Arc peptides to form protofibrils and fibrils at higher rates and in larger quantities than wild-type Aβ. ARC6 expresses lower levels of APP than J20, and ARC48 expresses higher levels of APP than J20. However, because of the fibrillogenic nature of Aβ-Arc peptides, ARC mice display aggressive amyloidosis beginning at 3 months in ARC6 and 2 months in ARC48, compared with 6 months in J20. Notably, ARC6 mice exhibit lower levels of soluble oligomeric Aβ peptides, perhaps due to the increased propensity of Aβ-Arc peptides to fibrillize. ARC6 mice also do not display behavioral deficits even in the presence of aggressive amyloidosis, supporting the hypothesis that oligomeric Aβ is the primary toxic species leading to cognitive deficits (32). ARC48 mice, which have high levels of both oligomeric Aβ and plaque deposition, do exhibit cognitive deficits. In another line of APP transgenic mice expressing APP with both Swedish and Arctic mutations (tg-APP_{ArcSwe}), increased accumulation of intraneuronal Aβ aggregates were observed (33). Tg-APP_{ArcSwe} also exhibit increased levels of protofibrils relative to non-Arctic mutation containing APP mice, and have behavioral deficits by 4 months.

9. *PSAPP*: There are several versions of PSAPP mice; the name generally refers to mice created by crossing APP transgenic mice (often Tg2576) with mice expressing presenilin containing one of several FAD mutations. Presenilin mutations increase the production of aggregation-prone Aβ42, increasing the Aβ42/Aβ40 ratio and facilitating amyloid deposition. One of the widely used versions of PSAPP mice is the Tg2576 X $PSEN1_{M146L}$ line, in which expression of presenilin carrying the M146L mutation is driven by the PDGF-β promoter (34, 35). These PSAPP mice develop amyloid pathology around 6 months, accompanied by reactive gliosis. Some cognitive deficits are observed at 3–5 months, while others are robustly measured at 15–17 months. Another line of mice expressing both human APPSwe and mutant presenilin is the APdE9 mouse, which expresses APPSwe as well as the exon-9-deleted variant of presenilin, $PS1_{dE9}$ (36). APdE9 mice were created by co-injection of APPSwe and $PS1_{dE9}$ vectors controlled by independent mouse prion promoter elements. The two transgenes co-integrated and co-segregate as a single locus, thereby facilitating the breeding of doubly transgenic mice.
10. *5XFAD*: These mice are APP/PSEN1 double transgenic mice that coexpress a total of five FAD mutations (37). APP695 carries three mutations: Swedish, London, and Florida (I716V); PSEN1 carries two mutations: M146L and L286V. Pronuclear co-injection of the transgenes, each controlled by independent mouse Thy-1 promoter elements, resulted in stable genomic co-integration and germline transmission of both genes. These mice generate Aβ42 almost exclusively, at very high levels. Intraneuronal Aβ accumulates around 1.5 months and amyloid deposition begins around 2 months, accompanied by reactive gliosis as well as hyperphosphorylated tau. Neurofibrillary tangles are absent. Progressive loss of synaptic markers begins around 4 months. 5XFAD mice also exhibit neuronal loss, which is most evident in deeper cortical layers (layer 5) as well as in the subiculum. The pattern of neuronal loss mirrors the distribution of intraneuronal Aβ accumulation and amyloid deposition. Cognitive deficits are observed at 4–6 months.

The APP models described above have been widely used by the AD research community to investigate how Aβ and/or amyloid pathology contribute to particular aspects of AD. Table 1 provides a comparison of the AD-related features exhibited by these mouse models.

2.2. Evaluating Tau and APP/Tau Transgenic Mice

Neurofibrillary tangles (NFTs), the other major pathological hallmark of AD, are composed mainly of hyperphosphorylated aggregates of tau. Tau is a microtubule-associated protein with numerous

Table 1
Summary of selected mouse models used in Alzheimer's disease research

Transgenic mouse	Transgene (mutation)[a]	Promoter	Strains	Amyloid plaques	NFTs	Neuron loss	Cognitive deficits	Primary references
PDAPP	APP695, 751, 770 (APPInd)	PDGF-β	C57Bl/6 J, DBA/2, Swiss-Webster	6–9 months	No	No	Yes	(20)
Tg2576	APP695 (APPSwe)	Hamster PrP	C57Bl/6SJL, C57Bl/6	9 months	No	No	Yes	(21)
APP23	APP751 (APPSwe)	Mouse Thy-1	C57Bl/6, DBA/2	6 months (severe CAA also present)	No	14 months	Yes	(26)
J20[b]	APP695, 751, 770 (APPSwe, Ind)	PDGF-β	C57Bl/6	6 months	No	No	Yes	(23)
TgCRND8	APP695 (APPSwe, Ind)	Hamster PrP	C3H, C57Bl/6	3 months	No	No	Yes	(28)
mThy1-hAPP751	APP695 (APPSwe, Lon)	Mouse Thy-1	C57Bl/6, DBA/2	3–4 months	No	No	Yes	(29)
APPDutch	APP751 (APPDutch)	Mouse Thy-1	C57Bl/6 J	22 months (CAA only)	No	Not reported	Not reported	(30)
ARC6, ARC48	APP695, 751, 770 (APPSwe, Ind, Arc)	PDGF-β	C57Bl/6	3 months (6) 2 months (48)	No (6) No (48)	No (6) No (48)	No (6) Yes (48)	(31)
PSAPP	Tg2576 X PSEN1-M146L	Hamster PrP PDGF-β	C57Bl/6SJL, C57Bl/6 B6D2F1, Swiss-Webster	6 months	No	No	Yes	(35)
5XFAD	APP695 (Swe, Lon, Flo) PSEN1-M146L, L286V	Mouse Thy-1 Mouse Thy-1	C57Bl/6SJL	2 months	No	9 months	Yes	(37)

(continued)

Table 1 (continued)

Transgenic mouse	Transgene (mutation)[a]	Promoter	Strains	Amyloid plaques	NFTs	Neuron loss	Cognitive deficits	Primary references
JNPL3	4R0N MAPT (Tau-P301L)	Mouse PrP	C57Bl/6 J, DBA/2, Swiss-Webster	No	9 months	6.5 months	No	(45)
rTg4510	4R0N MAPT (Tau-P301L)	Mouse PrP	129 S6, FVB/N	No	4 months (pre-tangles at 2.5 months)	5.5 months	Yes	(46)
Htau[c]	Human PAC, H1 haplotype	Human tau	Swiss-Webster, 129, SVJ, C57Bl/6	No	15 months (pre-tangles at 9 months)	>15 months	Not reported	(47)
TAPP	Tg2576 X JNPL3	Hamster PrP Mouse PrP	C57Bl/6SJL, C57Bl/6, DBA/2, Swiss-Webster	9 months	9 months	6.5 months	Yes	(49)
3XTG[d]	APP695 (Swe) 4R0N MsAPT (P301L) PSEN1-M146V (Knock-in)	Mouse Thy-1.2 Mouse Thy-1.2	129/C57Bl/6	6 months	12 months	No	Yes	(50)

[a]APP mutations: Ind (Indiana, V717F), Swe (Swedish, K670N/M671L), Lon (London, V717I), Dutch (E693Q), Arc (Arctic, E693G), Flo (Florida, I716V)
[b]J20 mice were originally created on a C57BL/6, DBA/2 background
[c]P1 artificial chromosome (PAC) contains entire tau gene plus upstream regulatory elements. Htau mice express human tau on a mouse tau knockout background
[d]APPSwe and Tau-P301L transgenes are expressed on a mouse PSEN1-M146V knock-in (KI) background

functions, including stabilizing microtubules and regulating neurite outgrowth as well as axonal transport. NFTs are thought to play an important role in the memory deficits in AD because the regional distribution and progression of NFTs closely parallels the brain regions involved in memory and the progressive cognitive loss characteristic of AD (38). Moreover, NFT counts correlate with the severity of clinical dementia, whereas amyloid plaque load does not (reviewed in (2, 11)). However, no mutations in the tau gene have been linked to AD, although tau mutations have been found in FTDP-17 patients as described above (FTDP-17, reviewed in (12, 13)). This and other findings demonstrate that tau dysfunction can lead to neurodegeneration and dementia (reviewed in (10)).

The tau gene does however contain several polymorphisms that lead to unique haplotypes. One of these haplotypes, H1c, is associated with increased tau expression as well as with AD (39–41). The finding that increased tau expression is associated with AD is particularly interesting with regards to recent findings that reducing tau expression in an APP transgenic mouse model of AD protects against excitotoxicity, alterations in synaptic plasticity-related protein expression, and memory deficits (42). These results suggest a serial relationship between APP/Aβ, tau dysfunction, and AD-related deficits. However, the interactions between APP/Aβ and tau may be more complex and may even be regulated by a common upstream factor (43).

Although mutations in APP and/or presenilins cause classic AD characterized by both amyloid plaques and neurofibrillary tangles, it is unclear why mice expressing mutant APP and/or presenilins fail to develop detectable tangles. It is therefore critical to understand the extent to which Aβ and tau pathologies interact in the development of AD. A number of tau transgenic mice have been created that exhibit tau aggregates and tangles (see Table 1 and Fig. 2); these mice have been used to study the role of tau in neurodegeneration (44). In addition, several experimental approaches have been taken to cross APP transgenic mice with tau transgenic mice to reveal pathogenic synergistic interactions between Aβ and tau. Several widely used models are described below, and a more complete listing can be found elsewhere (10). As in the previous section, the primary reference describing each mouse line is provided.

A few aspects of tau genetics are worth keeping in mind as we discuss tau transgenic models:

- There is a single MAPT (tau) gene, from which six isoforms are produced by alternative splicing (10). The isoforms contain either three or four repeats of a microtubule-binding domain, depending on whether exon 10 is included (3R or 4R). In addition, isoforms can contain two, one, or no amino-terminal inserts depending on the presence of exons

2 and 3 (2 N, 1 N, or 0 N). The adult mouse brain contains only 4R tau isoforms.

- The P301L mutation is one of the most common mutations associated with FTDP-17. This mutation decreases the microtubule-binding properties of tau, leading to microtubule disorganization. The P301L mutation has also been shown to promote tau aggregation.

1. *JNPL3*: The JNPL3 mouse expresses 4R0N MAPT with the P301L mutation, driven by the mouse prion promoter (45). Heterozygous JNPL3 mice express transgenic tau at roughly equivalent levels to endogenous tau; homozygous JNPL3 mice express mutant tau at twofold that of endogenous mouse tau. Heterozygous mice develop progressive motor and behavioral abnormalities together with neurofibrillary pathology and neuronal loss in the spinal cord as early as 6.5 months. By 10 months, 90% of mice have severe motor impairment. Pre-tangles are observed throughout the brain, and NFTs are evident in spinal cord, brainstem, and cerebellum. Extracellular tangles are consistent with the 50% loss of motor neurons in the spinal cord that are lost. This was the first transgenic mouse that demonstrated that tau alone can cause neuronal damage and cell loss.
2. *rTg4510*: These mice are inducible MAPT transgenic mice expressing tau with the P301L mutation (46). Transgene expression can be suppressed by doxycycline (TET-off system, meaning that tau is expressed when the mice are fed regular chow and turned off when they are on doxycycline chow). rTg4510 mice express mutant tau at 13 times the levels of endogenous mouse tau, form pre-tangles as early as 2.5 months, and tangle-like inclusions by 4–5 months. Neuronal loss is also evident coinciding with tangle formation, resulting in overall brain weight loss by 5.5 months, including nearly 60% loss of CA1 neurons. By 10 months, gross atrophy of the forebrain is evident. Memory deficits are observed in very young mice as early as 1.5–2.5 months and progress with age. Notably, suppression of mutant tau expression improves cognitive performance and reduces neuronal loss even though NFT pathology continues to progress. These results suggest a dissociation between memory loss and NFT pathology as well as a dissociation between NFTs and neuronal loss.
3. *Htau*: Htau mice express human genomic MAPT on a mouse MAPT knock-out background (47). The transgene was originally derived from a human P1 artificial chromosome (PAC) driven by the human tau promoter, from which all six human tau isoforms are produced (48). These mice exhibit hyperphosphorylated tau in neuronal cell bodies by 6 months and

NFTs as well as neuronal loss by 15 months. Both hyperphosphorylated tau and NFTs were found in neocortical and hippocampal regions, with little or no presence in striatum, cerebellum, or spinal cord, similar to human AD. These mice do not display motor abnormalities as observed in the JNPL3 mice. Notably, mice expressing human tau in the presence of mouse tau do not develop NFT pathology, whereas these Htau mice (on the mouse tau knock-out background) do, suggesting that mouse tau interferes with the ability of human tau to develop pathology.

4. *TAPP*: These mice are a cross of Tg2576 (APP) transgenic mice and JNPL3 mice, creating doubly-transgenic mice that exhibit both amyloid and neurofibrillary pathology (49). Aβ production and amyloid pathology are similar in Tg2576 single transgenics and TAPP mice; a few plaques are observed at 6 months but are numerous by 9 months. Similar to singly transgenic JNPL3 mice, a few tangles are present in spinal cord and brainstem at 3 months but are consistently present by 9–10 months. However, relative to JNPL3 mice, NFT pathology in TAPP mice is markedly enhanced in forebrain areas. This finding suggests that pathogenic synergistic interactions exist between Aβ and tau pathologies, and that similar pathogenic interactions may exist also in human AD.
5. *3XTG*: A triple transgenic model was created by micro-injecting APP_{Swe} and tau_{P301L} transgenes into single-cell embryos from $PSEN_{M146V}$ knock-in mice (50). The two transgenes co-integrated and co-segregate as a single locus in $PSEN_{M147L}$ knock-in mice, creating a triply transgenic mouse that breeds essentially as a single transgenic mouse. Expression of the APP and tau transgenes is controlled by the Thy1.2 promoter. Intraneuronal Aβ is evident in the neocortex around 3–4 months, and in hippocampal regions (CA1) by 6 months. Extracellular Aβ deposits from around 6 months, beginning in frontal cortex and spreading to other cortical and hippocampal areas with age. Notably, although the APP and tau transgenes are overexpressed to similar levels in 3XTG mice, tau pathology is not evident until 12 months, where it is first observed in the hippocampus and spreads to cortical regions with age. There is little evidence of neuronal loss in these mice. Synaptic deficits and LTP impairment initiate before plaque and tangle pathology. Cognitive deficits are also observed prior to plaque and tangle pathology, and appear to correlate with the progression of intraneuronal Aβ accumulation (51).

Tau transgenic mouse models such as those described here (summarized in Table 1) have enabled an understanding of the role of tau dysfunction and pathology in neurodegenerative

diseases, including FTD as well as AD. Tau transgenic mice do not exhibit Aβ or amyloid pathology to any extent, suggesting that amyloid pathology is not downstream of tau pathology. Whereas APP transgenic mice with high levels of Aβ do exhibit some degree of hyperphosphorylated tau, true tau pathology does not develop. The creation of doubly or triply transgenic mice expressing both APP and tau have highlighted the pathogenic synergistic interactions between Aβ and tau, and suggest that tau dysfunction is downstream of Aβ. However, it is also possible that both Aβ and tau dysfunction are downstream of a common factor, and develop with different time courses (43).

3. Considerations in Selecting a Mouse Model of AD

There are numerous avenues of investigation into the mechanisms underlying AD. The particular questions to be addressed and the methodology of intended use should guide the selection of the AD mouse model to be used. We have reviewed above several lines of transgenic mice expressing various combinations of APP, presenilin, and tau, which provide a general description of the utility of these mice for various aspects of research. We list here a few additional considerations to keep in mind when selecting a mouse model of AD.

1. It is important to remember that none of the currently available transgenic mouse models of AD fully recapitulate all aspects of AD, although several lines are able to recreate one or more of the major pathological hallmarks of the disease. However, this lack of full recapitulation should not deter researchers from utilizing mouse models; these models are of great utility in understanding how particular proteins affect neuronal function and lead to neuronal impairments and pathology, regardless of their ability to reproduce every aspect of the pathology and impairment associated with AD.
2. Different lines of transgenic mice exhibit varying ages of onset of impairments. This is an important consideration for both scientific as well as practical reasons. An earlier age of onset increases the efficiency (and decreases costs) of breeding and aging mice for research. However, extremely aggressive disease progression and very early age of onset may decrease the range of time and types of experiments that can be performed. While this may be suitable or even ideal for some biochemical investigations, it may make it difficult to run some types of behavioral experiments that require longer training and testing periods. Some lines of investigation aimed at understanding these processes as they relate to aging may benefit

from a model with a later age of onset or slower disease progression in order to evaluate possible synergistic interactions with the aging process.

3. The background strains on which transgenic mice have been created are important to consider, particularly for behavioral analyses. Inbred mice often show less behavioral variability than outbred mice, sometimes allowing reduced sample sizes to show differences between transgenic and nontransgenic mice. Outbred mice have been used in many studies that have advanced our understanding of AD, but it is important to keep in mind that larger sample sizes may be required for some behavioral analyses.

   In addition, different strains of mice are phenotypically different, even in the absence of any transgene expression. Inbred strains are extremely stable and spontaneous mutations are rare, but many have occurred within various inbred strains and contribute to the phenotype of those mice. An understanding of such mutations and their resulting phenotypes in different inbred strains is important to have when planning experiments (particularly behavioral) for particular strains of mice (52). Although many of the mutations will not substantially affect the majority of experiments, some mutations should be considered. For example, a mutation leading to age-related hearing loss present in a number of inbred strains (including the commonly studied C57BL/6 strain) will not affect studies to be performed in mice less than approximately 15 months, but would affect older mice to be tested in behavioral paradigms requiring sensitive hearing.

   Lastly, different inbred strains have different behavioral profiles, and some strains are "better learners" than others or are more active than others, etc. (53, 54). Particular strains of mice are often used for particular types of research as certain characteristics of mice make them more or less suitable for research. Reference materials are available that discuss such characteristics, as well as practical considerations for choosing, breeding, and testing mice in behavioral assays (55, 56). Understanding the inherent differences in behavioral profiles of different mouse strains will aid in the planning of experiments and interpretation of results.

4. For More Information

Particularly useful reviews providing detailed descriptions of transgenic mouse models of AD can be found in the References section of this chapter (9, 17, 18, 44, 57–61). In addition, a large,

although incomplete, listing of widely used AD mouse models is maintained by the Alzheimer Research Forum (AlzForum) and can be found at the following link: http://www.alzforum.org/res/com/tra/default.asp. For more information regarding the effects of background genetic strain on various phenotypes and behaviors, see (52, 54–56).

References

1. Walsh, D. M., and Selkoe, D. J. (2004) Deciphering the molecular basis of memory failure in Alzheimer's disease. *Neuron* **44**, 181–193.
2. Chin, J., Roberson, E. D., and Mucke, L. (2008) in "Learning and Memory: A Comprehensive Reference" (Byrne, J. H., ed.), pp. 245–293, Elsevier, London.
3. Glenner, G. G., and Wong, C. W. (1984) Alzheimer's disease: Initial report of the purification and characterization of a novel cerebrovascular amyloid protein. *Biochem. Biophys. Res. Commun.* **120**, 885–890.
4. Masters, C. L., Simms, G., Weinman, N. A., Multhaup, G., McDonald, B. L., and Beyreuther, K. (1985) Amyloid plaque core protein in Alzheimer's disease and Down's syndrome. *Proc. Natl. Acad. Sci. U S A* **82**, 4245–4249.
5. Hardy, J. A., and Higgins, G. A. (1992) Alzheimer's disease: The amyloid cascade hypothesis. *Science* **256**, 184–185.
6. Tanzi, R., and Bertram, L. (2005) Twenty years of the Alzheimer's disease amyloid hypothesis: A genetic perspective. *Cell* **120**, 545–555.
7. Chartier-Harlin, M. -C., Crawford, F., Houlden, H., Warren, A., Hughes, D., Fidani, L., Goate, A., Rossor, M., Roques, P., Hardy, J., and Mullan, M. (1991) Early-onset Alzheimer's disease caused by mutations at codon 717 of the beta-amyloid precursor protein gene. *Nature* **353**, 844–846.
8. Goate, A., Chartier-Harlin, M. -C., Mullan, M., Brown, J., Crawford, F., Fidani, L., Giuffra, L., Haynes, A., Irving, N., James, L., Mant, R., Newton, P., Rooke, K., Roques, P., Talbot, C., Pericak-Vance, M., Roses, A., Williamson, R., Rossor, M., Owen, M., and Hardy, J. (1991) Segregation of a missense mutation in the amyloid precursor protein gene with familial Alzheimer's disease. *Nature* **349**, 704–706.
9. Newman, M., Musgrave, I. F., and Lardelli, M. (2007) Alzheimer disease: amyloidogenesis, the presenilins and animal models. *Biochim. Biophys. Acta* **1772**, 285–297.
10. Ballatore, C., Lee, V. M., and Trojanowski, J. Q. (2007) Tau-mediated neurodegeneration in Alzheimer's disease and related disorders. *Nat. Rev. Neurosci.* **8**, 663–672.
11. Giannakopoulos, P., Gold, G., Kovari, E., von Gunten, A., Imhof, A., Bouras, C., and Hof, P. R. (2007) Assessing the cognitive impact of Alzheimer disease pathology and vascular burden in the aging brain: The Geneva experience. *Acta Neuropathol.* **113**, 1–12.
12. Lee, V. M., Goedert, M., and Trojanowski, J. Q. (2001) Neurodegenerative tauopathies. *Annu. Rev. Neurosci.* **24**, 1121–1159.
13. Roberson, E. D. (2006) Frontotemporal dementia. *Curr. Neurol. Neurosci. Rep.* **6**, 481–489.
14. Bertram, L., and Tanzi, R. E. (2008) Thirty years of Alzheimer's disease genetics: the implications of systematic meta-analyses. *Nat. Rev. Neurosci.* **9**, 768–778.
15. Radde, R., Duma, C., Goedert, M., and Jucker, M. (2008) The value of incomplete mouse models of Alzheimer's disease. *Eur. J. Nucl. Med. Mol. Imaging* **35 Suppl 1**, S70–S74.
16. Jankowsky, J. L., Younkin, L. H., Gonzales, V., Fadale, D. J., Slunt, H. H., Lester, H. A., Younkin, S. G., and Borchelt, D. R. (2007) Rodent Aβ modulates the solubility and distribution of amyloid deposits in transgenic mice. *J. Biol. Chem.* **282**, 22707–22720.
17. Games, D., Buttini, M., Kobayashi, D., Schenk, D., and Seubert, P. (2006) Mice as models: transgenic approaches and Alzheimer's disease. *J. Alzheimers Dis.* **9**, 133–149.
18. Duyckaerts, C., Potier, M. C., and Delatour, B. (2008) Alzheimer disease models and human neuropathology: similarities and differences. *Acta Neuropathol.* **115**, 5–38.
19. Turner, P. R., O'Connor, K., Tate, W. P., and Abraham, W. C. (2003) Roles of amyloid precursor protein and its fragments in regulating neural activity, plasticity and memory. *Prog. Neurobiol.* **70**, 1–32.
20. Games, D., Adams, D., Alessandrini, R., Barbour, R., Berthelette, P., Blackwell, C., Carr, T., Clemens, J., Donaldson, T., Gillespie, F., Guido, T., Hagopian, S., Johnson-Wood, K., Khan, K., Lee, M., Leibowitz, P., Lieberburg, I., Little, S., Masliah, E.,

McConlogue, L., Montoya-Zavala, M., Mucke, L., Paganini, L., Penniman, E., Power, M., Schenk, D., Seubert, P., Snyder, B., Soriano, F., Tan, H., Vitale, J., Wadsworth, S., Wolozin, B., and Zhao, J. (1995) Alzheimer-type neuropathology in transgenic mice overexpressing V717F β-amyloid precursor protein. *Nature* **373**, 523–527.

21. Hsiao, K., Chapman, P., Nilsen, S., Eckman, C., Harigaya, Y., Younkin, S., Yang, F. S., and Cole, G. (1996) Correlative memory deficits, Aβ elevation, and amyloid plaques in transgenic mice. *Science* **274**, 99–102.
22. Lesné, S., Ming Teng, K., Kotilinek, L., Kayed, R., Glabe, C. G., Yang, A., Gallagher, M., and Ashe, K. H. (2006) A specific amyloid-β protein assembly in the brain impairs memory. *Nature* **440**, 352–357.
23. Mucke, L., Masliah, E., Yu, G. -Q., Mallory, M., Rockenstein, E. M., Tatsuno, G., Hu, K., Kholodenko, D., Johnson-Wood, K., and McConlogue, L. (2000) High-level neuronal expression of $A\beta_{1-42}$ in wild-type human amyloid protein precursor transgenic mice: Synaptotoxicity without plaque formation. *J. Neurosci.* **20**, 4050–4058.
24. Palop, J. J., Chin, J., Roberson, E. D., Wang, J., Thwin, M. T., Bien-Ly, N., Yoo, J., Ho, K. O., Yu, G. -Q., Kreitzer, A., Finkbeiner, S., Noebels, J. L., and Mucke, L. (2007) Aberrant excitatory neuronal activity and compensatory remodeling of inhibitory hippocampal circuits in mouse models of Alzheimer's disease. *Neuron* **55**, 697–711.
25. Palop, J. J., and Mucke, L. (2009) Epilepsy and cognitive impairments in Alzheimer disease. *Arch. Neurol.* **66**, E1–E6.
26. Sturchler-Pierrat, C., Abramowski, D., Duke, M., Wiederhold, K. H., Mistl, C., Rothacher, S., Ledermann, B., Bürki, K., Frey, P., Paganetti, P. A., Waridel, C., Calhoun, M. E., Jucker, M., Probst, A., Staufenbiel, M., and Sommer, B. (1997) Two amyloid precursor protein transgenic mouse models with Alzheimer disease-like pathology. *Proc. Natl. Acad. Sci. U S A* **94**, 13287–13292.
27. Calhoun, M. E., Wiederhold, K. H., Abramowski, D., Phinney, A. L., Probst, A., Sturchler-Pierrat, C., Staufenbiel, M., Sommer, B., and Jucker, M. (1998) Neuron loss in APP transgenic mice. *Nature* **395**, 755–756.
28. Chishti, M. A., Yang, D. S., Janus, C., Phinney, A. L., Horne, P., Pearson, J., Strome, R., Zuker, N., Loukides, J., French, J., Turner, S., Lozza, G., Grilli, M., Kunicki, S., Morissette, C., Paquette, J., Gervais, F., Bergeron, C., Fraser, P. E., Carlson, G. A., George-Hyslop, P. S., and Westaway, D. (2001) Early-onset amyloid deposition and cognitive deficits in transgenic mice expressing a double mutant form of amyloid precursor protein 695. *J. Biol. Chem.* **276**, 21562–21570.
29. Rockenstein, E., Mallory, M., Mante, M., Sisk, A., and Masliah, E. (2001) Early formation of mature amyloid-β protein deposits in a mutant APP transgenic model depends on levels of $A\beta_{1-42}$. *J. Neurosci. Res.* **66**, 573–582.
30. Herzig, M. C., Winkler, D. T., Burgermeister, P., Pfeifer, M., Kohler, E., Schmidt, S. D., Danner, S., Abramowski, D., Sturchler-Pierrat, C., Burki, K., Van Duinen, S. G., Maat-Schieman, M. L., Staufenbiel, M., Mathews, P. M., and Jucker, M. (2004) Aβ is targeted to the vasculature in a mouse model of hereditary cerebral hemorrhage with amyloidosis. *Nat. Neurosci.* **7**, 954–960.
31. Cheng, I., Palop, J., Esposito, L., Bien-Ly, N., Yan, F., and Mucke, L. (2004) Aggressive amyloidosis in mice expressing human amyloid peptides with the Arctic mutation. *Nat. Med.* **10**, 1190–1192.
32. Cheng, I., Scearce-Levie, K., Legleiter, J., Palop, J., Gerstein, H., Bien-Ly, N., Puoliväli, J., Lesné, S., Ashe, K., Muchowski, P., and Mucke, L. (2007) Accelerating amyloid-β fibrillization reduces oligomer levels and functional deficits in Alzheimer disease mouse models. *J. Biol. Chem.* **282**, 23818–23828.
33. Lord, A., Kalimo, H., Eckman, C., Zhang, X. -Q., Lannfelt, L., and Nilsson, L. N. G. (2006) The Arctic Alzheimer mutation facilitates early intraneuronal Aβ aggregation and senile plaque formation in transgenic mice. *Neurobiol. Aging* **27**, 67–77.
34. Duff, K., Eckman, C., Zehr, C., Yu, X., Prada, C. M., Perez-Tur, J., Hutton, M., Buee, L., Harigaya, Y., Yager, D., Morgan, D., Gordon, M. N., Holcomb, L., Refolo, L., Zenk, B., Hardy, J., and Younkin, S. (1996) Increased amyloid-β42(43) in brains of mice expressing mutant presenilin 1. *Nature* **383**, 710–713.
35. Holcomb, L., Gordon, M. N., McGowan, E., Yu, X., Benkovic, S., Jantzen, P., Wright, K., Saad, I., Mueller, R., Morgan, D., Sanders, S., Zehr, C., O'Campo, K., Hardy, J., Prada, C. M., Eckman, C., Younkin, S., Hsiao, K., and Duff, K. (1998) Accelerated Alzheimer-type phenotype in transgenic mice carrying both mutant amyloid precursor protein and presenilin 1 transgenes. *Nat. Med.* **4**, 97–100.
36. Jankowsky, J. L., Fadale, D. J., Anderson, J., Xu, G. M., Gonzales, V., Jenkins, N. A., Copeland, N. G., Lee, M. K., Younkin, L. H., Wagner, S. L., Younkin, S. G., and Borchelt, D. R. (2004) Mutant presenilins specifically elevate the levels of the 42 residue beta-amyloid

peptide in vivo: Evidence for augmentation of a 42-specific gamma secretase. *Hum. Mol. Genet.* **13**, 159–170.

37. Oakley, H., Cole, S. L., Logan, S., Maus, E., Shao, P., Craft, J., Guillozet-Bongaarts, A., Ohno, M., Disterhoft, J., Van Eldik, L., Berry, R., and Vassar, R. (2006) Intraneuronal β-amyloid aggregates, neurodegeneration, and neuron loss in transgenic mice with five familial Alzheimer's disease mutations: Potential factors in amyloid plaque formation. *J. Neurosci.* **26**, 10129–10140.
38. Braak, H., and Braak, E. (1991) Neuropathological stageing of Alzheimer-related changes. *Acta Neuropathol.* **82**, 239–259.
39. Kwok, J. B., Teber, E. T., Loy, C., Hallupp, M., Nicholson, G., Mellick, G. D., Buchanan, D. D., Silburn, P. A., and Schofield, P. R. (2004) Tau haplotypes regulate transcription and are associated with Parkinson's disease. *Ann. Neurol.* **55**, 329–334.
40. Myers, A. J., Kaleem, M., Marlowe, L., Pittman, A. M., Lees, A. J., Fung, H. C., Duckworth, J., Leung, D., Gibson, A., Morris, C. M., de Silva, R., and Hardy, J. (2005) The H1c haplotype at the MAPT locus is associated with Alzheimer's disease. *Hum. Mol. Genet.* **14**, 2399–2404.
41. Myers, A. J., Pittman, A. M., Zhao, A. S., Rohrer, K., Kaleem, M., Marlowe, L., Lees, A., Leung, D., McKeith, I. G., Perry, R. H., Morris, C. M., Trojanowski, J. Q., Clark, C., Karlawish, J., Arnold, S., Forman, M. S., Van Deerlin, V., de Silva, R., and Hardy, J. (2007) The MAPT H1c risk haplotype is associated with increased expression of tau and especially of 4 repeat containing transcripts. *Neurobiol. Dis.* **25**, 561–570.
42. Roberson, E. D., Scearce-Levie, K., Palop, J. J., Yan, F., Cheng, I. H., Wu, T., Gerstein, H., Yu, G.-Q., and Mucke, L. (2007) Reducing endogenous tau ameliorates amyloid β-induced deficits in an Alzheimer's disease mouse model. *Science* **316**, 750–754.
43. Small, S. A., and Duff, K. (2008) Linking Abeta and tau in late-onset Alzheimer's disease: A dual pathway hypothesis. *Neuron* **60**, 534–542.
44. Götz, J., Deters, N., Doldissen, A., Bokhari, L., Ke, Y., Wiesner, A., Schonrock, N., and Ittner, L. M. (2007) A decade of tau transgenic animal models and beyond. *Brain Pathol.* **17**, 91–103.
45. Lewis, J., McGowan, E., Rockwood, J., Melrose, H., Nacharaju, P., Van Slegtenhorst, M., Gwinn-Hardy, K., Paul Murphy, M., Baker, M., Yu, X., Duff, K., Hardy, J., Corral, A., Lin, W. L., Yen, S. H., Dickson, D. W., Davies, P., and Hutton, M. (2000) Neurofibrillary tangles, amyotrophy and progressive motor disturbance in mice expressing mutant (P301L) tau protein. *Nat. Genet.* **25**, 402–405.
46. SantaCruz, K., Lewis, J., Spires, T., Paulson, J., Kotilinek, L., Ingelsson, M., Guimaraes, A., DeTure, M., Ramsden, M., McGowan, E., Forster, C., Yue, M., Orne, J., Janus, C., Mariash, A., Kuskowski, M., Hyman, B., Hutton, M., and Ashe, K. H. (2005) Tau suppression in a neurodegenerative mouse model improves memory function. *Science* **309**, 476–481.
47. Andorfer, C., Kress, Y., Espinoza, M., de Silva, R., Tucker, K. L., Barde, Y. -A., Duff, K., and Davies, P. (2003) Hyperphosphorylation and aggregation of tau in mice expressing normal human tau isoforms. *J. Neurochem.* **86**, 582–590.
48. Duff, K., Knight, H., Refolo, L. M., Sanders, S., Yu, X., Picciano, M., Malester, B., Hutton, M., Adamson, J., Goedert, M., Burki, K., and Davies, P. (2000) Characterization of pathology in transgenic mice over-expressing human genomic and cDNA tau transgenes. *Neurobiol. Dis.* **7**, 87–98.
49. Lewis, J., Dickson, D. W., Lin, W. L., Chisholm, L., Corral, A., Jones, G., Yen, S. H., Sahara, N., Skipper, L., Yager, D., Eckman, C., Hardy, J., Hutton, M., and McGowan, E. (2001) Enhanced neurofibrillary degeneration in transgenic mice expressing mutant tau and APP. *Science* **293**, 1487–1491.
50. Oddo, S., Caccamo, A., Shepherd, J. D., Murphy, M. P., Golde, T. E., Kayed, R., Metherate, R., Mattson, M. P., Akbari, Y., and LaFerla, F. M. (2003) Triple-transgenic model of Alzheimer's disease with plaques and tangles: Intracellular Aβ and synaptic dysfunction. *Neuron* **39**, 409–421.
51. Billings, L. M., Oddo, S., Green, K. N., McGaugh, J. L., and Laferla, F. M. (2005) Intraneuronal Aβ causes the onset of early Alzheimer's disease-related cognitive deficits in transgenic mice. *Neuron* **45**, 675–688.
52. Stevens, J. C., Banks, G. T., Festing, M. F., and Fisher, E. M. (2007) Quiet mutations in inbred strains of mice. *Trends Mol. Med.* **13**, 512–519.
53. Holmes, A., Wrenn, C. C., Harris, A. P., Thayer, K. E., and Crawley, J. N. (2002) Behavioral profiles of inbred strains on novel olfactory, spatial and emotional tests for reference memory in mice. *Genes Brain Behav.* **1**, 55–69.
54. Crawley, J. N. (2008) Behavioral phenotyping strategies for mutant mice. *Neuron* **57**, 809–818.
55. Linder, C. C. (2006) Genetic variables that influence phenotype. *ILAR J.* **47**, 132–140.

56. Crawley, J. N. (2008) "What's Wrong with My Mouse? Behavioral Phenotyping of Transgenic and Knockout Mice", John Wiley & Sons Inc., Hoboken, NJ.
57. Dodart, J. C., and May, P. (2005) Overview on rodent models of Alzheimer's disease. *Curr. Protoc. Neurosci.* Chapter 9, Unit 922.
58. Kobayashi, D. T., and Chen, K. S. (2005) Behavioral phenotypes of amyloid-based genetically modified mouse models of Alzheimer's Disease. *Genes Brain Behav.* **4**, 173–196.
59. McGowan, E., Eriksen, J., and Hutton, M. (2006) A decade of modeling Alzheimer's disease in transgenic mice. *Trends Genet.* **22**, 281–289.
60. Götz, J., and Ittner, L. M. (2008) Animal models of Alzheimer's disease and frontotemporal dementia. *Nat. Rev. Neurosci.* **9**, 532–544.
61. Howlett, D. R., and Richardson, J. C. (2009) The pathology of APP transgenic mice: a model of Alzheimer's disease or simply overexpression of APP? *Histol. Histopathol.* **24**, 83–100.
62. LaFerla, F. M., and Oddo, S. (2005) Alzheimer's disease: Abeta, tau and synaptic dysfunction. *Trends Mol. Med.* **11**, 170–176.

Chapter 14

Monitoring Spatial Learning and Memory in Alzheimer's Disease Mouse Models Using the Morris Water Maze

Kimberly Scearce-Levie

Abstract

Mouse models of Alzheimer's Disease are essential for understanding how pathological cascades alter neural circuitry and eventually disrupt cognitive function. A key prerequisite for the use of such models, therefore, is the ability to accurately and reliably measure cognitive function. The Morris Water Maze has emerged in the field as the standard test for assessing spatial cognition. There are many variations on the exact procedures and types of analysis that can be done within the framework of this test. We detail a procedure, with variations, that can be used to robustly detect cognitive deficits in Alzheimer's Disease mouse models as well as factors that ameliorate those deficits.

Key words: Spatial learning, Retention, Hippocampal function, Mouse behavior, Morris Water Maze, Cognition

1. Introduction

In order to understand the pathological processes underlying a disorder of cognition like Alzheimer's disease, it is essential to be able to understand and measure the central cognitive deficits. While the availability of transgenic mouse models has greatly increased our understanding of Alzheimer's disease, it remains challenging to accurately and reproducibly measure cognition in a mouse. One of the most robust methods of assessing spatial cognition in rodents is the Morris Water Maze. Developed by Richard Morris in the 1980s and initially used to assess hippocampal function in rats (1), the test has become the most common assay of memory function in mouse models of Alzheimer's disease.

There are several key advantages that make the Morris Water Maze well-suited to the assessment of cognition in

Erik D. Roberson (ed.), *Alzheimer's Disease and Frontotemporal Dementia*, Methods in Molecular Biology, vol. 670,
DOI 10.1007/978-1-60761-744-0_14, © Springer Science+Business Media, LLC 2011

Alzheimer's disease models. The test of spatial learning is quite sensitive to hippocampal dysfunction, and is thus well suited to Alzheimer's disease. Despite the complexity of the assay, it is remarkably robust. A study comparing the reproducibility of different behavioral phenotypes measured in different laboratories showed that the water maze was one of the only tests where the test site did not significantly affect the results (2). Moreover, the prevalence of the test throughout the field simplifies the interpretation of data and facilitates meaningful comparisons between studies.

Despite the robustness and validity of the test, its complexity opens the door for misinterpretation. There are a wide range of factors than can affect an animal's performance on the task besides its ability to learn, including health, motivation, sex, age, body weight, thermoregulation, eyesight, motor coordination, and stress. Moreover, environmental factors like water temperature, noise, lighting, cue placement, experimenter, time of day, etc., can seriously impact the test. While it is impossible to eliminate all such unwanted variables, an experimenter who carefully balances groups, standardizes procedures and incorporates appropriate controls can still consistently produce high-quality water maze data.

2. Materials

2.1. Essential Components

1. Circular water tank (see Note 1).
2. Opaque water (see Note 2).
3. Escape platform made from clear or white plexiglas, 10–12 cm^2.
4. Large (10 cm high, 1–2 cm wide), high-contrast removable marker for cued trials.
5. Large, high-contrast visual spatial cues for room.
6. For pretraining, a plexiglas alley measuring the length of the pool diameter and the width of the platform.
7. A high-resolution CCD (charge-coupled device) camera mounted to the ceiling above the center of tank and sending output to a personal computer.
8. Videotracking software (see Note 3).
9. Extra data capacity for storage/backup of large digital video files.
10. Appropriate test subjects (see Note 4).

2.2. Useful Accessories

1. Immersion heater.
2. Immersion pump (see Note 5).

3. Aquarium thermometer attached to a float (see Note 6).
4. Aquarium net (see Note 7).

3. Methods

3.1. Planning

1. Once an appropriate cohort of mice has been indentified, the cohort should be divided into subgroups of 9–12 mice each. These subgroups should be balanced by genotype, treatment, sex, and age.
2. Experimenter should be blinded to genotype and/or treatment. Someone else can blind-code the animals so the experimenter knows only a code number that corresponds to test order.
3. If possible, the experimental cohort should be moved to the testing room or a nearby housing room 5–10 days before the beginning of testing to reduce stress and disruption. Ideally, the animals should be singly housed. This speeds the training, reduces the likelihood of experimenter errors, and insures identical housing for each animal tested.
4. For drug testing, a number of additional considerations are critical to consider at this point. The logistics of dosing the animals should be carefully coordinated with the behavioral testing of the animal. Specifically,
   (a) someone other than the experimenter should perform the dosing. This helps insure the experimenter is treatment-blind. More importantly, the mouse should not learn to fear the person training it, which is a danger if the water maze examiner is also performing restraint and injections.
   (b) painful treatments (injections, gavage) should be avoided at the start of a training day. If possible, it is best to entirely avoid dosing on training days. However, if the kinetics of the drug requires frequent dosing, doses should be administered at the end of the training day whenever possible.
   (c) for treatments such as stereotactic injection or minipump implantation that require a survival surgery it is important to allow sufficient postsurgical recovery time before beginning water maze training. 5–10 days is usually sufficient. It is also crucial that the control animals undergo sham treatment that mimics the treatment as closely as possible.

3.2. Preparing the Tank

1. Fill the tank with tap water to the appropriate depth (20–30 cm, depending on size of tank). Check temperature as water is filling and adjust to 18–20°C.
2. Add nontoxic white paint, stirring constantly, until water is a uniformly opaque white color.

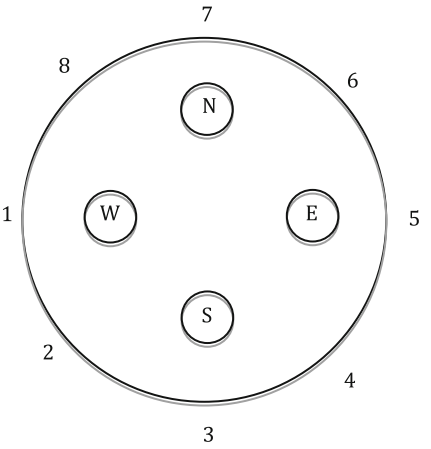

Fig. 1. Platform and drop locations. Potential platform locations within the pool are referred to by cardinal direction (*N* north, *E* east, *S* south, and *W* west). Potential drop locations are indicated by numbers around the perimeter of the pool. See Tables 1 and 2.

3.3. Pretraining

In most cases, allowing the mice some exposure to the tank before training begins speeds acquisition of the task.

1. Set up alley near the center of tank (Fig. 1).
2. Place platform approximately 1/3 of the distance from the end of the alley, centered within width of alley. The top of the platform should be approximately 1.5 cm below surface of the water. Platform should not be clearly visible from above.
3. Place the animal into the pool at the end of the alley furthest from the platform. The animal should be facing pool wall when placed into the water.
4. Start timing with a stopwatch when the animal enters the water.
5. Stop the trial after 90 s or when the animal reaches the platform and remains on it for 5 s, whichever occurs first.
6. If the animal fails to reach platform in 90 s, gently guide it to the platform, either by encouraging it to follow experimenter's hand or by allowing it to "surf" on the hand. Once the animal is on the platform, experimenter should step back and allow mouse to sit on platform undisturbed for 5 s. Always remove mouse from platform rather than taking it out of the pool directly from the water.
7. Record the length of time required for animal to settle on platform and any unusual behaviors, including:
   - *Climbing*: attempting to climb out of pool facing walls and making climbing movements.
   - *Jumping*: attempting to use platform to jump out of pool rather than waiting on platform.

- *Circling*: swimming in repetitive small circles, rather than in a line down length of alley.
- *Floating*: floating motionless in the pool. Making a loud noise (by using a clicker or snapping gloves) can startle animal and cause it to resume swimming.

8. After removing animal from platform, walk to other end of alley and repeat trial.
9. Repeat for a total of four consecutive trials for each mouse.
10. After testing all mice, review data. The goal is for 90% of mice in cohort to reach platform in <90 s without jumping off. If this criterion has not been reached, repeat pretraining with a second session of four consecutive trials. Depending on strain and mutation, one to four sessions may be necessary to achieve criterion. Mice that have consistently failed to remain on platform or that display an obvious motor deficit that affects swimming should be removed from the experiment at this stage.

3.4. Cued Platform Training

Cued platform training was originally designed as a control to verify that experimental subjects could see and swim well enough to complete the task. However, it should be noted that learning to swim to a cued platform is actually a complex task, requiring associative learning, episodic memory, motivation, navigation, and other modalities beyond visuomotor. The cued training can be performed either before or after the hidden portion platform of the task (see Note 8), but it is important to perform it for every animal tested. We perform two training sessions per day, each with two trials.

1. Adjust temperature, depth and opacity of water so that it is the same as for the pretraining.
2. Place platform with prominent marker on top at a pool location corresponding to North (N, see Fig. 1).
3. Place mouse into pool, facing the wall, at location #2 in Fig. 1.
4. Start recording/timing the trial and immediately get out of the way (see Note 9).
5. Allow the mouse to swim until it either:
   (a) finds the platform. End trial when mouse finds platform and remains on it for >5 s.
   (b) searches for platform for >60 s. After 60 s, end trial. Guide mouse to platform with hand. Allow mouse to climb onto platform by itself and sit for at least 5 s before removing. Always remove mouse from the platform, not the water. Trials in which the mouse fails to find the platform in 60 s should be recorded as "not found" with the maximum latency of 60 s.

6. Test all mice in the first subgroup of 9–12 mice in this manner, using drop location #2.
7. Testing all 9–12 mice in a group in the first trial should take 10–15 min. Once this intertrial interval has passed, return to the first mouse in the group, and place it into the pool, facing the wall, at location #4 (see Fig. 1) for trial 2.
8. Train all mice in the subgroup as before, using drop location #4.
9. Move on to the next subgroup of 9–12 mice. Test using the same procedures as for the first group, using drop location #2, then #4.
10. Continue in this manner until all mice in the cohort have been tested twice, from two different drop locations.
11. Allow mice to rest 2–4 h before beginning session 2.
12. Move platform to pool location corresponding to South (S, Fig. 1).
13. Repeat all steps from the first session using drop locations 8 and 6 from Fig. 1.
14. Allow mice to rest overnight in home cages.
15. Repeat procedure the following day, selecting platform and drop locations according to Table 1 and Fig. 1.
16. In general, 2–3 days of training is sufficient to train most mouse strains in the cued version of the task. Ideally, at the end of training, (1) control mice should be able to find the platform in <15 s on average and (2) control and experimental mice should be performing at the same level. Additional training may be required to achieve these criteria.

3.5. Hidden Platform Training

Hidden platform training is performed similar to cued platform training, except the platform has no visible cue above the water surface, the platform location is not moved between sessions, and three trials are performed per session.

Table 1
Visible platform

	Platform location	Drop location
Day 1, session 1	North	2, 4
Day 1, session 2	South	8, 6
Day 2, session 1	West	6, 4
Day 2, session 2	East	8, 2
Day 3, session 1	West	4, 6
Day 3, session 2	North	4, 2

1. Adjust temperature, depth and opacity of water so that it is the same as for the pretraining.
2. Place unmarked platform at a pool location corresponding to East (E, see Fig. 1 and Note 10).
3. Place mouse into pool, facing the wall, at location corresponding to 2 in Fig. 1.
4. Proceed as outlined for cued trial, with the following important differences:
   (a) Keep platform location constant for each mouse. Different platform locations may be used for each subgroup, if desired, to minimize a location bias (see Note 10), but the location must be held constant for each group throughout hidden training.
   (b) Perform three trials/session and two sessions/day for a total of six daily trials.
   (c) Proceed using the drop locations outlined in Table 2.
5. In general, 3–5 days of training are sufficient for wild type mice to learn to efficiently find the hidden platform. It is useful to download and check the data daily. Control mice should be able to find the platform within 15 s, on average, after 3–4 days of training.

3.6. Probe Trials

In a probe trial, the platform is removed, and the mice are tracked during a 60-s exploration of the pool. This provides important information about the strategy mice are using to locate the hidden platform (see Note 11).

Table 2
Hidden platform

	Drop location (East platform)	Drop location (South platform)
Day 1, session 1	2, 8, 1	6, 8, 7
Day 1, session 2	7, 1, 3	5, 7, 1
Day 2, session 1	2, 3, 1	8, 1, 7
Day 2, session 2	8, 7, 3	6, 1, 5
Day 3, session 1	3, 1, 7	1, 7, 5
Day 3, session 2	8, 2, 3	6, 8, 1
Day 4, session 1	7, 8, 1	5, 6, 8
Day 4, session 2	1, 8, 3	7, 6, 1
Day 5, session 1	3, 2, 8	8, 5, 6
Day 5, session 2	1, 7, 3	7, 5, 1

1. Remove platform from pool completely.
2. Place first mouse into pool at location opposite where the platform had been (i.e., for East platform location, use drop location #1 in Fig. 1).
3. Allow mice to swim in pool for 60 s, recording, if possible:
   (a) time spent in target quadrant surrounding old platform location
   (b) time spent in other three control quadrants
   (c) crossings over old target platform location
   (d) crossings over control areas the same size as the platform but located in nontarget quadrants
   (e) latency to the first crossing over target platform location
   (f) mean distance from platform location.
4. After 60 s, remove mouse from pool and return to home cage.
5. Repeat steps 2–4 for each mouse in entire cohort so that there is one probe trial per mouse.
6. Probe trials can be repeated at different time points during the experiment (see Note 12), but should be interspersed with rewarded trials in which the platform is present in the correct location. Otherwise, the memory of the platform location will be extinguished by repeated failures to find the platform (see Note 13).

3.7. Reversal Training

Once an animal has acquired the task, it is sometimes useful to move the platform and attempt to train the animal to the new location. This is a more demanding task, requiring cognitive flexibility as well as spatial learning. Reversal training can often reveal deficits that were not apparent during the first hidden platform training or probe trial.

1. Select a new hidden platform location (see Note 14).
2. Proceed with hidden platform training only, as outlined in Subheading 3.5, for 1–2 days (see Note 15).
3. Perform a probe trial at the end of reversal training, noting crossings over both old and new platform location.
4. Reversal training can be repeated as many times as necessary, either immediately after the initial training or separated by several weeks or months.

3.8. Data Analysis

Due to the tremendous amount of data generated during the course of a typical water maze experiment, the analysis and interpretation is often more complicated and time consuming that the actual process of collecting the data. There is no general

consensus in the field about the best way to present data or the optimal statistical techniques to apply. Often investigators make a post hoc selection of the data representation that best supports their hypothesis, a practice that may contribute to a high false-positive rate in the field. A good analysis is planned in advance and includes the following elements:

1. Visualize the learning curve by plotting the distance to the platform (see Note 16) on the Y axis and trials, sessions or day on the X axis (see Note 17).
2. Check for statistical differences in learning curves between groups by performing a repeated measures analysis of variance (rmANOVA) (see Note 18) with session as the repeated measure, and distance as the dependent measure. You should see a highly significant effect of trial or session overall, indicating that learning is occurring. Group differences that do not interact with the repeated measure suggest that the groups are performing differently across all trials, but are learning at a similar rate. Interactions of group with session indicate that the groups learn at different rates.
3. It is useful to calculate the average swim speed for each animal across the different sessions. A persistent difference in swim speeds throughout training may suggest differences in motor abilities. Animals with very low swim speeds (<10 cm/s) may need to be excluded from further analysis due to low motivation and failure to perform the task.
4. Thigmotaxis can be calculated by measuring the amount of time that a mouse spends within an annulus around the edge of the pool that covers approximately 20–30% of the pool surface area. Thigmotaxic behavior is quite common and normal, especially during the initial days of training, but it should decline with repeated exposure to the pool. Animals that exhibit thigmotaxis as a dominant behavior throughout training (>50% of time in outer annulus) should be excluded from analysis. Since thigmotaxic animals fail to perform the learning task at all, conclusions about learning ability cannot be drawn from an increased prevalence of thigmotaxis in one experimental group. However, it may reflect increased anxiety or stress in that group.
5. The probe trial is the ultimate measure of spatial memory. There are several key measures that can be used to determine a mouse's performance on a probe trial. There is still little consensus in the field about the most sensitive and/or least error-prone measure (3). Reviewing multiple measures of performance is the most informative and robust approach (see Note 19).

(a) *Dwell time in target quadrant*. For mice that have learned the task, this should be significantly higher than chance (25% of the trial or 15 s). Statistically, dwell time can be compared between groups in an ANOVA with treatment/genotype as between factors. Within groups, it can also be compared to time in nontarget quadrants using paired *t*-tests.

(b) *Crossings over old platform location*. The number of times each mouse crosses over the location of the target platform can be compared using ANOVAs between groups. For comparison, crossings over "dummy" platform locations in other quadrants can be calculated and compared to crossings over the real platform location. This data can be used to calculate an Annulus Crossing Index (ACI).

$$\mathrm{ACI} = \mathrm{TargetCrosses} - \frac{\mathrm{Dummy1\ Crosses} + \mathrm{Dummy2\ Crosses} + \mathrm{Dummy3\ Crosses}}{3}$$

An ACI > 1 indicates learning of the task.

(c) *Mean distance to platform location*. Some software programs will allow you to calculate a running average of the mouse's distance to the platform throughout the trial. While this is not as commonly reported as dwell time or platform crossings, a recent meta-analysis of water maze experiments demonstrated that this was the most sensitive measure (3).

(d) *Latency to reach old platform location*. This measure is essentially the same as the latency measures used during training and is useful primarily as a quality control. The mean latency to reach the platform location on the probe trial for each group should be roughly equal to the mean target latency on the previous training day. If it is very different, it suggests that something unusual during the probe trial is disrupting the animals' behavior.

4. Notes

1. For mice, the ideal water tank diameter is 120–150 cm. Mice require more time to learn the task in larger pools. Water depth should be 20–30 cm, with the rim of the tank 10–15 cm above the water surface. The tank should be as uniform as possible, since large visible marks (e.g., a welding seam) can become proximal cues.

2. Normal tap water is made opaque by the addition of white nontoxic paint. The ideal temperature of the water depends somewhat on the strain of mouse used, but should be kept consistent throughout the experiment. 18–20°C works well to motivate animals to keep moving; 22–26°C is better for frail or small animals that might be subject to hypothermia.
3. Several vendors provide software that processes the video image using contrast- or edge-detection algorithms to record the animal's *x* and *y* coordinates over time. This *x* and *y* data is then translated by the software to more user-friendly data like "path length." This software is typically the most expensive part of the set up. A simpler version of the task can be conducted by only an experimenter with a stopwatch, but some of the richness of the data will be lost. For example, without video tracking, the only measure of training will be latency to find the platform, which can be confounded by differing swim speeds.
4. Selection of an appropriate number of age-, sex-, and strain-matched subjects is one of the most crucial determinants of the success of this test. Subjects should be adult (minimum of 10 weeks old). With aging, water maze performance is expected to decline, with the deficits observed in females before males. For Alzheimer's research, it is often necessary to use aged mice, but efforts should be made to avoid testing females older than 20 months or males older than 24 months. In most mouse strains, wild type animals above this age have major deficits that will make it difficult to detect transgene-related deficits. Animals tested in a given experiment should be as closely age-matched as possible (<6 week range in ages).
5. An immersion pump is useful to help with drainage of tank.
6. An aquarium thermometer attached to a float is useful to measure water temperature.
7. An aquarium net is useful for the removal of debris from pool.

Genetic background strain has a profound influence on water maze performance (1, 4, 5). Some strains have visual or motor defects that prevent them from performing the task at all. For example, FVB/NJ, a strain commonly used for genetic manipulations due to the large litter size and good maternal behaviors, has retinal degeneration, and is therefore unable to perform the cued version of the task (6). Other common strains, such as 129/SvJ and DBA/2 are documented to be poor learners in the water maze and are not well suited to this type of experiment (7, 8). Despite between strain differences in learning ability, good data can be obtained as long as the strain composition of control and experimental groups is identical. Danger arises, however, when

the strains are mixed. F1 hybrids, where each animal has one allele from each parent strain can yield consistent data since all animals are genetically identical. However, testing other types of mixed backgrounds is very risky, since each animal will have a different genetic contribution from the parent strains. In this case, it is nearly impossible to determine if learning differences are attributable to the intended experimental variation or to genetic background variation. It is never recommended to perform the water maze on mixed backgrounds. Any results achieved in such a situation must be replicated in a genetically homogenous population of mice. More detailed guidance on appropriate background strains and breeding strategies for behavioral experiments can be found in recent guidelines from the journal *Genes, Brain, and Behavior* (9).

Even with "ideal" cohorts of mice, both within-subject and between-subject variation is quite high for water maze performance. Therefore, large cohorts of mice are necessary to achieve reliable, statistically significant data. Twelve to fifteen mice/group is a good target. Manipulations that introduce additional variability, such as drug dosing, may require higher n's.

8. Performing cued platform training before hidden platform training allows the animal to form the association between the platform and escape from the pool and can thereby facilitate learning of the hidden platform version of the task. When working with mice that are particularly poor learners or extremely susceptible to the stress of being placed in the pool, it is often helpful to perform the cued task first. However, if the cued and hidden tasks are to be performed in the same room, the mice begin forming a spatial map of the room during the cued training. Even though the platform is moved to a new location for the hidden training, the spatial map helps animals find the hidden platform much more quickly, as evidenced by improved performance in the very first hidden training session. Some Alzheimer's Disease mouse models seem to be less able to form this spatial map of the room and therefore can show deficits on the very first trial of hidden training relative to nontransgenic controls (unpublished observations). Since this difference can complicate interpretation of data, it is generally best to perform cued training after the hidden, unless (1) two training rooms are available or (2) the mice are completely unable to learn the hidden version without learning the cued first.
9. The experimenter is one of many visual cues that the mouse can use in navigating the pool. Moreover, the primary reward for the mouse is to be lifted off the platform by the experimenter and returned to the safe, dry, home cage. Since the mouse will typically learn to associate the experimenter with escape, many

mice will attempt to swim toward the experimenter rather than to the platform. To avoid training the mouse to follow the experimenter, it is important for the experimenter to get out of sight quickly. Ideally, the experimenter can step behind a screen or curtain and monitor the trial on video.

10. In an ideally uniform room, it is sufficient to train all mice to the same hidden platform location. However, in the real word, there are often environmental cues or experimenter behaviors that will lead to a "quadrant bias," i.e., a general preference for an area of the pool besides the one containing the platform. If this is the case, you will consistently see that mice spend more time in one of the nontarget quadrants relative to the others during probe trials. Since it may be impossible to find and eliminate the source of the bias, an experimenter can adjust for it by using two different platform locations and training balanced subgroups of mice to each location. This approach takes a bit of extra time and is more prone to experimenter errors, but can yield cleaner data when performed correctly.
11. After mice have been trained so that latency to find platform is clearly improving, probe trials can begin. Probe trials are critical because mice may improve performance on training trials using a number of strategies other than spatial memory. There are, in fact, clear cases of mice that dramatically improve their performance on training trials, but show no spatial learning on the probe trial (10). Correct performance on a probe trial is the proper confirmation that mice are using a spatial strategy to solve the maze.
12. The timing of the probe trials depends both on the experimental question and the learning performance of the mice being studied. In general, probe trials can be used to interrogate three types of memory:
    (a) *Short-term memory*: trial should be performed within 15–30 min of last training session.
    (b) *Long-term memory*: trial should be performed 18–24 h after last training session.
    (c) *Long-term retention*: trial can be performed 2 days or more after last training session. Performing a delayed probe trail several days after training can unmask deficits in mice that might not be apparent with a less demanding 18-h probe trial. Well-trained C57BL/6 mice have no difficulty remembering platform location for 2 weeks posttraining. After that, probe trial performance begins to degrade until no clear target preference is apparent after about 4 weeks.

In addition to performing probe trials when hidden platform training is complete, it can be useful to perform a probe trial at an intermediate stage of training. This allows the experimenter to

confirm that the animals are in fact learning the task using a spatial strategy. It is also useful for detecting delays in learning, as evidenced by good performance by one group but poor performance by another. Poor learners can be "overtrained" so that their latency improves to control levels. Performing the probe trial at that time can mask learning deficits.

13. In selecting a new platform location, avoid any quadrant that the mice have shown some bias toward in earlier training/probe trials. Choose a location that is a different distance from the center of the tub. This avoids animals relying on a "chaining" strategy of swimming in circles, a fixed distance from the edge of the pool, until they bump into the platform.
14. To avoid extinction during probe trials, some investigators utilize what is called an "Atlantis platform." An Atlantis platform can move up and down underwater under the experimenter's control. Thus, it can be deeply submerged (and effectively absent) during the 60 s probe trial, but then can rise to the usual location of the hidden platform so that the mouse still ends up being "rewarded" by finding the platform in the correct location, and avoiding an extinction trial.
15. The animals have extensive experience with the water maze task by the time reversal training begins, and therefore typically learn the task much more quickly than they learned the initial hidden platform location. Some animals are unable to learn the new location, but additional training does not provide much benefit to those animals.
16. Investigators often plot time to reach platform because the number of seconds to target seems more intuitive than the distance traveled to reach the platform. However, the latency data can be biased by differences in swim speeds: a fast swimming mouse may use a less efficient search strategy but still reach the platform before a slower swimming mouse that navigates directly to the target. To correct for this, it is preferable to plot the distance traveled to the platform.
17. Plotting the data for each individual trial is typically too noisy for the purposes of presentations or publication. However, taking a look at the trial by trial data can often reveal some interesting points. For instance, a pattern in which one group always performs very poorly on the first trial of the day; improves quickly throughout the day; and then, performs worse again at the beginning of the next day would suggest that those mice have intact learning ability but a retention deficit. In contrast, animals that improve slowly but steadily over the entire course of the trial would suggest a deficit in learning acquisition. However, that important difference could be missed by inspecting only the average data for each day.

18. It is important to use the repeated measures ANOVA rather than a factorial ANOVA or a *t*-test at individual time points. The analysis adds power by taking into account all individual measures taken, without biasing it by assuming that the measures taken each session are independent of one another. When a difference is apparent in an rmANOVA analysis, post hoc comparisons can then be performed to compare individual time points. It is not appropriate to choose a single time point and compare the groups at that time point by *t*-test or ANOVA. In a typical experiment, in which two groups of mice were run for ten training sessions, there are ten potential comparison points. One of those will be significant at the $p < 0.05$ level by pure chance in half the experiments run (20 comparisons). Appropriate use of rmANOVA, therefore, reduces false positive results.
19. There are several advantages to using multiple measures. If they all agree, it can increase your confidence in your finding. If there are discrepancies, it can be quite informative. For example, an animal with good performance as measured by quadrant dwell time but poor performance on target crossings may have learned the general location of the platform, but have difficulty with fine navigation.

References

1. Morris, R. G., Garrud, P., Rawlins, J. N., and O'Keefe, J. (1982) Place navigation impaired in rats with hippocampal lesions. *Nature* **297**, 681–683.
2. Crabbe, J. C., Wahlsten, D., and Dudek, B. C. (1999) Genetics of mouse behavior: interactions with laboratory environment. *Science* **284**, 1670–1672.
3. Maei, H. R., Zaslavsky, K., Teixeira, C. M., and Frankland, P. W. (2009) What is the most sensitive measure of water maze probe test performance? *Frontiers in Integrative Neuroscience* **3**, 1–9.
4. Nguyen, P. W., Abel, T., Kandel, E. R., and Bourtchouladze, R. (2000) Strain-dependent differences in LTP and hippocampus-dependent memory in inbred mice. *Learning and Memory* **7**, 170–179.
5. Owen, E. H., Logue, S. F., Rasmussen, D. L., and Wehner, J. W. (1997) Assessment of learning by the Morris water task and fear conditioning in inbred mouse strains and F1 hybrids: implications of genetic background for single gene mutations and quantitative trait loci analysis. *Neuroscience* **80**, 1087–1099.
6. Wahlsten, D., Cooper, S. F., and Crabbe, J. C. (2005) Different rankings of inbred mouse strains on the Morris maze and a refined 4-arm water escape task. *Behavioral Brain Research* **165**, 36–51.
7. Wehner, J. M., Sleight, S., and Upchurch, M. (1990) Hippocampal protein kinase C activity is reduced in poor spatial learners. *Brain Research* **523**, 181–187.
8. Hengemihle, J. M., Long, J. M., Betkey, J., Jucker, M. and Ingram, D. K. (1999) Age-related psychomotor and spatial learning deficits in 129/SvJ mice. *Neurobiology of Aging* **20**, 9–18.
9. Crusio, W. E., Goldowitz, D., Holmes, A., and Wolfer, D. (2009) Standards for the publication of mouse mutant studies. *Genes, Brain and Behavior* **8**, 1–4.
10. Steiner, R. A., Hohmann, J. G., Holmes, A., Wrenn, C. C., Cadd, G., Juréus, A., Clifton, D.K., Luo, M., Gutshall, M., Ma, S. Y., Muffson, E. J., and Crawley, J. N. (2007) Galanin transgenic mice display cognitive and neurochemical deficits characteristic of Alzheimer's disease. *Proceedings of the National Academy of Sciences (USA)* **98**, 4184–4189.

Chapter 15

Step-by-Step In Situ Hybridization Method for Localizing Gene Expression Changes in the Brain

Jorge J. Palop, Erik D. Roberson, and Inma Cobos

Abstract

RNA in situ hybridization is a powerful technique for examining gene expression in specific cell populations. This method is particularly useful in the central nervous system with its high cellular diversity and dynamic gene expression regulation associated with development, plasticity, neuronal activity, aging, and disease. Standard quantitative techniques such as Western blotting and real-time PCR allow the detection of altered gene or protein expression but provide no information about their cellular source or possible alterations in expression patterns. Here, we describe a step-by-step RNA in situ hybridization method on adult and embryonic brain sections for quantitative neuroscience. We include fully detailed protocols for RNase-free material preparation, perfusion, fixation, sectioning, selection of expressed sequence tag cDNA clones, linearization of cDNA, synthesis of digoxigenin-labeled RNA probes (riboprobes), in situ hybridization on floating and mounted sections, nonradioactive immunohistochemical detection of riboprobes for light and fluorescence microscopy, and double labeling. We also include useful information about quality-control steps, key online sites, commercially available products, stock solutions, and storage. Finally, we provide examples of the utility of this approach in understanding the neuropathogenesis of Alzheimer's disease. With virtually all genomic coding sequences cloned or being cloned into cDNA plasmids, this technique has become highly accessible to explore gene expression profiles at the cellular and brain region level.

Key words: In situ hybridization, RNA, RNA probes, Riboprobes, Brain sections, Sliding microtome, Cryostat, EST, Expressed sequence tag, cDNA, In vitro transcription, Transcripts, Digoxigenin-labeled probes, NTB, BCIP, HNPP, Fast red, Light and fluorescence microscopy, Alzheimer's disease, Frontotemporal dementia, NPY, ARC, Nav1.1

1. Introduction

The central nervous system is an extremely complex structure containing hundreds of distinct cell types. This diversity is also present at the local level. Circuits or local networks are usually assembled through contributions from a diverse array of cells with

Erik D. Roberson (ed.), *Alzheimer's Disease and Frontotemporal Dementia*, Methods in Molecular Biology, vol. 670,
DOI 10.1007/978-1-60761-744-0_15,

distinct gene expression profiles. In addition, patterns of gene expression often overlap between cell types and are dynamically regulated by age, synaptic plasticity, brain activity, aging, or disease. This cellular diversity and the dynamic regulation of gene expression pose tremendous challenges for understanding in vivo regulation of gene expression. Standard quantitative techniques such as Western blotting and real-time PCR can detect changes in gene or protein expression, but provide no information about the cellular source. This missing piece of information makes it very difficult to assess the functional significance of a given change in expression level. For example, a change could have opposite functional outcomes depending on whether it occurred in excitatory or inhibitory neurons. In situ hybridization is a powerful technique that effectively addresses cellular localization of gene expression.

Two landmark projects, the Integrated Molecular Analysis of Genomes and their Expression (IMAGE) Consortium and the National Institutes of Health's Mammalian Gene Collection (MGC), have made virtually all human and mouse genomic coding sequences accessible in cDNA plasmids, which can be readily used to generate RNA probes for in situ hybridization. Although there are remarkable efforts to map expression patterns of thousands of genes in normal brain tissue (for example, the Allen Institute for Brain Science at http://www.brain-map.org/; Mousebrain Gene Expression Map at St. Jude Children's Research Hospital at http://www.stjudebgem.org/; GenePaint.org at http://www.genepaint.org/), these sources are not designed to address alterations in gene expression patterns induced by experimental manipulations or disease processes, which can be critical for understanding pathogenic processes. For example, we found de novo, ectopic neuropeptide Y (NPY) gene expression in the granule cells of transgenic mouse models of Alzheimer's disease (Fig. 2d). The NPY gene, which is exclusively expressed by GABAergic inhibitory cells in healthy brain, is transcribed ectopically in glutamatergic cells in the disease state, with important implications for the function of the hippocampal circuit (1). Although granule cells are easily identifiable by anatomy, in other cases, additional information is necessary to identify specific cellular sources. For example, the sodium channel Nav1.1 is expressed in cells of the CA1 hippocampal region (Fig. 1d, left). However, only after double labeling for Nav1.1 mRNA and parvalbumin it is possible to identify the specific cellular source of Nav1.1 as parvalbumin-positive inhibitory interneurons, rather than pyramidal cells (Fig. 1d, right).

In situ hybridization is the procedure for labeling a particular sequence of DNA or RNA with a specific complementary detection probe. Originally described by Gall and Pardue (2) and John et al. (3), this method has been extensively used and adapted

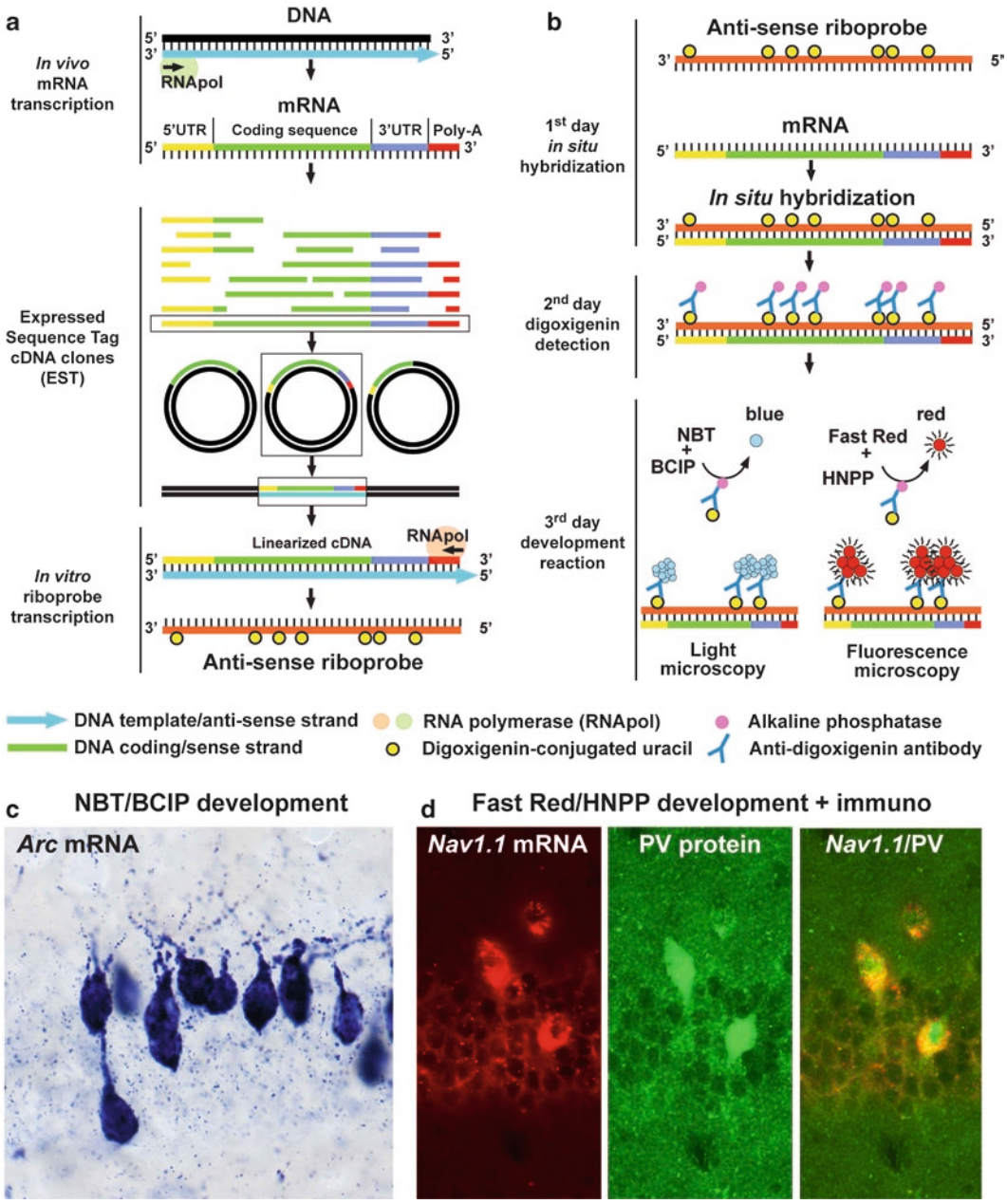

Fig. 1. Overview of the in situ hybridization method. (**a**) mRNA is transcribed from the DNA template (anti-sense strand, *light blue*) by RNA polymerases moving from 3′ to 5′ along the template, as indicated by the *arrow*. The mRNA or transcript is synthesized 5′ to 3′ and contains a 5′UTR (untranslated region, *yellow*), a coding sequence (*green*), a 3′UTR (*blue*), and a poly-A signaling tail (*red*). Transcripts or expressed sequence tags (ESTs) from virtually all mouse genes have been cloned into cDNA plasmids, which can be readily used to generate RNA in situ probes. RNA probes can target the full length of the transcript, including coding sequences and untranslated regions, or only parts. RNA probes are synthesized in vitro from the cDNA coding or sense strand of EST clones by RNA polymerases. This synthesis generates a digoxigenin-labeled RNA probe complementary to the mRNA. (**b**) RNA in situ hybridization is the procedure by which a particular mRNA is hybridized with a specific, complementary, labeled RNA probe. The process includes the hybridization of an mRNA with the digoxigenin-labeled complementary riboprobe, immunohistochemical detection of digoxigenin, and development for light or fluorescence microscopy. (**c**) Activity-regulated cytoskeletal-associated protein (Arc) in situ hybridization for light microscopy on 30-μm floating sections. Note intense labeling in some, but not all, granule cells in the dentate gyrus of the hippocampus (for more info, see (4)). (**d**) Double in situ hybridization for Nav1.1 (*red*) and immunohistochemistry for parvalbumin (PV, *green*) for fluorescence microscopy on 10-μm cryosections. Note that Nav1.1 is expressed in PV-positive GABAergic interneurons.

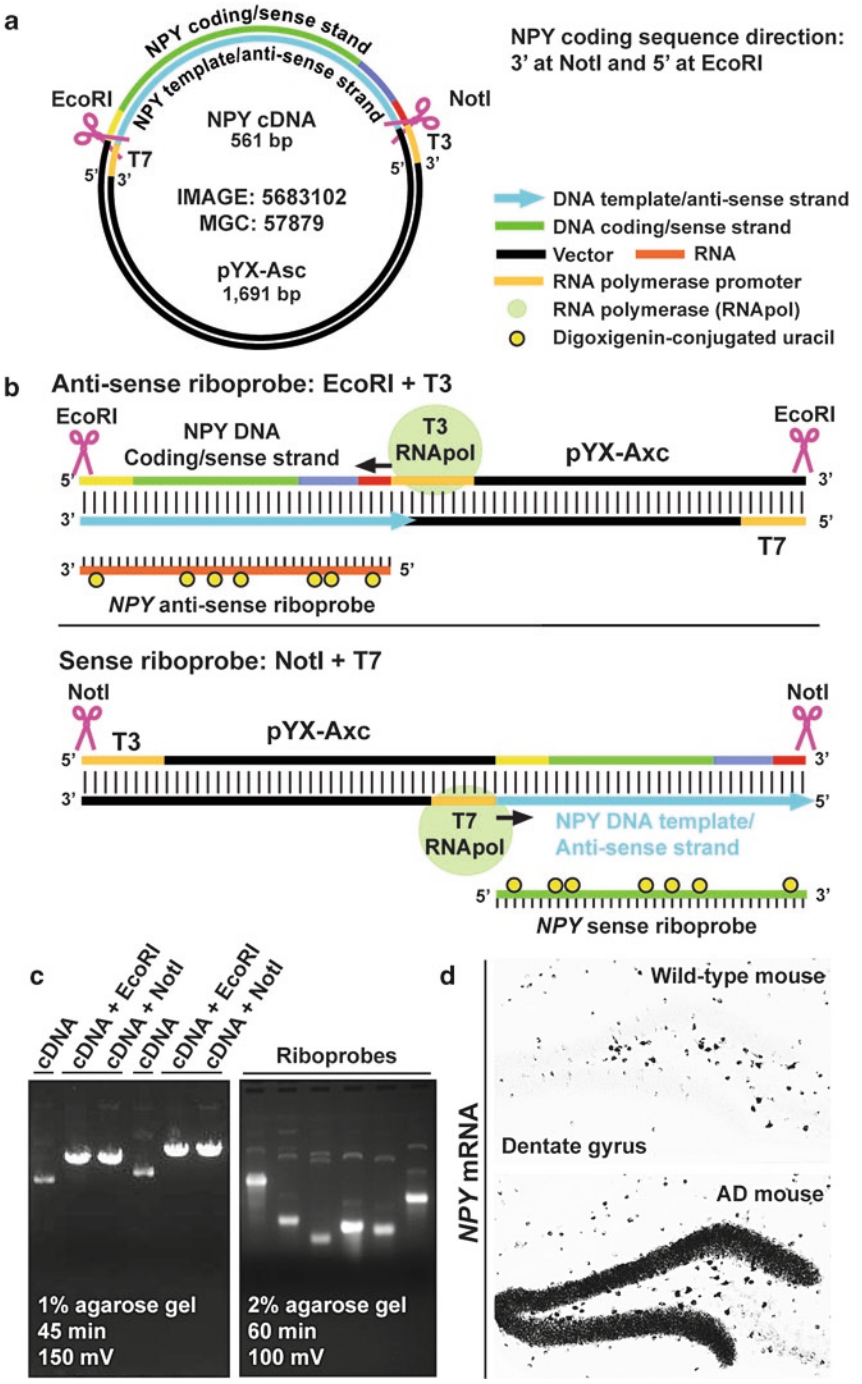

Fig. 2. Synthesis of RNA probes from cDNA clones. The IMAGE and MGC consortiums have created extensive cDNA libraries of ESTs and made them available to the research community. (**a**) There are approximately 40 cDNA clones available for mouse neuropeptide Y (NPY). The diagram illustrates one of them (IMAGE: 5683102), containing the NPY full-length transcript inserted into a pYX-Asc vector. It is important to know the polymerase promoters (in this case, T3 and T7), the restriction enzyme sites flanking the fragment (*Not*I and *Eco*RI), and the direction of the transcript (3′ at *Not*I and 5′ at *Eco*RI). (**b**) Sense and anti-sense RNA probes are generated as illustrated. NPY anti-sense riboprobe, which will hybridize

for studying gene expression in a wide variety of animal models, tissues, and experimental conditions. This paper focuses on the detection of messenger RNA (mRNA) on brain tissue sections by complementary RNA probes (riboprobes). We have been optimizing this technique over the course of several years of studying adult and embryonic brain tissue from mouse models of Alzheimer's disease and neurodevelopmental disorders (1, 4–6). The protocols described are suitable for adult or embryonic tissue, floating or mounted sections, and a broad range of mRNA lengths (200–3,000 bp). We describe step-by-step and fully detailed protocols for RNase-free material preparation, perfusion, fixation, sectioning, selection of cDNA clones, synthesis of digoxigenin-labeled riboprobes, in situ hybridization on floating and mounted brain sections, immunohistochemical detection of riboprobes for light and fluorescence microscopy, and double in situ and immuno detection. We also include useful information about tips, quality-control steps, key online sites, commercially available products, and storage.

2. Materials

2.1. Avoiding RNase Contamination

1. Gloves.
2. RNase-inactivating wipes.
3. Autoclave and oven.
4. Aluminum foil.
5. RNase-free water (see Note 1).
6. 0.22-μm Filter units.

2.2. Perfusing, Fixing, and Sectioning Brain Tissue

All of the reagents listed below must be prepared using RNase-free conditions, as described in Subheading 3.1.

1. Anesthetic agent, such as pentobarbital.
2. Perfusion pump or large-capacity syringes and tubing.
3. Surgical tools.

Fig. 2. (continued) with NPY mRNA in tissue sections, can be synthesized after linearizing the plasmid with *Eco*RI and transcribing it with T3 RNA polymerase. The sense riboprobe, which does not hybridize with NPY mRNA, serves as a control and can be synthesized after linearizing the plasmid with *Not*I and transcribing it with T7 RNA polymerase. (**c**) cDNA clones, DNA templates, and riboprobes are run in agarose gels to verify size and quality. *Lanes 1–3* and *4–6* represent two different cDNA clones. (**d**) NPY in situ hybridization for light microscopy on 30-μm floating sections from a normal (non-transgenic; *upper panel*) and an Alzheimer's disease (AD) mouse (for more info, *see* (1)). Note the ectopic expression of NPY in the granule cells of the hippocampus in the AD mouse.

4. Normal saline: 0.9% NaCl.
5. 2× Phosphate buffer (2× PB): 160 mM Na_2HPO_4, 400 mM NaH_2PO_4, pH 7.4. For a 1-L stock solution, dissolve 22.72 g of Na_2HPO_4 and 5.52 g of $NaH_2PO_4 \times 1H_2O$ in diethyl pyrocarbonate (DEPC)-treated water, and adjust pH to 7.4. Filter through 0.22-μm filter. Store at room temperature for weeks or at –20°C for months.
6. 1 M NaOH: 40 g of NaOH in 1 L of water.
7. 1× Phosphate buffer (1× PB): Prepared from 2× PB by diluting 1:1 in DEPC-treated water.
8. 8% Paraformaldehyde (8% PFA, w/v): For 1 L, measure 80 g of PFA (see Note 2). Add about 600 ml of DEPC-treated water that has been heated to ~65°C in a microwave. Place the mixture on a hotplate in a fume hood and stir with continued heating until the solution reaches, but does not exceed, 85°C (see Note 3). Turn off the heat and continue stirring. At this point, the solution should be semi-white and cloudy. Add 2–4 drops of 1 M NaOH and wait for 2–4 min. The solution will become less cloudy and more transparent. Repeat the addition of NaOH until the PFA goes fully into solution. The goal is to obtain a completely transparent solution with minimal addition of NaOH, because high concentrations of NaOH increase the pH and affect the fixative properties of PFA. Add heated water to a volume of 1 L. Let the solution cool to room temperature while stirring. For transcardial perfusion, filter the solution with a 0.22-μm pore size. Aliquot and store at 4°C for use within 1–2 days or at –20°C for any longer period of storage.
9. 4% PFA in 1× PB: Prepared as a 1:1 mixture of 8% PFA and 2× PB. If the solutions are stored at –20°C, thaw in a 40–50°C water bath. Wait until both solutions are transparent. Do not use a microwave to thaw PFA.
10. Phosphate-buffered saline (PBS): Purchase 10× sterile stock solution (pH 7.4), dilute to 1×.
11. 30% Sucrose in PBS (w/v).
12. Sliding microtome, cryostat, or vibratome.
13. 10% Sucrose in PBS.
14. Cryoprotectant solution (for microtome and vibratome sections): 30% ethylene glycol, 30% glycerin, 40% 1× PBS (v/v/v). Store at –20°C.
15. Embedding molds (for cryostat sections).
16. TBS medium (Triangle Biomedical Science, for cryostat sections of postnatal and adult brains) or Tissue-Tek OCT (for cryostat sections of embryonic brains).
17. Superfrost Plus slides (Fisher Scientific).

2.3. Synthesis of Digoxigenin-Labeled Riboprobes

1. EST clones for the gene of interest (see Subheading 3.3.1 below for instructions on selection).
2. T7, T3, and/or SP6 sequencing primers (see Subheading 3.3.2 below for instructions on selection). Standard primers for each are available from a variety of commercial sources.
3. Restriction enzymes and buffers (see Subheading 3.3.2 below for instructions on selection).
4. Vortex.
5. Microcentrifuge.
6. UltraPure phenol:chloroform:isoamyl alcohol solution (25:24:1, Invitrogen). Store in 1 ml aliquots at 4°C or –20°C.
7. 3 M Sodium acetate buffer solution, pH 7.0 (Sigma).
8. 100% Ethanol.
9. 70% Ethanol.
10. TE buffer: 10 mM Tris–HCl, pH 8.0, 1 mM EDTA, in DEPC-treated water.
11. Spectrophotometer.
12. Parafilm.
13. Agarose gel electrophoresis apparatus and power supply.
14. Agarose.
15. Tris–acetate EDTA (TAE) buffer: 40 mM Tris–acetate, 1 mM EDTA. To prepare a 50× TAE stock solution, dissolve 242 g of Tris base in approximately 750 ml of deionized water. Add 57.1 ml of glacial acid and 100 ml of 0.5 M EDTA (pH 8.0), and adjust the solution to a final volume of 1 L. The pH of this buffer should be about 8.5 and does not need to be adjusted. Store at room temperature.
16. Ethidium bromide solution, 10 mg/ml (Bio-Rad).
17. BlueJuice buffer (Invitrogen).
18. 1-kb DNA ladder.
19. T7, T3, and/or Sp6 RNA polymerase (Promega). Store at –20°C.
20. 5× Transcription buffer (Promega, provided with polymerase enzyme). Store at –20°C.
21. 100 mM dithiothreitol (DTT; Promega, provided with polymerase enzyme). Store at –20°C.
22. 10× Digoxigenin-labeled nucleotide mix (Roche DIG RNA labeling mix: contains ATP, CTP, GTP, UTP, and DIG-11-UTP). Store at –20°C.
23. Protector RNase inhibitor (Roche). Store at –20°C.
24. RNeasy Mini Kit for RNA purification (Qiagen).
25. 100% UltraPure formamide, redistilled (Invitrogen). Store at 4°C.

2.4. RNA In Situ Hybridization

1. 24-Well plates (for floating sections).
2. Clean glass Pasteur pipettes with their tips sealed in a flame, for handling sections.
3. PBS/0.5% Tween: 0.5% Tween-20 in 1× PBS, pH 7.4.
4. Shaking platform.
5. 4% PFA in PBS: Dilute 8% PFA stock in 2× PBS.
6. Tris/EDTA/Tween buffer: 50 mM Tris–HCl, pH 8.0, 5 mM EDTA, 0.5% Tween-20. For 100 ml, mix 94 ml of DEPC-treated water, 5 ml of 1 M Tris–HCl, pH 8.0 stock solution, 1 ml of 500 mM EDTA stock solution, and 500 µl of 100% Tween-20.
7. Proteinase K buffer: 50 mM Tris–HCl, pH 8.0, 5 mM EDTA, 0.5% Tween-20, 1 µg/ml recombinant, PCR-grade proteinase K (Roche 3 115 828). Add 1 µl of Proteinase K stock solution (~20 µg/µl) per 20 ml of Tris/EDTA/Tween buffer. Omit Tween-20 for cryostat sections.
8. Acetylation solution: 1.355% triethanolamine, 0.175% HCl, and 0.25% acetic anhydride. Mix 9.8 ml of water, 133.5 µl of triethanolamine (Fisher Chemical, certified), and 17.5 µl of 12 M HCl in a safety hood. Once dissolved, add 25 µl of acetic anhydride (Sigma, reagent grade, ≥98%), mix well, and use immediately.
9. 50× Stock Denhardt's solution: 1% bovine serum albumin (BSA), 1% Ficoll, 1% polyvinyl pyrolidone. To prepare 100 ml, mix 1 g of BSA, 1 g of Ficoll PM 400 (Type 400, Sigma), 1 g of polyvinyl pyrolidone, average molecular weight 40,000 (Sigma), and 100 ml of water. Warm mixture to dissolve each, filter, and aliquot to 15 ml each. Store at –20°C. 50× Denhardt's solution is also commercially available.
10. In situ pre-hybridization buffer: 50% formamide, 5× salt sodium citrate (SSC) buffer, pH 7.0, 5× Denhardt's solution, 0.25 mg/ml salmon sperm DNA, 0.5 mg/ml yeast tRNA. To prepare a 200-ml stock solution, mix 100 ml of 100% UltraPure formamide (Invitrogen), 50 ml of 20× SSC (Roche), 20 ml of 50× Denhardt's, 30 ml of water, 50 mg of UltraPure salmon sperm DNA (Invitrogen), and 100 mg of yeast tRNA (Invitrogen). Store at –20°C.
11. Slide humidity incubation box.
12. Precise temperature control oven (see Note 4).
13. 5× SSC/0.5% Tween buffer: Prepare from commercially purchased 20× SSC (Roche) and Tween-20. For cryostat sections, use 5× SSC without Tween.
14. 0.2× SSC/0.5% Tween buffer: Prepare from commercially purchased 20× SSC (Roche) and Tween-20. For cryostat sections, use 0.2× SSC without Tween.

15. Tris-HCl/saline/Tween buffer: 100 mM Tris–HCl, pH 7.5, 150 mM NaCl, 0.5% Tween-20. To prepare 1 L, mix 870 ml of water, 100 ml of 1 M Tris, pH 7.5, 30 ml of 5 M NaCl stock, and 5 ml of Tween. For cryostat sections, omit the Tween-20.
16. Heat-inactivated sheep serum (HISS): Heat sheep serum (Sigma) at 56°C for 20 min.
17. Blocking buffer: 10% HISS in Tris-HCl/saline/Tween buffer. For cryostat sections, omit the Tween-20.
18. Alkaline phosphatase-conjugated anti-digoxigenin antibody (Anti-digoxigenin-AP, Fab fragment, from sheep; Roche).
19. PBS/EDTA solution: 0.1 M PBS, 1 μM EDTA pH 8.0, 0.5% Tween. For 1,000 ml of total volume, mix 900 ml of water, 100 ml of 10× PBS, 2 ml of 0.5 M EDTA, and 2.5 ml of Tween 20. Omit the Tween for cryostat section.
20. 1% Gelatin (for mounting floating sections). Mix 1 g of gelatin from porcine skin, type A (Sigma) in 100 ml of warm water.
21. Xylene.
22. RNase-free glass coverslips.

For light microscopic detection:

23. NTMT Buffer: 0.1 M Tris–HCl, pH 9.5, 0.1 M NaCl, 50 mM $MgCl_2$. To prepare 400 ml, mix 332 ml of water, 40 ml of 1 M Tris, pH 9.5, 8 ml of 5 M NaCl, and 20 ml of 1 M $MgCl_2$.
24. NBT/BCIP stock solution: 18.75 mg/ml nitroblue tetrazolium chloride and 9.4 mg/ml 5-bromo-4-chloro-3-indolyl-phosphate, toluidine salt in 67% dimethyl sulfoxide (DMSO; Roche).
25. #1 Size sable paintbrush.
26. Cytoseal or Permount mounting medium.

For fluorescent microscopic detection:

27. Fluorescence detection buffer: 100 mM Tris–HCl, pH 8.0, 100 mM NaCl, 5 mM $MgCl_2$. To prepare 1 L, mix 100 ml of 1 M Tris–HCl, pH 8.0, 20 ml of 5 M NaCl, and 5 ml of 1 M $MgCl_2$.
28. HNPP/Fast Red TR developing mix: 100 μg/ml HNPP, 250 μg/ml Fast Red TR, 100 mM Tris–HCl pH 8.0, 100 mM NaCl, and 5 mM $MgCl_2$. To prepare 1 ml, mix 10 μl of 10 mg/ml HNPP in dimethylformamide and 10 μl of 25 mg/ml Fast Red in redistilled H_2O with 1 ml of fluorescence detection buffer. We purchase HNPP and Fast Red TR together in the HNPP fluorescence detection set (Roche).
29. Fluorescence mounting medium.

3. Methods

3.1. Avoiding RNase Contamination

The first step of in situ hybridization is to create a clean environment to preserve the RNA from the samples. mRNA is very susceptible to degradation by ribonucleases (RNases). To ensure maximal mRNA preservation, all solid and liquid materials must be free of RNases and stored in semi-sterile condition throughout the procedure.

1. Assign an RNase-free dedicated area at your bench to keep all RNase-free solutions and materials. Regularly wipe your work area and equipment with RNase-free wipes.
2. Avoid skin contact with reagents and work surfaces, and use clean gloves at all times.
3. All glassware (e.g., Coplin jars, beakers, cylinders, and coverslips) and metal tools (i.e., forceps, scissors, and stir bars) used during the perfusion, sectioning, and staining must be baked. Seal the glassware opening, or wrap up the metal materials with aluminum foil and bake for 6 h at 220°C in an oven. Sterile plastic products are considered RNase-free material and do not need to be autoclaved.
4. Prepare RNase-free water. All buffers used during the procedure must be prepared using water treated with 0.1% diethyl pyrocarbonate (DEPC, Sigma D-5758), a standard method to inactivate RNases (see Note 5). Mix 1 ml of DEPC per liter of milli-Q water, and stir for 10 h at room temperature. Autoclave 0.1% DEPC-treated water for 30 min at 125°C to eliminate residual DEPC. Store for weeks at room temperature. We routinely prepare batches of 5 L at a time.
5. Ensure that all buffers for subsequent steps (including perfusion and fixation) are RNase free by purchasing RNase-free reagents, using autoclaved glassware and tools, preparing the solutions with DEPC-treated water, and filtering through a 0.22-μm pore size membrane. Solutions that do not have primary amine groups can be treated directly with DEPC and then autoclaved (but see Note 6 regarding Tris-based solutions). Keep the bottles in an RNase-free designated location and make sure that these products are always handled with clean gloves (see Notes 7 and 8).

3.2. Perfusing, Fixing, and Sectioning Brain Tissue

3.2.1. Perfusing and Fixing Brain Tissue

1. If a perfusion pump is used, clean the tubing by flushing first with 1 M NaOH for 15–30 s and then with DEPC-treated water. Sterile syringes and needles can be used as an alternative.
2. Anesthetize animals.

3. Flush-perfuse transcardially with 1× PB or normal saline for 10–20 s until most of the blood is washed out from the circulatory system.
4. Perfuse with 4% phosphate-buffered PFA (4% PFA in 1× PB) for 5 min (see Notes 9 and 10). Keep the 4% PFA at 4°C or on ice during the perfusion.
5. Remove the brain, cut into hemibrains, and drop-fix in the same fixative (4% PFA in 1× PB) for 24–48 h at 4°C. Make sure that the fixative volume is at least ten times larger than the volume of the brain sample.
6. After the brains have been fixed at 4°C for 24–48 h, rinse twice for 2–5 h with PBS at 4°C. This reduces background during immunohistochemistry.
7. For immunohistochemistry, brains can be stored for 2–4 weeks at 4°C before sectioning. For in situ hybridization, brains must be sectioned immediately to reduce RNA degradation. We recommend either microtome (Subheading 3.2.2) or cryostat (Subheading 3.2.3) sectioning. A vibratome can also be used, although it provides less accurate sectioning throughout the extent of the sample.

3.2.2. Microtome Sectioning

1. Transfer the brains into 30% sucrose in PBS for 24 h at 4°C. Initially, the brains will float. They will sink when cryoprotected and ready for sectioning; do not section until the brains sink. Make sure that the volume of sucrose solution is at least ten times greater than the volume of the sample.
2. Place the hemibrains on the freezing stage of the microtome at room temperature and add a few drops of 10% sucrose around the hemibrains (see Note 11). Once the stage temperature is lowered, the 10% sucrose base will freeze and firmly attach the samples to the stage.
3. Set the temperature of the freezing stage at –20°C and wait for 5–10 min until the hemibrain and 10% sucrose base are completely frozen.
4. Collect ten subseries of floating sections (30 μm) per mouse hemibrain in 1.5-ml Eppendorf tubes with 1.2 ml of ethylene glycol-based cryoprotectant medium. Each tube will contain 8–12 equidistant sections, 300 μm apart, throughout the rostro–caudal extent of the hemibrain. (These are standard parameters that could change depending on the experiment or animal model.)
5. Store the sections at –20°C until use.

3.2.3. Cryostat Sectioning

1. Transfer the brains into 30% sucrose in PBS for 24 h at 4°C. Initially, the brains will float. They will sink when cryoprotected and ready for sectioning; do not section until the brains sink.

Make sure that the volume of sucrose solution is at least ten times greater than the volume of the sample.

2. Embed the hemibrains in tissue-freezing medium using embedding molds. For better embedding, gently remove excess 30% sucrose from the surface of the brains before embedding. For postnatal and adult brain tissue, use TBS medium. For embryonic brains, use Tissue-Tek OCT compound.
3. For TBS medium, allow the tissue to set for 3–5 min at room temperature while gently stirring the brain with a sterile pipette tip. For OCT medium, allow the tissue to set for 1 h at 4°C on a shaker or stir regularly.
4. After orienting the sample, freeze on dry ice and wait for 30–60 min before cutting the samples in a cryostat or storing them at –80°C.
5. Set the cryostat at –25°C. Note that different embedding media have different optimal temperatures (around –25°C for TBS and –18°C for OCT).
6. Collect 20 subseries of cryosections (10 μm) per mouse hemibrain on RNase-free Superfrost Plus slides. Each slide will contain 6–8 equidistant sections, 200 μm apart, throughout the rostro–caudal extent of the hemibrain. These are standard conditions that might change depending on the experiment.
7. Store the slides at –80°C in a clean slide box with desiccant caps. Place each slide box inside of a plastic zip bag.

3.3. Generating Digoxigenin-Labeled Riboprobes

Anti-sense and sense RNA probes (riboprobes) are generated from a linearized cDNA plasmid containing the complete or a partial transcript of a particular gene. The mRNA transcript of a gene includes the 5′UTR (untranslated region), the coding sequence, the 3′UTR, and a poly-A tail (Fig. 1a). RNA probes can target any sequence of the transcript. In 1993, the Integrated Molecular Analysis of Genomes and their Expression (IMAGE) Consortium was created with the primary goal of creating extensive cDNA libraries and associated bioinformatics tools, and making them available to the research community (more information at http://image.hudsonalpha.org/). In addition, the Mammalian Gene Collection (MGC), a trans-NIH initiative, provides researchers with sequence-validated full-length protein-coding cDNA clones (http://mgc.nci.nih.gov/). These cDNA plasmids or clones called expressed sequence tags (ESTs) are commercially available through IMAGE, Invitrogen, American Type Culture Collection (ATCC), Open Biosystems, RIKEN, and other sources. Virtually all human and mouse gene transcripts or expressed sequences have been cloned into EST clones. This creates a tremendous resource of expressed sequences ready to be used for in situ hybridization.

3.3.1. Selecting cDNA/EST Clones

1. The first step is to identify two or three EST clones per gene of interest by using an online genome browser (e.g., http://www.ncbi.nlm.nih.gov/unigene or http://genome.ucsc.edu). Search for the name of the gene and organism to find the gene's web page. mRNA and EST sequences are constantly updated in these web pages. Select cDNA clones containing full or partial transcript sequences of lengths of 200–3,000 bp (ideally 500–1,000 bp). Although an RNA probe can be selected from the 3′UTR, 5′UTR, or the coding region of a gene, the 3′UTR regions usually reduce the probability of cross-hybridization with other genes. Throughout this chapter, we will use in situ hybridization for mouse NPY as an example. Mouse NPY has six mRNA and 40 EST sequences. One of them, an IMAGE cDNA clone (IMAGE:5683102; MGC:57879), contains the full transcript sequence of NPY (561 bp), including 77 bp of 5′UTR, 294 bp of coding sequence, 176 bp of 3′UTR, and 18 bp of poly-A tail (Fig. 2a). We successfully used this clone in a recent publication (1).
2. Once two or three EST clones per gene have been selected, it is important to determine whether the sequence of the selected clone is specific for the gene of interest by performing a BLAST search against the full genomic transcript (http://www.ncbi.nlm.nih.gov/BLAST/). Avoid clones with sequences that overlap with other genes. Using the 3′UTR regions reduces the probability of cross-hybridization with other genes.
3. In an EST clone, a transcribed sequence is inserted into a cloning vector. Check whether the selected cDNA plasmid contains RNA polymerase promoter sites (i.e., T7, T3, and SP6) and determine the orientation of the transcript sequence. The query tool at http://image.hudsonalpha.org/html/query_tools.shtml or the web sites of EST clone providers are useful for this purpose. For example, our NPY complete transcript sequence cDNA (IMAGE:5683102) was cloned into the pYX-Asc vector with the 5′ end at *Eco*RI and 3′ end at *Not*I (Fig. 2a). This information is used later to generate the riboprobes.
4. Once cDNA clones are received, sequence them using primers based in the polymerase promoters to verify the gene and the orientation of the coding sequence (Fig. 2b).
5. Perform a BLAST search for the resulting sequences and confirm that they correspond with the gene of interest.
6. Check the sequence orientation and determine which promoter will synthesize the sense and anti-sense strands (Fig. 2). Because the sequencing primers are complementary to the polymerase promoter, the sequence generated represents

what the polymerase will transcribe. If the sequencing reaction from a given polymerase promoter generates a sequence *complementary* to the mRNA (termed plus/minus), then the polymerase will transcribe an "anti-sense" RNA probe, which will be used to detect the mRNA of interest during the in situ hybridization. If the sequencing reaction from a primer complementary to the polymerase promoter generates a sequence *equivalent* to the mRNA (termed plus/plus), then the promoter will transcribe a "sense" RNA probe, which will be used as a control. In Fig. 2b, the sequencing primers that bind to T3 would produce a sequence complementary to the mRNA (plus/minus), so T3 polymerase is used to synthesize the anti-sense riboprobe. Sequencing primers that bind to T7 would produce a sequence equivalent to the mRNA (plus/plus), so T7 polymerase is used to generate the sense riboprobe.

7. Once the cDNA clones containing the full or partial transcript sequence of the gene of interest have been sequenced and verified, it is useful to elaborate EST clone maps containing information about the location of polymerase promoters and restriction enzymes, as well as the direction of the transcript sequence and sizes (Fig. 2a).

3.3.2. Synthesizing Digoxigenin-Labeled Riboprobes

To generate riboprobes, cDNA plasmids are first linearized with vector-specific restriction enzymes (steps 1–4). Then the linearized template is purified from the restriction enzyme solution (steps 5–24). Finally, to generate digoxigenin-labeled RNA probes, anti-sense and sense DNA templates are transcribed in vitro from the linearized template with RNA polymerases and digoxigenin-labeled nucleotides and then purified from the other components of the polymerase reaction (steps 25–33). Potential overnight stopping points are after step 4 or step 24.

For our NPY example, the anti-sense probe was generated by linearizing the cDNA plasmid with *Eco*RI and transcribing with T3 polymerase, and the sense probe was generated by linearizing with *Not*I and transcribing with T7 polymerase (Fig. 2b).

1. Prepare a restriction digest in 200 µl of volume, containing 160 µl of water, 10 µg of cDNA, and 20 µl of 10× buffer (provided with enzyme). Vortex for 1 s.
2. Add 50 units of the restriction enzyme (five units of enzyme/µg of DNA). Do not vortex after the enzymes are added.
3. Incubate for 2 h at the appropriate temperature for your restriction enzyme.
4. Place tubes on wet ice or at 4°C (or for long-term storage keep them at –20°C).
5. Place the Eppendorf tubes containing the restriction digest on wet ice.

6. Add 200 µl of phenol:chloroform:isoamyl alcohol (25:24:1) on ice.
7. Vortex for 5 s.
8. Centrifuge at 21,000 × *g* for 5 min at 4°C. After centrifugation, the DNA remains in the upper aqueous phase, whereas most proteins localize in the interface and organic phase.
9. Label a new set of Eppendorf tubes.
10. With a micropipette, collect around 150 µl from the clear upper phase without disturbing the interface. This fraction contains the DNA templates. The next step is to precipitate and concentrate the DNA templates from this fraction.
11. Add 15 µl of 3 M sodium acetate, pH 7.0, at 4°C to the 150 µl of supernatant containing the DNA templates.
12. Add 330 µl of 100% ethanol stored at –20°C. It is important that the temperature of the ethanol be –20°C when added to the sample.
13. Vortex for 5 s.
14. Place the samples at –80°C for 30 min or at –20°C for 60 min.
15. Centrifuge the samples at 21,000 × *g* for 20 min at +4°C.
16. The DNA templates will precipitate in a very clear, almost invisible, white pellet. Remove most of the supernatant (leave around 10–20 µl).
17. Add 500 µl of 70% ethanol stored at –20°C (do not vortex or agitate the tubes). The goal is to wash the DNA pellet but not to resuspend it.
18. Immediately centrifuge the samples, before the pellet resuspends, at 21,000 × *g* for 5 min at 4°C.
19. Remove almost all of the ethanol with a pipette and wait for 2–5 min until the ethanol evaporates. The white DNA pellet might be difficult to observe.
20. Resuspend the pellet with TE buffer to achieve a final concentration of 1 µg of DNA/µl, about 8 µl (see Note 12).
21. Incubate for 1–2 min at room temperature to resuspend the cDNA.
22. Measure the DNA concentration with a spectrophotometer and adjust the concentration to 1 µg/µl (optional).
23. For quality control, run 1 µg samples of DNA on a 1% agarose gel containing 0.25 mg/ml of ethidium bromide (see Note 13). On a piece of parafilm, place a drop of 1 µg of DNA (1 µl of the purified DNA templates). Add 8 µl of water and 1 µl of 10× BlueJuice Buffer. Run uncut plasmid (cDNA), anti-sense template (cDNA + Enzyme A), sense template

(cDNA + Enzyme B), and 1 kb of DNA Ladder in TAE buffer at 150 mV for 30–45 min. Verify the size and number of bands. The uncut, supercoiled cDNA should run faster than the linearized templates (Fig. 2c). A single band should appear per lane. If several bands are found, check for potential restriction sites in the plasmid or coding sequence (use online restriction-mapping tools such as http://www.restrictionmapper.org/ or http://tools.neb.com/NEBcutter2/). Note that digesting within the transcript sequence may be useful to reduce the size and/or increase the specificity of the riboprobe.

24. Store the DNA templates at −20°C.
25. Mix the following for a 50-µl in vitro transcription reaction:
    (a) 21.25 µl of Water
    (b) 2.5 µg of DNA template (~2.5 µl of the template in TE buffer)
    (c) 10 µl of Promega 5× transcription buffer
    (d) 5 µl of 100 mM of DTT
    (e) 5 µl of 10× DIG RNA labeling mix
    (f) 2.5 µl of Roche Protector RNAse inhibitor
    (g) 5 µl RNA polymerase (T3, T7, or SP6, depending on design).
26. Do not vortex. Mix the solutions by tapping with the fingers and keep the tubes on ice.
27. Incubate for 2 h at 37°C.
28. Add 50 µl of water to the 50 µl of incubation synthesis solution (see above) to obtain a final volume of 100 µl (see Note 14).
29. Use Qiagen RNeasy Mini columns according to the manufacturer's directions to clean up the riboprobes (see Note 15). This procedure will purify RNA molecules longer than 200 nucleotides.
30. At the final step of the column purification, elute the high-quality RNA from the column with 50 µl of water. We do not routinely check the RNA concentration with a spectrophotometer, although it is important to check the quality of the probe by electrophoresis (step 8).
31. Add 50 µl of 100% UltraPure formamide.
32. Run samples of purified riboprobes on a 2% agarose gel to verify RNA integrity and size. On a piece of parafilm, place a drop of 10 µl of RNA/formamide solution and add 4 µl of water and 1 µl of 10× BlueJuice Buffer. Load samples on a 2% agarose gel containing ethidium bromide and run in TAE buffer at 100 mV for 60 min.
33. Store purified RNA probes at −80°C.

3.4. RNA In Situ Hybridization

The in situ hybridization protocol is divided into 3 days (Fig. 1b). On day 1, digoxigenin-labeled RNA probes are hybridized with the mRNA in the tissue. On day 2, anti-digoxigenin antibodies conjugated to alkaline phosphatase are added to label digoxigenin-labeled RNA probes for detection by immunohistochemistry. On day 3, the catalytic activity of alkaline phosphatase is used to precipitate the NBT/BCIP chromogen for light microscopy, or the HNPP/Fast Red TR chromogen for fluorescence microscopy.

3.4.1. RNA In Situ Hybridization for Floating Microtome Sections

Day 1: Tissue Preparation and In Situ Hybridization

1. Place the floating brain sections stored at −20°C in 24-well plates (4–8 sections per well) containing PBS/Tween 0.5% (400 µl per well). Handle the sections with a clean, sealed glass Pasteur pipette tip. For all incubations, shake gently at room temperature, unless indicated otherwise.
2. Fix in 4% PFA in PBS (pH 7.4) for 20 min. Save PFA at +4°C for step 5.
3. Wash 3 × 10 min with PBS/0.5% Tween.
4. Digest sections with 1 µg/ml of proteinase K in Tris/EDTA/Tween buffer at room temperature with very slow shaking. For 30-µm adult sections, digest for 12–15 min. Adjust the incubation time for different tissue and fixation conditions. Proceed to step 5 without washing.
5. Fix in 4% PFA 1× PBS for 10 min. Fixation increases the stability of the tissue after proteolytic digestion.
6. Wash 3 × 10 min in PBS/Tween 0.5%.
7. Incubate in acetylation solution for 10 min. Acetylation reduces the nonspecific binding of riboprobes to the tissue.
8. Wash 3 × 10 min in PBS/Tween 0.5%.
9. Incubate the sections in pre-hybridization buffer for 4–6 h at room temperature. Add 300–400 µl per well and shake gently.
10. Prepare hybridization solution containing digoxigenin-labeled anti-sense riboprobe, and separate aliquots of hybridization solution containing sense riboprobe and no riboprobe as controls. Heat the riboprobes, which have been stored at −80°C, at 70°C for 3–5 min. Heat pre-hybridization buffer, which has been stored at −20°C, at 70°C for 3–5 min. Add the riboprobes to the pre-hybridization buffer. RNA probe concentration is typically 200–400 ng/ml of RNA probe in pre-hybridization buffer (1:200–1:500 dilution of the RNA/formamide mixture from Subheading 3.3.2., steps 33).
11. Remove the pre-hybridization buffer from the wells, but do not discard. Place it between the wells of the plate to help keep the sections humidified during the hybridization incubation.

12. Keep the hybridization solution at 70°C and add 300–400 µl per well.
13. Seal the plate with parafilm, and place the plate inside a sealed humidified chamber with water. Do not shake. Incubate without shaking for 12–14 h at 65–68°C.

Day 2: Immunohistochemical Labeling of Digoxigenin-Labeled RNA Probes

14. Wash 1×30 min in 5× SSC/0.5% Tween at 72°C. After this point, it is no longer necessary to maintain RNase-free conditions.
15. Wash 6×30 min in 0.2× SSC/0.5% Tween at 72°C. The stringent wash conditions (low salt concentration and high temperature) help to eliminate nonspecific binding of probes. Adjust the total washing time to different riboprobes and experimental conditions.
16. Wash 1×15 min in 0.2× SSC/0.5% Tween at room temperature.
17. Wash 1×10 min in Tris-HCL/Saline/Tween buffer at room temperature.
18. To block nonspecific binding, incubate the sections with 10% heat-inactivated sheep serum (HISS) in Tris-HCl/Saline/Tween buffer (400 ml per well) for 1 h.
19. Overnight primary antibody incubation. Add 1:5,000 anti-digoxigenin antibody-AP in Tris-HCl/Saline/Tween buffer with 3% HISS. Incubate overnight at 4°C on a shaker.

Day 3, Option 1: Washes and Development Reaction for Light Microscopy

The in situ labeled RNA can be visualized by light microscopy using a colorimetric detection reagent (continue to **step 20**), or by fluorescence microscopy (skip to **step 30**).

20. Wash 6×30 min in Tris-HCl/saline/Tween buffer.
21. Equilibrate 5 min with freshly prepared NTMT buffer.
22. Develop with NTMT containing NBT/BCIP stock solution (1:50) in the dark (NBT/BCIP, Roche, 11681451001).
23. Incubate at room temperature for 2–24 h in dark without shaking. Check progress of the development reaction periodically. If the developing solution turns blue and/or starts to precipitate, wash with NTMT and add fresh NTMT containing NBT/BCIP.
24. Stop reaction with 3×5 min washes of PBS/EDTA buffer.
25. Fix the colorimetric reaction with 4% PFA for 5–10 min. Recycled 4% PFA from day 1 can be used. Without this fixation step, some mounting media can dissolve the precipitate.
26. Wash 2×10 min in 1× PBS

27. Keep at 4°C until mounting.
28. To mount floating sections, wash twice with warmed 1% gelatin in water (see Note 16). Gently mount sections on SuperFrost Plus slides in 1% gelatin using a #1 size sable paintbrush, arranging them on the slide in the desired order. Air dry overnight. Wash the slides 2×5 min in xylene or equivalent. Coverslip with mounting medium.
29. Go to celebrate!

Day 3, Option 2: Washes and Development Reaction for Fluorescence Microscopy

30. Wash 6 × 30 min in Tris-HCl/Saline/Tween buffer.
31. Wash 2 × 10 min in fluorescence detection buffer at room temperature.
32. Prepare fresh HNPP/Fast Red TR developing mix (Roche, Cat. No. 11 758 888 001) and filter with a 0.22-μm pore size. Protect the developing mix from the light.
33. Develop with fresh HNPP/Fast Red TR developing mix in the dark.
34. Incubate at room temperature for 0.5–3 h in the dark with out shaking. Monitor the developing under a fluorescence microscope at 30 min intervals.
35. Stop reaction with 3 × 5 min washes of PBS/EDTA buffer. Protect the developed sections from light.
36. Fix the colorimetric reaction with 4% PFA for 5–10 min.
37. Wash 2 × 10 min in 1× PBS at room temperature with gentle shaking.
38. Keep at 4°C in the dark until mounting.
39. Mount as in step 28 and coverslip with fluorescence mounting medium.

3.4.2. RNA In Situ Hybridization for Cryostat Sections

The in situ hybridization can also be performed on cryosections that are already slide-mounted. The protocol is similar, except that many of the incubation times are altered and Tween is not necessary in the buffers (see Note 17).

Day 1: Tissue Preparation and In Situ Hybridization

1. Remove the slides from –80°C storage, place in Coplin jars, and equilibrate at room temperature for 1 h (see Note 18).
2. Fix in 4% PFA in PBS (pH 7.4) for 10 min. Save PFA at 4°C for step 5.
3. Wash 3 × 3 min with 1× PBS.
4. Digest sections with 1 μg/ml of proteinase K in 50 mM Tris–HCl (pH 8.0)/5 mM EDTA buffer, at room temperature

with very slow shaking. Incubation time for embryonic tissue is 5–10 min, postnatal tissue 10–15 min, and adult 30–45 min.

5. Fix in 4% PFA in 1× PBS for 5 min. Fixation increases the stability of the tissue after proteolytic digestion.
6. Wash 3 × 3 min with 1× PBS.
7. Incubate in acetylation solution for 10 min. Shake vigorously. Acetylation reduces the nonspecific binding of riboprobes to the tissue.
8. Wash 3 × 3 min with 1× PBS.
9. Thaw an aliquot of pre-hybridization buffer. Place the slides horizontally in a humidified chamber containing a mix of 50 ml of formamide and 50 ml of 5× SSC. Let the sections air dry for 1–3 min and add 500 μl of hybridization buffer on each slide (do not coverslip the slides). Incubate the sections for 4–6 h at room temperature.
10. Prepare hybridization solution containing digoxigenin-labeled anti-sense riboprobe, and separate aliquots of hybridization solution containing sense riboprobe and no riboprobe as controls. Heat the riboprobes, which have been stored at −80°C, at 70°C for 3–5 min. Heat pre–hybridization buffer, which has been stored at −20°C, at 70°C for 3–5 min. Add the riboprobes to the pre-hybridization buffer. RNA probe concentration is typically 200–400 ng/ml of RNA probe in pre-hybridization buffer (1:200–1:500 dilution of the RNA/formamide mixture from Subheading 3.3.2, steps 3 and 7).
11. Remove the pre-hybridization buffer from the sections.
12. Add 70–100 μl of hybridization solution per slide and coverslip with RNAse-free glass coverslips. To avoid bubbles, use small forceps to slowly slide the coverslips from one end to the other.
13. Seal the humidified chamber with tape and incubate at 72°C for 12–14 h.

Day 2: Immunohistochemical Labeling of Digoxigenin-Labeled RNA Probes

14. Wash 1 × 5 min in 5× SSC at 72°C. After this point, it is no longer necessary to maintain RNase-free conditions. Transfer the slides to holding racks and wash in 5× SSC buffer at 72°C. The coverslips should slide off easily (use forceps if needed).
15. Wash 2–3 × 30 min in 0.2× SSC at 72°C. The stringent wash conditions (low salt concentration and high temperature) help to eliminate nonspecific binding of probes. Adjust the total washing time to different riboprobes and experimental conditions.

16. Wash 1 × 5 min in 0.2× SSC at room temperature.
17. Wash 1 × 5 min in Tris-HCl/saline buffer at room temperature.
18. To block nonspecific binding, transfer the slides to the humidified chamber and place them horizontally. Add 500 µl of Tris-HCl/saline buffer with 10% HISS on each slide. Incubate for 1 h at room temperature.
19. Overnight primary antibody incubation. Replace blocking solution with 500 µl of 1:5,000 anti-digoxigenin antibody-AP in Tris-HCl/saline buffer with 3% HISS (no coverslips are needed). Incubate overnight at 4°C, without shaking or otherwise disturbing the specimens.

Day 3, Option 1: Washes and Development Reaction for Light Microscopy

The in situ labeled RNA can be visualized either by light microscopy using a colorimetric detection reagent (continue to step 20), or by fluorescent microscopy (skip to step 28).

20. Wash 6 × 15 min in Tris-HCl/saline buffer.
21. Equilibrate for 5 min with freshly prepared NTMT buffer.
22. Develop with NTMT containing NBT/BCIP stock solution (1:50) in the dark (NBT/BCIP, Roche, 11681451001).
23. Incubate at room temperature for 2–24 h in the dark without shaking. Check progress of the development reaction periodically. If the developing solution turns blue and/or starts to precipitate, wash with NTMT and add fresh NTMT containing NBT/BCIP. The colorimetric reaction can be greatly attenuated at 4°C. Consider this temperature for overnight periods.
24. Stop reaction with 3 × 5 min washes with PBS/EDTA buffer.
25. Fix the colorimetric reaction with 4% PFA for 5–10 min. Recycled 4% PFA from day 1 can be used.
26. Wash 2 × 10 min in 1× PBS.
27. Rinse the slides with 0.01 M Tris pH 7.5 (to remove salts), air dry overnight, wash with xylene, and coverslip.

Day 3, Option 2: Washes and Development Reaction for Fluorescence Microscopy

28. Wash 6 × 15 min in Tris-HCl/Saline buffer.
29. Wash 2 × 10 min in fluorescence detection buffer at room temperature.
30. Prepare fresh HNPP/Fast Red TR developing mix and filter with a 0.22-µm pore size. Protect the developing mix from light.

31. Develop with fresh HNPP/Fast Red TR developing mix in the dark. Incubate at room temperature for 0.5–3 h without shaking. Monitor the development reaction under a fluorescence microscope at 30-min intervals.
32. Stop reaction with 3×5 min washes of PBS/EDTA buffer. Protect the developed sections from light.
33. Fix the colorimetric reaction with 4% PFA for 5–10 min.
34. Wash 2×10 min in 1× PBS at room temperature with gentle shaking.
35. Keep at 4°C in the dark until coverslipping.
36. Coverslip with fluorescence mounting medium.

3.4.3. Combined Fluorescence In Situ Hybridization and Immunohistochemistry

In some cases, it is desirable to combine in situ hybridization with protein immunohistochemistry (e.g., Fig. 1d). In general, the immunohistochemistry should be carried out after the in situ hybridization. It is important to consider the following key points.

1. Proteinase K digestion and high temperatures could alter protein structure and affect the immunoreactivity of the tissue. Include positive control sections without digestion and high temperature incubations.
2. Increase primary antibody concentration (typically, 5–10×).
3. Avoid detergents in the immunohistochemistry buffers, as they can dissolve in situ precipitates.
4. For combined in situ hybridization and immunohistochemistry, fluorescence labeling is preferred over colorimetric detection.
5. When using microtome or vibratome sections, we prefer to do the immunohistochemistry on floating sections and mount sections after all staining is complete.

4. Notes

1. RNase-free water can be purchased commercially. However, it is easily prepared in the laboratory by treatmeant with 0.1% DEPC as described in Subheading 3.1, step 4.
2. PFA is a toxic and volatile compound and must be handled in a fume hood.
3. PFA does not go into solution well at room temperature. However, avoid temperatures above 85°C, which will compromise the fixative properties of PFA.

4. Temperature accuracy and stability during the hybridization are critical for result reproducibility across experiments. Note that a 2–3°C change in temperature could significantly alter the results.
5. DEPC is a toxic and volatile compound and must be handled in a fume hood.
6. Although 0.1% DEPC can be directly added to most buffers and solutions, this procedure is not suitable for Tris-based solutions, because the primary amine in Tris reacts with DEPC. To prepare Tris-based solutions, use a bottle of Tris dedicated to RNA work (handle with gloves, do not use spatulas, do not return excess Tris from weighing paper to bottle) and dilute in DEPC-treated water that has already been autoclaved to remove residual DEPC.
7. Ultrafiltered solutions (0.22-μm pore size) are also considered RNase free.
8. Sterile liquid products (e.g., 10× PBS) are considered RNase free and do not need to be baked or autoclaved.
9. Transcardial perfusion of fixatives is the best way to ensure rapid fixation and preservation of brain tissue and mRNA. However, this step (Subheading 3.2.1, step 4) can be avoided if the other hemibrain is needed for other experimental procedures that are not compatible with fixed tissue (e.g., Western blotting, ELISA). Simply drop-fix the hemibrain intended for in situ hybridization in 4% PFA.
10. Large animals may need longer perfusion time.
11. We routinely make small amounts of 10% sucrose by a 1:3 dilution of the 30% sucrose solution used for cryoprotection.
12. The desired final concentration of the cDNA templates is 1 μg of DNA/μl. The expected yield from this protocol is 8 μg of DNA, which would call for adding 8 μl of TE buffer. The exact amount to add should be determined empirically.
13. Ethidium bromide is a carcinogenic compound that must be handled with caution in a safety hood.
14. DNase digestion of the DNA template is not required for in situ hybridization applications.
15. Although the RNeasy cleanup procedure is carried out at room temperature, purified RNA should be kept on ice when aliquots are used for subsequent applications.
16. It is important not to dissolve the gelatin in saline buffers, as the salts will crystallize on the sections as they dry.
17. The main purpose for including Tween in the buffers with floating sections is to prevent the sections from sticking to each other or to the plasticware. This precaution is unnecessary

when the sections are already mounted on slides or when performing the protocol with in toto embryos.

18. If the sections are wet when exposed to abrupt temperature changes, they can detach from the slides.

Acknowledgments

We thank members of the Lennart Mucke and John Rubenstein laboratories, particularly Nga Bien-Ly and Alice Thwin, who contributed to the development of these protocols, and Stephen Ordway and Gary Howard for editorial comments. This work was supported by the Stephen D. Bechtel Jr. Young Investigator Awards (J.J.P and E.D.R), NIH grant NS054811 (E.D.R.), and the Ramon y Cajal Investigator Award (I.C.).

References

1. Palop JJ, Chin J, Roberson ED, Wang J, Thwin MT, Bien-Ly N, Yoo J, Ho KO, Yu G-Q, Kreitzer A, Finkbeiner S, Noebels JL, Mucke L (2007) Aberrant excitatory neuronal activity and compensatory remodeling of inhibitory hippocampal circuits in mouse models of Alzheimer's disease. *Neuron* **55**, 697–711.
2. Gall JG, Pardue ML (1969) Formation and detection of RNA-DNA hybrid molecules in cytological preparations. *Proc Natl Acad Sci USA* **63**, 378–383.
3. John HA, Birnstiel ML, Jones KW (1969) RNA-DNA hybrids at the cytological level. *Nature* **223**, 582–587.
4. Palop JJ, Chin J, Bien-Ly N, Massaro C, Yeung BZ, Yu G-Q, Mucke L (2005) Vulnerability of dentate granule cells to disruption of Arc expression in human amyloid precursor protein transgenic mice. *J Neurosci* **25**, 9686–9693.
5. Cobos I, Calcagnotto ME, Vilaythong AJ, Thwin MT, Noebels JL, Baraban SC, Rubenstein JL (2005) Mice lacking Dlx1 show subtype-specific loss of interneurons, reduced inhibition and epilepsy. *Nat Neurosci* **8**, 1059–1068.
6. Cobos I, Borello U, Rubenstein JL (2007) Dlx transcription factors promote migration through repression of axon and dendrite growth. *Neuron* **54**, 873–888.

Chapter 16

Real-Time Visualization of Axonal Transport in Neurons

Yasuko Osakada and Bianxiao Cui

Abstract

The normal function of neurons depends on the integrity of microtubule-dependent transport of cellular materials and organelles to/from their cell bodies or axon terminus. In this chapter, we describe the design and implementation of a fluorescence imaging method to visualize axonal transport in neurons directly. We combine a pseudo total internal reflection microscopy, quantum dot fluorescence labeling, microfluidic neuronal culture chamber, and single molecule detection methods to achieve a high spatial and temporal resolution in tracking nerve growth factor transport in dorsal root ganglia neurons.

Key words: Axonal transport, Nerve growth factor, Live imaging, Quantum dot, Microfluidic, Total internal reflection microscopy, Single molecule imaging

1. Introduction

Neurons are highly asymmetric cells with long axons and dendrites extending from the cell body, which play a critical role in carrying information to and from synapses. While neuronal cell bodies are typically in the range of 20–50 μm, their axons can be as long as 1 m, roughly 30,000 times the diameter of the cell body. Thus, organelles, proteins, slipids, and neurotransmitters that are made in the cell body have to travel a great distance before they can reach the nerve terminal. Similarly, extracellular stimuli originating in the axonal terminus – such as trophic signals derived from target cells that are known to be essential for the survival and maintenance of neurons and neuronal circuits – are carried back to the cell body in axons. The failure of either anterograde or retrograde transport inevitably disrupts neuronal function (1–3).

Rates of axonal transport were first measured via pulse-chase experiments of radioactive tracers in nerves (4–6). Great advances

Erik D. Roberson (ed.), *Alzheimer's Disease and Frontotemporal Dementia*, Methods in Molecular Biology, vol. 670,
DOI 10.1007/978-1-60761-744-0_16,

in the development of fluorescent proteins and other fluorophores in the last decade have enabled the development of methods to measure axonal transport using fusion proteins and various dyes (7–9). Although the process has been captured by various fluorescence microscopic techniques, real-time visualization of axonal transport in live neurons is generally hindered by fast bleaching of GFP fluorescence and a strong background due to auto-fluorescence of the cells.

Nerve growth factor (NGF) is a particularly important neurotrophin. It is transported in neurons by the microtubule-dependent motor protein dynein. In this chapter, we describe a method that combines a microfluidic culture platform, total internal reflection microscopy, quantum dot fluorescence labeling, and ultrasensitive single molecule detection methods to measure axonal transport of NGF in neurons (10). This method allows one to track the movement of an axonal endosome for more than 20 min, over a distance of several millimeters. In addition, this method provides a temporal resolution of 100 ms and a spatial resolution of 30 nm, which offers unprecedented detailed information about axonal transport.

2. Materials

2.1. Preparation of Microfluidic Chamber

1. Photolithography clean room.
2. 3-in Si Wafer (Silicon Inc., Boise, ID).
3. Hexamethyldisilazane (HDMS, Sigma).
4. Precision spin coater (Headway Research Inc.).
5. Photoresist, SU-8 2 and SU-8 50 (Microchem, Newton, MA).
6. High-resolution transparency masks (Artnetpro, San Jose, CA).
7. Mask aligner.
8. Propylene glycol monomethyl ether acetate (PGMEA) photoresist developer (Sigma).
9. Polydimethyl siloxane (PDMS) Sylgard 184 (Dow Chemical Co., Midland, MI).
10. PDMS release agent, trimethylchlorosilane (TMCS, Dow Chemical Co.).
11. High-temperature vacuum cure oven (Yield Engineering Systems).
12. Alconox detergent.
13. Autoclave.
14. 1 M potassium hydroxide.
15. 70% Ethanol.

16. 0.1 M borate buffer. Mix 1.54 g of boric acid and 2.38 g of sodium tetraborate in 500 ml of DI water, adjust pH to 8.5. Sterilize by filtering through 0.2-μm pore-size filter.
17. Poly-L-Lysine (PLL): 500 mg/ml in 0.1 M borate buffer.
18. Glass coverslips.

2.2. Cell Culture

1. Micro coverglass and Petri dishes.
2. Timed pregnant rats at embryonic day 15 (E15).
3. Dissection microscope and surgical tools.
4. NGF: native NGF was purified from mouse submaxillary glands following a well-established protocol (11). NGF can also be purchased from Sigma–Aldrich and BD Biosciences.
5. Dissection buffer: 1× Hank's Buffered Salt Solution (HBSS, GIBCO), 100 U/ml penicillin, and 100 μg/ml streptomycin. The antibiotics are diluted from a Pen-Strep stock solution of 10,000 U/ml penicillin and 10,000 μg/ml (Cellgro).
6. Solution of 0.25% trypsin in HBSS w/o Ca2+ and Mg2+ (cellgro).
7. Quenching medium (DMEM+15% FBS): 1× Dulbecco's Modified Eagle's Medium (DMEM), 15% fetal bovine serum (FBS, GIBCO), 100 U/ml penicillin, and 100 μg/ml streptomycin.
8. Plating medium: 1× DMEM, 10% FBS, 200 U/ml penicillin, 200 μg/ml streptomycin, and 50 ng/ml NGF.
9. Maintenance medium: 1× B-27 supplement (diluted from a stock of 50×, GIBCO), 2 mM glutamax (diluted from a stock of 100 mM, GIBCO), 100 U/ml penicillin, and 100 μg/ml streptomycin, 50 ng/ml NGF in 1× neurobasal medium.
10. Hemocytometer.
11. Anti-mitotic medium: maintenance medium supplemented with 4 μM cytosine-B-D arabinofuranoside hydrochloride (Sigma).
12. CO_2 independent medium (GIBCO).

2.3. Real-time Imaging of Axonal Transport

1. 1-Ethyl-3-[3-dimethylaminopropyl]carbodiimide hydrochloride (EDC, Thermo Scientific).
2. NGF (purified as described in (11)).
3. EZ-link Biotin PEO-Amine (Thermo Scientific).
4. MES-NaOH buffer: 20 mM morpholinoethanesulfonic acid (MES). Dissolve 3.9 g of anhydrous MES in 1 L of DI water and adjust pH to 5.0 with 2 N NaOH solution.
5. HPLC system with C4 column.
6. 0.1% Trifluoroacetic acid.

7. 60% Acetonitrile in 0.1% trifluoroacetic acid.
8. FluoReporter Biotin Quantification kit (Molecular Probes).
9. Qdot 605-Streptavidin conjugate (Invitrogen).
10. Pseudo Total Internal Reflection Microscope. Commercial systems can be purchased. We built our setup using an inverted Nikon Eclipse Ti-U microscope with a 60× 1.49NA oil immersion objective (Nikon, Japan) modified for TIRF imaging as follows.
    - A 523-nm CW diode green excitation laser beam is expanded to 3 cm diameter and focused at the back focal plane of the objective lens.
    - The focal point is moved off-axis so that the light undergoes total internal reflection at the glass–water interface.
    - The angle of refraction is carefully tuned by moving a focusing lens mounted on a translation stage. The incident angle is adjusted to be slightly smaller than the critical angle so that the laser beam penetrates ~1 μm into the aqueous solution.
    - Fluorescence emission from Qdot605 is collected by the objective lens, filtered with a QD605/20 emission filter, and focused onto a cascade 512B CCD camera.
    - The sample temperature is controlled by an external water bath. The insert of the microscope stage is custom machined to incorporate copper tubing that is connected to a circulating water bath. The microscope objective is wrapped by a coil of copper tubing that connects to the same circulating water bath.
11. Laser safety glasses (Sperian, Smithfield, RI).
12. Optics-lenses, neutral density filters, mirrors, dichroic mirrors, and emission filters.
13. EMCCD camera (Andor, South Windsor, CT).
14. Recirculating water bath.

3. Methods

In order to make precise quantitative measurements of axonal transport, it is essential to obtain a good signal-to-noise ratio. The experiment described in this section has single molecule precision, which is achieved by combining a few cutting-edge techniques. A microfluidic neuronal culture (MNC) chamber is used to keep environments of the cell bodies physically isolated from that of the distal axons (12), thereby ensuring that any Qdot-NGF signal arises from

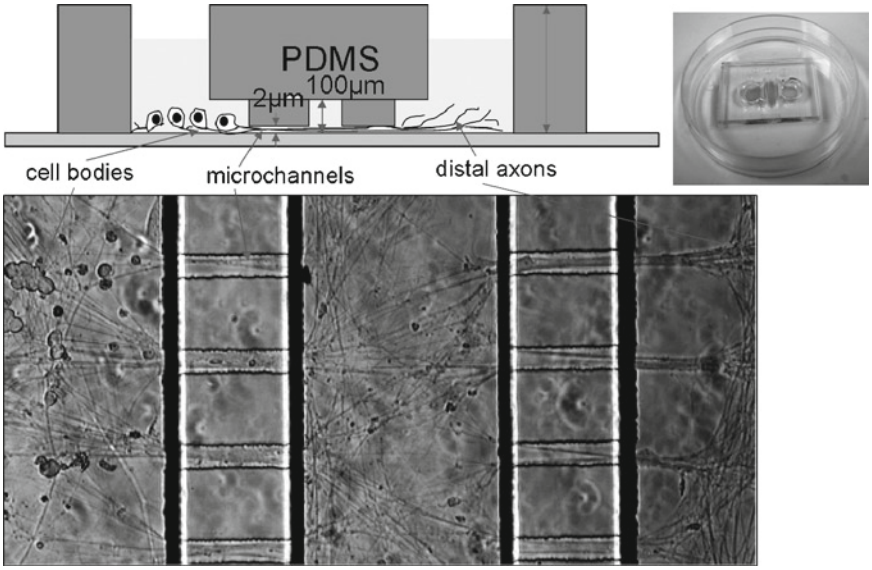

Fig. 1. DRG neurons cultured inside an MNC chamber. Cell bodies are plated to the left most chamber. Three days after plating, axons have extended across the middle compartment and into the distal axon compartment to the right.

axonal transport (Fig. 1). A pseudo-TIRF imaging system is used to cut down on background noise. In TIRF, only evanescent waves penetrate into the sample to a depth of several hundred nanometers, thereby eliminating much of the cellular autofluorescence.

3.1. Preparation of Microfluidic Neuronal Culture Chamber

3.1.1. Fabrication of Master Pattern on Si Wafer

Master patterns on a Si wafer are fabricated using photolithography in a clean room facility (we use the Stanford nanofabrication center, but commercial services are also available). The master pattern is composed of two photoresist layers of different thickness. The thin layer is ~2 μm, while the thick layer is ~100 μm thick. Details of photolithography are beyond the scope of this chapter, but the procedure is outlined as follows (Fig. 2).

1. Clean a 3-in. Si wafer with DI H_2O and blow-dry using pressurized air.
2. Prime with HDMS in a vacuum oven.
3. Place the clean wafer polished side up on the vaccum chuck of a spin coater.
4. Pour 2 ml of SU8-2 negative photoresist on the center of the wafer and spin at 2,000 rpm for 60 s (~2 μm thick).
5. Bake the wafer for 3 min at 100°C on a hotplate.
6. Expose the photoresist-coated Si wafer to ultraviolet (UV) light using a mask aligner through a high-resolution transparency mask, on which the channel pattern is printed. The exposure time was optimized to be 37 s at 200 W.

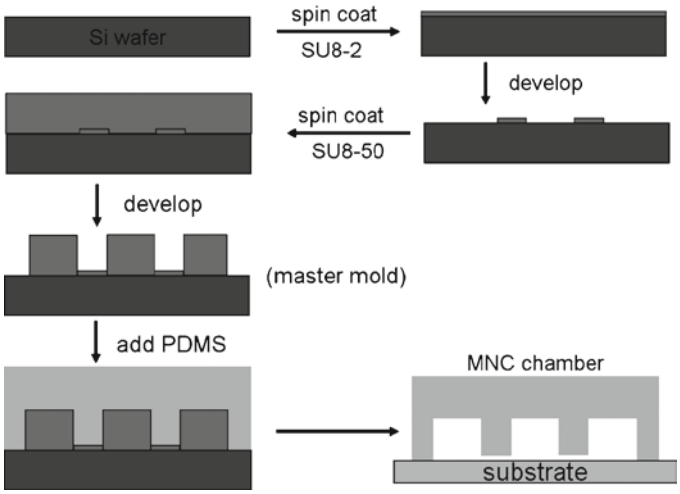

Fig. 2. Fabrication steps of microfluidic neuronal culture (MNC) chamber. The master mold is composed of two layers of SU-8 photoresist on a 3-in. Si wafer. The MNC chamber is made by sealing PDMS mold with a PLL-coated coverglass substrate.

7. After exposure to UV light, bake at 100°C for 3 min on the hotplate.
8. Develop in PGMEA (SU-8 developer) for 3–6 min with gentle rocking. Rinse with isopropyl alcohol and dry with pressurized air.
9. Spin the second layer photoresist (SU8-50) at 1,000 rpm for 60 s to achieve 100 μm thickness.
10. Bake at 100°C for 10 min on the hotplate so that the photoresist layer is even and smooth.
11. Place the second transparency mask, which has the pattern of three chambers, on the mask aligner. Align the substrate with the mask by alignment marks.
12. Expose for 150 s at 200 W. Post-exposure, bake for 10 min at 100°C.
13. Develop in PGMEA for 5 min, then change to a fresh developer solution. Repeat three times. Rinse with EPA and dry.

3.1.2. Preparation of PDMS Chamber by Replica Molding

1. Weigh 50 g total PDMS mixture (weight ratio of cross-linking reagent:base = 1:10) in a disposable plastic container. Thoroughly mix by stirring with a glass rod, and degas for 5 min inside a vacuum desiccator.
2. Prime the master Si wafer by vapor coating with TMCS. Place a 100-mm Petri dish with the master Si wafer facing up inside a large plastic container. Add 1 ml of TMCS in the flat glass Petri dish inside the container. Cap the container and prime for 5 min. TMCS treatment helps release PDMS from the Si wafer surface.

3. Pour the PDMS liquid mix on the wafer. Place the Petri dish in the vacuum desiccator and thoroughly degas for 15 min. Use a pipette tip to push any remaining bubbles to the edge of the Petri dish.
4. Place the Petri dish in an oven with temperature pre-set at 70°C. Incubate for 2 h. It is important that the temperature should not surpass 80°C at any time. The plastic Petri dish will melt above 80°C.
5. Gently peel off PDMS from the Si wafer. The designed pattern is printed on PDMS by replica molding.
6. Trim the PDMS pattern to fit the 24×40 mm coverglass using a razor blade.
7. Punch access holes at appropriate locations. Two large holes provide direct access to the cell body chamber and the distal axon chamber. Two small holes located at the end of the central compartment allow fluid access to the proximal axons (see Note 1).
8. Clean PDMS chips in detergent solution for 2 h. Rinse with water and ethanol. Dry in a clean hood.
9. Wrap PDMS chips in aluminum foil and dry-autoclave for 15 min. Autoclave will sterilize the device and increase the degree of cross-linking.

3.1.3. PLL Coating of Coverglass Substrate

1. Soak a 24×40 mm coverglass in detergent solution. Sonicate for 30 min. Rinse three times with DI water (see Note 2).
2. Immerse the coverglass in 1 M KOH solution. Sonicate for 15 min. Rinse three times with DI water.
3. Sterilize the coverglass with 70% ethanol and dry in a sterile laminar flow hood.
4. Dissolve 500 mg of PLL into 500 ml of 0.1 M borate buffer. Sterilize by filtering through 0.2-μm pore-size filter.
5. Place dry and clean glass coverslips into a 100 mm Petri dish containing PLL coating solution. Be careful to immerse the coverslips one by one so that all surfaces are exposed to the PLL solution. Place the Petri dish in a 37°C incubator for 3 h.
6. Rinse with DI water three times, 5 min each.
7. Dry in a sterile laminar flow hood.

3.2. Culture DRG Neurons Inside Microfluidic Chambers

3.2.1. Assembly of MNC Chamber

1. Assemble microfluidic neuronal culture chamber as neuronal dissection is in progress.
2. Prepare freshly cleaned and autoclaved PDMS chips. Fresh PDMS surface is necessary in order to form a tight seal to the coverglass substrate.
3. Place a PLL-coated coverglass in a 60-mm sterile Petri dish.

4. Use sterile forceps to hold a PDMS chip by side wall of a large hole, with the pattern facing down. Place the PDMS chip in the center of the coverglass and lightly press it down to form a water-tight seal to the substrate.
5. Gently press the middle part of the PDMS chip to ensure complete sealing around micro-channel area.

3.2.2. Harvest DRG Neurons from Embryonic Rats

1. Collect E15 embryos from pregnant rats. One pregnant rat generally produces 10–15 embryos (see Note 3).
2. Separate the body, where DRG neurons will be collected, from the head, where cortical neurons will be collected.
3. To collect dorsal root ganglia, cut along the spinal column from ventral side to expose the spinal column. Use curved forceps to grab the most cervical segment of the spinal cord and gently pull up and along the spinal column to remove the cord.
4. Place the spinal cord in a 60 mm Petri dish with dissection buffer. Check under the dissection microscope. Dorsal root ganglion should be visible as semi-transparent tissue flapping on the side of the spinal cord, one per spinal nerve.
5. Pull individual dorsal root ganglia off the spinal cord and collect all ganglia into a 15-ml centrifuge tube filled with dissection buffer.
6. Wait for 5 min for the ganglia to settle down to the bottom of the tube by gravity. Gently pipette out the dissection buffer. Wash three times with 5 ml fresh dissection buffer.
7. Add 5 ml of 0.25% trypsin solution and incubate for 45 min at 37°C in a water bath. Gently shake the tube every 5 min.
8. Quench the trypsin by adding DMEM containing 15% FBS. Spin down the cells at 800 rpm and decant the trypsin/DMEM/FBS solution. Resuspend cells in 1.0 ml plating medium w/NGF.
9. Pipette the resuspended cells using 1 ml pipette tip for a maximum of ten times to further dissociate the cells.
10. Count total cell density using a hemocytometer.
11. Spin down the cells at 800 rpm. Resuspend in appropriate volume of plating medium to make the concentration at least 5×10^6 cells/ml.

3.2.3. Plating DRG or Cortical Neurons in MNC Chamber

1. Take 10 μl of cell suspension and add to the cell body compartment. Add the cell suspension next to the middle separation wall, so that some cells are located very close to the channel by capillary attraction (see Note 4).

2. Wait for 10 min for the cells to attach to the substrate surface. During the waiting time, place the chamber in a humidity controlled 37°C, 5% CO_2 incubator.
3. Add 200 µl of plating medium to the cell culture chamber after the cells are attached to the substrate.
4. Flush the middle compartment with plating medium. Place a 200-µl pipette tip very close to the channel opening inside the small hole. Pipette up and down for three to five times to flush out any air trapped inside the middle compartment. Add 50 µl of plating medium to fill the small holes that connect the middle compartment.
5. Add 200 µl of plating medium to the distal axon chamber. Place the culture inside a CO_2 incubator.

3.2.4. Selection and Maintenance of DRG Neurons in MNC Chamber

1. Three hours after plating, exchange the plating medium to maintenance medium that contains no FBS. Maintenance medium curbs the growth of non-neuronal cells.
2. At 36 h after plating, change the culture to anti-mitotic medium. The anti-mitotic medium inhibits the growth of dividing cells including fibroblasts, Schwann cells, phagocytes, and various other cell types.
3. At 48 h after plating, change the culture medium back to maintenance medium.
4. Exchange half of the cell medium with fresh maintenance medium every 3 days.

3.3. Real-time Imaging of Axonal Transport of Qdot-NGF

3.3.1. Preparation of Qdot-NGF

1. Biotinylate lyophilized native NGF at the carboxyl group. Add 40 µl of 0.5 M EDC, 0.5 mg of purified and lyophilized NGF, and 14.4 mg of EZ-link biotin-PEO-amine to 710 µl of 20 mM MES-NaOH buffer, pH 5.0. Incubate at RT for 2 h. EDC catalyzes the coupling reaction between the carboxyl group on NGF and the amine group on biotin-PEO-amine. Excess biotin-PEO-amine prevents cross-linking among NGF molecules.
2. Biotinylated NGF is purified from the reaction mixture by reverse-phase HPLC over a C4 column (13). Inject 0.5 ml of the NGF biotinylation reaction mixture into a 1-ml sample loop on a HPLC. Aqueous solutions of 0.1% trifluoroacetic acid containing 0% and 60% acetonitrile are mixed to create a gradient elution. The reaction mixture runs on the C4 column using the elution solution that increases linearly from 0 to 60% acetonitrile in 60 min. Biotinylated NGF is recovered in the 30–40% acetonitrile elution fraction.
3. Quantify the amount of biotin per NGF using the FluoReporter Biotin Quantification kit according to the manufacturer's instructions. (On average, there will be 3–4 biotin per NGF dimer).

4. Prepare Qdot-NGF by mixing streptavidin-coated quantum dot (605 nm) with biotin-NGF at a molar ratio of 1:1 and incubating at room temperature for 1 h. Conjugated Qdot-NGF should be stored at 4°C and is stable for several weeks.

3.3.2. Loading Qdot-NGF in the Distal Axon Compartment

1. DRG neurons cultured 5–7 days in a microfluidic chamber extend their axons across the middle compartment and into the distal axon compartment.
2. Prior to the addition of Qdot-NGF, the DRG culture is starved of NGF for 3–4 h. All compartments of the microfluidic chamber are washed and supplied with maintenance medium without NGF.
3. Prepare 100 µl of 1 nM Qdot-NGF in maintenance medium without NGF. Completely withdraw fluid from the distal axon compartment, while keeping 130 µl of medium in the cell body compartment.
4. Add 100 µl of Qdot-NGF to distal axon compartment. The liquid volume in the cell body compartment is slightly larger than that in the distal axon chamber (130 versus 100 µl). The volume difference creates a positive pressure working against diffusion from the distal axon to the cell body compartment, ensuring that any Qdot-NGF seen on the cell body side was brought there by axonal transport.
5. Place the culture back in CO_2 incubator to allow NGF binding, internalization, and transport in axons. Be careful not to tilt the chamber so as to minimize fluid flow through the channels.

3.3.3. Fluorescence Imaging of Qdot-NGF Transport in Axons

Extra care should be taken when dealing with lasers. Laser light may permanently damage vision. Ensure that all personnel have been properly trained in laser use and that all safety protocols are followed. Always wear goggles for the specific wavelength of laser excitation being used (see Note 5).

1. Wash out unbound Qdot-NGF using DMEM for three times, 2 h after Qdot-NGF is added to the distal axon compartment. During this process, the liquid level in the cell body compartment must always be kept higher than the liquid level in the distal axon compartment in order to maintain a positive hydraulic pressure against Qdot-NGF diffusion.
2. Change the maintenance medium to CO_2-independent DMEM buffer for imaging. CO_2-independent medium minimizes any pH change induced by CO_2 withdrawal.
3. Place the microfluidic culture on the stage of the TIRF microscope. Maintain temperature at 37°C.
4. Open laser shutter to excite the Qdot-NGF (see Note 6).

5. Locate surface-binding Qdots in the distal axon compartment. Qdot-NGF binds to its TrkA receptor at the axon membrane. While some Qdot-NGF molecules are internalized upon receptor binding, the majority of Qdot-NGF remains on the surface of the axon membrane in the distal axon compartment. These surface-binding Qdots will outline the shape of axons.
6. Move the microscope stage to observe the middle compartment. Many Qdots can be seen actively moving toward the cell body compartment, but some surface-binding Qdots are still visible.
7. Move the microscope stage to the micro-channels connecting the cell body compartment and the middle compartment. All Qdots undergo retrograde transport toward the cell body compartment.
8. Take time-lapse movies of axonal transport in the microchannels, where axons are relatively flat and straight. Time-lapse images are collected at a speed of 10 frames/s (Fig. 3).
9. Data analysis can be performed in Matlab, Sigmaplot, IDL, or other software capable of image processing to obtain information such as transport speed, pausing location, frequency and duration, etc.

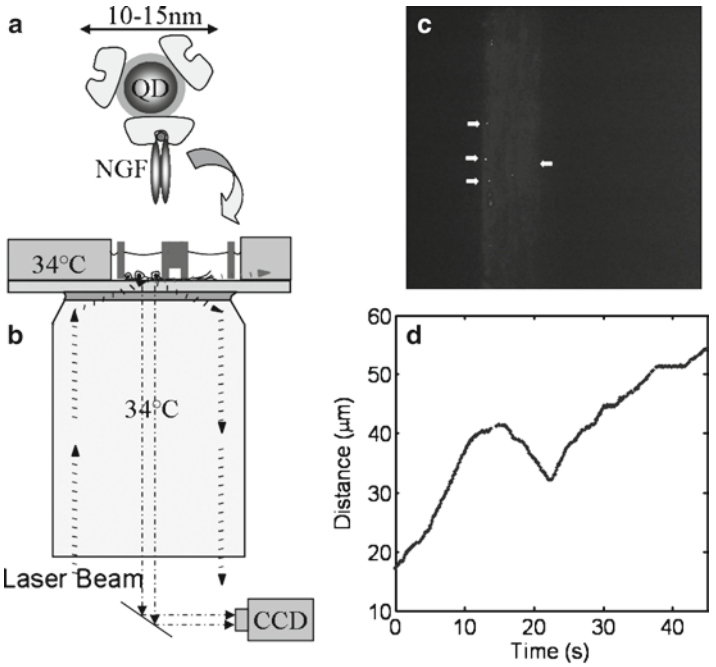

Fig. 3. (**a**) Illustration of NGF labeled with quantum dot (Qdot-NGF). (**b**) Schematic drawing of pseudo-TIRF microscope setup. Qdot-NGF is added exclusively to the distal axon compartment. (**c**) A sample image of Qdot-NGF traveling in axons that are confined inside microgrooves. (**d**) A typical trajectory of retrograde transport of Qdot-NGF.

4. Notes

1. When punching holes in the PDMS chambers, it is important to cut through a small part of the 2-μm thick layer to ensure that fluid can flow freely through. These chambers can be reused as long as they are intact, given that proper care is taken to clean and sterilize them before each use.
2. When coating the coverglasses with PLL, it is important that all the detergent in the washing step be washed off thoroughly. Otherwise, the glass surface will remain slightly hydrophobic and proper coating will not take place.
3. If using rat embryos older than age E15, the DRG will not come out attached when the spinal cord is pulled out. They will remain in the spinal column in between the vertebrae, in which case they would have to be pulled out one by one. This procedure is much more difficult and tedious, hence it is recommended that, when possible, only E15 embryos are used.
4. When plating cells in the microfluidic chambers, it is desirable to deposit them close to the microchannels so that they do not have to extend their axons to long distances to reach the microchannels and extend to the next chamber.
5. This section has been greatly abridged. A detailed description of the construction of the TIRF system is beyond the scope of this chapter. Construction of the system is non-trivial and requires familiarity with optics. However, commercial TIRF systems are available.
6. To minimize light-induced cell toxicity, one should use the longest wavelength possible light to excite quantum dots. For example, use 532-nm laser as the excitation light source for 605-nm QDot. It is also advantageous to photobleach the area being imaged for a few minutes prior to taking data to reduce autofluorescence.

References

1. Huang, E. J. & Reichardt, L. F. (2003) Trk receptors: roles in neuronal signal transduction. *Annu Rev Biochem* **72**, 609–642.
2. Zweifel, L. S., Kuruvilla, R. & Ginty, D. D. (2005) Functions and mechanisms of retrograde neurotrophin signalling. *Nat Rev Neurosci* **6**, 615–625.
3. Huang, E. J. & Reichardt, L. F. (2001) Neurotrophins: roles in neuronal development and function. *Annu Rev Neurosci* **24**, 677–736.
4. Senger D. L. & Campenot, R. B. (1997) Rapid retrograde tyrosine phosphorylation of trkA and other proteins in rat sympathetic neurons in compartmented cultures. *J Cell Biol* **138**, 411–421.
5. Korsching S. & Thoenen H. (1983) Quantitative demonstration of the retrograde axonal transport of endogenous nerve growth factor. *Neurosci Lett* **39**, 1–4.
6. von Bartheld C. S. (2001) Tracing with radiolabeled neurotrophins. *Methods Mol Biol* **169**, 195–216.
7. Jullien J., Guili, V., Derrington E. A., Darlix J., Reichardt L. F. & Rudkin, B. B. (2003) Trafficking of TrkA-green fluorescent protein

chimerae during nerve growth factor-induced differentiation. *J Biol Chem* **278**, 8706–8716.

8. Lalli G. & Schiavo G. (2002) Analysis of retrograde transport in motor neurons reveals common endocytic carriers for tetanus toxin and neurotrophin receptor p75. *J Cell Biol* **156**, 233–240.
9. Tani T., Miyamoto Y., Fujimori K. E., Taguchi T., Yanagia T., Sako Y. & Harada Y. (2005) Trafficking a ligand-receptor complex on the growth cones as an essential step for the uptake of nerve growth factor at the distal end of the axon: a single-molecule analysis. *J Neurosci* **25**, 2181–2191.
10. Cui B., Wu C., Chen L., Ramirez A., Bearer E. L., Li W., Mobley W. C. & Chu S. (2007) One at a time, live tracking of NGF axonal transport using quantum dots. *Proc Natl Acad Sci U S A* **104**, 13666–13671.
11. Mobley, W. C., Schenker, A. & Shooter, E. M., (1976) Characterization and isolation of proteolytically modified nerve growth factor. *Biochemistry* **15**, 5543–5552.
12. Taylor A. M., Rhee S. W., Tu C. H., Cribbs D. H., Cotman C. W. & Jeon N. L. (2003) Microfluidic multicompartment device for neuroscience research. *Langmuir* **19**, 1551–1556.
13. Bronfman F. C., Tcherpakov M., Jovin T. M. & Fainzilber M. (2003) Ligand-induced internalization of the p75 neurotrophin receptor: a slow route to the signaling endosome. *J Neurosci* **23**, 3209–3220.

Chapter 17

Quantifying Biomarkers of Cognitive Dysfunction and Neuronal Network Hyperexcitability in Mouse Models of Alzheimer's Disease: Depletion of Calcium-Dependent Proteins and Inhibitory Hippocampal Remodeling

Jorge J. Palop, Lennart Mucke, and Erik D. Roberson

Abstract

High levels of Aβ impair neuronal function at least in part by disrupting normal synaptic transmission and causing dysfunction of neural networks. This network dysfunction includes abnormal synchronization of neuronal activity resulting in epileptiform activity. Over time, this aberrant network activity can lead to the depletion of calcium-dependent proteins, such as calbindin, Fos, and Arc, and compensatory inhibitory remodeling of hippocampal circuits, including GABAergic sprouting and ectopic expression of the inhibitory neuropeptide Y (NPY) in dentate granule cells. Here we present detailed protocols for detecting and quantifying these alterations in mouse models of Alzheimer's disease (AD) by immunohistochemistry. These methods are useful as surrogate measures for detecting chronic aberrant network activity in models of AD and epilepsy. In addition, since we have found that the severity of these changes relates to the degree of Aβ-dependent cognitive impairments, the protocols are useful for quantifying biomarkers of cognitive impairment in mouse models of AD.

Key words: Hippocampus, Dentate gyrus, Granule cell, Mossy fiber, Hilus, Neuropeptide Y, NPY, Calbindin, Seizure, Epilepsy, Excitability, GABA, GABAergic sprouting, Ectopic expression, Excitatory, Inhibitory, Immunohistochemistry, Aβ, Alzheimer's disease, Biomarkers, Immediate early gene, Fos, Arc, Neuronal activity

1. Introduction

Transgenic mice expressing Alzheimer's disease (AD)-related genes, such as genes encoding mutant amyloid precursor protein (APP) and presenilin 1, have become a mainstay for studying the molecular pathogenesis of AD and for the preclinical development of new therapeutic strategies. These mouse models have proved

Erik D. Roberson (ed.), *Alzheimer's Disease and Frontotemporal Dementia*, Methods in Molecular Biology, vol. 670,
DOI 10.1007/978-1-60761-744-0_17,

useful because their brain architecture and circuitry are similar in many ways to those of humans, and because they display deficits in learning and memory that can be quantified by standard behavioral measures of hippocampal functions, including the Morris water maze, radial arm maze, and contextual fear conditioning. However, these tests have considerable downsides, including requirements for specialized equipment and dedicated space, expertise in the neurobehavioral analysis of mice, and high inter-animal variability in behavior, which increases the number of mice required to obtain conclusive results and makes the procedures very labor intensive (1, 2).

While behavior likely will never be supplanted as the ultimate measure of brain function, more convenient surrogate measures that provide reliable correlates of hippocampal dysfunction in AD mouse models would be very useful. Amyloid plaque load was initially considered a potential surrogate marker for the severity of AD-related changes in mouse models, but it is now clear that plaque density does not correlate with learning and memory deficits in AD mouse models (3–7), or indeed in patients with AD (8–10). Here, we present a protocol for other immunohistochemical measures that do correlate with cognitive deficits in mouse models of AD. In the dentate gyrus of different lines of hAPP transgenic mice, we have detected depletion of the calcium-binding protein calbindin D-28K (Fig. 1), aberrant expression of the neuromodulator neuropeptide Y (NPY) (Fig. 2), and reductions in the number of Fos- or Arc-positive granule cells (Fig. 3) (7, 11–15). Some of these changes have also been observed by other groups in other AD models (16), as well as in patients with AD (7). Importantly, the changes in calbindin, NPY, and Fos/Arc in individual mice and in transgenic lines correlate with the severity of learning and memory impairments (7, 11–14, 17), and with each other (Figs. 3 and 4).

Changes in calbindin, NPY, Fos, and Arc expression in dentate granule cells probably share a common neurobiological basis, representing compensatory responses to excessive neuronal activity (13, 18). Indeed, evidence has been accumulating that imbalances between excitation and inhibition may be a major mode by which Aβ disrupts normal cognitive functioning at the network level (13, 15, 16, 19–21). For example, hAPP mice have interictal epileptiform spikes and nonconvulsive seizures (13, 16, 22). This aberrant excitatory activity likely causes the depletion of calcium-dependent proteins and compensatory inhibitory remodeling in the hippocampus, including changes in calbindin, Fos, Arc, and NPY (13, 16). Here we describe how to detect and quantify changes in these functionally relevant biomarkers in AD mouse models by immunohistochemistry.

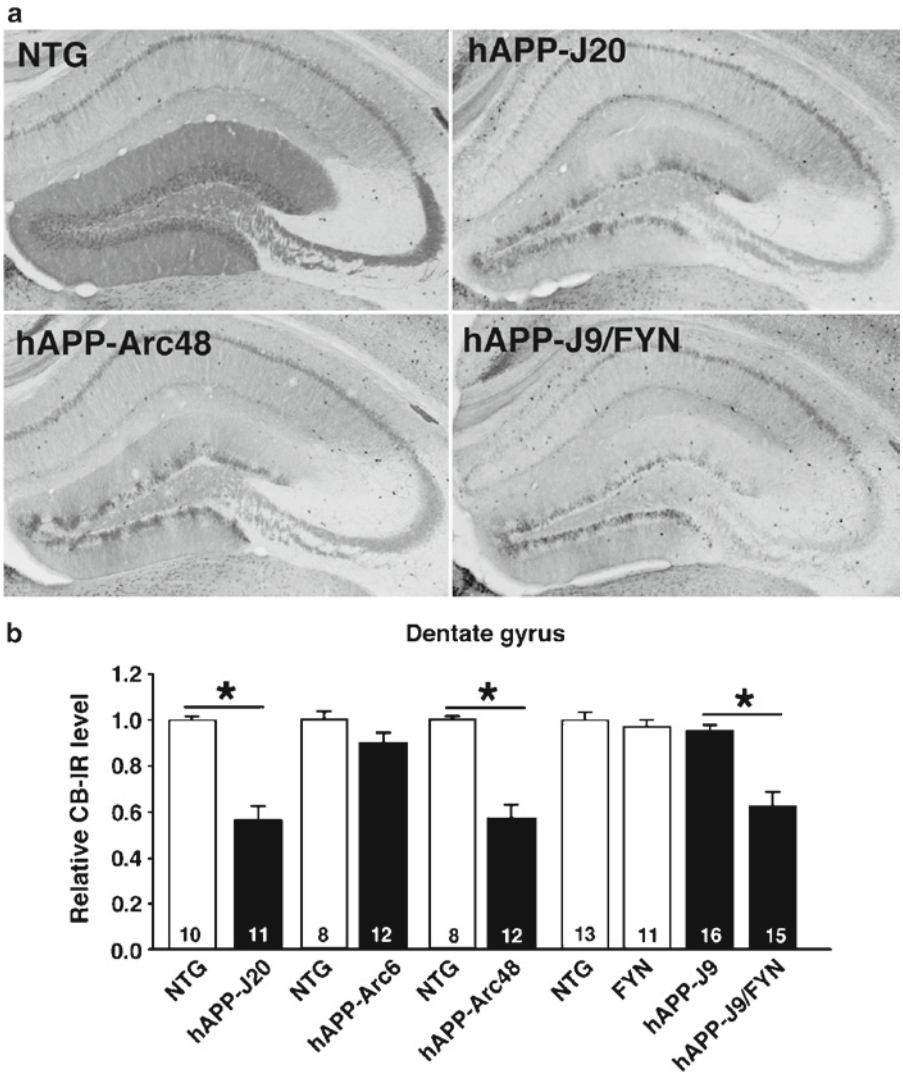

Fig. 1. Calbindin depletion in multiple lines of cognitively impaired hAPP transgenic mice. Calbindin immunohistochemistry was performed and quantified as described here. (**a**) Calbindin depletion relative to levels in nontransgenic (NTG) mice was observed in transgenic mice from lines hAPP-J20 (expressing human APP [hAPP] with Swedish and Indiana mutations), hAPP-Arc48 (expressing hAPP with Swedish, Indiana, and Arctic mutations), and hAPP-J9/FYN (expressing both hAPP with Swedish and Indiana mutations and the Src-family tyrosine kinase Fyn). (**b**) Quantification of calbindin immunoreactivity (CB-IR) in the different lines. Calbindin was depleted in lines with Aβ-dependent cognitive impairments, including hAPP-J20 (originally demonstrated in ref. 7), hAPP-Arc48 (originally demonstrated in ref. 14), and hAPP-J9/FYN (originally demonstrated in ref. 12). Calbindin was not depleted or only slightly reduced in lines that do not display significant cognitive deficits, including hAPP-Arc6 (originally demonstrated in ref. 14) and hAPP-J9 (originally demonstrated in ref. 12). *$P < 0.05$ by Student's t-test or Tukey–Kramer test.

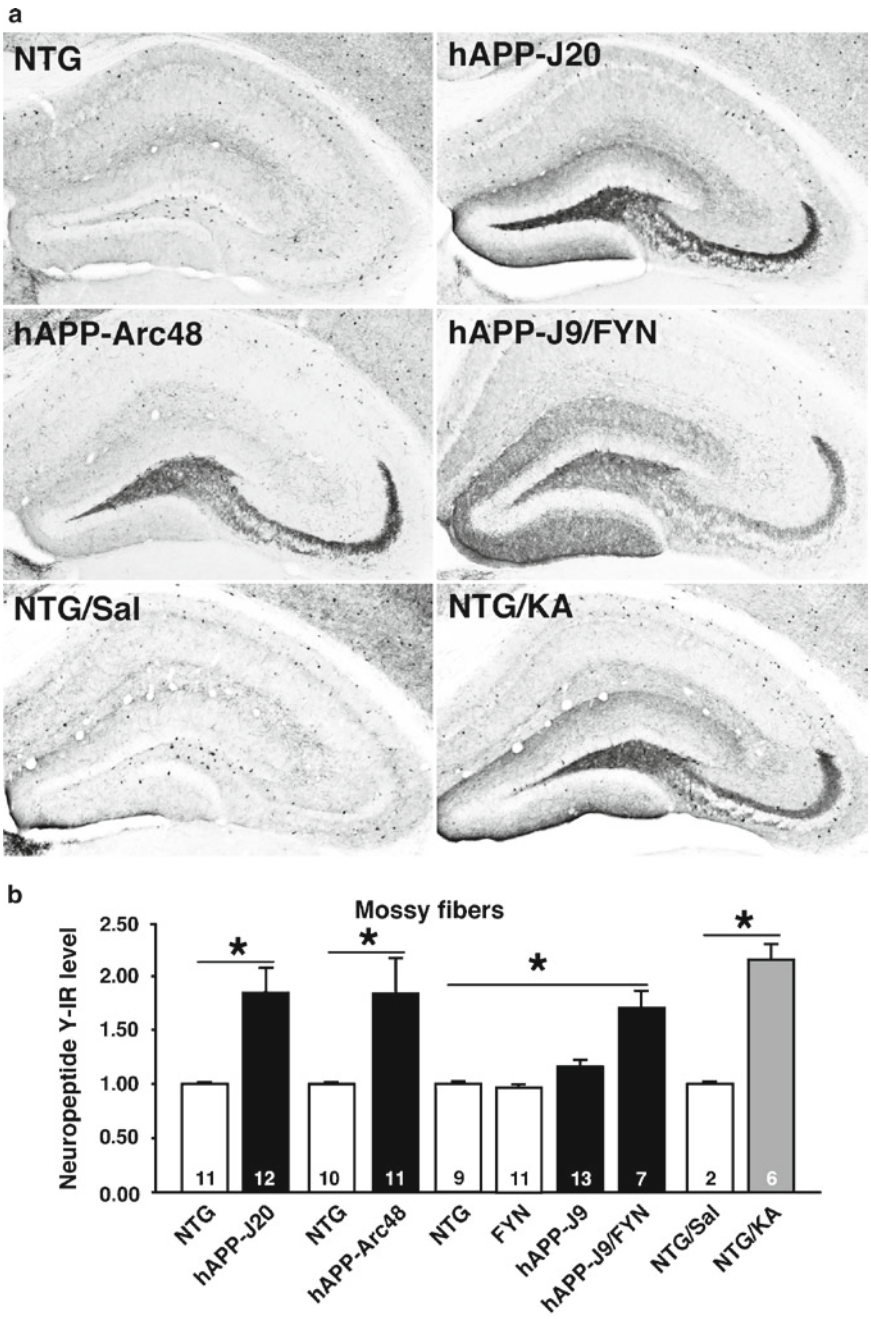

Fig. 2. Aberrant NPY expression in multiple lines of hAPP transgenic mice. NPY immunohistochemistry was performed and quantified as described here. (**a**) Aberrant NPY expression was observed in transgenic mice from lines hAPP-J20, hAPP-Arc48, and hAPP-J9/FYN. Similar changes were seen 3 days after pharmacological induction of seizures by intraperitoneal injection of 25 mg/kg kainic acid in NTG mice (NTG/KA), but not in saline-treated NTG mice (NTG/Sal). (**b**) Quantification of NPY immunoreactivity (IR) in different groups of mice. NPY expression in mossy fibers was increased in lines with Aβ-dependent cognitive impairment, including hAPP-J20, hAPP-Arc48, and hAPP-J9/FYN, as well as after KA injection in NTG mice (originally demonstrated in ref. 13). $^{*}P < 0.05$ by Student's *t*-test or Tukey–Kramer test.

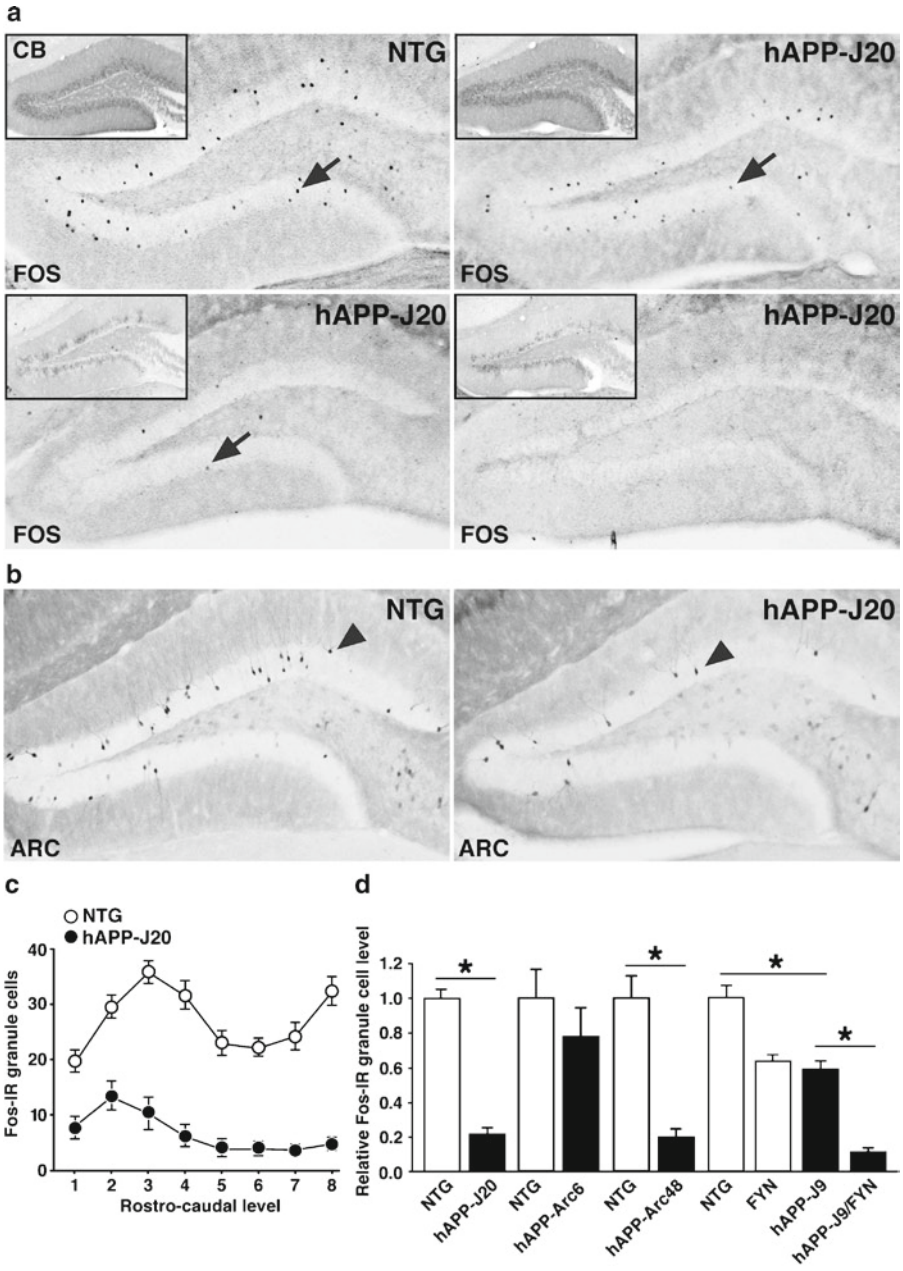

Fig. 3. Reduced number of Fos- and Arc-positive dentate granule cells in hAPP mice. (**a**) Sections through the hippocampus of NTG or three different hAPP-J20 transgenic mice were immunostained for Fos. Inset shows calbindin immunoreactivity from the same animals. Some hAPP mice show normal levels of Fos and calbindin immunoreactivity (*upper right*), whereas most show varying degrees of reductions in both Fos and calbindin. (**b**) Arc-positive granule cells are also reduced in hAPP-J20 mice (originally demonstrated in ref. 11). (**c**) Plot of Fos-positive granule cells along the rostro–caudal axis of the dentate gyrus (1 = most rostral/dorsal; 8 = most caudal/ventral). The number of Fos-positive cells was reduced in hAPP-J20 mice along the entire axis. N = 12–18 mice per genotype. (**d**) Quantification revealed reduced numbers of total Fos-positive granule cells in hAPP-J20 mice (originally demonstrated in ref. 7), hAPP-J9/FYN mice (originally demonstrated in ref. 12), and hAPP-Arc48 mice (originally demonstrated in ref. 14). *$P < 0.05$ by Student's t-test or Tukey–Kramer test.

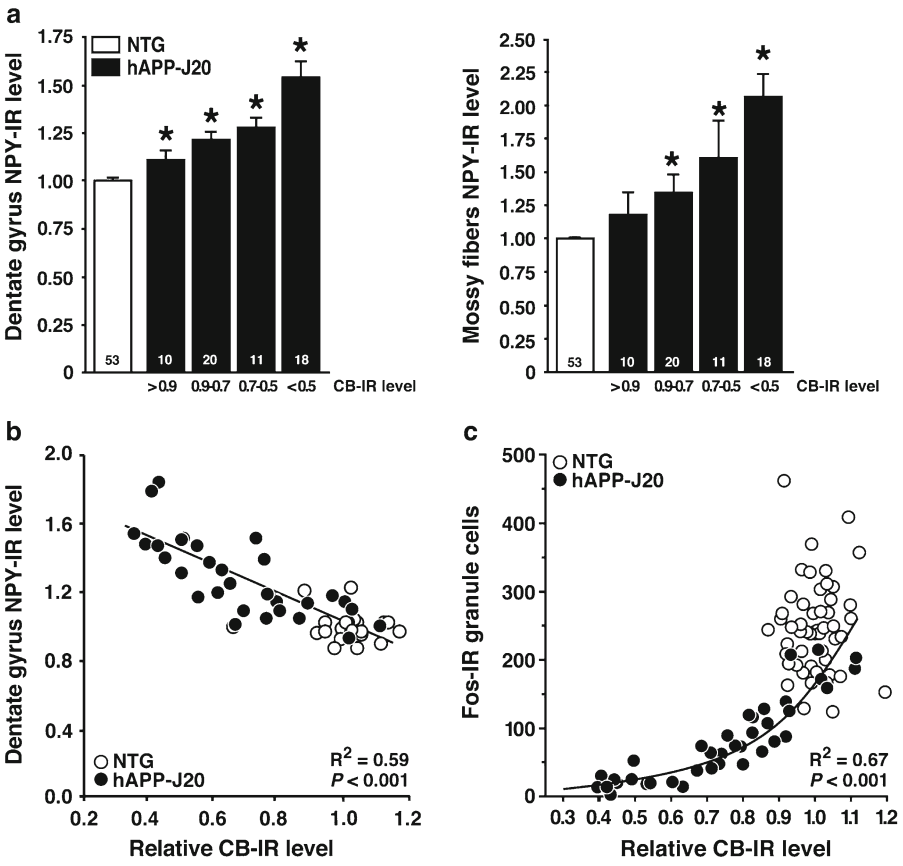

Fig. 4. Correlations between calbindin, NPY, and Fos immunoreactivity in hAPP-J20 mice. (**a**) Compared with NTG controls, NPY expression was increased in the molecular layer of the dentate gyrus (*left*) and in the mossy fibers (*right*) in hAPP-J20 mice. Aberrant NPY expression was more prominent in hAPP-J20 mice with severe reductions in calbindin immunoreactivity. Numbers on bars indicate numbers of mice. * $P < 0.05$ versus NTG by Tukey–Kramer test. (**b**) hAPP-J20 transgenic mice showed interindividual variation in calbindin and NPY. Interestingly, these alterations were tightly correlated, suggesting a common underlying mechanism. The correlation and resulting R^2 and *P*-value are for hAPP-J20 mice only. (**c**) Nonlinear correlation between calbindin immunoreactivity and the number of Fos-immunoreactive granule cells in hAPP-J20 mice. A few hAPP-J20 mice displayed normal levels of both calbindin- and Fos-immunoreactive cells. The number of Fos-immunoreactive cells is a highly sensitive measure and can be strongly reduced in hAPP-J20 mice with only mild calbindin depletion. See also refs. 7, 13. R^2 and *P*-values are for hAPP-J20 mice.

2. Materials

2.1. Perfusion and Fixation of Brain Tissue

1. Anesthetic agent, such as pentobarbital.
2. Perfusion pump or large-capacity syringes and tubing.
3. Surgical tools.
4. Normal saline: 0.9% NaCl.
5. 2× Phosphate buffer (2× PB): 160 mM Na_2HPO_4, 400 mM NaH_2PO_4, pH 7.4. For a 1-L stock solution, dissolve 22.72 g of Na_2HPO_4 and 5.52 g of $NaH_2PO_4 \times 1H_2O$ in water and

adjust pH to 7.4. Store at room temperature for weeks or at –20°C for months.

6. 1 M NaOH: 40 g of NaOH in 1 L of water.
7. 8% Paraformaldehyde (8% PFA, w/v): For 1 L, measure 80 g of PFA (see Note 1), add about 600 ml of water that has been heated to ~65°C in a microwave, place the mixture on a hotplate in a fume hood, and stir with continued heating until the solution reaches, but does not exceed, 85°C (see Note 2). Turn off the heat and continue stirring. At this point, the solution should be whitish and cloudy. Add two to four drops of 1 M NaOH and wait for 2–4 min. The solution will become less cloudy and more transparent. Repeat the addition of NaOH until the PFA mixes fully in the solution. The goal is to obtain a completely transparent solution with minimal addition of NaOH, because high concentrations of NaOH increase the pH and affect the fixative properties of PFA. Add heated water to a volume of 1 L. Let the solution cool to room temperature while stirring. Aliquot and store at 4°C for use within 1–2 days or at –20°C for longer periods of storage.
8. 4% PFA in 1× PB: Prepared as 1:1 mixture of 8% PFA and 2× PB. If the solutions are stored at –20°C, thaw in a 40–50°C water bath. Wait until both solutions are transparent. Do not use a microwave to thaw PFA.

2.2. Sectioning of Brain Tissue

1. Phosphate-buffered saline (PBS): Purchase 10× sterile stock solution (pH 7.4), dilute to 1×.
2. 30% Sucrose in PBS (w/v).
3. Sliding microtome or vibratome (see Note 3).
4. 10% Sucrose in PBS.
5. Cryoprotectant solution: 30% ethylene glycol, 30% glycerol, 40% 1× PBS (v/v/v). Store at –20°C.
6. #1 sable paintbrush.

2.3. Immunohistochemistry

1. Shaking platform, such as IKA Vibrax.
2. 10-cm dishes.
3. 24-well plates.
4. Transfer pipettes, pipette tips, and Parafilm (see Note 4).
5. PBS/Tx: 0.5% Triton X-100 in PBS.
6. Peroxidase quenching solution: 3% H_2O_2 and 10% methanol in PBS.
7. Blocking solution: 10% normal goat serum (Vector Laboratories), 1% blocking-grade dry milk (Bio-Rad), and 0.2% gelatin from porcine skin, type A (Sigma) in PBS/Tx.

8. Antibody incubation solution: 3% normal goat serum (Vector Laboratories) and 0.2% gelatin from porcine skin, type A (Sigma) in PBS.
9. Rabbit anti-calbindin D-28K antibody (Swant).
10. Rabbit anti-NPY antibody (Immunostar).
11. Rabbit anti-c-Fos (Ab-5, EMD Biosciences).
12. Rabbit anti-Arc (gift from Dr. Paul F. Worley).
13. Biotinylated goat anti-rabbit antibody (Vector Laboratories).
14. Vectastain Elite ABC Kit Standard (Vector Laboratories).
15. 100 mM Tris-HCl, pH 7.4.
16. DAB solution: 0.25 mg/ml 3,3′-diaminobenzidine tetrahydrochloride (DAB) and 0.036% H_2O_2 in 100 mM Tris-HCl, pH 7.4. Dissolve one 10 mg tablet of DAB (Sigma) in 40 ml of 100 mM Tris (see Note 5). Filter through filter paper. Place 10 ml of filtered DAB solution in a glass scintillation vial and add 12 µl of 30% H_2O_2 (see Note 6). Use immediately.
17. Dissecting microscope (for visualizing progress of development reaction).
18. 1% Gelatin. Mix 1 g of gelatin from porcine skin, type A (Sigma) in 100 ml of warm water (see Note 7).
19. Superfrost Plus slides.
20. Slide racks and staining jars.
21. Xylene.
22. Cytoseal or Permount mounting medium.

2.4. Quantification of Results

1. Digital microscope and camera.
2. Image analysis software capable of densitometry.
3. Spreadsheet software.
4. Tally counter.

3. Methods

3.1. Perfusion and Fixation of Brain Tissue

1. Anesthetize animals. Levels of immediate-early genes such as Fos and Arc are tightly regulated by activity-dependent neuronal activity (11). Changes in levels of these proteins can be observed as soon as 45 min after environmental modification, such as moving the mice to the necropsy room, changing mouse cages, switching lights, etc. The day before perfusion, notify laboratory personnel and animal care staff to avoid any disturbance to the cages. When ready to perfuse, remove only a cage or two at a time from the home room, and proceed as

quickly as possible to minimize the time to fixation. We perfuse mice from one or two cages every five or 10 min to ensure that all mice have a similar experience before the perfusion.

2. Flush-perfuse transcardially with normal saline for 45–60 s until the perfusate returns clear and no longer contains blood.
3. Remove the brain, bisect (see Note 8), and drop-fix one hemibrain in 4% PFA in 1× PB for 24–48 h at 4°C. Make sure that the fixative volume is at least ten times larger than the volume of the brain sample.
4. After the brains have been fixed at 4°C for 24–48 h, rinse twice for 2–5 h with PBS at 4°C. This reduces background during immunohistochemistry. Brains can be stored for 2–4 weeks in PBS at 4°C before sectioning.

3.2. Sectioning of Brain Tissue

1. Transfer the brains into 30% sucrose in PBS for 24–48 h at 4°C. Initially, the brains will float. They will sink when cryoprotected and ready for sectioning; do not section until the brains sink. Make sure that the volume of sucrose solution is at least ten times greater than the volume of the sample. Brains can be kept for 2 weeks at 4°C in 30% sucrose before sectioning. We recommend sectioning the brains within 1 month from the perfusion.
2. Place the hemibrains on the freezing stage of the microtome at room temperature and add a few drops of 10% sucrose around the hemibrains (see Note 9). Once the stage temperature is lowered, the 10% sucrose base will freeze and firmly attach the samples to the stage.
3. Set the temperature of the freezing stage at –20°C and wait for 5–10 min until the hemibrain and 10% sucrose base are completely frozen.
4. Collect ten subseries of floating sections (30 μm) per mouse hemibrain and place in 1.5-ml Eppendorf tubes containing 1.2 ml of ethylene glycol-based cryoprotectant medium (see Note 10). Each tube will contain 8–12 equidistant sections, 300 μm apart, throughout the rostro–caudal extent of the hemibrain. (These are standard parameters that could change depending on the experiment or animal model.)
5. Store the sections at –20°C until use.

3.3. Immunohistochemical Staining

The primary steps in the procedure are quenching endogenous peroxidase activity, blocking nonspecific binding, and incubating first with anti-calbindin, anti-NPY, anti-Fos, or anti-Arc primary antibody, then with a biotinylated secondary antibody, and finally with a horseradish peroxidase (HRP)-conjugated avidin–biotin complex. The HRP is detected by reaction with DAB, and the sections are mounted for quantification (see Note 11).

We routinely conduct the immunohistochemistry on floating microtome sections in a 24-well plate, with a 400-µl volume per well for most incubations and washes (the volume can be decreased to a minimum of ~250 µl for primary antibody reactions or other situations where reagents are limited). Unless indicated otherwise, all steps are conducted at room temperature (RT), and incubations/washes are done on a gently shaking platform.

1. Select one subseries for each animal.
2. Remove the sections from the cryoprotectant solution into a 10-cm dish containing PBS. Select the sections for immunohistochemical staining. For calbindin and NPY, the most important sections are those through the dorsal (rostral) hippocampus. Sections that are either anterior or posterior to the hippocampus can be discarded. For Fos and Arc, it is important to include every section through the dentate gyrus, from the most anterior where only the lower blade is visible, to the most posterior where the dentate takes on a circular shape. Transfer the desired sections to a 24-well plate, one well per animal, containing 400 µl of PBS per well.
3. Wash the sections 4×10 min at RT in PBS to remove cryoprotectant (see Note 12).
4. Wash the sections 2×15 min at RT in PBS/Tx.
5. Quench endogenous peroxidase activity by incubating the sections in PBS containing 3% H_2O_2 and 10% methanol for 15 min at RT. See Note 13.
6. Wash 4×15 min at RT in PBS/Tx.
7. Block nonspecific binding. Incubate the sections in PBS/Tx containing 10% normal goat serum (i.e., the normal serum from the species used to generate the secondary antibody), 1% dry milk, and 0.2% gelatin for 60 min at RT.
8. Wash 1×10 min in PBS/Tx at RT.
9. Primary antibody. Incubate the sections in PBS/Tx containing 3% normal goat serum, 0.2% gelatin, and primary antibody (1:30,000 rabbit anti-calbindin antibody, 1:8,000 rabbit anti-NPY antibody, 1:10,000 rabbit anti-Fos antibody, or 1:8,000 rabbit anti-Arc antibody) overnight at 4°C. Optimal primary antibody concentrations may differ between antibody batches. We recommend adjusting primary antibody concentration such that the development time is about 5 min.
10. Wash 5×15 min at RT in PBS/Tx.
11. Secondary antibody. Incubate the sections in PBS/Tx containing 3% normal goat serum, 0.2% gelatin, and 1:200 biotinylated goat anti-rabbit antibody for 60 min at RT.

12. Wash 5 × 15 min at RT in PBS/Tx. During these washes, prepare the ABC reagent for the next step. For a 24-well plate, add 45 μl of Reagent A (avidin) and 45 μl of Reagent B (biotinylated HRP) to 10 ml PBS/Tx and gently mix for 30 min at RT. The amount to prepare will depend on how many wells are being developed and can be scaled up or down, using 4.5 μl of each reagent per ml of PBS/Tx.
13. Avidin–biotin complex. Incubate the sections for 60 min at RT in ABC reagent that has been mixed as above.
14. Wash 1 × 15 in PBS/Tx at RT.
15. Wash 2 × 15 min in PBS at RT.
16. Wash 1 × 15 min in 100 mm Tris at RT (see Note 14).
17. Prepare the DAB solution as directed in Subheading 2.3.
18. Development reaction. We generally develop 24 wells at a time (one plate). Add DAB solution to each well at a constant interval. We typically use 10 s per well, which takes 4 min to add the DAB solution to a full 24-well plate. Monitor the progress of the development reaction under a dissecting microscope. The development time will vary depending on factors such as the batch and concentration of antibody and how the tissue was handled, but we generally aim for 5–6 min (see Note 15). Do not overdevelop and saturate the signal; light staining can be quantitated more reliably than dark staining. When the first well has reached the desired degree of development, stop the reaction by removing the DAB solution (see Note 5) and replacing it with 100 mM Tris. Continue to stop subsequent wells, again staggered 10 s apart (see Note 16).
19. Wash another 2 × 5 min in 100 mM Tris at RT.
20. Wash 2 × 15 min in PBS at RT (see Note 17).
21. Wash for 5 min with warmed 1% gelatin in water.
22. Move the sections to a 10-cm dish containing warm 1% gelatin and arrange in anatomical order for mounting.
23. Rest a clean SuperFrost Plus slide against the back of the 10-cm dish, wet the slide with gelatin, and use a paintbrush to gently slide the sections up onto the slide.
24. Blot excess gelatin solution from the edge of the slide and air dry overnight in a location protected from dust.
25. Clear the slides 2 × 5 min in xylene.
26. Coverslip with mounting medium and dry overnight.

3.4. Quantification of Results

Quantification of the results is an important aspect of the protocol and is performed on a digital microscope with image-analysis software that allows for densitometric measurement. All quantification

should be performed by an experimenter blinded to the genotypes of the animals.

3.4.1. Quantification of Calbindin Immunoreactivity

Calbindin depletion occurs in dentate granule cells and is visible in both the cell bodies (granule cell layer) and their dendrites (molecular layer) (Fig. 1). We quantify calbindin immunoreactivity in the molecular layer. Calbindin immunoreactivity in area CA1 was not altered in the hAPP transgenic lines we have analyzed so far (Fig. 5); we therefore use this region as an internal control to normalize for nonspecific variations in signal intensity (see Note 18).

1. Prepare the microscope, camera, and computer for image analysis. Adjust white balance.
2. Image the section at 10×.

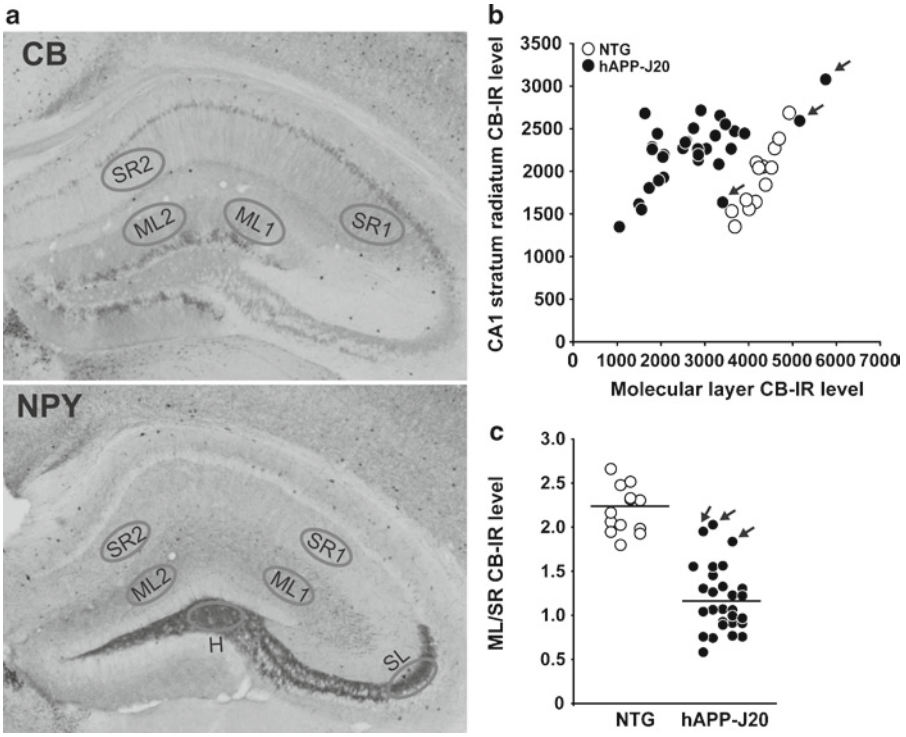

Fig. 5. Quantification of calbindin and NPY immunoreactivity. (**a**) Images demonstrate calbindin depletion (*top*) and aberrant NPY expression (*bottom*) in hAPP-J20 mice. Regions of interest for densitometric quantification are indicated in the dentate molecular layer (ML) and hilus (H), CA1 stratum radiatum (SR), and CA3 stratum lucidum (SL). (**b**) Calbindin immunoreactivity in the dentate ML and CA1 SR. Most hAPP-J20 mice have reduced calbindin in the dentate ML relative to NTG mice, with three exceptions indicated by *arrows*. In contrast, there are no differences between the groups in CA1 SR. Plotting dentate ML versus CA1 SR, as shown here, reveals a correlation between calbindin IR in the ML and in SR, indicating nonspecific variation in immunostaining. Because there are no differences between NTG and hAPP-J20 mice in calbindin levels in CA1 SR, this measurement can be used to normalize these non-biological differences in staining and reduce the variability in the measurement of calbindin in dentate ML (see Subheading 3.4.1, Eq. 1). (**c**) The ratio of ML/SR calbindin immunoreactivity reveals calbindin levels in the dentate ML to be lower in hAPP-J20 mice than in NTG controls, with reduced interindividual variability compared to raw ML data. *Arrows* indicate the three hAPP mice with normal ML/SR calbindin levels.

3. Create an elliptical region of interest (ROI) roughly the width of the dentate gyrus molecular layer.
4. For each animal, select two sections (a and b) through the dorsal hippocampus (roughly around –1.6 mm and –1.9 mm from bregma). Quantify the density of immunoreactivity in four areas of each section using the ROI tool: two segments of the dentate molecular layer (ML1a and ML2a) and two corresponding segments of the CA1 stratum radiatum (SR1a and SR2a) (see Fig. 5). Repeat for the second section (ML1b, ML2b, SR1b, and SR2b).
5. Repeat step 4 for each animal in the experiment.
6. Calculate the calbindin immunoreactivity for each animal as follows:

$$\frac{\frac{(\mathrm{ML1a}+\mathrm{ML2a})}{(\mathrm{SR1a}+\mathrm{SR2a})}+\frac{(\mathrm{ML1b}+\mathrm{ML2b})}{(\mathrm{SR1b}+\mathrm{SR2b})}}{2} \quad (1)$$

   This equation sums the ML density in two segments of each histological section, normalizes to the SR density for each section, and then averages the two sections to obtain the calbindin immunoreactivity for that animal. The resulting value should be ~2 for NTG mice. A lower value might indicate that the sections have been overdeveloped.
7. To enable comparison of data between experiments, determine the average calbindin level for all of the NTG animals in the experiment, and normalize every animal's calbindin level to this value. The average value of the NTG animals will thus be 1.0 after normalization.

3.4.2. Quantification of NPY Immunoreactivity

In the normal mouse hippocampus, NPY is expressed in a subset of inhibitory interneurons. Dark staining is visible in the soma of these cells, and faint staining from the axons of these inhibitory interneurons is visible in the molecular layer, where they synapse onto the dendrites of granule cells (Fig. 2). In AD mouse models, NPY is aberrantly expressed by granule cells themselves, most prominently in their axons (the mossy fibers), which is visible as dark staining along the course of the mossy fibers through the hilus to their termination in stratum lucidum of area CA3 (Fig. 2). hAPP transgenic mice also exhibit axonal sprouting of NPY-expressing hilar interneurons, resulting in increased immunoreactivity in the dentate molecular layer (Fig. 2). We quantify both processes, measuring NPY immunoreactivity in the mossy fibers and in the dentate molecular layer. Because NPY immunoreactivity in area CA1 was not altered in the hAPP lines we have analyzed so far, we use this region as an internal control to normalize the signal (Fig. 5).

1. Prepare the microscope, camera, and computer for image analysis. Adjust the white balance.
2. Image the section at 10×.
3. Create an elliptical ROI roughly the width of the dentate gyrus molecular layer.
4. For each subject animal, select two sections (a and b) through the dorsal hippocampus with good dentate anatomy (roughly around –1.6 mm and –1.9 mm from the bregma). Quantify the density of immunoreactivity in six areas of each section using the ROI tool: two segments of the dentate molecular layer (ML1a and ML2a), two corresponding segments of the CA1 stratum radiatum (SR1a and SR2a), the dentate hilus (Ha), and CA3 stratum lucidum (SLa) (see Fig. 5). Repeat for the second section (ML1b, ML2b, SR1b, SR2b, Hb, and SLb).
5. Repeat step 4 for each animal in the experiment.
6. Calculate the NPY immunoreactivity in the molecular layer for each animal as follows:

$$\frac{\frac{(\mathrm{ML1a}+\mathrm{ML2a})}{(\mathrm{SR1a}+\mathrm{SR2a})}+\frac{(\mathrm{ML1b}+\mathrm{ML2b})}{(\mathrm{SR1b}+\mathrm{SR2b})}}{2} \qquad (2)$$

   This equation sums the ML density in two segments of each histological section, normalizes to the SR density for each section, and then averages the two sections to obtain the NPY immunoreactivity in the molecular layer for that animal. This measure reflects axonal sprouting of NPY-positive hilar interneurons onto granule cell dendrites in the molecular layer.

7. Calculate the NPY immunoreactivity in the mossy fibers for each subject animal as follows:

$$\frac{\frac{(\mathrm{Ha})}{(\mathrm{SR1a}+\mathrm{SR2a})}+\frac{(\mathrm{Hb})}{(\mathrm{SR1b}+\mathrm{SR2b})}}{2}+\frac{\frac{(\mathrm{SLa})}{(\mathrm{SR1a}+\mathrm{SR2a})}+\frac{(\mathrm{SLb})}{(\mathrm{SR1b}+\mathrm{SR2b})}}{2}}{2} \qquad (3)$$

   This equation calculates the hilus density, normalizes to SR density, for each histological section, then averages the two sections. Similar normalization and averaging are performed for the CA3 stratum lucidum signals from the two sections. Then the hilar and CA3 stratum lucidum signals are averaged to obtain the NPY immunoreactivity in the mossy fibers for each animal. This measure reflects the aberrant expression of NPY in granule cell axons.

8. To enable comparison of data between experiments, determine the average NPY value for all of the NTG animals in the experiment, and normalize every animal's NPY level to this value. The average value of the NTG animals will be 1.0.

3.4.3. Quantification of Fos and Arc Immunoreactivity

In the normal mouse hippocampus, Fos and Arc are expressed in a small proportion of dentate granule cells. Fos-positive granule cells are easily visualized by their dark, round, nuclear staining (Fig. 3a), whereas Arc-positive granule cells show intense labeling in the soma and dendrites (Fig. 3b). The number of Fos- and Arc-positive granule cells are markedly reduced in hAPP transgenic mice with high levels of Aβ in the hippocampus (Fig. 3).

1. Starting at the most anterior section through the dentate gyrus, count the number of Fos- or Arc-positive cells in the granule cell layer in each section with a tally counter. Most positive cells exhibit strong and unequivocal staining, but there will be a few cells with less intense immunoreactivity. The experimenter must develop a consistent threshold for what will be considered a positive cell. All animals in a given cohort should be counted by the same experimenter at the same time. See Note 19.
2. Data can be plotted either as the number of Fos- or Arc-positive cells at a given rostro–caudal level (Fig. 3c) or as the total number of positive cells counted (Fig. 3d).

4. Notes

1. PFA is a toxic and volatile compound and must be handled in a fume hood.
2. PFA does not go into solution well at RT. However, avoid temperatures above 85°C, which will compromise the fixative properties of PFA.
3. We prefer the microtome over the vibratome, as it produces more uniform sections.
4. For washing, we use a transfer pipette with a fine (10 μl) Pipetman tip attached to the end with Parafilm. Remove as much liquid from the well as possible without damaging the sections. Tipping the plate back and forth can help collect the sections on one side of the well while removing the liquid from the other side.
5. DAB is a suspected carcinogen. When working with DAB and DAB-containing solutions, wear gloves, lab coat, and eye protection. Anything that comes into contact with DAB, including pipette tips, glassware and plasticware, and filter paper,

should be treated with bleach or a solution of 3% potassium permanganate ($KMnO_4$) and 2% sodium carbonate (Na_2CO_3).

6. Hydrogen peroxide is a substrate for peroxidase, and DAB is an electron donor in this reaction. The resulting oxidation of DAB produces a brown precipitate that is insoluble in xylenes and thus serves as a good immunohistochemical detection label.
7. It is important not to dissolve the gelatin in saline buffers, as the salts will crystallize on the sections as they dry.
8. We typically flash freeze one hemisphere on dry ice for future biochemical analyses, and drop-fix the other for immunohistochemistry. If desired, the entire brain can be fixed for immunohistochemistry without bisecting into separate hemibrains.
9. We routinely make small amounts of 10% sucrose by a 1:3 dilution of the 30% sucrose solution used for cryoprotection.
10. If the sections are intended for immunohistochemistry within a few days, the sections can be placed into PBS rather than cryoprotectant and stored at 4°C. This saves some time later, as the washes to remove cryoprotectant solution can be omitted.
11. A similar protocol can be performed for fluorescent labeling of calbindin or NPY. The following steps in Subheading 3.3 are modified. (a) Steps 5 and 6: quenching endogenous peroxidase and subsequent washing can be omitted. (b) Step 9: primary antibody concentrations are usually increased by 2–3× for fluorescence microscopy. (c) Step 11: use a fluorescent-labeled secondary antibody and incubate for 2 h. (d) Steps 13–26 (avidin–biotin–HRP complex, DAB development, and dry mounting in gelatin) are omitted. Instead, mount the PBS-washed sections with a fluorescence mounting medium and keep slides at 4°C.
12. If the sections were in PBS rather than cryoprotectant, this step can be omitted.
13. Some tissues contain endogenous peroxidase activity that could react with DAB to induce deposition of stain during development, even in the absence of antigen/antibody/HRP. This step quenches endogenous peroxidase to avoid this problem. In brain sections, the main source of endogenous peroxidase is erythrocytes, and failure to block endogenous peroxide will result in staining of the vasculature.
14. Developing in Tris-based solution instead of PBS produces lower background.
15. If the reaction proceeds much faster (e.g., 1 min), it is difficult to ensure that each well is developed for equal times, and antibody concentrations or DAB concentrations should be reduced. If the reaction takes too long (e.g., >10 min), then concentrations can be increased.

16. We routinely have two people involved in stopping the development reaction. One person removes the DAB from the well, and the other person immediately adds the Tris. This allows us to move from well to well in 10-s intervals. If it takes longer than this to stop the reaction in each well, use a longer interval between wells when adding the DAB, so that each well has the same duration of development in DAB.
17. Sections can be stored at 4°C in PBS for up to a week before sectioning. If the sections will be mounted immediately, it is not necessary to change from Tris to PBS, and this step can be omitted.
18. Different sections may have different staining intensity due to different times of development or immunoreactivity of the tissue. An internal control effectively cancels out this non-biological variation. It is important to verify in pilot experiments that the signal of the control area (e.g., radiatum of CA1) is not significantly changed in the experimental groups.
19. Around 5% of hAPP-J20 mice have abnormally increased Fos and Arc levels due to recent epileptiform activity (13). We do not typically count the number of positive granule cells in these mice.

Acknowledgments

We thank members of the Mucke laboratory, particularly Nga Bien-Ly and Alice Thwin, who helped develop these protocols; Jeannie Chin, Irene Cheng, and Julie Harris for helpful comments on the manuscript; Paul Worley for Arc antibody; and Stephen Ordway and Gary Howard for editorial review. This work was supported by Stephen D. Bechtel Jr. Young Investigator Awards (J.J.P and E.D.R), and NIH grants NS054811 (E.D.R.), AG023501 (L.M.) and AG022074 (L.M.).

References

1. Crabbe, J. C., Wahlsten, D., and Dudek, B. C. (1999) Genetics of mouse behavior: interactions with laboratory environment. *Science* **284**, 1670–72.
2. Richter, S. H., Garner, J. P., and Würbel, H. (2009) Environmental standardization: cure or cause of poor reproducibility in animal experiments? *Nat. Methods* **6**, 257–61.
3. Holcomb, L., Gordon, M. N., McGowan, E., Yu, X., Benkovic, S., Jantzen, P., Wright, K., Saad, I., Mueller, R., Morgan, D., Sanders, S., Zehr, C., O'Campo, K., Hardy, J., Prada, C. M., Eckman, C., Younkin, S., Hsiao, K., and Duff, K. (1998) Accelerated Alzheimer-type phenotype in transgenic mice carrying both mutant amyloid precursor protein and presenilin 1 transgenes. *Nat. Med.* **4**, 97–100.
4. Westerman, M. A., Cooper-Blacketer, D., Mariash, A., Kotilinek, L., Kawarabayashi, T., Younkin, L. H., Carlson, G. A., Younkin, S. G., and Ashe, K. H. (2002) The relationship between Aβ and memory in the Tg2576 mouse model of Alzheimer's disease. *J. Neurosci.* **22**, 1858–67.

5. Kobayashi, D. T., and Chen, K. S. (2005) Behavioral phenotypes of amyloid-based genetically modified mouse models of Alzheimer's disease. *Genes Brain Behav.* **4**, 173–96.
6. Lesné, S., Ming, T. K., Kotilinek, L., Kayed, R., Glabe, C. G., Yang, A., Gallagher, M., and Ashe, K. H. (2006) A specific amyloid-β protein assembly in the brain impairs memory. *Nature* **440**, 352–57.
7. Palop, J. J., Jones, B., Kekonius, L., Chin, J., Yu, G. -Q., Raber, J., Masliah, E., and Mucke, L. (2003) Neuronal depletion of calcium-dependent proteins in the dentate gyrus is tightly linked to Alzheimer's disease-related cognitive deficits. *Proc. Natl. Acad. Sci. U S A* **100**, 9572–77.
8. Arriagada, P. V., Growdon, J. H., Hedley-Whyte, E. T., and Hyman, B. T. (1992) Neurofibrillary tangles but not senile plaques parallel duration and severity of Alzheimer's disease. *Neurology* **42**, 631–39.
9. Ingelsson, M., Fukumoto, H., Newell, K. L., Growdon, J. H., Hedley-Whyte, E. T., Frosch, M. P., Albert, M. S., Hyman, B. T., and Irizarry, M. C. (2004) Early Aβ accumulation and progressive synaptic loss, gliosis, and tangle formation in AD brain. *Neurology* **62**, 925–31.
10. Giannakopoulos, P., Gold, G., Kövari, E., von Gunten, A., Imhof, A., Bouras, C., and Hof, P. R. (2007) Assessing the cognitive impact of Alzheimer disease pathology and vascular burden in the aging brain: the Geneva experience. *Acta Neuropathol.* **113**, 1–12.
11. Palop, J. J., Chin, J., Bien-Ly, N., Massaro, C., Yeung, B. Z., Yu, G. -Q., and Mucke, L. (2005) Vulnerability of dentate granule cells to disruption of Arc expression in human amyloid precursor protein transgenic mice. *J. Neurosci.* **25**, 9686–93.
12. Chin, J., Palop, J. J., Puoliväli, J., Massaro, C., Bien-Ly, N., Gerstein, H., Scearce-Levie, K., Masliah, E., and Mucke, L. (2005) Fyn kinase induces synaptic and cognitive impairments in a transgenic mouse model of Alzheimer's disease. *J. Neurosci.* **25**, 9694–703.
13. Palop, J. J., Chin, J., Roberson, E. D., Wang, J., Thwin, M. T., Bien-Ly, N., Yoo, J., Ho, K. O., Yu, G. -Q., Kreitzer, A., Finkbeiner, S., Noebels, J. L., and Mucke, L. (2007) Aberrant excitatory neuronal activity and compensatory remodeling of inhibitory hippocampal circuits in mouse models of Alzheimer's disease. *Neuron* **55**, 697–711.
14. Cheng, I., Scearce-Levie, K., Legleiter, J., Palop, J., Gerstein, H., Bien-Ly, N., Puoliväli, J., Lesné, S., Ashe, K., Muchowski, P., and Mucke, L. (2007) Accelerating amyloid-β fibrillization reduces oligomer levels and functional deficits in Alzheimer disease mouse models. *J. Biol. Chem.* **282**, 23818–28.
15. Palop, J. J., and Mucke, L. (2009) Epilepsy and cognitive impairments in Alzheimer disease. *Arch. Neurol.* **66**, 435–40.
16. Minkeviciene, R., Rheims, S., Dobszay, M. B., Zilberter, M., Hartikainen, J., Fülöp, L., Penke, B., Zilberter, Y., Harkany, T., Pitkänen, A., and Tanila, H. (2009) Amyloid β-induced neuronal hyperexcitability triggers progressive epilepsy. *J. Neurosci.* **29**, 3453–62.
17. Roberson, E. D., Scearce-Levie, K., Palop, J. J., Yan, F., Cheng, I. H., Wu, T., Gerstein, H., Yu, G. -Q., and Mucke, L. (2007) Reducing endogenous tau ameliorates amyloid β-induced deficits in an Alzheimer's disease mouse model. *Science* **316**, 750–54.
18. Vezzani, A., Sperk, G., and Colmers, W. F. (1999) Neuropeptide Y: emerging evidence for a functional role in seizure modulation. *Trends Neurosci.* **22**, 25–30.
19. Palop, J. J., Chin, J., and Mucke, L. (2006) A network dysfunction perspective on neurodegenerative diseases. *Nature* **443**, 768–73.
20. Busche, M. A., Eichhoff, G., Adelsberger, H., Abramowski, D., Wiederhold, K. H., Haass, C., Staufenbiel, M., Konnerth, A., and Garaschuk, O. (2008) Clusters of hyperactive neurons near amyloid plaques in a mouse model of Alzheimer's disease. *Science* **321**, 1686–89.
21. Palop, J. J., and Mucke, L. (2010) Amyloid-β-induced neuronal dysfunction in Alzheimer's disease: from synapses toward neural networks. *Nat. Neurosci.* **13**:812–818.
22. Vogt, D. L., Thomas, D., Galvan, V., Bredesen, D. E., Lamb, B. T., and Pimplikar, S. W. (2009) Abnormal neuronal networks and seizure susceptibility in mice overexpressing the APP intracellular domain. *Neurobiol. Aging.* doi:10.1016/j.neurobiolaging. 2009.09.002.

Chapter 18

Epigenetic Changes in the Brain: Measuring Global Histone Modifications

Gavin Rumbaugh and Courtney A. Miller

Abstract

Recent years have witnessed an explosion of research on the role of epigenetic modifications, such as DNA methylation and histone protein acetylation and phosphorylation, in neuroscience. These changes exert control over gene expression and have been shown to play important roles in a variety of neural processes, including learning and memory. We and others have also recently shown that epigenetic changes may contribute to neurodegenerative disorders, such as Alzheimer's disease. Western blot analysis with antibodies raised against specific histone modifications is a relatively simple technique able to reveal the type, location, and degree of histone posttranslational modifications produced by an experimental manipulation. Here we provide a step-by-step protocol for isolating histone proteins from tissue and measuring these posttranslational modifications.

Key words: Epigenetics, Histone, Chromatin, Acetylation, Phosphorylation, Methylation, Western blot

1. Introduction

The term epigenetics, coined by Conrad Waddington (1), refers to modifications that occur above ("epi-") the genetic level. These changes do not alter the underlying DNA nucleotide sequence, but are capable of persisting through cell division and influencing gene transcription. The most commonly studied epigenetic modifications are DNA methylation and chromatin modification. This chapter will focus on a method used to assay the latter, chromatin modifications.

Chromatin consists of a complex of DNA and core histone proteins, which act as a spool to package DNA to fit inside the nucleus. These core histone proteins (H2A, H2B, H3, and H4) are subject to posttranslational modification on their N-terminal tails.

Erik D. Roberson (ed.), *Alzheimer's Disease and Frontotemporal Dementia*, Methods in Molecular Biology, vol. 670,
DOI 10.1007/978-1-60761-744-0_18,

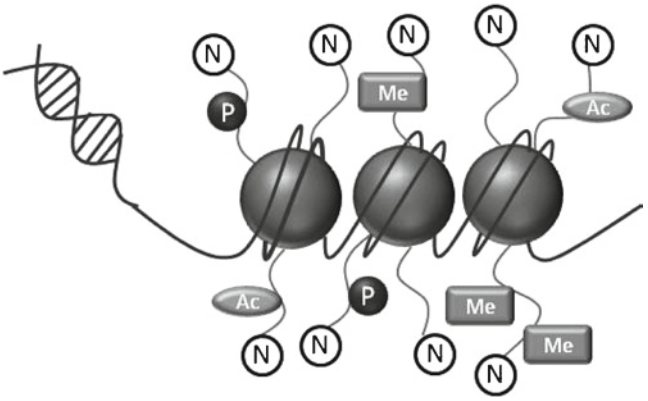

Fig. 1. Schematic representation of DNA spooled around core histone proteins to form chromatin, along with potential posttranslational modifications (*P* phosphorylation, *Ac* acetylation, *Me* methylation) of the N-terminal tails.

The most common modifications are acetylation, phosphorylation, and methylation, all of which are capable of influencing the rate of gene transcription by controlling physical access to the gene (Fig. 1). Both phosphorylation and acetylation are associated with transcriptional activation, while histone methylation's transcriptional consequences are dependent on the number and location of the methyl groups (2).

In recent years, the field of neuroscience has begun to realize the importance of epigenetic mechanisms in both development and cognition. A critical role for chromatin modifications in learning has now been demonstrated in several rodent behavioral models, including tasks dependent on the hippocampus and cortex (3–7). Moreover, chromatin modifications play an important role in psychiatric disorders such as schizophrenia, depression, and drug addiction (8).

Histone deacetylases (HDACs) are the enzymes responsible for the removal of acetyl groups from the N-terminal of histones. Several HDAC inhibitors have been developed, including SAHA, a compound approved by the FDA for the treatment of T-cell lymphoma. With the discovery that HDAC inhibitors not only increase acetylation levels, but also enhance cognition (9, 10), a number of laboratories have turned a therapeutic eye to the role of histone modifications in Alzheimer's disease. In accordance with this, a recent publication from our group reported that memory deficits in a mouse model of Alzheimer's disease can be rescued by treatment with HDAC inhibitors that specifically target class I HDACs (11).

The following protocol will provide investigators with an excellent technique to begin their own research in the field of epigenetics.

2. Materials

2.1. Extracting Histone Proteins

1. Tissue to be assayed.
2. 1 M Tris-HCl stock, pH 7.4.
3. 1 M KCl stock. Dissolve 3.73 g of KCl in 50 mL of ddH_2O.
4. 100 mg/mL (900 mM) sodium butyrate. Dissolve 100 mg in 1 mL of ddH_2O. Store aliquots at –20°C. Sodium butyrate is used as a HDAC inhibitor.
5. 100 mM sodium orthovanadate. Dissolve 18.39 mg of sodium orthovanadate in 1 mL of ddH_2O. Store aliquots at –20°C. Sodium orthovanadate is used as a phosphotyrosine phosphatase inhibitor.
6. 0.2 M phenylmethylsulphonyl fluoride (PMSF). Dissolve 34.8 mg of PMSF in 1 mL of 100% EtOH. Store at 4°C. PMSF is used as a serine protease inhibitor.
7. 100× protease inhibitor cocktail (Sigma).
8. Homogenization buffer: 50 mM Tris-HCl, pH 7.5, 25 mM KCl, 250 mM sucrose, 2 mM sodium butyrate, 1 mM sodium orthovanadate, 0.5 mM PMSF, 1× protease inhibitor cocktail. To make 10 mL, mix 855.8 mg of sucrose, 500 µl of 1 M Tris-HCl stock, and 250 of µl 1 M KCl stock in 9.13 mL of ddH_2O. Then add 22 µl of 100 mg/mL sodium butyrate, 100 µl of 100 mM sodium orthovanadate, 25 µl of 0.2 M PMSF, and 100 µl of 100× protease inhibitor cocktail immediately before use. Large volume stocks containing the first three ingredients can be prepared and stored at 4°C, but the inhibitors should always be added immediately before use.
9. Dounce homogenizers or RNase-free tubes with tissue grinding pestles.
10. 0.4 N H_2SO_4 (sulfuric acid): Mix 111.12 µl of 18 M H_2SO_4 in 9.88 mL of ddH_2O. Store at 4°C.
11. Trichloroacetic acid (TCA) with 10 mM sodium deoxycholate. Mix 160 mg of sodium deoxycholate in 40 mL of 6.1 N TCA. Store at 4°C.
12. Acidified acetone: Mix 5 mL of acetone (HPLC grade) and 5 mL of hydrochloric acid (32–38% trace metal grade). Store at 4°C.
13. 100% acetone. Store at 4°C so it is cold for use.
14. 10 mM Tris-HCl, pH 8.0.
15. Bradford reagent for protein assay.

2.2. Western Blotting for Posttranslational Histone Modifications

1. Gel casting and electrophoresis apparatus, including power supply.
2. 30% Acrylamide/Bis (37.5:1) solution.
3. 1.5 M Tris-HCl, stock, pH 8.8.
4. 10% sodium dodecyl sulfate (SDS) solution (w/v). Dissolve 1 g of SDS in 10 mL of ddH_2O.
5. 50% glycerol solution (v/v). Disolve 50 mL of glycerol in 50 mL of ddH_2O.
6. 10% ammonium persulfate (APS) solution (w/v). Dissolve 1 g of APS in 10 mL of ddH_2O, and allow it to settle.
7. TEMED.
8. 15% Resolving gel solution: 375 mM Tris-HCl, pH 8.8, 15% acrylamide/bis (37.5:1), 0.1% SDS, 2.5% glycerol, 0.1% APS, 0.1% TEMED. To make 40 mL, mix 20 mL of 30% acrylamide, 10 mL of 1.5 M Tris-HCl, 400 µl of 10% SDS, 2 mL of 50% glycerol, and 400 µl of 10% APS with 7.2 mL of ddH_2O. Add 40 µl of TEMED immediately prior to pouring gel.
9. Stacking gel solution: 360 mM Tris-HCl, pH 8.8, 4% acrylamide/bis (37.5:1), 0.1% SDS, 15% glycerol, 0.1% APS, 0.1% TEMED. To make 20 mL, mix 2.6 mL of 30% acrylamide, 4.8 mL of 1.5 M Tris-HCl, 200 µl of 10% SDS, 6 mL of 50% glycerol, and 200 µl of 10% APS with 6.2 mL of ddH_2O. Add 20 µl of TEMED immediately prior to pouring gel.
10. Running buffer: 250 mM glycine, 25 mM Tris-HCl base, 0.1% SDS. To prepare 2 L, mix 37.54 g of glycine, 6 g of Tris-HCl base, and 2 g of SDS in ddH_2O.
11. Protein molecular weight standard.
12. Transfer buffer: 250 mM glycine, 25 mM Tris-HCl base, 10% methanol. To prepare 2 L, mix 37.54 g of glycine, 6 g of Tris-HCl base, and 200 mL of methanol in ddH_2O.
13. Gel transfer apparatus.
14. PVDF membrane and filter paper.
15. Methanol.
16. Tris-Buffered Saline (TBS): 50 mM Tris-HCl, pH 7.5, 150 mM NaCl. To prepare 2 L, mix 17.54 g of NaCl and 100 mL of 1 M Tris-HCl, pH 7.5, in ddH_2O.
17. TBS with Tween-20 (TBST): 50 mM Tris-HCl, pH 7.5, 150 mM NaCl, 0.1% Tween 20. To prepare 1 L, mix 999 mL of TBS with 1 mL of Tween-20.
18. TBST with 5% bovine serum albumin (BSA): 50 mM Tris-HCl, pH 7.5, 150 mM NaCl, 0.1% Tween 20, 5% BSA. To prepare 200 mL, dissolve 10 g of BSA in TBST.
19. Sealable plastic pouches for antibody incubation.

Table 1
Primary antibodies for Western blotting to detect changes in histone modifications

To Detect	Antibody	Source
Acetylated H3	Rabbit anti-acetyl-histone H3 (Lys9/Lys14)	Cell Signaling Technology 9677
Phosphorylated H3	Rabbit anti-phospho-histone H3 (Ser28)	Millipore 07-145
Trimethylated H3	Rabbit anti-trimethyl-histone H3 (Lys4)	Millipore 07-473
Total H3	Mouse anti-histone H3 (clone 96C10)	Cell Signaling Technology 3638
Acetylated H4	Rabbit anti-acetyl-histone H4 (Lys5/Lys8/Lys12/Lys16)	Millipore 06-598
Total H4	Rabbit anti-histone H4	Millipore 07-108

20. Primary Antibodies. See Table 1. We use each of these antibodies at 1:1,000, but conditions may need to be re-optimized in each laboratory.
21. Secondary Antibodies: HRP-conjugated anti-rabbit and anti-mouse IgG (depending on the source of primary antibody).
22. ECL Western blotting substrate.
23. Kodak bioMax light film.
24. 0.2 N sodium hydroxide (NaOH): Dilute 10 N NaOH 1:50.

2.3. Analysis of Western Blots

1. Flat bed scanner.
2. ImageJ analysis software. You can download this freeware program at http://rsbweb.nih.gov/ij/index.html.

3. Methods

The protocol described below outlines procedures for extraction of histone proteins from a tissue sample, performing the Western blot analysis of histone posttranslational modifications, and quantifying and interpreting the results.

3.1. Extracting Histone Proteins

1. Prepare two sets of 1.5-mL sterile microfuge tubes per treatment condition.
2. Prepare fresh homogenization buffer (1.5 mL per sample) according to Subheading 2.1, step 8.

3. Fill Dounce homogenizers or RNase-free tubes with tissue grinders with 1 mL of homogenization buffer and place on ice (see Note 1).
4. Transfer tissue from dry ice or –80°C storage into tube and homogenize with approximately six strokes.
5. Transfer homogenate to microfuge tube.
6. Centrifuge at 7,700 × *g* for 1 min at 4°C to pellet nuclei (see Note 2).
7. Transfer supernatant to a fresh 1.5-mL microfuge tube and store at –20°C if desired (see Note 3).
8. Resuspend pellets containing nuclear fraction in 500 µl of 0.4 N H_2SO_4 by thorough trituration. Vortex samples if necessary.
9. Incubate on ice for 30 min, with brief vortexing every 10 min.
10. Centrifuge extracts at maximum speed for 10 min at 4°C.
11. Transfer supernatant to fresh 1.5-mL tube and discard pellet (see Note 4).
12. Add 250 µl of trichloroacetic acid and sodium deoxycholate to supernatant to precipitate histones.
13. Slowly invert the tubes to mix by hand; the solution should immediately turn cloudy.
14. Incubate on ice for 30 min.
15. Centrifuge solution at maximum speed for 30 min at 4°C.
16. Discard supernatant (see Note 5), rinse tube with 1 mL of *cold*, *acidified* acetone (see Note 6), and invert to mix.
17. Incubate on ice for 5 min.
18. Centrifuge at maximum speed for 5 min at 4°C.
19. Discard supernatant and rinse tube with 1 mL *cold* (4°C) 100% acetone as in Note 6. This provides a safe method of removing acid from the solution without affecting the histone (protein) pellet. Carefully invert tube to mix and incubate on ice for 5 min.
20. Centrifuge at maximum speed for 5 min at 4°C.
21. Decant supernatant and allow the pellet to dry for approximately 5 min (see Note 7).
22. Resuspend protein extract in 50 µl of 10 mM Tris-HCl, pH 8.0 (see Note 8).
23. Quantify the protein concentration of each sample using a Bradford reagent-based commercial protein assay kit.
24. Store sample at –80°C. We prefer to add SDS-PAGE sample buffer before storage, to further protect the samples.

3.2. Western Blotting for Posttranslational Histone Modifications

1. Determine the number of gels needed and the number of lanes per gel.
2. Prepare gel casting apparatus.
3. Make Resolving and Stacking Gel solutions, but do not add TEMED until *immediately* before pouring each of the solutions, in steps 4 and 5.
4. Pour Resolving Gel solution between glass plates, taking care not to produce any bubbles, and wait for 10 min.
5. Pour Stacking Gel solution on top of resolving gel and insert gel combs.
6. Wait for 15 min for the gel to set.
7. While the gels are setting up, make Running Buffer.
8. Load gel in electrophoresis apparatus and fill with Running Buffer.
9. Remove gel combs and load 1 μg of histone extract per lane. Load molecular weight standards in desired lane(s).
10. Run the gel at 100 V for 1 h and 45 min, or until protein marker has run down the gel.
11. While the gel is running, prepare Transfer Buffer and make distinct marks on each PVDF membrane (e.g., cut a corner off with scissors) for later identification.
12. Prepare PVDF membranes for transfer by pre-incubation in methanol for 1 min, followed by a dip in ddH_2O. Leave membrane in Transfer Buffer until the gel finishes running.
13. Prepare the gel for transfer by setting up the transfer cassette in the following order: (a) pad, (b) filter paper, (c) gel, (d) PVDF membrane, (e) filter paper and (f) pad (see Note 9).
14. Set up transfer chamber with stir bar and place in an ice bath on stir plate.
15. Run at 75 V for 2 h.
16. Make TBS, TBST, and TBST with 5% BSA during transfer.
17. Remove blots from cassettes and place in methanol for 1 min.
18. Dry at room temperature for 15 min (see Note 10) and prepare primary antibody solutions.
19. Cut plastic sealing bags to size for blots and incubate blots with primary antibody in TBST + 5% BSA on rotator overnight at 4°C (see Note 11).
20. Remove the blot from the primary antibody and perform 3×5 min washes in TBST.
21. During these washes, prepare the secondary antibody solution.

22. Incubate blots with secondary antibody, 1:5,000 in TBST + 5% BSA, for 60 min at room temperature (see Note 12).
23. Perform 3 × 5 min washes in TBST, followed by 3 × 5 min washes in TBS.
24. Set up for development by chemiluminescence by preparing ECL substrate (1 mL per blot) and sections of plastic wrap for each blot.
25. At the end of washing, place each blot on square of plastic wrap.
26. Add 1 mL of ECL reagent to each blot and wait for 1 min.
27. Wrap blots in plastic wrap, being careful not to create any uneven surfaces.
28. Expose to film in dark room, developing after 30 s, 2 min, and 10 min (see Note 13).
29. After exposing to film, the antibody must be stripped and reprobed with a second antibody (see Note 14). Place blot in a solution of 0.2 N NaOH for 15 min, rotating on an orbital shaker at maximum speed.
30. Perform 1 × 5 min wash in TBS.
31. Block the membrane in TBST with 5% BSA.
32. Continue Western blotting with control antibody, as described above in steps 19–28.

3.3. Analysis of Western Blots

To quantify the relative change in a histone modification, it is necessary to measure bands from both the blot exposed to the antibody of interest, and the blot exposed to a control protein (such as total histone H4). This can be done using an image analysis program. ImageJ is a freely available program capable of providing a quantitative readout of band densities.

1. Take exposed films of both blots (let us use the example of acetylated H3 [AcH3] and total H4 [TH4]) and scan each (using a consumer-grade scanner) to a separate TIFF file at a resolution of 300 dpi. Turn off all image processing filters and acquire the image in 8-bit grayscale.
2. Open the AcH3 scan (blot) with Image J.
3. Crop the image close to the bands to remove unnecessary area.
4. Invert the image (CTRL + SHFT + I). This command results in the band having higher gray values relative to the film (see Fig. 2).
5. Open the "Set Measurements" dialog box located in the "Analyze" menu.
6. Check the "Integrated Density" box.

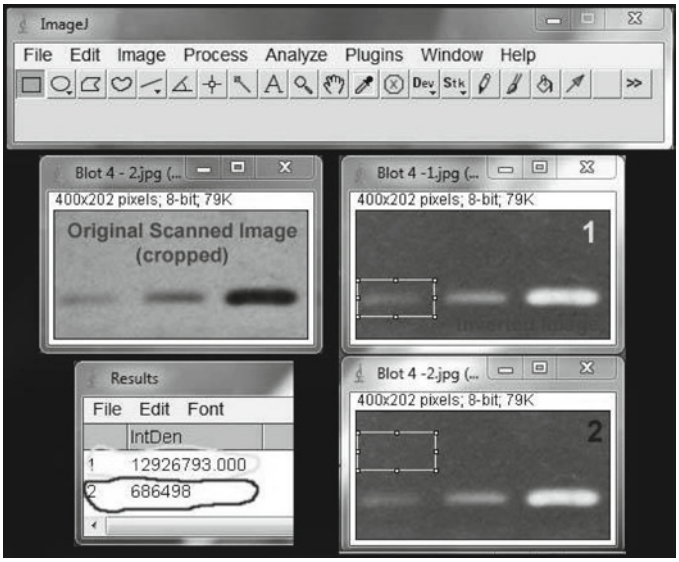

Fig. 2. Using ImageJ software to quantify the intensity of bands after Western blotting.

7. Click on the image and draw a rectangle around the first band – Inverted Image 1 (see Fig. 2).
8. To measure the density of this area, use the "Measure" command in the "Analyze" menu. You can also use the shortcut (CTRL + M). This command will sum the value of all pixels (see Fig. 2).
9. To uncover the "true integrated density" of the band, you must now measure and subsequently subtract the value of the film in this region. This is equivalent to a background subtraction. To do this, move the rectangle to a blank area above the band and repeat the "measure" command (see Fig. 2). The integrated density for this region is smaller than the first measurement. Subtract this value from the first to yield the true integrated density of your band's signal. It is essential to use the same size rectangle for all measurements on a given scan (blot). Different sized rectangles can be used for different scans (blots).
10. Repeat this procedure for all bands.
11. Open the scan from your "TH4" blot.
12. Repeat steps 3–10 for the "TH4" blot.
13. For each sample/lane, divide the "true integrated density" of the AcH3 band by the "true integrated density" of the TH4 band. This normalization yields a relative acetylated histone value for each sample.

4. Notes

1. We typically work with 40 mg or more of starting brain tissue. However, the protocol can easily be adapted for smaller tissue amounts, as we have successfully isolated sufficient histone protein concentrations from just a few 1 mm^2 tissue punches. Simply reduce the volume of the homogenization buffer (e.g., 500 µl).
2. It is particularly important to develop a standard practice of orienting the tubes in the same direction for each spin in the centrifuge. In many cases, the small histone pellet's location will not be obvious and will be inferred from how the tube was oriented during the spin.
3. This is the cytoplasmic fraction and can, if desired, be used for other assays.
4. Acid extraction by H_2SO_4 is a common method for separating histones. Following incubation on ice and centrifugation, nuclear proteins and nucleic acids will precipitate and pellet. Investigators specifically interested in examining histone phosphorylation may consider a high salt-based extraction method instead. Phosphorylation is particularly acid labile.
5. Do not expect to see a pellet at this point.
6. When rinsing the pellet with acidified acetone, run the acetone down the side of the tube that is expected to have product based on the way the tube was oriented in the centrifuge. Carefully run your pipette tip along the tube's side to help "peel" the sample off the side of the tube and into the acetone.
7. Use care to not *over-dry* the pellet, as this will make resuspension extremely difficult.
8. Resuspension requires patience. Carefully pipette the Tris-HCl down the side of the tube where the product is from centrifugation. Repeat by pulling up Tris-HCl at the bottom of the tube and running it down the side again. Then let Tris-HCl sit for several minutes while you prepare protein assay or add Tris-HCl to additional samples. Finally, *gently* triturate to complete resuspension. Some of the pellet will likely remain at the bottom of the tube, but histones have resuspended.
9. To ensure complete transfer, be careful to remove any bubbles between layers in transfer cassette using a 15-mL conical vial or similar.
10. This drying step precludes the need to include a blocking step.
11. We typically incubate blots with the primary antibody overnight at 4°C at a concentration of 1:1,000. However, a rapid version of this protocol can be performed in which blots are incubated with the primary antibody for 90 min at room

temperature. These times and concentrations may need to be optimized in your laboratory. Be sure all bubbles are removed from plastic bags before sealing to ensure proper contact between all parts of blot and antibody during incubation.

12. As with the primary antibody, the incubation time and secondary antibody concentration will need to be optimized in your laboratory. We have found that the time can range from 45 min to 2 h, with a concentration range of 1:5,000–10,000.
13. In order to use this analysis for publication, one must first confirm that their detection system is in the "linear range." To test if your system is indeed linear, perform a serial dilution (over a tenfold concentration) of your sample and then blot with one of your antibodies. Then perform the analysis from Subheading 3.3 to determine the linear range. Using an HRP-conjugated secondary antibody, ECL, and high quality film, one should have at least a fivefold range of linearity using this system. If you do not, then the Western blotting protocol and exposure time must be optimized. The two most common causes of reduced linearity using this system are film over-exposure and suboptimal primary/secondary antibody ratios/incubation times. One can achieve >100-fold linearity using more sophisticated detection systems based on direct fluorescence (e.g. LiCOR or Typhoon).
14. A second (control) antibody for a protein that is not expected to change with the experimental manipulation should be used to normalize the signal from the first antibody. This serves as an excellent loading control in addition to normalizing based on the results of the protein assay. We recommend that the control antibody recognize an antigen with a different molecular weight than the first. This ensures that the first antibody will not influence the results of the second, in case the stripping did not fully remove all of the first antibody. For example, if probing for acetylation of histone H3 on a blot is performed first, we recommend normalizing to total H4 protein to avoid the confounding of both antibodies having a molecular weight of 17 kDa. Also, we recommend stripping a blot no more than once to avoid stripping protein from the blot.

References

1. Waddington, C.H. (1957) The Strategy of Genes. New York: Macmillan.
2. Spencer, V.A. and Davie, J.R. (1999) Role of covalent modifications of histones in regulating gene expression. *Gene* **240**, 1–12.
3. Levenson, J.M., O'Riordan, K.J., Brown, K.D., Trinh, M.A., Molfese, D.L. and Sweatt, J.D. (2004) Regulation of histone acetylation during memory formation in the hippocampus. *J. Biol. Chem.* **279**, 40545–59.
4. Wood, M.A., Kaplan, M.P., Park, A., Blanchard, E.J., Oliveira, A.M., Lombardi, T.L. and Abel, T. (2005) Transgenic mice expressing a truncated form of CREB-binding

protein (CBP) exhibit deficits in hippocampal synaptic plasticity and memory storage. *Learn. Mem.* **12**, 111–19.

5. Miller, C.A., Campbell, S.L. and Sweatt, J.D. (2008) DNA methylation and histone acetylation work in concert to regulate memory formation and synaptic plasticity. *Neurobiol. Learn. Mem.* **89**, 599–603.
6. Swank, M.W. and Sweatt, J.D. (2001) Increased histone acetyltransferase and lysine acetyltransferase activity and biphasic activation of the ERK/RSK cascade in insular cortex during novel taste learning. *J. Neurosci.* **21**, 3383–91.
7. Koshibu, K., Graff, J., Beullens, M., Heitz, F.D., Berchtold, D., Russig, H., Farinelli, M., Bollen, M. and Mansuy, I.M. (2009) Protein phosphatase 1 regulates the histone code for long-term memory. *J. Neurosci.* **29**, 13079–89.
8. Graff, J. and Mansuy, I.M. (2008) Epigenetic codes in cognition and behaviour. *Behav. Brain. Res.* **192**, 70–87.
9. Vecsey, C.G., Hawk, J.D., Lattal, K.M., Stein, J.M., Fabian, S.A., Attner, M.A., Cabrera, S.M, McDonough, C.B., Brindle, P.K., Abel, T. and Wood, M.A. (2007) Histone deacetylase inhibitors enhance memory and synaptic plasticity via CREB:CBP-dependent transcriptional activation. *J. Neurosci.* **27**, 128–40.
10. Bredy, T.W. and Barad, M. (2008) The histone deacetylase inhibitor valproic acid enhances acquisition, extinction and reconsolidation of conditioned fear. *Learn. Mem.* **15**, 39–45.
11. Kilgore, M., Miller, C.A., Fass, D.M., Hennig, K.M., Haggarty, S.J., Sweatt, J.D. and Rumbaugh, G. (2009) Inhibitors of class I histone deacetylases reverse contextual memory deficits in a mouse model of Alzheimer's disease. *Neuropharm.* **35**, 870–80.

INDEX

A

Aβ. *See* Amyloid-beta (Aβ) protein
Acetylation 214, 223, 226, 264, 273
Aggregation 3, 4, 13–30, 33, 45, 57–68, 72, 93, 109–122, 135, 136, 141, 143, 147, 150, 174, 178, 182
Aging..... 45, 176, 184, 185, 201, 208
Alzheimer's disease 1–5, 33, 34, 45, 57, 85, 93, 109, 125, 141, 169–186, 191–205, 208, 211, 245–261, 264
Amyloid.....2, 20, 57, 170, 171, 175–178, 183, 184
Amyloid-beta (Aβ) protein 2, 20, 33–43, 45, 58, 71, 141, 169
Amyloid plaques..... 2, 3, 5, 38, 45, 166, 169, 173, 181, 246
Amyloid precursor protein (APP) 2, 34, 45, 58, 71, 85, 169, 245
Antigen retrieval..... 86, 88–90
ApoE structure 125
Apolipoprotein E..... 125–137
APP. *See* Amyloid precursor protein
APP C-terminal fragments 71–83
APP intracellular domain (AICD)..... 74, 85–91
ARC 177
Arc.....177, 209, 246, 249, 252–254, 259, 261
Atomic force microscopy (AFM) 3, 22, 26, 57–68
Axonal transport.....5, 181, 231–242

B

BACE. *See* Beta-site APP cleaving enzyme
β-amyloid 2, 20, 33–43, 45, 58, 71, 141, 169
BCIP 207, 215, 223, 224, 227
Behavior 5, 13, 59, 194, 199–201, 203, 246
Beta-site APP cleaving enzyme (BACE) 45, 71, 169, 174
Biomarkers 5, 245–261
Brain.....3, 5, 33–43, 45–56, 58, 72–74, 76, 79–80, 82, 85–91, 141, 145, 149, 159, 164–166, 171–174, 176, 181, 182, 207–230, 246, 250–253, 260, 262–273
Brain sections 211, 223, 260

C

Calbindin..... 246, 247, 249, 250, 252, 254, 256–257, 260
cDNA..... 127, 174, 208–211, 218–222, 229
Cell culture 14, 21, 24, 26, 94, 95, 97–99, 102, 106, 107, 142–146, 150, 233, 239
Cell death 141
Central nervous system..... 4
Cerebrospinal fluid (CSF), 3, 33–43, 83
Chromatin 263, 264
Cognition 191, 264
Cognitive deficits.....3, 175, 177, 178, 183, 191, 246, 247
Cryostat..... 212, 214, 215, 217–218, 225–228
Cultured hippocampal neurons 142, 148, 149

D

Dementia.....2, 141, 170, 181
Dentate gyrus 209, 246, 249, 250, 254, 257–259
digoxigenin-labeled probes
Disinhibition 1

E

Ectopic expression 211
Epigenetics 5, 263, 264
Epilepsy..... 245
EST. *See* Expressed sequence tag
Excitability 245
Excitatory 208, 246
Expressed sequence tag (EST) 209, 210, 213, 218–220

F

Fast Red..... 215, 223, 225, 227, 228
Fibrils 17–19, 66
Fluorescence 215, 228, 234, 240–241
Fos 246, 249, 250, 252, 254, 259, 261
Frontotemporal dementia 1–5

G

GABA 245
GABAergic sprouting 245
Gel filtration..... 136
Gene expression..... 5, 86, 155–167, 207–230
Glia-conditioned medium 147, 150
Glycogen synthase kinase 3-β 86, 111, 113, 118–120
Granule cell 208, 209, 211, 246, 249, 250, 256–259, 261
GSK3-β. *See* Glycogen synthase kinase 3-β

Erik D. Roberson (ed.), *Alzheimer's Disease and Frontotemporal Dementia*, Methods in Molecular Biology, vol. 670,
DOI 10.1007/978-1-60761-744-0, © Springer Science+Business Media, LLC 2011

H

Hilus 256–258
Hippocampal function 191, 246
Hippocampus 79, 82, 88, 145, 146, 149, 166, 175, 176, 183, 209, 211, 246, 249, 254, 257–259, 264
Histone 5, 263–273
HNPP 215, 223, 225, 227, 228

I

Immediate early gene 252
Immunohistochemistry 90, 209, 217, 223, 228, 246–248, 253, 254, 260
In-Cell Western (ICW) 4, 94–101, 104, 106
Inhibitory 208, 245–261
In situ hybridization 5, 207–230
In vitro transcription 222

L

Lentiviral vector 155–167
Light and fluorescence microscopy 225
Live imaging 231

M

Memory 1, 182, 191–205
Methods 17–19, 23–28, 37–40, 48–55, 61–68, 76–82, 88–90, 97–103, 113–121, 129–136, 143–147, 158–166, 193–200, 207–230, 234–241, 252–259, 267–271
Methylation 263, 264
Microfluidic 232–237, 240, 242
Mild cognitive impairment 1
Morris water maze 5, 191–205, 246
Mossy fiber 248, 250, 257, 258
Mouse behavior 191
Mouse model 3–5, 86, 125, 169–185, 191–205, 208, 211, 245–261, 264

N

Nav1.1 ..... 208, 209
Near-infrared 94, 95, 104
Nerve growth factor (NGF) 232–234, 238–241
Neurodegeneration 170, 181
Neurofibrillary tangles (NFTs) 2, 4, 45, 110, 141, 169, 170, 173, 175, 178, 181–183
Neuronal activity 246
Neuropathology 2, 13, 170–172
Neuropeptide Y (NPY) 208, 210, 211, 219, 220, 246, 248, 250, 256–60
NGF. *See* Nerve growth factor
NPY. *See* Neuropeptide Y
NTB 207

O

Odyssey 36, 94–97, 99, 100, 104–106
Oligomers 3, 14, 15, 17–21, 24–25, 27–30, 33–43, 45–56, 58, 62, 63, 68, 110, 147, 148

P

Personality change 2
Phosphorylation 107, 119, 142, 170, 264, 272
Preaggregated Aβ 147, 148
Presenilin 2, 85, 170, 172, 177, 178, 181, 184, 245
Primary neural culture 162–164
Progranulin 3
Protocols 3, 4, 17, 19, 29, 40, 42, 46, 48, 55, 61, 63, 68, 73, 83, 86, 90, 94, 106, 110, 113, 118, 129, 147, 149, 161, 211, 223, 225, 229, 230, 240, 246, 255, 261, 264, 267, 272, 273
Protofibrils 3, 19, 30, 58, 62, 66–68, 177

Q

Quantum dot 232, 240–242

R

Recombinant protein expression 125
Retention 204, 293
Riboprobes. *See* RNA probes
RNA 155, 208–211, 213–217, 219, 220, 222–229
RNA probes 208–211, 213, 218–224, 226

S

SDS-PAGE. *See* Sodium dodecylsulfate-polyacrylamide gel electrophoresis
Seizure 175, 176, 246, 248
Single molecule imaging 232
Sliding microtome 212, 251
Sodium dodecylsulfate-polyacrylamide gel electrophoresis (SDS-PAGE) 16, 18, 21, 25, 30, 39, 46, 51–55, 83, 86, 89, 103, 129, 131–136, 175, 268
Spatial learning 191–205
Split GFP complementation 109–122
Stereotaxic injection 158, 159, 164–165

T

Tau 1, 3, 4, 45, 93–107, 109–122, 141, 142, 170–173, 175, 176, 178–184
TDP-43 3
Total internal reflection microscopy 234

Transcripts.....209, 210, 218, 219, 222
Transgenic 72, 79, 80, 82, 86, 87, 125, 170–185, 245–250, 256, 257
Transgenic mouse model 86, 171, 173, 174, 181, 183–185, 191, 208

W

Western blot ..18, 21, 42, 52, 55, 72, 74, 77–79, 82, 89, 103, 105–107, 164, 165, 267, 270–271
Western blotting.....21, 33–37, 40–42, 46–48, 51, 72, 79, 86–88, 90, 94–97, 103, 111–113, 120–121, 161, 208, 229, 266–267, 269–271, 273